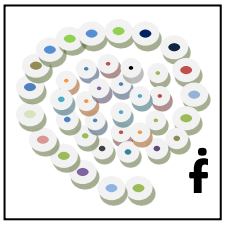

# International Journal of Mathematical Analysis and Modelling

**(Formerly Journal of the Nigerian Society for Mathematical Biology)**

**Volume 5, Issue 1 (May), 2022**

**ISSN (Print): 2682 - 5694**
**ISSN (Online): 2682 - 5708**

**International Journal of Mathematical Analysis and Modelling (Formerly Journal of the Nigerian Society for Mathematical Biology)**

**Volume 5, Issue 1 (May), 2022**

**ISSN (Print): 2682 – 5694**

**ISSN (Online): 2682 - 5708**



**A publication of the Nigerian Society for Mathematical Biology**

## Editorial Board

**International Journal of Mathematical Analysis and Modelling**
**Volume 5, Issue 1, May 2022, Pages 1 – 17**

# A mathematical study of effect of constriction and extra cellular matrix gel on aqueous humor flow and IOP

**B. A. Ngwu[*†], C. O. Mmaduakor[*], O. E. Abolarin[*], O. A. Akintunde[*], M. Iorkua[‡], and S.U. Isienyi[§]**

**Abstract**

Increase in Intraocular Pressure (IOP) in the eye has been pointed out as a primary risk factor for Glaucoma and; Glaucoma is a leading cause of sight loss globally. Despite this knowledge, the site where this increase in pressure occurs is still under studies. The junction between the endothelia-cell wall of the Schlemn's canal and the juxtacanalicular tissue is known to contain funnel shaped pores which are surrounded by extra cellular matrix gel. The flow of Aqueous Humour through these pores generates a funneling effect (which can be considered as a flow through constricted channel) on the TM. Furthermore, the extra cellular matrix may (exert) contribute some force on the flow dynamics, in the form of drag to Aqueous Humour flow. This study investigated the combined effect of the pores and extra cellular matrix gel (as a drag force) on Aqueous Humour flow dynamics such as Aqueous Humour flow resistance, and hydraulic conductivity respectively. Our results show that these structures affect the flow resistance and hydraulic conductivity, and might likely contribute to increase in IOP.

***Keywords:*** constricted channel flow; constriction and drag; aqueous humuor flow; intraocular pressure; hydraulic conductivity and resistance.

## 1. Introduction

Aqueous humor (AH) is a fluid in the eyes secreted through ciliary process which leaves through the trabecular meshwork [9]. The conventional outflow route comprises of the trabecular meshwork (TM), the juxtacanalicular connective tissue (JCT), the endothelial lining of Schlemm's canal (SC)

[*] Department of Mathematics, Federal University, Oye-Ekiti, Ekiti State, Nigeria
[†] Corresponding Author: benitho.ngwu@fuoye.edu.ng; benamaobi@gmail.com
[‡] Department of Statistics, Benue State Polytechnic, Ugbokolo, Benue State, Nigeria
[§] Department of Mathematics/Statistics, Akanu Ibiam Federal Polytechnic, Unwana, Afikpo, Nigeria

and the Schlemm's canal (SC) itself [20,29]. As a fenestrated beams and sheets of extra cellular matrix (ECM) covered with endothelial-like cells (TM), the TM is adjacent to SC. Its primary function is to regulate the bulk of the AH outflow from the anterior chamber [32], thereby controlling the intraocular pressure (IOP). The junction between the innermost portion of the TM and the inner wall endothelium cells of SC is the JCT [32]. Extracellular matrix has been discovered in the cells of the TM beams, JCT and SC inner wall of the eye. Basement and stromal ECM are found in the TM beams and JCT region [1]. The TM beam cells which have discontinuous tight junction strands in addition to possessing gap junctions is known to cover the ECM [ 6, 18,25]. ECM is implicated in outflow resistance because it is critical in maintaining outflow resistance [1] despite that it seems more likely a candidate for the outflow resistance [22]. The SC cells and the JCT ECM are also considered to be responsible for the maintenance of AH outflow resistance. The inner wall cells of the SC have some pores that make funneling possible [18] which creates a hydrostatic effect on the outflow facility [20]. The ECM has a role in the outflow facility of AH as it is primarily thought to cause AH outflow resistance [12, 15, 20, 21, 24, 30], because the ECM and the inner wall cells of SC provides outflow resistance [1] and contribute and control the final the pressure drop by forcing funneling through SC cellular pores [32]. Despite being a candidate for causing outflow resistance, the ECM plays a role also in regulating outflow activity and maintaining IOP. About 25 to 30 pores of the SC which serve as collector channels should allow free circumferential flow of AH but due to segmental flow witnessed in some eyes the fluids do not flow freely, as expected [11, 17, 19].This outflow resistance destabilizes IOP homeostasis which its loss is clearly central to the progression of glaucoma [13, 32]. Glaucoma results from an increase in the resistance of the aqueous humor outflow, which in turn elevates the intraocular pressure (IOP) [31, 33]. Because of this reason it will not be out of place to study the combined effect of these players on AH flow dynamics. See [16, 20, 24] for details.

Earlier, some mathematical works have looked at this problem through different perspectives. These works include [3] that carried out a study of flow of aqueous humor in Schlemm's canal in the eye. They treated the canal segment along which the aqueous humor flows as an elliptic narrow tube. Further, they considered that the inner endothelial wall in contacts with TM is porous and collapsible, and that the inner wall of the SC is deformable as well. By considering that the same quantity of aqueous humor drains through each collector channel is somehow unrealistic. In 2008, Fitt A.D, (2008 ) [14] also carried a similar study on the SC to determine its influence on Primary open angle glaucoma (POAG). In the study, he considered the flow of aqueous humor from the anterior chamber through the TM into the SC. This he did using lubrication theory. After a study of the flow dynamics of the AH through the iris-lens channel, David M. Silver and Harry A. Quigley, (2004) [10] agrees that there is a pressure difference between the posterior and anterior chambers. In 2018, the circulation of AH through its route is considered as a flow with constriction in a channel [23]. The authors considered the funneling effect as a constriction in the channel of flow. By adjusting the stenosis length and other flow parameters they established that the stenosis length and height has a significant effect on the flow dynamics. Other works that studied the dynamics of the AH outflow activity and its effect on IOP include [2, 4, 5]. These works motivated us to extend [23] by incorporating into the flow a drag force term representing the effect of the ECM gel on the flow dynamics, which, to the best of our knowledge, has not been carried out on the AH flow dynamics. Therefore we here try to investigate the effect of constriction (due to the funneling effect of the SC) and ECM (considered as a form of drag force on the flow dynamic) on the AH flow through the TM and SC.

For ease of communication and understanding, we splited the paper into four sections. The first section is the introduction where a background of the study is presented in addition to review of some related literatures to the work. The definition of the problem and its model equations follows from the second section. In this section is contained some of the assumptions guiding the study with some explanations. The third section is where the mathematical analysis of the model is carried out before the last section. This last section takes care of the numerical results, findings from the work and its conclusion.

## 2. Definition and model formulation

Here we consider the flow of AH in the eye as a flow through constriction with drag. Consider that at the point of interest (i.e. the junction between the JCT and the inner wall of SC) the channel is a cylindrical tube with stenosis, which is mild and symmetric. In addition, there is a drag force opposing the outflow of AH through the JCT since it is assumed embedded in the ECM and open on the surface. The flow channel is such that fluid (AH in this case) enters through the point z = 0 and continues until it gets to the mouth of the stenosis at z = d where the funneling effect starts. Within the constricted region the flow is steady and continues until the point z = d + l after which the flow profile fills the non-constricted region. But on getting to z = d +3.5l, the effect of the gel manifests thereby causing a drag on the flow velocity. The flow through the ECM (we represented the ECM with the circle in red) is represented by an arrow around the circular region in the channel and signifies nothing but the effect of drag on the flow profile. This is to sya that there is no tangential flow. In doing so, we have assumed a one dimensional flow with a very low convective momentum. In addition, we assumed that the relationship between the axial velocity and axial direction is not significant. This is because of the nature of the channel and the fluid under consideration here. The geometry of flow channel is considered as shown in figure 1.

R is the radius of the free channel, $R_\delta$ is the radius of the constricted part of the channel, $\delta$ is the radius of constriction, L is the length of the channel, a is the radius of the drag-free channel, $R_a$ is the radius of the drag-filled channel, d is the distance between the entrance and the constriction and L is the length of the constriction.

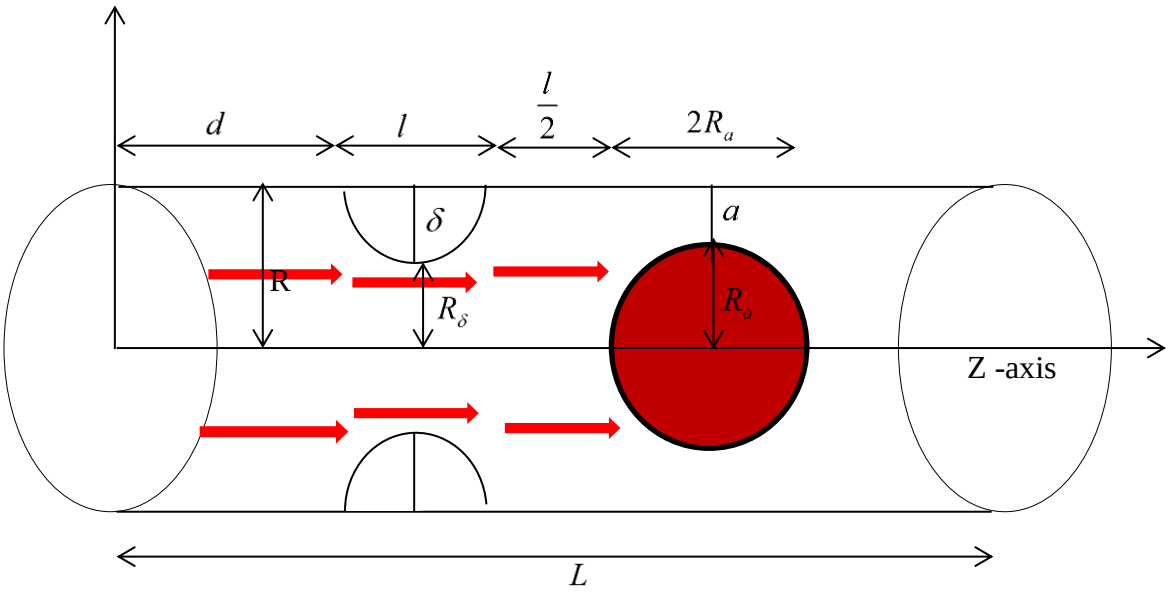


**Figure 1.** Geometry of the flow channel.

## 2.1. Model formulation

The equations governing the geometry of the flow channel is defined as presented in equations (1) and (2) respectively.

$$\frac{R_\delta}{R} = \begin{cases} 1-\dfrac{2\delta}{Rl}(z-d); & d \le z \le d+\dfrac{l}{2} \\ 1-\dfrac{\delta}{2R}\left[1+\cos\dfrac{2\pi}{l}\left(z-d-\dfrac{l}{2}\right)\right]; & d+\dfrac{l}{2} \le z \le d+l \end{cases} \tag{1}$$

$$\frac{R_a}{R} = \begin{cases} 1-\dfrac{a}{Rl_a}(z-d_a); & d_a \le z \le d_a+\dfrac{l_a}{2} \\ 1-\dfrac{a}{2R}\left[1+\cos\dfrac{2\pi}{l_a}\left(z-d_a-\dfrac{l_a}{2}\right)\right]; & d_a+\dfrac{l_a}{2} \le z \le d+l_a \\ 1 & \text{otherwise} \end{cases} \tag{2}$$

In the light of the above, the equation governing the AH flow in this case is given by

$$\rho\frac{D\overline{U}}{Dt} = -\overline{\nabla}P + \mu\overline{\nabla}^2 U + \bar{f}$$

where $\overline{U} = (u_1, u_2, u_3)$ is the velocity of the flow, $\frac{D\overline{U}}{Dt}$ is the instantaneous accelerations, $\overline{\nabla}P$ is the pressure gradient, i.e. the pressure drop across the channel length of flow and $\bar{f}$ is the external body force. Since there is no external body, $\bar{f} = 0$. (The aqueous flow is driven by the pressure drop in the channel, which is the difference between the flow at the entrance and exit of the channel). We shall assume that $(u_1, u_2, u_3) = (u_1, 0, 0)$, which is to say that there is only flow along the channel. This in other words means that we consider only a one dimensional flow system. Because of the funneling effect on aqueous flow caused by the JCT on the inner wall of the SC, the dynamics of the flow is considered as a flow with constriction.

Suppose that the channel of flow is such that the point z = d is the end of the hydrodynamic entrance region where the flow stooped developing. Because of this, we shall assume that the flow is fully developed having travelled through the entrance length where the flow was developing. As a result of this, we consider the equations governing the flow (see [23, 27] ) to be

$$\frac{\mu}{r}\frac{\partial}{\partial r}\left[r\frac{\partial U}{\partial r}\right] = P_x, \tag{3}$$

$$U(R) = 0, \tag{4}$$

$$U(R_\delta) = \frac{-R_\delta\sqrt{D_a}}{\alpha}U_\delta, \tag{5}$$

$$\frac{\partial U(R_a)}{\partial r} = U_\delta - U_a, \tag{6}$$

where $U_\delta$ is the slip velocity at the stenosis and $U_a = -\pi r\mu U$ is the drag velocity due to ECM.

## 2.2. Analysis of the Problem

We obtain the slip velocity of the flow at the stenosis throat as equation (7) and the velocity profile of the flow as equation (8) below.

$$U_\delta = \frac{p_x}{4\mu}\left[\frac{2R_a^2\ln\left(R_\delta/R\right) - \left(R_\delta^2 - R^2\right) + \pi\mu R_a^2\left(\left(R_a^2 - R^2\right)\ln\left(R_\delta/R\right) - \left(R_\delta^2 - R^2\right)\ln\left(R_a/R\right)\right)}{R_a\ln\left(R_\delta/R\right) + \frac{\pi\mu R_\delta R_a^2\sqrt{D_a}}{\alpha}\ln\left(R_a/R\right) + \frac{R_\delta\sqrt{D_a}}{\alpha}}\right] \tag{7}$$

$$U(r) = \frac{p_x}{4\mu}\left[ r^2 - R^2 + \gamma R_a{}^2 \frac{\ln\left(r/R\right)}{\ln\left(R_\delta/R\right)} - \left(R_\delta{}^2 - R^2\right)\frac{\ln\left(r/R\right)}{\ln\left(R_\delta/R\right)}\right], \tag{8}$$

where

$\gamma$

$$= \left(\frac{R}{R_\delta}\right)\frac{2\left(\frac{R_a}{R}\right)^2 \ln\left(R_\delta/R\right) - \left(\left(\frac{R_\delta}{R}\right)^2 - 1\right) + \pi\mu R_a{}^2\left(\left(\left(\frac{R_a}{R}\right)^2 - 1\right)\ln\left(R_\delta/R\right) - \left(\left(\frac{R_\delta}{R}\right)^2 - 1\right)\ln\left(R_a/R\right)\right)}{\left(\frac{R_a}{R_\delta}\right)\ln\left(R_\delta/R\right) + \frac{\pi\mu R_a{}^2\sqrt{D_a}}{\alpha}\ln\left(R_a/R\right) + \frac{\sqrt{D_a}}{\alpha}}$$

Next we calculate the flux of the flow but in doing so we shall consider only the flux of the region of constriction and that of the ECM respectively. The part of the channel without any obstruction is considered the standard as it is assumed that the flow in those regions is free of any resistance. To get the flux we use the following equation adapted from [28]:

$$Q = 2\pi\left[\int_0^{R_\delta} rU dr + \int_{R_a}^{R} rU dr\right]. \tag{9}$$

By employing equation (8) in equation (9) and simplifying we obtain the flux of the flow as

$Q$

$$= \frac{\pi R^4 p_x}{8\mu}\left\{\begin{array}{l}\left(\frac{R_\delta}{R}\right)^4 + \left(\frac{R_a}{R}\right)^4 - 2\left[\left(\frac{R_\delta}{R}\right)^2 + \left(\frac{R_a}{R}\right)^2\right] + \frac{\beta}{R}\left(\frac{R_a}{R}\right)\left(\frac{R_\delta}{R}\right)\left[2\log\left(\frac{R_\delta}{R}\right) - 1\right] \\ \qquad + \frac{\beta}{R}\left(\frac{R_a}{R}\right)^3\left[2\log\left(\frac{R_a}{R}\right) - 1\right]\end{array}\right\}, \tag{10}$$

where $\dfrac{\beta}{R} = \dfrac{\pi R_a R_\delta \mu^2\sqrt{D_a}\left[\left(\frac{R_a}{R}\right)^2 - 1\right] - \alpha\left[\left(\frac{R_\delta}{R}\right)^2 - 1\right] - 2\left(\frac{R_a}{R}\right)\left(\frac{R_\delta}{R}\right)\mu\sqrt{D_a}}{\left(\frac{R_\delta}{R}\right)\sqrt{D_a} + \alpha\left(\frac{R_a}{R}\right)\log\left(\frac{R_\delta}{R}\right) - \left(\frac{R_a}{R}\right)^2 R R_\delta \pi\mu\sqrt{D_a}\log\left(\frac{R_a}{R}\right)}$.

From equation (10) we obtain the pressure gradient as

$$p_x = \frac{8\mu Q}{\pi R^4 \Gamma}, \tag{11}$$

where

$$\Gamma = \left(\frac{R_\delta}{R}\right)^4 + \left(\frac{R_a}{R}\right)^4 - 2\left[\left(\frac{R_\delta}{R}\right)^2 + \left(\frac{R_a}{R}\right)^2\right] + \frac{\beta}{R}\left(\frac{R_a}{R}\right)\left(\frac{R_\delta}{R}\right)\left[2\log\left(\frac{R_\delta}{R}\right) - 1\right] + \frac{\beta}{R}\left(\frac{R_a}{R}\right)^3\left[2\log\left(\frac{R_a}{R}\right) - 1\right].$$

Integrating (11) with respect to the variable $x$ along the channel length $L$ yields the pressure gradient as

$$\nabla p = \int_0^L p_x \, dx = \frac{8\mu Q}{\pi R^4}\Phi, \tag{12}$$

where

$$\Phi = \int_0^d \frac{1}{\Gamma}dx + \int_d^{d+\frac{l}{2}} \frac{1}{\Gamma}dx + \int_{d+\frac{l}{2}}^{d+l} \frac{1}{\Gamma}dx + \int_{d+l}^{\frac{3}{2}d+l} \frac{1}{\Gamma}dx + \int_{\frac{3}{2}d+l}^{\frac{3}{2}d+l+R_a} \frac{1}{\Gamma}dx + \int_{\frac{3}{2}d+l+R_a}^{\frac{3}{2}d+l+2R_a} \frac{1}{\Gamma}dx + \int_{\frac{3}{2}d+l+2R_a}^{L} \frac{1}{\Gamma}dx.$$

Evaluating the first, fourth and seventh integrals yields $L - l - 2R_a = L\left(1 - \frac{l + 2R_a}{L}\right)$, and with this the flow resistance in the stenosis region becomes

$$\bar{\lambda} = \frac{\nabla p}{Q} = \frac{8\mu}{\pi R_\delta^{\,4}}\left(\frac{L - l - 2R_a}{\Gamma} + \Theta\right), \tag{13}$$

where $\Theta = \frac{1}{L}\left[\int_{d}^{d+\frac{1}{2}} \frac{1}{\Gamma} dx + \int_{d+\frac{1}{2}}^{d+l} \frac{1}{\Gamma} dx + \int_{\frac{3}{2}d+l}^{\frac{3}{2}d+l+R_a} \frac{1}{\Gamma} dx + \int_{\frac{3}{2}d+l+R_a}^{\frac{3}{2}d+l+2R_a} \frac{1}{\Gamma} dx\right]$.

From equation (13), we obtain the non-dimensional form of flow resistance, as described in [7, 8, 26] from the stenosis region as

$$\lambda = \frac{\overline{\lambda}}{\lambda_0} = \Omega\left\{\frac{1-(l-2a)/L}{\Gamma_0} + \frac{1}{\Gamma_0}\Theta\right\}, \tag{14}$$

where $\lambda_0 = \frac{8\mu}{\Gamma_0 \pi R^4}$, $\Gamma_0 = \varepsilon^4 - 2\varepsilon^2 + \frac{\beta_0}{R}\left\{\varepsilon^3\left[\log(\varepsilon) - 1\right] - \varepsilon\right\} - 1$,

$\frac{\beta_0}{R} = \frac{\pi\mu^2\varepsilon\left(\varepsilon^2 - 1\right) - 2\frac{\mu\varepsilon}{R^2}}{\frac{1}{R^2} - \varepsilon^2\pi\mu\log(\varepsilon)}$, $\varepsilon = \frac{R_\delta}{R_a}$ and $\Omega = 2\left(2\mu^2 R^2 - 1\right)$.

Since our numeric result is in two parts we obtained the following expressions to be used in each of these regions. Expressions for the stenosis free region are with subscript 'a', whereas those for the ECM free regions are subscripted '$\delta$'.

ECM free region: $\frac{\beta_\delta}{R} = \frac{\pi R_a R_\delta \mu^2 \sqrt{D_a}\left[\varepsilon^2 - 1\right] - \alpha\left[\left(\frac{R_\delta}{R}\right)^2 - 1\right] - 2\varepsilon\left(\frac{R_\delta}{R}\right)\mu\sqrt{D_a}}{\frac{R_\delta}{R}\sqrt{D_a} + \alpha\varepsilon\log\left(\frac{R_\delta}{R}\right) - \varepsilon^2 R R_\delta \pi\mu\sqrt{D_a}\log(\varepsilon)}$ and

$\Gamma_\delta = \left(\frac{R_\delta}{R}\right)^4 + \left(\frac{R_\delta}{R}\right)^2 - 2\left[\left(\frac{R_\delta}{R}\right)^2 + \left(\frac{1}{\varepsilon}\right)^2\right] + \frac{\beta_\delta}{R}\varepsilon\left\{\left(\frac{R_\delta}{R}\right)^2\left[2\log\left(\frac{R_\delta}{R}\right) - 1\right] + \varepsilon^2\left[2\log(\varepsilon) - 1\right]\right\}$

Stenosis free region; $\frac{\beta_a}{R} = \frac{\pi R_a R \mu^2\left[\left(\frac{R_a}{R}\right)^2 - 1\right] - 2\left(\frac{R_a}{R}\right)\mu}{1 - \left(\frac{R_\delta}{R}\right)^2 R^2 \pi\mu\log\left(\frac{R_\delta}{R}\right)}$ and

$\Gamma_a = \left(\frac{R_a}{R}\right)^4 - 2\left(\frac{R_a}{R}\right)^2 - 1 + \frac{\beta_a}{R}\left(\frac{R_a}{R}\right)\left\{\left(\frac{R_a}{R}\right)^2\left[2\log\left(\frac{R_a}{R}\right) - 1\right] - 1\right\}$.

We also considered the hydraulic conductivity of the flow duct following the definition given in [18] and obtained the dimensionless hydraulic conductivity, $L_p$, as

$$L_p = \frac{1}{\lambda A}. \tag{15}$$

## 3. Numerical results and discussion

Because of the fact that solutions for the resistance and hydraulic conductivity is not possible analytically, we resorted to numerical solution approach. The flow channel is partitioned into two, the first is $0 \leq z_1 \leq 0.5$ and the second is $0.5 \leq z_2 \leq 1$. We assumed equal length for both ECM and stenosis and considered that $d$ which locates the stenosis in the channel is zero. The first two integrals are evaluated with equations 1(a) and (b) respectively whereas 2(a) and (b) are used to evaluate the second and fourth integrals. We followed [3, 14] closely, in simulation and the numerical results, and obtained different results as presented and discussed in the figures shown below.

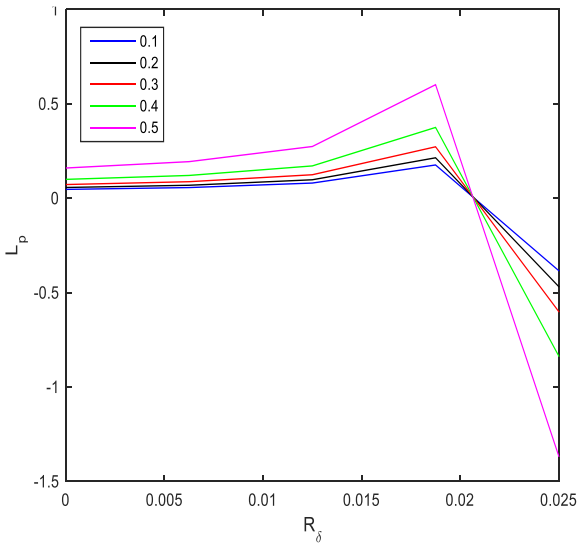


**Figure 2**: The effect of stenosis radius on Hydraulic conductivity with different varying slip paremeters.

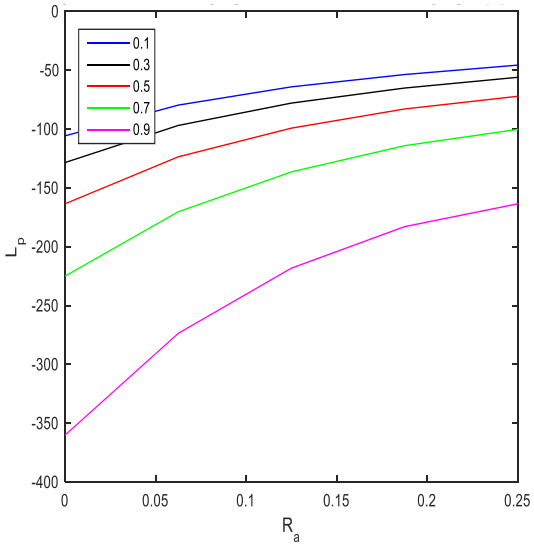


**Figure 3**: The relationship between Hydraulic conductivity and the ECM.

Figures 2 and 3 show that hydraulic conductivity increases in the presence of stenosis and ECM with varying slip parameter. On one hand, it increases with increasing slip parameter, gradually though, in the presence of stenosis until the flow starts to come just immediately after the stenosis throat when the hydraulic conductivity starts to decline in a reverse order with the slip parameter. This concept, as we think, may be due to the drag force caused by the presence of ECM in the flow profile.

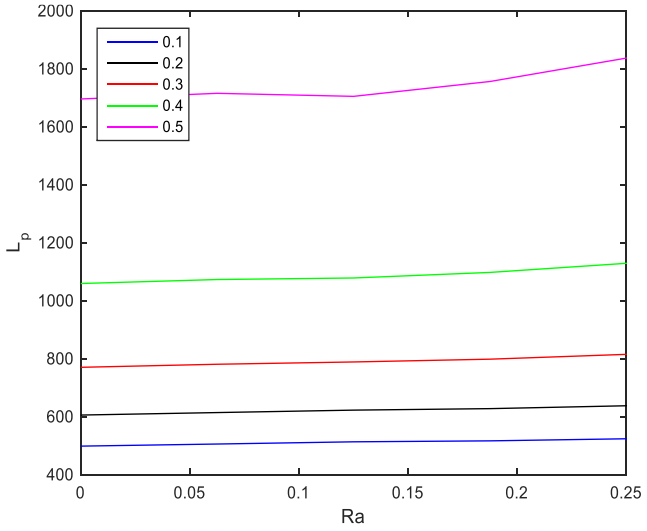


**Figure 4**. The effect of Darcy Number on Hydraulic conductivity and ECM.

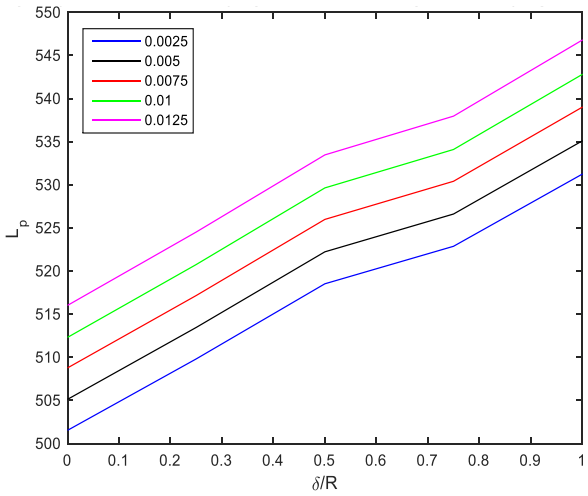


**Figure 5.** This shows how stenosis height affects Hydraulic conductivity in the presence of ECM.

In Figure 4 we see that the Hydraulic conductivity varies directly with the Darcy number in the presence of the ECM. As shown in this figure, the hydraulic conductivity of the flow gradually increases with higher Darcy number despite the increase in ECM diameter. It appears from this that the effect of Darcy number and the ECM cancel out each other, to some extent. This is open for further study. As is expected, Figure 5 shows that, in the presence of ECM, the stenosis height affects hydraulic conductivity. If a smaller area of the flow channel is under the influence of the drag from the ECM, the ease with which AH moves through the channel is lower than when a larger area is covered by the ECM. It then means that the presence of ECM contributes more pressure to the flow profile.

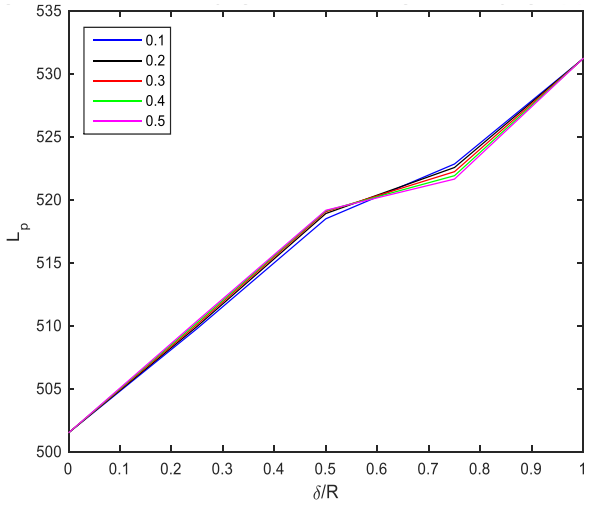


**Figure 6.** How Hydraulic conductivity behaves against stenosis height with varying slip parameters.

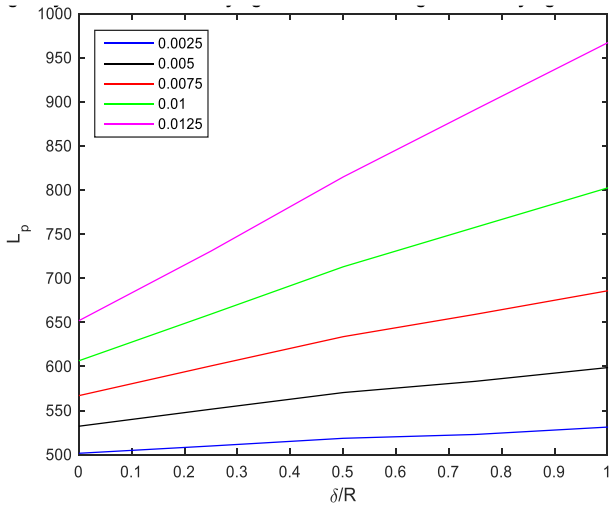


**Figure 7.** Display of how stenosis height affects Hydraulic conductivity in the varying stenosis radius.

Figure 6 shows that the slip parameters has little or no effect on the flow profile with respect to the Hydralc conductivity and the stenosis height. Nevertheless, it can be seen that the hadraulic conductivity responds directly to the stenosis with the slip parameter up to the mouth of the middle of the stenosis where the eefct of the slip is noticed. This is seen in the way the slip parameters switchs their positions, insignificantly though. From Figure 7, it is evident that the flow starts out with less ease due to, may be, the funneling effect caused by the pores considered as the stenosis but eases out as the flow moves out of the pores. It is also observable that with longer radii, the ease of flow through the pores increases. The effect of the stenosis is seen to delay hydraulic conductivity around the stenosis throat.

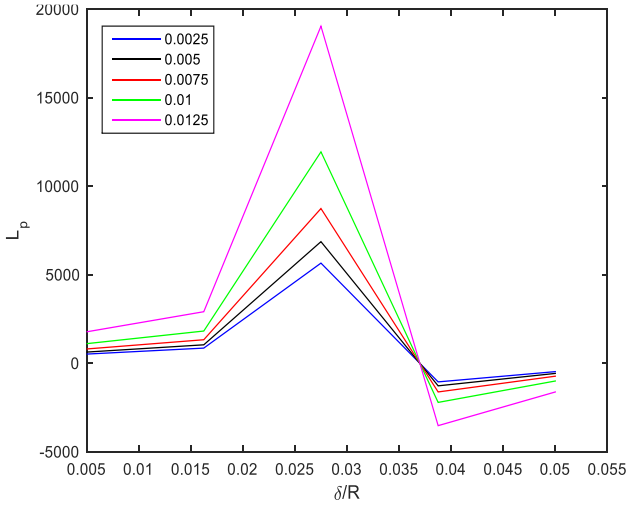


**Figure 8**. A display of effect of ECM on hydaraulic conductivity and stenosis radius.

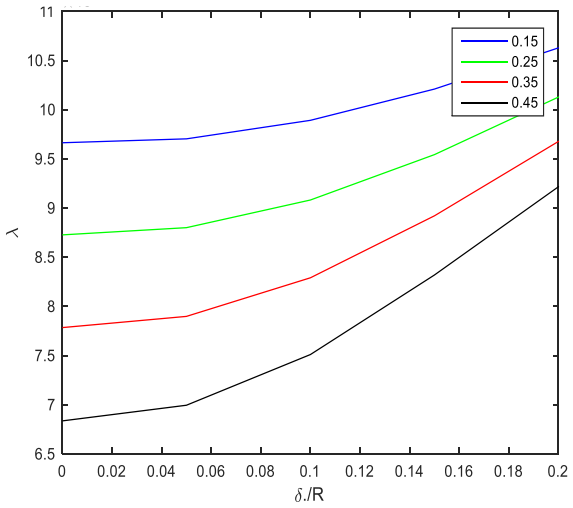


**Figure 9**. A plot showing the effect of stenosis height on Resistance in the presence of ECM.

Figure 8 displays the combined effect of stenosis and ECM on hydraulic conductivity. As is expected increase in ECM radius affects hydraulic conductivity of the flow. On the other hand, presence of stenosis is seen to affect hydraulic conductivity since it declines just immediately after the stenosis throat. Remarkable is Fgure 9 which shows how resistance is affected by ECM. It shows that increase in ECM radius increases the resistance. The steepness of the resistance profile is deeper with increasing ECM which agrees with our expectation.

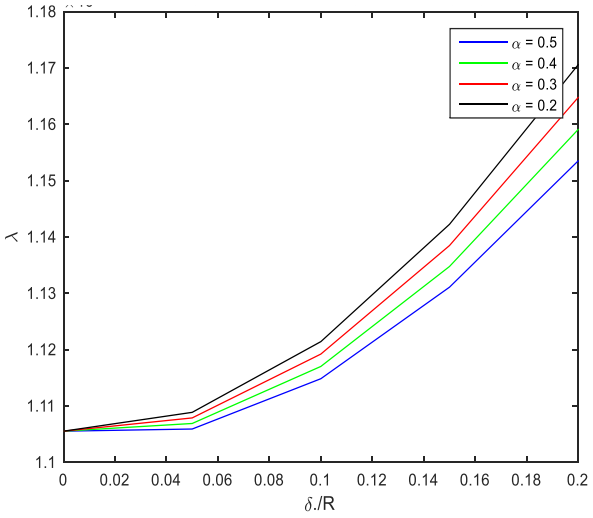


**Figure 10**. How resistance is affected by stenosis in the presence of different slip parameters.

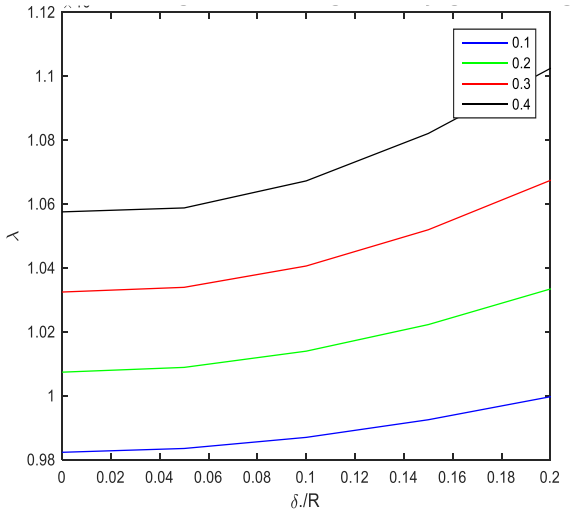


**Figure 11**. A plot of how stenosis height and radius affect resistance.

Figure 10 shows that resistance is increases with increasing stenosis height. However, the result is different in the presence of slip parameter. As can be seen from this figure, resistance decreases with higher slip parameter value but reduces otherwise. İt goes on to show the the role of slip parameter in the resistance profile of the flow through constriction. On the other hand, we see from Figure 11 that the height of the stenosis directly affects the resistance. İn other words, the more steep the constriction the more the resistance.

## 4. Conclusion

Based on these results from numeric solution and simulations we conclude that these structures affect the flow resistance and hydraulic conductivity, and might likely contribute to increase in IOP. We can then infer from the study that reducing the stenosis height can reduce resistance to AH flow, in addition to regulating ECM spread.

## References

[1] Acott T.S. and Kelley M.J. (2008). Extracellular matrix in the trabecular meshwork. Exp. Eye Res., 86:543–61.

[2] Akbar S. and Shah S. (2020). The effects of prostaglandin analogs on intraocular pressure in human eye for open angle glaucoma. International Journal of Innovative Technology and Exploring Engineering, 10(2): 176 - 180.

[3] Avtar R., Srivastava S., and Srivastava R. (2014). Modelling the flow of aqueous humor in schlemm's canal in the eye. AAM: Intern. J., 9(1). http://pvamu.edu/aam.

[4] Avtar R. and Srivastava R. (2006). Modelling the flow of aqueous humor in anterior chamber of the eye. Applied Mathematics and Computation 181: 1336–1348.

[5] Avtar R. and Srivastava R. (2006). Aqueous outflow in Schlemms canal. Applied Mathematics and Computation 174 : 316–328.

[6] Bhatt K., Gong H., and Fredo T.F. (1995). Freeze-fracture studies of interendothelial junctions in the angle of the human eye. Invest Ophthalmol Vis Sci, 36(7):1379–1389.

[7] Bird R.B., Stewart W. E., and Lightfoot E.N. (2002). Transport Phenomena. John Wiley & Sons, Singapore, p97.

[8] Biswas D. and Chakraborty U.S. (2010). Pulsatile blood flow through a catheterized artery with an axially nonsymmetrical stenosis. Applied Mathematical Science, 4 (58); 2865-2880.

[9] Braunger B.M, Fuchshofer R., and Tamm E.R. (2015). The aqueous humor outflow pathways in glaucoma: A unifying concept of disease mechanisms and causative treatment. Eur J Pharm Biopharm, 95 (Pt B):173-81.

[10] David M. S. and Harry A. Q. (2004). Aqueous flow through the iris–lens channel: estimates of differential pressure between the anterior and posterior chambers. J. Glaucoma, 13: 100 – 107.

[11] Ethier C.R, Chan D.W., and Johnson M. (2001). Cationic ferritin changes outflow facility in human eyes whereas anionic ferritin does not. Invest Ophthalmol Vis Sci.; 42:1795–1802. [PubMed: 11431444].

[12] Ethier C.R. (2002). The inner wall of Schlemm's canal. Exp Eye Res. 74:161–172. [PubMed: 11950226].

[13] Ficarrotta K.R., Mohamed Y.H., and Passaglia C.L. (2020). Experimental glaucoma model with controllable intraocular pressure history. Natureresearch, 10:126. https://doi.org/10.1038/s41598-019-57022-5.

[14] Fitt A.D. (2008). Flow in the canal of schlemm and its influence on primary open angle glaucoma. In Bonilla, L.L., Moscoso, M., Platero, G. and Vega, J.M. (eds), Progress in Industrial Mathematics, Germany, Springer, 843-847.

[15] Fuchshofer R. and Tamm E.R. (2009). Modulation of extracellular matrix turnover in the trabecular meshwork. Exp Eye Res.; 88:683–688. [PubMed: 19385040].

[16] Goel M., Picciani R.G., Lee R.K., and Bhattacharya S.K. (2010). Aqueous humor dynamics: a review. The Open Ophthalmology Journal,Vol. 4, 52-59.

[17] Gottanka J., Chan D., Eichhorn M., and Johnson M. (2004). Effects of TGF-beta2 in perfused human eyes. Invest Ophthalmol Vis Sci;45:153-158.

[18] Grierson I. and Lee W.R. (1974). Junctions between the cells of the trabecular meshwork. Albrecht Von Graefes Arch Klin, Exp Ophthalmol, 192:89–104.

[19] Hann C.R., Bahler C.K., and Johnson D.H. (2005). Cationic ferritin and segmental flow through the trabecular meshwork. Invest. Ophthalmol Vis Sci.; 46(1):1-7.

[20] Johnson M. and Tamm E.R. (2010). Biomechanics of aqueous humor outflow resistance. Elsevier 2010 Adapted from Johnson, M. (2006), What controls aqueous humour outflow resistance? Experimental Eye Research, 82: 545–557.

[21] Johnson M. (2006). What controls aqueous humor outflow resistance? Exp Eye Res; 82:545–57.

[22] Maepea O. and Bill A. (1992). Pressures in the juxtacanalicular tissue and Schlemm's canal in monkeys. Exp Eye Res, 54(6): 879-883.

[23] Ngwu B.A., Iorkua M., Mmaduakor C.O., and Odafi O.N. (2018). Mathematical model of aqueous humour flow through a constricted channel. Journal of the Nigerian Association of Mathematical Physics, 47: 47 – 54.

[24] Overby D.R., Stamer W.D., and Johnson M. (2009). The changing paradigm of outflow resistance generation: towards synergistic models of the JCT and inner wall endothelium. Exp Eye Res., 88:656-670.

[25] Raviola G. and Raviola E. (1981). Paracellular route of aqueous outflow in the trabecular meshwork and canal of Schlemm. A freeze-fracture study of the endothelial junctions in the sclerocorneal angel of the macaque monkey eye. Invest Ophthalmol Vis Sci., 21:52–72.

[26] Shah S.R., Siddiqui S.U., and Sing A. (2016). Performance of blood flow through two phase stenosed artery using Herschel-Bulkley model. International Journal of Applied and Pure Science and Agriculture, 02(2): 228-240.

[27] Srivastav R.K. (2015). Mathematical model of blood flow through a composite stenosis in catheterized artery with permeable wall. Application and Applied Mathematics: An International Journal, 9(1): 58-74.

[28] Srivastav V.P., Vishnoi R., Sing D., Medhavi A., and Mishra S. (2015). Response to blood flow through an overlapping stenosis in catheterized arteries. E-Journal of Science and Technology, 5(6): 93-103.

[29] Tamm E.R., Braunger B.M., and Fuchshofer R. (2015). Chapter Eighteen - Intraocular pressure and the mechanisms involved in resistance of the aqueous humor flow in the trabecular meshwork outflow pathways, In 'Progress in Molecular Biology and Translational Science', Academic Press, Volume 134: 301-314.

[30] Tamm E.R. and Johnson M. (2009). The trabecular meshwork outflow pathways: structural and functional aspects. Exp Eye Res., 88: 648–655. PubMed: 19239914.

[31] Villamarina A., Roy S., Hasballa R., Vardoulis O., Reymond P., and Stergiopulos N. (2012). 3D simulation of the aqueous flow in the human eye. Journal of Medical Engineering and Physics 34; 1462 – 1470. www. elsevier.com/locate/medengphy.

[32] Vranka J.A., Kelley M.J., Acott T.S., and Keller K.E. (2015). Extracellular matrix in the trabecular meshwork: Intraocular pressure regulation and dysregulation in glaucoma. Exp Eye Res, 133: 112–125. doi:10.1016/j.exer.2014.07.014.

[33] Yuan N., Li M., Chen X., Lu Y., Fang Y., Gong H., Qian L., Wu J., Zhang S., Shipp S., Andolina I.M., Sun X., and Wang W. (2020). Immediate impact of acute elevation of intraocular pressure on cortical visual motion processing. Invest Ophthalmol Vis Sci., 61(5):59. https://doi.org/10.1167/iovs.61.5.59.

**International Journal of Mathematical Analysis and Modelling**
**Volume 5, Issue 1, May 2022, Pages 18 – 35**

# The transmission dynamics of Lassa fever disease incorporating control measures

**V. Vegha***

**Abstract**

In this work, a mathematical model to study the transmission dynamics of Lassa fever with control measures like public health education campaign, isolation and treatment is formulated. The basic properties of the model are examined and the effective reproduction number $R_c$ is computed. Steady states of the model were analyzed for stability, it was found that whenever $R_c$ is $< 1$, the disease dies out while when $R_c$ is $> 1$, the disease persists in the population. We found from sensitivity analysis that the most sensitive parameter is the natural death rate of rodents $\mu_r$ with a sensitivity index of -2 while the least sensitive parameter is Lassa fever induced death rate with a sensitivity index of -0.0007. We carried out numerical simulation and results sows that isolation, treatment and public health education campaign can reduce the dynamical spread of the disease in the population.

***Keywords:*** Lassa fever; mathematical model; basic reproduction number; disease free equilibrium; stability; sensitivity analysis; endemic equilibrium; bifurcation; multimammate rat; zoonotic disease.

## 1. Introduction

Lassa fever is an acute viral illness that occurs in West Africa [5]. The illness was discovered in 1969 when two missionary nurses died in Nigeria. The virus is named after a town Lassa in Borno state of Nigeria where the first cases occurred [5, 16]. Lassa fever is a zoonotic disease, meaning that humans become infected from contact with infected animals [20]. The rodent reservoir, or host of Lassa virus is a rodent of genus *Mastomys natalensis*, commonly known as "*multimammate rat*". *Mastomys* rats infected with Lassa virus do not become ill, but can shed the virus in their urine and faeces [20]. Humans become infected with Lassa virus from exposure to urine or faeces of *infected Mastomys rats* [20]. Several cases of disease outbreak have been recorded in 19 states of Nigeria since it was first reported in 1969. The most affected states are Bauchi, Edo, Oyo and Taraba which account for 54% of the confirmed cases [7, 19]. The worst outbreak was recorded in 2012 where 1700 cases including 112 deaths were reported [7, 19].

* Department of Mathematics, Federal University of Agriculture, Makurdi, Nigeria

A review of earlier works on Lassa fever provides the perspective of this work. In [14], Ogabi *et al* formulated a basic SIR model for the control of Lassa fever in Northern part of Edo State of Nigeria. The disease control was studied based on the basic reproductive number. It was clearly shown in his work that to control the spread of Lassa fever in the endemic areas, the basic reproduction number $R_0$ must be brought below 1. If it is more than 1, the disease will not die out from the area.

In [12], Mohammed *et al* in their work titled 'sensitivity analysis in a Lassa fever deterministic model' formulated a model with five mutually exclusive compartments related to Lassa fever transmission. The result of their sensitivity analysis showed that the most sensitive parameter is the human immigration, followed by human recovery rate, then person to person contact. This suggests that control strategies should target human immigration, effective drugs for treatment and education to reduced person to person contact.

In [15],Onuorah *et al* developed a Lassa fever model using the sex structure approach. Key to his analysis was the basic reproductive number $R_0$ . Sensitivity indices of $R_0$ around the baseline parameter value were computed, which showed that the most sensitive parameter to $R_0$ is human birth rate, followed by condom efficacy and compliance. In [8], James *et al* proposed a mathematical model for the transmission dynamics of Lassa fever incorporating treatment. The equilibrium states were obtained and analyzed for stability. It was discovered that the zero-equilibrium state is stable when the birth rate of the human population is less than the death rate and same when the birth rate of the *mastomys natalensis* (reservoir) is less than the total death rates.

In [2], Adewale *et al* formulated a model with six compartments to gain insight into the effect of isolation of infected individuals and treatment of infected individuals in the dynamical spread of Lassa fever due to effective contact of human and infected rats. The result shows that the disease dies out whenever the threshold $R_0 < 1$ but spreads when it exceeds unity i.e., $R_0 > 1$ .

It is worthy of note that none of the models reviewed incorporated health education campaign as a control strategy, rather, most of the authors advised that health education campaign should be intensified in the affected areas in order to curb the endemic nature of the disease. Furthermore, most of the authors considered treatment of infected individuals without isolation. Our model therefore examines the effect of public health education campaign, isolation and treatment on the spread of Lassa fever disease (LFD) all incorporated at a time. Hence our model is an advanced one that seeks to provide a better study and understanding of the LFD transmission dynamics in a given population.

## 2. Model formulation

A diagrammatic representation of the model formulation is shown in Figure 1. The total human population $N_h(t)$ is sub-divided into sub-classes as follows: Susceptible humans $S_h(t)$, Exposed humans $E_h(t)$ infectious humans $I_h(t)$, Isolated humans $J_h(t)$, Recovered humans $R_h(t)$, so that $N_h(t) = S_h\ (t) + E_h(t) + I_h(t) + J_h(t) + R_h(t)$, Also, the total population of rats $N_r(t)$ is subdivided into Susceptible $S_r(t)$, and Infected $I_r(t)$, so that; $N_r(t) = S_r\ (t) + I_r(t)$.

The susceptible human population $S_h(t)$, increases by recruitment of individuals into the population by birth or immigration at the level $\Lambda_h$, the group also increases as a result of loss of immunity by recovered individuals at a rate $\Phi$. The population decreases by infection following effective contact with infectious rodents and infectious humans at the level $\beta_1$ and $\beta_2$ respectively. The population also decreases as a result of human natural death at a rate $\mu_h$.

The population of the exposed individuals $E_h(t)$ consists of newly infected individuals following contact with infectious rodents and infectious humans at the rate $\beta_1$ and $\beta_2$ respectively. The population declines as a result of progression to infectious class at a rate $\alpha$ and human natural death at a rate $\mu_h$.

The population of infectious individuals $I_h(t)$ increases as a result of progression from the exposed class at the rate $\alpha$. The class decreases as a result of isolation at a rate $\tau_1$, treatment at a rate $\tau_2$, natural death at a rate $\mu_h$ and disease induced death at a rate $\delta$. The population of isolated individuals $J_h(t)$ increases as a result of isolation of the infectious individuals at a rate $\tau_1$ .The population decreases due to natural death at the rate $\mu_h$, death due to disease at the rate $\delta$ and treatment at the rate $\tau_3$.

We introduce the Recovered compartment $R_h(t)$. The population of the individuals in this group increases as a result of treatment of infectious humans at a rate $\tau_2$ and isolated humans at a rate $\tau_3$. The population decreases as a result of natural death at a rate $\mu_h$ and loss of immunity at a rate $\Phi$.

Susceptible rodents ($S_r$) are generated at a constant recruitment level $\Lambda_r$ and acquire infection following effective contact with infected rodent at a rate $\beta_1$. The rodents suffer death at the rate $\mu_r$. The infected class of the rodents ($I_r$) has newly infected rodents and reduces by natural death at the rate $\mu_r$.

| Variable | Description |
|---|---|
| $S_h(t)$ | Susceptible humans at time t |
| $E_h(t)$ | Exposed humans at time t |
| $I_h(t)$ | Infectious humans at time t |
| $J_h(t)$ | Isolated humans at time t |
| $R_h(t)$ | Recovered humans at time t |
| $S_r(t)$ | Susceptible rats at time t |
| $I_r(t)$ | Infected rats at time t |

**Table 1**: Variables of the model

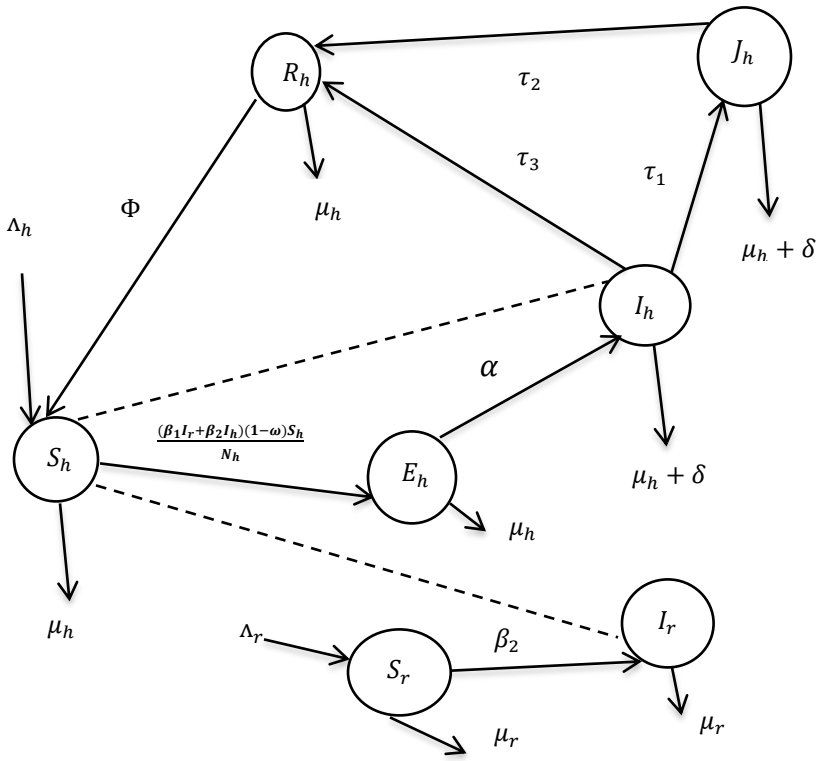


**Figure 1**: Schematic diagram for the model

## 2.1. Model equations

$$
\begin{aligned}
\frac{dS_h}{dt} &= \Lambda_h + \Phi R_h - \frac{(\beta_1 I_r + \beta_2 I_h)(1-\omega)S_h}{N_h} - \mu_h S_h \\
\frac{dE_h}{dt} &= \frac{(\beta_1 I_r + \beta_2 I_h)(1-\omega)S_h}{N_h} - (\alpha + \mu_h)E_h \\
\frac{dI_h}{dt} &= \alpha E_h - (\tau_1 + \tau_2 + \mu_h + \delta)I_h \\
\frac{dJ_h}{dt} &= \tau_1 I_h - (\tau_3 + \mu_h + \delta)J_h \\
\frac{dR_h}{dt} &= \tau_3 J_h + \tau_2 I_h - (\mu_h + \Phi)R_h \\
\frac{dS_r}{dt} &= \Lambda_r - \beta_1 S_r I_r - \mu_r S_r \\
\frac{dI_r}{dt} &= \beta_1 S_r I_r - \mu_r I_r,
\end{aligned} \tag{1}
$$

with initial condition

$S_h(0) = S_{h0}$, $E_h(0) = E_{h0}$, $I_h(0) = I_{h0}$, $J_h(0) = J_{h0}$ $R_h(0) = R_{h0}$, $S_r(0) = S_{r0}$, $I_r(0) = I_{r0}$,

$$N_h(t) = S_h(t) + E_h(t) + I_h(t) + J_h(t) + R_h(t), \quad (2)$$

where $N_h(t)$ denotes the total human population at a given time:

$$\frac{dN_h(t)}{dt} = \frac{dS_h}{dt} + \frac{dE_h}{dt} + \frac{dI_h}{dt} + \frac{dJ_h}{dt} + \frac{dR_h}{dt},$$
$$\frac{dN_h(t)}{dt} = \Lambda_h - \mu_h N_h(t) - (I_h + J_h)\delta.$$

$$N_r(t) = S_r(t) + I_r(t). \quad (3)$$

$N_r$(t) denotes the total population of rats at a given time:

$$\frac{dN_r(t)}{dt} = \frac{dS_r}{dt} + \frac{dI_r}{dt},$$
$$\frac{dN_r(t)}{dt} = \Lambda_r - \mu_r N_r(t).$$

## 3. Basic properties of the model

### 3.1. Positivity of solutions

Let the initial data be $\{S_h(0), E_h(0), I_h(0), J_h(0), R_h(0), S_r(0), I_r(0) \geq 0\} \in R_+^7$. Then the solution set $\{S_h(t), E_h(t), I_h(t), J_h(t), R_h(t), S_r(t), I_r(t)\}$ of the system (1.0) to (1.6) is positive for all t >0.

### 3.2. Feasibility of the model

The closed set $\Omega = \left\{(S_h, E_h, I_h, J_h, R_h, S_r, I_r) \in R_+^7 : N_h \leq \frac{\Lambda_h}{\mu_h}, N_r \leq \frac{\Lambda_r}{\mu_r}\right\}$ is positively Invariant and attracting with respect to the basic model (1).

## 4. The disease-free equilibrium (DFE)

The disease-free equilibrium (DFE) of a Lassa fever model is the steady state where there is no Lassa fever infection [3]. We denote the DFE by $E_0 = \{S_{h0}, E_{h0}, I_{h0}, J_{h0}, R_{h0}, S_{r0}, I_{r0}\}$. At the disease-free equilibrium,

$$\frac{dS_h}{dt} = \frac{dE_h}{dt} = \frac{dI_h}{dt} = \frac{dJ_h}{dt} = \frac{dT_h}{dt} = \frac{dS_r}{dt} = \frac{dI_r}{dt} = 0.$$

Thus, $E_0 = \{S_{h0}, E_{h0}, I_{h0}, J_{h0}, R_{h0}, S_{r0}, I_{r0}\} = \left\{\frac{\Lambda_h}{\mu_h}, 0,0,0,0, \frac{\Lambda_r}{\mu_r}, 0\right\}$ represents the state of the system (1) in which there is no infection.

## 5. The basic reproduction number

The basic reproduction number denoted by $R_0$ is the expected number of secondary Lassa fever infections produced in a completely susceptible population by a typical infective individual. It is one of the most useful threshold parameters in mathematical epidemiology [3].

If $R_0 < 1$, this implies that on average an infected individual produces less than one new infection during the infectious period and the disease dies out. Conversely, if $R_0 > 1$, then each infectious individual produces on average more than one new infection and disease spreads in the population [3]. For a single infected compartment, $R_0$ is simply the product of the infection rate and the mean duration of the infection. But for complicated models, this simple definition of $R_0$ is insufficient.

We therefore compute the basic reproduction number $R_0$ using the next generation method as follows [11]. For the model equations (1), the effective reproduction number (basic reproduction number with controls) is the spectra radius of the next generation matrix i.e., $R_C = \rho(FV^{-1})$ .

Our model has four Infective compartments namely the Exposed humans $E_h(t)$, infected humans $I_h(t)$, isolated humans $J_h(t)$ and infected rats $I_r(t)$. It follows that the associated matrices $F_i$ and $V_i$ for new infection in the infected compartments and the remaining transfer terms are given respectively by

$$F_i = \begin{pmatrix} \frac{(\beta_1 I_r + \beta_2 I_h)(1-\omega)S_h}{N_h} \\ 0 \\ 0 \\ \beta_1 S_r I_r \end{pmatrix},$$

$$V_i = \begin{pmatrix} (\alpha + \mu_h)E_h \\ -\alpha E_h + (\tau_1 + \tau_2 + \mu_h + \delta)I_h \\ -\tau_1 I_h + (\tau_3 + \mu_h + \delta)J_h \\ \mu_r I_r \end{pmatrix}.$$

Next, we evaluate F and V which are the Jacobean of $F_i$ and $V_i$ respectively at $E_0$ such that F is non-negative and V is a non-singular matrix.

Let $K_1 = (1-\omega)$ and $K_2 = \frac{\Lambda_r}{\mu_r}$, then,

$$F = \begin{pmatrix} 0 & \beta_2 K_1 & 0 & \beta_1 K_1 \\ 0 & 0 & 0 & 0 \\ 0 & 0 & 0 & 0 \\ 0 & 0 & 0 & \beta_1 K_2 \end{pmatrix}.$$

Let $a = (\alpha + \mu_h)$, $b = (\tau_1 + \tau_2 + \mu_h + \delta)$, $c = (\tau_3 + \mu_h + \delta)$, $d = \mu_r$, $e = \alpha$, $f = \tau_1$, then

$$\mathrm{V} = \begin{pmatrix} a & 0 & 0 & 0 \\ -e & b & 0 & 0 \\ 0 & -f & c & 0 \\ 0 & 0 & 0 & d \end{pmatrix},$$

$$FV^{-1} = \begin{pmatrix} \frac{\beta_2 K_1 e}{ab} & \frac{\beta_2 K_1}{b} & 0 & \frac{\beta_1 K_1}{d} \\ 0 & 0 & 0 & 0 \\ 0 & 0 & & 0 \\ 0 & 0 & 0 & \frac{\beta_1 K_2}{d} \end{pmatrix}.$$

We next compute $|FV^{-1} - \lambda I| = 0$ as follows

$$\begin{vmatrix} \frac{\beta_2 K_1 e}{ab} - \lambda & \frac{\beta_2 K_1}{b} & 0 & \frac{\beta_1 K_1}{d} \\ 0 & 0 - \lambda & 0 - \lambda & 0 \\ 0 & 0 & & 0 \\ 0 & 0 & 0 & \frac{\beta_1 K_2}{d} - \lambda \end{vmatrix} = 0 \tag{4}$$

From (4), we obtain the following characteristic equation

$$(\frac{\beta_2 K_1 e}{ab} - \lambda)(0 - \lambda)(0 - \lambda)\Big(\frac{\beta_1 K_2}{d} - \lambda\Big) = 0.$$

The Eigen values of (4) are $\lambda_1 = \frac{\beta_2 K_1 e}{ab}$, $\lambda_2 = \lambda_3 = 0$, $\lambda_4 = \frac{\beta_1 K_2}{d}$.

Let $R_h = \lambda_1 = \frac{\beta_2 K_1 e}{ab}$ and $R_r = \lambda_4 = \frac{\beta_1 K_2}{d}$

Then $R_h = \frac{\alpha\beta_2(1-\omega)}{(\alpha+\mu_h)(\tau_1+\tau_2+\mu_h+\delta)}$, (5)

and $R_r = \frac{\beta_1 \Lambda_r}{\mu_r^2}$. (6)

Thus, the effective reproduction number (basic reproduction number with controls) of our model is $R_c = Max\,(R_h, R_r)$.

When there are no controls $i.e.\ \omega = \tau_1 = \tau_2 = 0$, the basic reproduction number is

$R_h = \frac{\alpha\beta_2}{(\alpha+\mu_h)(\mu_h+\delta)}$. (7)

## 6. Stability of the disease-free equilibrium

**Theorem 6.1:** If the effective reproduction number $R_c < 1$ ,the model (1) is locally asymptotically stable at the disease-free equilibrium
$E_0 = \left\{\frac{\Lambda_h}{\mu_h}, 0,0,0,0,\frac{\Lambda_r}{\mu_r}, 0\right\}$ while $E_0$ is unstable otherwise.

Proof: To prove, we evaluate the Jacobian of the system (1) at the disease-free equilibrium and solve $|J(E_0) - \lambda I| = 0$ as follows:

$$\begin{vmatrix} -\mu_h - \lambda & 0 & -\beta_2(1-\omega) & 0 & \Phi & 0 & -\beta_1(1-\omega) \\ 0 & -(\alpha+\mu_h)-\lambda & \beta_2(1-\omega) & 0 & 0 & 0 & \beta_1(1-\omega) \\ 0 & \alpha & -(\tau_1+\tau_2+\mu_h+\delta)-\lambda & 0 & 0 & 0 & 0 \\ 0 & 0 & \tau_1 & -(\tau_3+\mu_h+\delta)-\lambda & 0 & 0 & 0 \\ 0 & 0 & \tau_2 & \tau_3 & -(\Phi+\mu_h)-\lambda & 0 & 0 \\ 0 & 0 & 0 & 0 & 0 & -\mu_r-\lambda & \frac{-\beta_1\Lambda_r}{\mu_r} \\ 0 & 0 & 0 & 0 & 0 & 0 & \frac{\beta_1\Lambda_r}{\mu_r}-\mu_r-\lambda \end{vmatrix} = 0 \quad (8)$$

Clearly, four eigenvalues of (8) are: $\lambda_1 = -\mu_h, \lambda_5 = -(\Phi + \mu_h)$ , $\lambda_6 = -\mu_r$ , and $\lambda_7 = \mu_r(R_r - 1)$. Clearly $\lambda_1 < 0, \lambda_5 < 0,\ \lambda_6 < 0\ and\ \ \lambda_7 < 0\ \ if\ \ R_r < 1$ .

The remaining matrix is given by

$$A = \begin{vmatrix} -a-\lambda & \beta_2 K_1 & 0 \\ e & -b-\lambda & 0 \\ 0 & f & -c-\lambda \end{vmatrix} = 0. \quad (9)$$

The characteristic polynomial is of (9) $A_0\lambda^3 + A_1\lambda^2 + A_2\lambda + A_3 = 0,$ where, $A_0 = 1,\ A_1 = a + b + c, A_2 = ab + ac + bc - e\beta_2 K_1 = ac + bc + ab(1 - R_h),$ and $A_3 = c(ab - e\beta_2 K_1) = abc(1 - R_h)$.

The Routh Hurwitz criterion as used in [1] and [18] will be employed to determine the nature of the roots, which states that all the roots of the polynomial will have negative real parts if and only if

$A_1 > 0,\ A_3 > 0$ and $A_1 A_2 > A_3$ .

Clearly that $A_1 > 0,\ \ A_3 > 0$ if $R_h < 1$ and $A_1 A_2 > A_3$ if $R_h < 1$. This completes the proof.

**Theorem 6.2**: The disease-free equilibrium is globally asymptotically stable if the effective reproduction number $R_c < 1$.

Proof: A comparison theorem as proposed by [10] and used in the works of [13] and [2] shall be used to prove the global stability of the disease-free equilibrium.
The rate of change of variables representing the infected components of the model equations (1) can be re-written as;

$$X' = (F - V)X - J_i X \tag{10}$$

where,

$$X = \begin{pmatrix} E_h \\ I_h \\ J_h \\ I_r \end{pmatrix} \quad , \qquad X' = \begin{pmatrix} E_h' \\ I_h' \\ J_h' \\ I_r' \end{pmatrix},$$

$$\mathrm{F} = \begin{pmatrix} 0 & \beta_2(1-\omega) & 0 & \beta_1(1-\omega) \\ 0 & 0 & 0 & 0 \\ 0 & 0 & 0 & 0 \\ 0 & 0 & 0 & \frac{\beta_1 \Lambda_r}{\mu_r} \end{pmatrix}$$

$$V = \begin{pmatrix} (\alpha + \mu_h) & 0 & 0 & 0 \\ -\alpha & (\tau_1 + \tau_2 + \mu_h + \delta) & 0 & 0 \\ 0 & -\tau_1 & (\tau_3 + \mu_h + \delta) & 0 \\ 0 & 0 & 0 & \mu_r \end{pmatrix}$$

$$J_i = \begin{pmatrix} 0 & \frac{\beta_2(1-\omega)S_h}{N_h} & 0 & \frac{\beta_1(1-\omega)S_h}{N_h} \\ 0 & 0 & 0 & 0 \\ 0 & 0 & 0 & 0 \\ 0 & 0 & 0 & \beta_1 S_r \end{pmatrix} = \left(1 - \frac{S_h}{N_h}\right) \begin{pmatrix} 0 & \beta_2(1-\omega) & 0 & \beta_2(1-\omega) \\ 0 & 0 & 0 & 0 \\ 0 & 0 & 0 & 0 \\ 0 & 0 & 0 & Q\beta_1 \end{pmatrix}, \text{ where}$$

$$Q = \frac{\left(1 - \frac{S_r}{N_r}\right)}{\left(1 - \frac{S_h}{N_h}\right)}.$$

$J_i$ is a non-negative matrix since $S_h(t) \leq N_h(t) \leq \frac{\Lambda_h}{\mu_h}$, $S_r(t) \leq N_r(t) \leq \frac{\Lambda_r}{\mu_r}$ in the invariant set, it follows that

$$X' \leq (F - V)X \tag{11}$$

$$F - V = \begin{pmatrix} -(\alpha + \mu_h) & \beta_2(1-\omega) & 0 & \beta_1(1-\omega) \\ \alpha & -(\tau_1 + \tau_2 + \mu_h + \delta) & 0 & 0 \\ 0 & \tau_1 & -(\tau_3 + \mu_h + \delta) & 0 \\ 0 & 0 & 0 & \frac{\beta_1 \wedge_r}{\mu_r} - \mu_r \end{pmatrix}.$$

All the eigen values of the matrix $(F - V)$ have negative real part whenever $R_c < 1$. See proof of local stability. It follows that the linearized differential in equality (11) is stable whenever $R_c < 1$. Consequently, by comparison theorem we have that $(E_h, I_h, J_h, I_r) \rightarrow$ (0,0,0,0) as t$\rightarrow \infty$ . Substituting, $E_h = I_h = J_h = I_r = 0$ into (2) and (3) we have that $N_h(0) \rightarrow S_{h0}$ as t$\rightarrow \infty$ . Similarly, $N_r(0) \rightarrow S_{r0}$ as t$\rightarrow \infty$ . Hence, we have a positive invariant region. It follows that disease free equilibrium is globally asymptotically stable whenever $R_c < 1$.

## 7. Sensitivity analysis

Sensitivity analysis is used to determine how "sensitive" a model is to changes in the value of the parameters of the model and to changes in the structure of the model. If the result is negative, then the relationship between the parameters and $R_c$ is inversely proportional. In this case, we will take the modulus of the sensitivity index so that we can deduce the size of the effect of changing that parameter. On the other hand, a positive sensitivity index means $R_c$ varies directly with the parameter [17]. Thus, we use it to discover parameters that have a high impact on $R_c$ and should be targeted by intervention strategies [12, 17]. The sensitivity indices of the respective parameters are derived using the normalized sensitivity index $S_\tau^{R_c}$ defined as $S_\tau^{R_c} = \frac{\partial R_c}{\partial \tau} . \frac{\tau}{R_c}$ [9].

| Parameter | Description | Value | Source | Sensitivity index |
|---|---|---|---|---|
| $\mu_r$ | Recruitment rate of rodents | 0.0038 | Mohammed (2015) | -2 |
| $\wedge_r$ | Recruitment rate of humans | 0.0250 | Mohammed (2015) | +1 |
| $\beta_1$ | Contact rate of humans | 0.8000 | Mohammed (2015) | +1 |
| $\beta_2$ | Contact rate of rodents | 0.2000 | Adewale (2016) | +1 |
| $\omega$ | Rate of public health education | 0.5000 | Assumed | -1 |
| $\mu_h$ | Natural death rate of humans | 0.0200 | CIA (2015) | -0.9172 |
| $\alpha$ | Rate of progression from exposed to infectious state | 0.3000 | Assumed | 0.8696 |
| $\tau_1$ | Isolation rate | 0.2000 | Adewale (2016) | -0.4759 |
| $\tau_2$ | Treatment rate | 0.1000 | Adewale (2016) | -0.4759 |
| $\delta$ | Lassa fever induced death rate | 0.0003 | Mohammed (2015) | -0.0007 |

**Table 2:** Parameters, description, values, sources and sensitivity indices

## 8. The endemic equilibrium

In the presence of Lassa fever infection, the model equations (1) have a non-trivial equilibrium called the endemic equilibrium $E^*(S_h^*, E_h^*, I_h^*, J_h^*, R_h^*, S_r^*, I_r^*)$ where:

$$S_h^* = \frac{\Lambda_h}{\left[1-\frac{\Phi\alpha\tau_2[(\tau_3+\mu_h+\delta)+\tau_1](1-\omega)\lambda^*}{(\alpha+\mu_h)(\tau_1+\tau_2+\mu_h+\delta)(\tau_3+\mu_h+\delta)(\Phi+\mu_h)}\right]+\mu_h} \quad ,$$

$$E_h^* = \frac{(1-\omega)\Lambda_h\lambda^*}{\left\{\left[1-\frac{\Phi\alpha\tau_2[(\tau_3+\mu_h+\delta)+\tau_1](1-\omega)\lambda^*}{(\alpha+\mu_h)(\tau_1+\tau_2+\mu_h+\delta)(\tau_3+\mu_h+\delta)(\Phi+\mu_h)}\right]+\mu_h\right\}(\alpha+\mu_h)} ,$$

$$I_h^* = \frac{\alpha(1-\omega)\Lambda_h\lambda^*}{\left\{\left[1-\frac{\Phi\alpha\tau_2[(\tau_3+\mu_h+\delta)+\tau_1](1-\omega)\lambda^*}{(\alpha+\mu_h)(\tau_1+\tau_2+\mu_h+\delta)(\tau_3+\mu_h+\delta)(\Phi+\mu_h)}\right]+\mu_h\right\}(\alpha+\mu_h)(\tau_1+\tau_2+\mu_h+\delta)} ,$$

$$J_h^* = \frac{\tau_1\alpha(1-\omega)\Lambda_h\lambda^*}{\left\{\left[1-\frac{\Phi\alpha\tau_2[(\tau_3+\mu_h+\delta)+\tau_1](1-\omega)\lambda^*}{(\alpha+\mu_h)(\tau_1+\tau_2+\mu_h+\delta)(\tau_3+\mu_h+\delta)(\Phi+\mu_h)}\right]+\mu_h\right\}(\alpha+\mu_h)(\tau_1+\tau_2+\mu_h+\delta)(\tau_3+\mu_h+\delta)} \quad ,$$

$$S_r^* = \frac{\mu_r}{\beta_1}, \quad I_r^* = \frac{\mu_r}{\beta_1}(R_r - 1) ,$$

$$R_h^* = \frac{\Phi\tau_2\alpha[(\tau_3+\mu_h+\delta)+\tau_1]\Lambda_h\lambda^*}{\left\{\left[1-\frac{\Phi\alpha\tau_2[(\tau_3+\mu_h+\delta)+\tau_1](1-\omega)\lambda^*}{(\alpha+\mu_h)(\tau_1+\tau_2+\mu_h+\delta)(\tau_3+\mu_h+\delta)(\Phi+\mu_h)}\right]+\mu_h\right\}(\alpha+\mu_h)(\tau_1+\tau_2+\mu_h+\delta)(\tau_3+\mu_h+\delta)(\Phi+\mu_h)},$$

$$\lambda^* = \frac{(\beta_1 I_r+\beta_2 I_h)}{N_h}.$$

The endemic equilibrium satisfies the equation

$f(\lambda^*) = A\lambda^{*2} + B\lambda^* + C = 0$ , $\lambda^* = \frac{-B\pm\sqrt{B^2-4AC}}{2A}$ , where

$A = \beta_1[\mu_r\Lambda_h(\Phi+\mu_h)(\tau_3+\mu_h+\delta)(\tau_1+\tau_2+\mu_h+\delta) + \mu_r\Lambda_h\alpha(\Phi+\mu_h)(\tau_3+\mu_h+\delta) + \Lambda_h\tau_1\alpha(\Phi+\mu_h) + \mu_r\Lambda_h\tau_1\tau_2\alpha + \beta_1\Lambda_r\Phi\tau_1\tau_2\alpha]$

$$B = \Lambda_h(\alpha+\mu_h)(\tau_1+\tau_2+\mu_h+\delta)(\tau_3+\mu_h+\delta)(\Phi+\mu_h)\left[(1-R_h)+(1-R_r)\frac{\beta_1(1-\omega)}{\Lambda_h}\frac{\mu_r}{\beta_1}\left\{\frac{\tau_2\Phi[(\tau_3+\mu_h+\delta)+\tau_1]}{(\alpha+\mu_h)(\tau_1+\tau_2+\mu_h+\delta)(\tau_3+\mu_h+\delta)(\Phi+\mu_h)}-1\right\}\right],$$

$$C = -\left[\frac{\mu_r}{\beta_1}(R_r-1)\beta_1(\Phi+\mu_h)(\tau_3+\mu_h+\delta)(\tau_1+\tau_2+\mu_h+\delta)(\Phi+\mu_h)\right].$$

In the case of backward bifurcation, multiple endemic equilibrium points must exist. Since all parameter values are positive and between 0 and 1, and A is positive. There are three cases we have to consider of $f(\lambda^*) = 0$ depending on the sign of B and C.

Case 1: $C < 0 \Rightarrow R_r > 1,$ there exists a unique positive root.
Case 2: $B < 0$, and $C = 0 \Leftrightarrow B^2 - 4AC = 0$ , there exists a unique positive root.
Case 3: $B < 0, C > 0,\ B^2 - 4AC > 0$, there exist two positive roots.

From case 1 to case 3, we establish the following theorem.

**Theorem 8.1**: The Lassa fever model has:
precisely one endemic equilibrium if $C < 0$ and $R_r > 1$ and no backward bifurcation;
precisely one endemic equilibrium if $B < 0,\ C = 0$ and $B^2 - 4AC = 0$ and no backward bifurcation;
two endemic equilibria if $B < 0,\ C > 0$ and $B^2 - 4AC > 0$ and it is possible for backward bifurcation;
otherwise, there is none.

## 8.1. Local stability of the endemic equilibrium

We will investigate the local stability of the endemic equilibrium using center manifold theorem. We make the following change of variables to apply the theorem:

$$S_h = x_1, E_h = x_2, I_h = x_3, J_h = x_4, R_h = x_5, S_r = x_6, I_r = x_7.$$

We now use the vector $X = (x_1, x_2, x_3, x_4, x_5, x_6, x_7)^T$, then, the model equations (1) can be written in the form $\frac{dx}{dt} = F = (f_1, f_2, f_3, f_4, f_5, f_6, f_7)^T$ giving

$$\begin{aligned}
\frac{dx_1}{dt} &= \Lambda_h + \Phi x_5 - \frac{(\beta_1 x_7 + \beta_2 x_3)(1-\omega)x_1}{N_h} - \mu_h x_1 \\
\frac{dx_2}{dt} &= \frac{(\beta_1 x_7 + \beta_2 x_3)(1-\omega)x_1}{N_h} - (\alpha + \mu_h)x_2 \\
\frac{dx_3}{dt} &= \alpha x_2 - (\tau_1 + \tau_2 + \mu_h + \delta +)x_3 \\
\frac{dx_4}{dt} &= \tau_1 x_3 - (\tau_3 + \mu_h + \delta)x_4 \\
\frac{dx_5}{dt} &= \tau_2 x_3 + \tau_3 x_4 - (\Phi + \mu_h)x_5 \\
\frac{dx_6}{dt} &= \Lambda_r - \beta_1 x_6 x_7 - \mu_r x_6 \\
\frac{dx_7}{dt} &= \beta_1 x_6 x_7 - \mu_r x_7
\end{aligned} \tag{12}$$

Taking $\beta_2 = \beta^*$ as our bifurcation constant and solving for $\beta^*$ when $R_h = 1$ gives

$$\beta^* = \frac{(\alpha + \mu_h)(\tau_1 + \tau_2 + \mu_h + \delta)}{\alpha(1-\omega)}.$$

The Jacobian of the system (12) when $\beta_2 = \beta^*$ and $R_h = 1$ at the DFE is given by

$$J(E_0) = \begin{vmatrix} -\mu_h & 0 & -\beta_2(1-\omega) & 0 & \Phi & 0 & -\beta_1(1-\omega) \\ 0 & -(\alpha+\mu_h) & \beta_2(1-\omega) & 0 & 0 & 0 & \beta_1(1-\omega) \\ 0 & \alpha & -(\tau_1+\tau_2+\mu_h+\delta) & 0 & 0 & 0 & 0 \\ 0 & 0 & \tau_1 & -(\tau_3+\mu_h+\delta) & 0 & 0 & 0 \\ 0 & 0 & \tau_2 & \tau_3 & -(\Phi+\mu_h) & 0 & 0 \\ 0 & 0 & 0 & 0 & 0 & -\mu_r & \frac{-\beta_1\Lambda_r}{\mu_r} \\ 0 & 0 & 0 & 0 & 0 & 0 & \frac{\beta_1\Lambda_r}{\mu_r} - \mu_r \end{vmatrix} \quad (13)$$

Let $V = (v_1, v_2, v_3, v_4, v_5, v_6, v_7)$ be the left and eigen vector of (13), then,

$$v_1 = 0, v_2 = v_2 > 0(free), v_3 = \left[\frac{(\alpha+\mu_h)-\beta^*(1-\omega)}{\alpha-(\tau_1+\tau_2+\mu_h+\delta)}\right] v_2 \, , v_4 = 0 \, , v_5 = 0,$$
$$v_6 = 0 \, , \quad v_7 = \frac{\beta_1(1-\omega)v_2}{\left(\mu_r - \frac{\beta_1\Lambda_r}{\mu_r}\right)}.$$

Also, if $W = (w_1, w_2, w_3, w_4, w_5, w_6, w_7)^T$ is the right eigen vector of (13), then,

$$w_1 = \left[\frac{\Phi\tau_1\tau_2}{\mu_h(\tau_3+\mu_h+\delta)(\Phi+\mu_h)} - \frac{\beta^*(1-\omega)}{\mu_h}\right] w_3 \, , \; w_2 = \left[\frac{\beta^*(1-\omega)}{\mu_h} - \frac{(\tau_1+\tau_2+\mu_h+\delta)}{\mu_h}\right] w_3,$$
$$w_3 = w_3 > 0(free) \, , \; w_4 = \frac{\tau_1 w_3}{(\tau_2+\mu_h+\delta)} \, , w_5 = \frac{[\tau_3(\tau_3+\mu_h+\delta)+\tau_1\tau_3]w_3}{(\tau_3+\mu_h+\delta)(\Phi+\mu_h)} \, , w_6 = 0 \, , w_7 = 0.$$

After computing the right and left eigenvectors we have the theorem in [4] to establish the conditions for the existence of backward and forward bifurcation by determining the sign of a and b as indicated in the theorem which is restated as Theorem 8.2 in this work.

**Theorem 8.2**: Consider the following general system of ordinary differential equations with a parameter $\beta^*$.

$$\frac{dx}{dt} = f(x, \beta^*), f: R^n \times R^n \to R^n \; and \; f \epsilon C^2(R^n \times R^n), \quad (14)$$

where 0 is an equilibrium point of the system, that is $f(0, \beta^*) \equiv 0 \; \forall \; \beta^*$ and $A = D_x f(0,0) = \left[\frac{\partial f_i}{\partial x_i}(0,0)\right]$ is linearization matrix of the system evaluated around 0 and with $\beta^*$ evaluated at 0.

Zero is a simple eigen value of A and other eigen values of A have negative real parts.
Matrix A has a right eigen vector W and a left eigen vector V corresponding to the zero eigen value.
Let $f_k$ be the $kth$ component of $f$ and $a = \sum_{k,i,j=1}^{n} v_k w_i w_j \frac{\partial^2 f_k}{\partial x_i \partial x_j}(0,0)$ ,

$b = \sum_{k,i=1}^{n} v_k w_i \frac{\partial^2 f_k}{\partial x_i \beta^*}(0,0)$ .

The local dynamics of (14) around 0 are completely governed by the signs of a and b.
a > 0, b > 0. When $\beta^* < 0$ with $|\beta^*| << 1$, 0 is locally asymptotically stable, and there exists a positive unstable equilibrium; when $0 < \beta^* << 1$, 0 is unstable and there exists a negative and locally asymptotically stable equilibrium.
a < 0, b < 0. When $\beta^* < 0$ with $|\beta^*| << 1$, 0 is unstable; when $0 < \beta^* << 1$, 0 is locally asymptotically stable, and there exists a positive unstable equilibrium.

(iii) a > 0, b < 0. When $\beta^* < 0$ with $|\beta^*| << 1$, 0 is unstable, and there exists a locally asymptotically stable negative equilibrium; when $0 < \beta^* << 1$, 0 is stable, and a positive unstable equilibrium appears.

(iv) a < 0, b > 0. When $\beta^*$ changes from negative to positive, 0 changes its stability from stable to unstable. The corresponding negative unstable equilibrium becomes positive and locally asymptotically stable.
Particularly if a>0, b>0, then a backward bifurcation occurs while when a<0, b>0, there is forward bifurcation.

**Computation of a and b**

Since $v_1 = v_6 = 0$ for $k = 1$ and 6, we consider only $k = 2,3,4,5,7$. The only non-zero second order partial derivatives are: $\frac{\partial^2 f_2(0,0)}{\partial x_1 \partial x_3} = \frac{\beta^*(1-\omega)}{N_h}$, $\frac{\partial^2 f_2(0,0)}{\partial x_1 \partial x_7} = \frac{\beta_1(1-\omega)}{N_h}$

$a = \left[\frac{\Phi\tau_1\tau_3}{\mu_h(\tau_3+\mu_h+\delta)(\Phi+\mu_h)} - \frac{\beta^*(1-\omega)}{N_h\mu_h}\right]\frac{\beta^*(1-\omega)}{N_h} w_3^2 v_2$

Let $p = \frac{\Phi\tau_1\tau_3}{\mu_h(\tau_3+\mu_h+\delta)(\Phi+\mu_h)}$ and $q = \frac{\beta^*(1-\omega)}{N_h\mu_h}$,

$$a = (p-q)\frac{\beta^*(1-\omega)}{N_h} w_3^2 v_2 \ . \tag{15}$$

Similarly, the only non –zero second order partial derivative when calculating b is
$\frac{\partial^2 f_2(0,0)}{\partial x_3 \partial \beta^*} = \frac{(1-\omega)}{N_h}$ , $b = v_2 w_3 \frac{\partial^2 f_2(0,0)}{\partial x_3 \partial \beta^*}$, $b = v_2 w_3 \frac{(1-\omega)}{N_h} > 0$ .

The sign of *a* in (15) depends on the sign of (p-q), if $p < q$, then $a < 0$, but if $p > q$, then $a > 0$. Thus we have established the following theorem.

**Theorem 8.3:** (i) If $p < q$,when $\beta^*$ changes from negative to positive, the disease-free equilibrium changes its stability from stable to unstable. Correspondently, the negative unstable endemic equilibrium becomes positive and locally asymptotically stable when $R_c > 1$.
(ii) If $p > q$, when $\beta^* < 0$ with $|\beta^*| \ll 1$, the disease-free equilibrium is locally asymptotically stable and there exists a positive unstable endemic equilibrium; when $0 < \beta^* \ll 1$, the disease-free equilibrium is unstable and there exists a negative and locally asymptotically stable endemic equilibrium.

## 9. Numerical Simulations

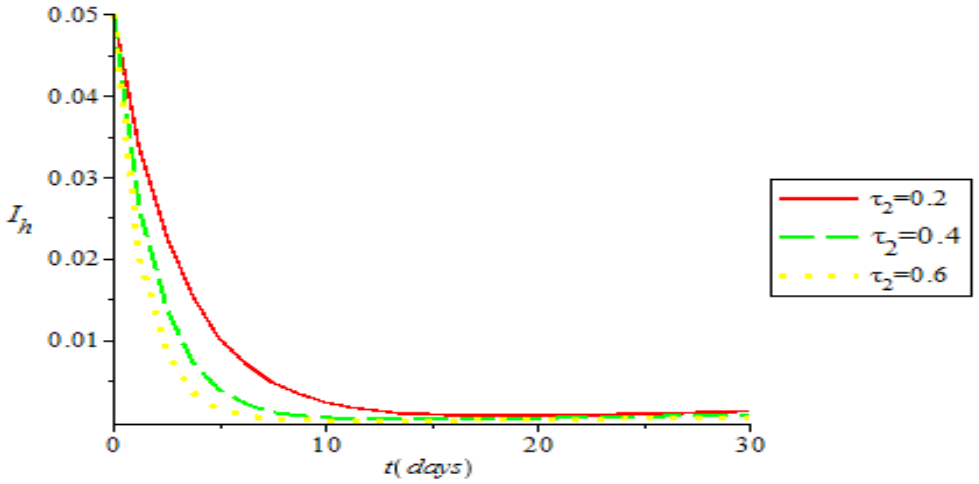


**Figure 2:** A graph of infectious individuals against time with varying treatment rate.

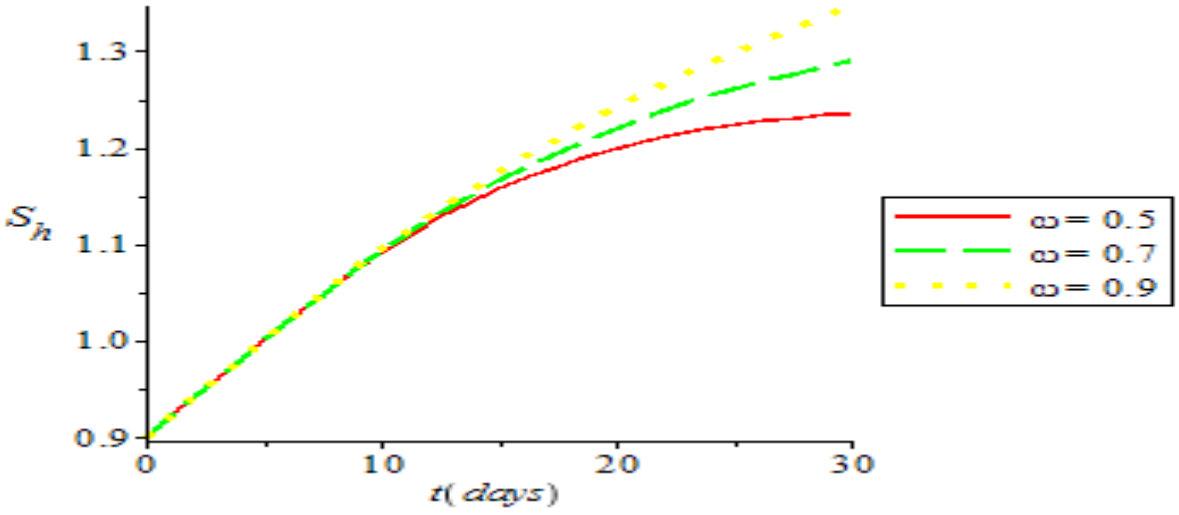


**Figure 3:** A graph of susceptible individuals against time with varying rate of public health education

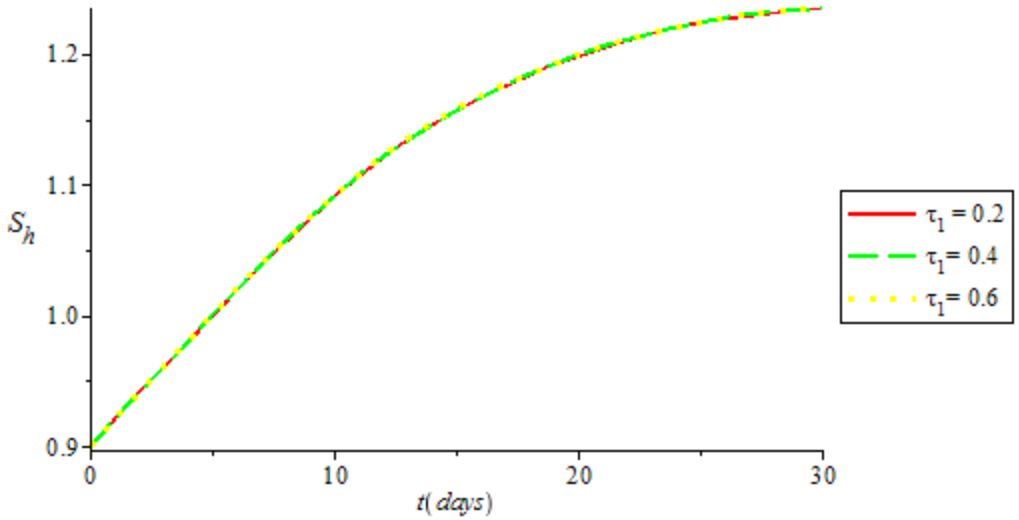


**Figure 4:** A graph of susceptible individuals against time with varying isolation rate

## 10. Discussion of results

In Figure 2, we observed the progression of the infectious human population $I_h(t)$ with time in the presence of varying treatment rate $\tau_2$. The infectious human population decreases for all treatment rate. We observe that the infectious human population decreases faster as treatment rate increases. At $\tau_2 = 0.2$ and 0.4, as shown in figure 1, the infectious human population takes 15 to 20 days to attain its minimum while it takes 10 days to attain its minimum at $\tau_2 = 0.6$. This agrees with reality because the more the infectious population is being treated, the lesser it becomes.

Figure 3 shows the progression in susceptible human population $S_h(t)$ with time in the presence of varying public health education campaign rate $\omega$. It is observed that the number of susceptible individuals increases with time for all values of $\omega$ . We further observed that increased public health enlightenment reduces the rate at which the susceptible population is being invaded by the disease. When public health enlightenment $\omega$ is 0.5 and 0.7, the susceptible population $S_h(t)$ is less than when $\omega$ is 0.9. This agrees with reality because an increased public health education campaign will keep people aware of the dangers of the disease, its mode of transmission and preventive strategies there by reducing the infection rate.

In Figure 4, we studied the progression of the Susceptible human population $S_h(t)$ with time in the presence of varying isolation rate $\tau_1$. The susceptible population increases for all isolation rates. This is also in line with reality, because as infectious individuals are being isolated from the susceptible ones, the infection rate reduces there by leading to an increase in the susceptible population.

## 11. Conclusion

In this work, a deterministic model has been formulated to study the transmission dynamics of Lassa fever disease. The model incorporates three control parameters, isolation $\tau_1$ , treatment $\tau_2$and public health education campaign $\omega$. We obtained an important threshold parameter called the effective reproduction number $R_c$. It is known that when $R_c < 1$ the disease dies out, and when $R_c > 1$ the disease persists in the population.

Because we are interested in control, we carried out a sensitivity analysis of the effective reproduction number, which shows that the most sensitive parameter to the effective reproduction number $R_c$ is the natural death rate of rodents $\mu_r$ followed by the human contact rate $\beta_2$, rodents contact rate $\beta_1$, recruitment level of rodents $\Lambda_r$ and the rate of public health education campaign $\omega$ while the least sensitive parameter is the Lassa fever induced death rate $\delta$. We conducted numerical simulation and results shows that isolation, treatment and public health education can reduce the number of infections.

## References

[1] Andam E. A. (2013). Analysis of transmission dynamics of tuberculosis (tb) using differential equations. a case study of Amansie West District of Ghana. M.Sc. Thesis. Department of Mathematics, Nkwam Nkrumah University of Science and Technology, pp. 90.

[2] Adewale S. O., Olopade I. A., Ajao S. O., Adeniran G. A., and Oyedemi O. T. (2016). Mathematical analysis of Lassa fever model with isolation. Asian Journal of Applied and Natural Sciences, 5 (3): 47-57.

[3] Benyah F. (2009). Mathematical models of infectious disease. A seminar paper presented at the 11th regional College on Modeling, Simulation, and Optimization, University of Cape Coast Ghana.32pp.

[4] Castillo-Chavez C. and Song B. (2004). Dynamical models of tuberculosis and their application. Mathematical Bioscience and Engineering, 1 (2): 361-404.

[5] CDC (2015). Lassa Fever. Retrieved from https://www.cdc.gov/vhf/lassa/outbreaks/index.html. (September 9, 2017).

[6] CIA (2015). World Fact Book for the Year 2014.Retrieved from http:/www.cia/library/publication/the-wworld factbook/geos/ni.htm. (July 18, 2017).

[7] CNN (2016). Lassa Fever Death Rates in Nigeria Higher than Expected Retrieved from edition.cnn /2016//03/17/ health/lassa-fever-outbreak/inde x.html. (September 9, 2017).

[8] James T. O., Abdulrahman S., Akinyemi S., and Akinwande N. I. (2015). Dynamics transmission of Lassa fever disease. International Journal of Innovation and Research in Education Sciences, 2 (1): 2349–5219.

[9] Josephine E. A. (2009). The basic reproduction number: bifurcation and stability. Postgraduate Diploma Thesis. African Institute for Mathematical Sciences.41pp.

[10] Lakshmikantham V. and Mitropolskii Y. A. (2006). Nonlinear dynamics and systems theory. Informath Publishing Group, 6 (1): 1–15.

[11] Lungu E. M., Kgosimore F., and Nyabadza M. (2007). Mathematical epidemiology. Lecture Note, Department of Mathematics, University of Botswana.72pp. Retrieved from http://ms.mcmaster.ca/earn/paper/pdf/Earn20 08lig ht. Pdf. (March 31, 2018).

[12] Mohammed B. A., Umar C. D., and Mamman M. (2015). Sensitivity analysis in a Lassa fever model. American Institute of Physics (AIP)Conference Proceedings. Retrieved from http://dx.doi.org/10.1063/1.491\5683. (July 18, 2017).

[13] Mudassar I., Muhammad H., Muhammad D., and Adnan K. (2013). A comparison of a deterministic and stochastic model for hepatitis c with an isolation stage. Biological Dynamics, 7(1) : 276-301.

[14] Ogabi C. O., Olusa T. V., and Madufor M.A. (2012). Controlling Lassa fever transmission in northern part of Edo State, Nigeria Using Sir Model. New York Science *J*ournal, 5 (12): 190-197.

[15] Onuorah M. O., Akinwande N. I., Nasir M. O., and Ojo M. S. (2016). Sensitivity analysis of Lassa fever model. International Journal of Mathematics and Statistics Studies, 4 (1): 30 – 49.

[16] PAMJ (2016). Outbreak of Lassa fever in Nigeria: measures for prevention and control. Retrieved from https://www.ncbi.nlm.nih.gov/pmc/articles/PMC 490 77 47/ . (June 4, 2017).

[17] Stephen E. and Nkuba N. (2015). A mathematical Model for the dynamics of Cholera with control measures. Applied and computational mathematics, 4(2):43-53.

[18] Tahir K., Gul Z., and Chohan I. M. (2017). The transmission dynamic and optimal control of acute and chronic hepatitis B. Biological Dynamics, 11(1) : 172 -189.

[19] WHO (2016). Lassa Fever. Retrieve from www.who.int/csr/disea se/Lassa fever /en/. (April 18, 2017)

[20] WHO (2017). Lassa Fever. Retrieved from www.afro.who.int/health-topics/las sa-fever. (February 8, 2018).

**International Journal of Mathematical Analysis and Modelling**
**Volume 5, Issue 1, May 2022, Pages 36 – 55**

# Application of open network queuing model in a banking system to reduce waiting time of customers

**E. Jocob[*], L. Adamu[*†], E. N. Didigwu[‡], A. Abdullahi[§], and S. D. Yakubu[**]**

**Abstract**

The need to use scientific techniques to determine optimal number of banking personnel (Servers) at different units of a banking system is the thrust of this work. In this paper, a network queuing model that determines optimal numbers of servers at different nodes of First City Monument Bank Minna Branch to reduce waiting time is presented. The relevant data were collected for a period of four (4) weeks, through direct observations and personal interview. The total expected waiting time of customers in the current system before modification was 52 minutes with total number of 11 servers in the system while the total new expected waiting time of the customers in the system after modification was reduced to 11 minutes with optimal number of 17 servers (personnel) in all the nodes. The study has determined optimal number of servers (personnel) at different nodes of the bank network system. Result from this study is important information to the management of the First City Monument Bank, Minna branch for efficient and better service delivery.

***Keywords***: FCMB; nodes; servers; customers; waiting time; network of queue.

## 1. Introduction

A Common situation that occurs in everyday life is that of queuing or waiting in line, when the demand for a service exceeds the capacity of the service, waiting is unsurprising and inevitable [14]. Queues or waiting lines are usually seen at hospitals, bus stops, supermarkets, traffic, airports, gas stations, bank counters and so on. Service delay is unavoidable as a system gets blocked [13]. When too much service is been provided, it's involves excessive cost and not providing enough service capacity causes the waiting line to become excessively long. The ultimate goal is to achieve an economic balance between the cost of service and the cost associated with the waiting for that service. Queuing systems theories have been used to study waiting time and predict the efficiency of services to be provided. In queuing theory, there are three basic components of a queuing process which are: - Arrivals patterns, the actual waiting line and service facilities. Customers arrive to the facility from an infinite calling population, with a random arrival pattern following

[*] Department of Mathematics, Federal University of Technology, Minna, Nigeria
[†] Corresponding Author; lawal.adamu@futminna.edu.ng
[‡] Department of Mathematics, Enugu State University of Science and Technology, Enugu, Nigeria
[§] Department of Mathematics, Faculty of Science, Air Force Institute of Technology, Kaduna, Nigeria
[**] Department of Mathematical Science, Ibrahim Badamasi Babagida University, Lapai, Nigeria

poison process. Once customers arrive, they are served immediately if the server(s) is empty, or otherwise the customers wait in the queue for the next empty server. Mostly, the service is on a first come first serve (FCFS) basis although other methods like service at random order (SARO) can be used. Preference service depending on the level of risk, urgency or the social, economic or political standing of the customers and hold on line (HL) discipline, where important arriving customer takes the lead of the queue is rampant in many facilities. Customers who may feel to have waited for long in queue can balk or renege and seek alternative equivalent services elsewhere, however, the queue length and waiting time depends on the traffic intensity, which is the ratio of arrival and service rates. The service discipline follows an exponential pattern, with individual service time variation due to different nature of the problems to be handled [19]. Successful application of queuing models has been reported in the following works: ([1], [3], [11], [16]).

## 2. Materials and methods

The type of queuing system adopted by an organization solely dependent on the type of service being provided [11]. First City Monument Bank practice network type of queuing system. Queuing network is composed of several random queue systems, mostly limited and single queue systems. Diverse types of customers go by through the network in many ways and are served by the service nodes within the network system. A queuing network system has a set of nodes ($i$). Each node has a number of servers ($s$) and a single node can be regarded as a queuing system. customers can have access to the queuing network from any node. The arrival rate from the outside is $\lambda$ and the arrival rate of Node $i$ is $\lambda_i$. After the customer queues and gets the service at a node (the service rate of Node $i$ is $\mu_i$), he /she can leave the network system or go to another node, or even return to the former node [11].

### 2.1. Model formulation

The First City Monument Bank Minna branch consists of five main units, they are the Meter Greeter Unit, Customers Service Unit, Marketing Unit, Tellers Unit, and Customers Service Manager Unit. In this study, each department is regarded as a node of the network system. The data used in this research were collected from the five different departments of the Bank and they were collected based on the arrival and departure rate as well as time spent at each node. The method adopted for the data collection was direct observation and personal interview, for a period of one month. The collection of the data was for a total of six (6) hours at different time of the day, for each node. In a day, the number of arrivals and departures together with service time were taken at intervals of 5 minutes arrivals of customers into a node ($\lambda$), while the departure rate was obtained also by the average number of five (5) minutes departures of customers at that particular node.

### 2.2. Model Assumptions

The following are the model assumptions made for Network Queuing System of the First City Monument Bank (FCMB), Minna Branch.

i. The First City Monument Bank in the network queuing system is considered as an independent queuing system.
ii. Queuing discipline is usually first come first served in the bank.
iii. The arrival of the customers in the bank follows a Poisson arrival process.
iv. The service follows exponential distribution

v. The way customers enter the bank is not restricted.
vi. The banking personnel are regarded as servers
vii. All the banking personnel in the bank are working in full capacity
viii. Service rate is independent of line length.

We consider a banking network queuing system based on Jackson open network queuing model, the First City Monument Bank, Minna constitutes of five units. In this study, we assumed that customers who come in to bank for services will start by going first to the meter greeter unit and then move to the customer's service unit, then some customers proceed to tellers unit or customers service manager until all customers depart from the bank as captured by Figure 1 below,

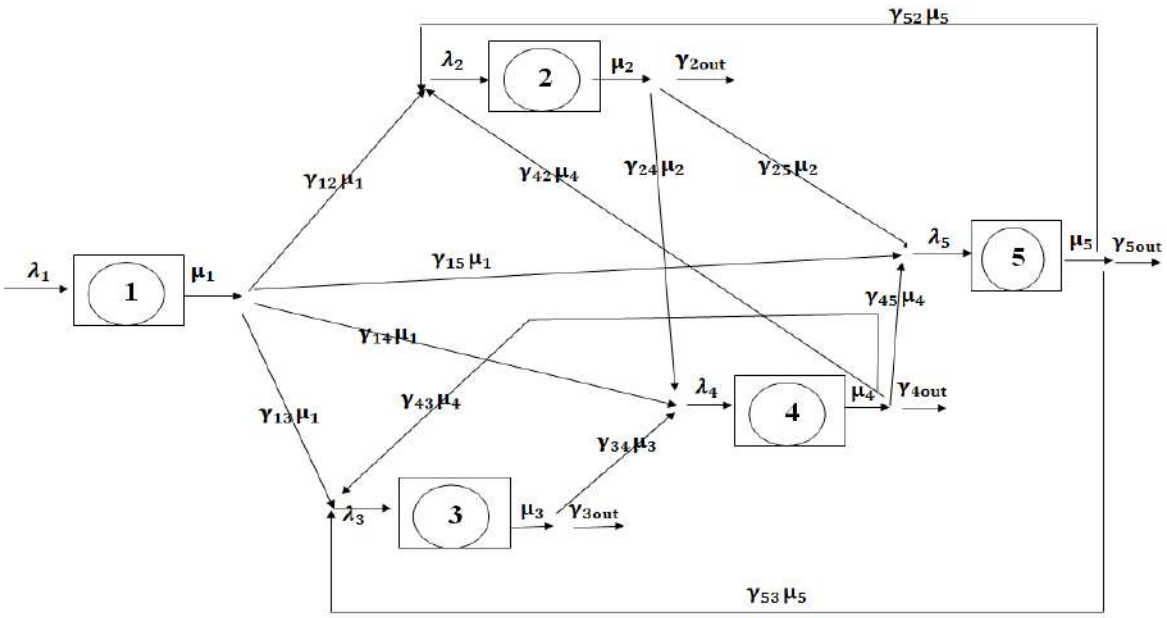


Figure 1 A Schematic diagram of the Bank (FCMB) Queuing Network

where: $\lambda_i$ Is the arrival rate of the customer, for i = 1, 2,...5,

$\mu_i$ Is the departure rate out of the system, for i = 1, 2,…5,

$\gamma_{ij}$ Are the weights of moving from server i to server j,

$m_i$ for i= 1…,5, is the number servers at the various node points in the system.

The following are the nodes in the network queuing system of the bank where Node1, Node2, Node3, Node4, Node5 are defined as follow: Meter Greeter Unit denoted by node1; Customer Service Unit denoted by node2; Marketing Unit denoted by node3; Tellers Unit denoted by node4; Customer Service Manager Unit denoted by node5.

From Figure1, we obtained the following equations

$$\lambda_2 = \gamma_{12}\mu_1 + \gamma_{42}\mu_4 + \gamma_{52}\mu_5\,, \tag{1}$$

$$\lambda_3 = \gamma_{13}\mu_1 + \gamma_{43}\mu_4 + \gamma_{53}\mu_5, \tag{2}$$

$$\lambda_4 = \gamma_{14}\mu_1 + \gamma_{24}\mu_2 + \gamma_{34}\mu_3, \tag{3}$$

$$\lambda_5 = \gamma_{15}\mu_1 + \gamma_{25}\mu_2 + \gamma_{45}\mu_4. \tag{4}$$

Also,

$$\mu_1 = \gamma_{12}\mu_1 + \gamma_{13}\mu_1 + \gamma_{14}\mu_1 + \gamma_{15}\mu_1, \tag{5}$$

$$\mu_2 = \gamma_{24}\mu_2 + \gamma_{25}\mu_2 + \gamma_{2out}\mu_2, \tag{6}$$

$$\mu_3 = \gamma_{34}\mu_3 + \gamma_{3out}\mu_3, \tag{7}$$

$$\mu_4 = \gamma_{42}\mu_4 + \gamma_{43}\mu_4 + \gamma_{45}\mu_4 + \gamma_{4out}\mu_4, \tag{8}$$

$$\mu_5 = \gamma_{52}\mu_5 + \gamma_{53}\mu_5 + \gamma_{5out}\mu_5, \tag{9}$$

where,
$\gamma_{12}, \gamma_{13}, \gamma_{14}, \gamma_{15}, \gamma_{24}, \gamma_{25}, \gamma_{2out}, \gamma_{34}, \gamma_{3out}, \gamma_{42}, \gamma_{43}, \gamma_{45}, \gamma_{4out}, \gamma_{52}, \gamma_{53}, \gamma_{5out}$
are to be determined.

Equation (1 – 9) can also be represented in the following forms, thus:

$$\begin{aligned}\lambda_2 = {} & \mu_1\gamma_{12} + 0\gamma_{13} + 0\gamma_{14} + 0\gamma_{15} + 0\gamma_{24} + 0\gamma_{25} + 0\gamma_{2out} + 0\gamma_{34} + 0\gamma_{3out} \\ & + \mu_4\gamma_{42} + 0\gamma_{43} + 0\gamma_{45} + 0\gamma_{4out} + \mu_5\gamma_{52} + 0\gamma_{53} + 0\gamma_{5out}\end{aligned} \tag{10}$$

$$\begin{aligned}\lambda_3 = {} & 0\gamma_{12} + \mu_1\gamma_{13} + 0\gamma_{14} + 0\gamma_{15} + 0\gamma_{24} + 0\gamma_{25} + 0\gamma_{2out} + 0\gamma_{34} + 0\gamma_{3out} \\ & + 0\gamma_{42} + \mu_4\gamma_{43} + 0\gamma_{45} + 0\gamma_{4out} + 0\gamma_{52} + \mu_5\gamma_{53} + 0\gamma_{5out}\end{aligned} \tag{11}$$

$$\begin{aligned}\lambda_4 = {} & 0\gamma_{12} + 0\gamma_{13} + \mu_1\gamma_{14} + 0\gamma_{15} + \mu_2\gamma_{24} + 0\gamma_{25} + 0\gamma_{2out} + \mu_3\gamma_{34} + 0\gamma_{3out} \\ & + 0\gamma_{42} + 0\gamma_{43} + 0\gamma_{45} + 0\gamma_{4out} + 0\gamma_{52} + 0\gamma_{53} + 0\gamma_{5out}\end{aligned} \tag{12}$$

$$\begin{aligned}\lambda_5 = {} & 0\gamma_{12} + 0\gamma_{13} + 0\gamma_{14} + \mu_1\gamma_{15} + 0\gamma_{24} + \mu_2\gamma_{25} + 0\gamma_{2out} + 0\gamma_{34} + 0\gamma_{3out} \\ & + 0\gamma_{42} + 0\gamma_{43} + \mu_4\gamma_{45} + 0\gamma_{4out} + 0\gamma_{52} + 0\gamma_{53} + 0\gamma_{5out}\end{aligned} \tag{13}$$

$$\mu_1 = \mu_1\gamma_{12} + \mu_1\gamma_{13} + \mu_1\gamma_{14} + \mu_1\gamma_{15} + 0\gamma_{24} + 0\gamma_{25} + 0\gamma_{2out} + 0\gamma_{34} + 0\gamma_{3out}$$

$$+0\gamma_{42}+0\gamma_{43}+0\gamma_{45}+0\gamma_{4out}+0\gamma_{52}+0\gamma_{53}+0\gamma_{5out}\,, \tag{14}$$

$$\mu_2 = 0\gamma_{12}+0\gamma_{13}+0\gamma_{14}+0\gamma_{15}+\mu_2\gamma_{24}+\mu_2\gamma_{25}+\mu_2\gamma_{2out}+0\gamma_{34}+0\gamma_{3out}$$
$$+0\gamma_{42}+0\gamma_{43}+0\gamma_{45}+0\gamma_{4out}+0\gamma_{52}+0\gamma_{53}+0\gamma_{5out}\,, \tag{15}$$

$$\mu_3 = 0\gamma_{12}+0\gamma_{13}+0\gamma_{14}+0\gamma_{15}+0\gamma_{24}+0\gamma_{25}+0\gamma_{2out}+\mu_3\gamma_{34}+\mu_3\gamma_{3out}$$
$$+0\gamma_{42}+0\gamma_{43}+0\gamma_{45}+0\gamma_{4out}+0\gamma_{52}+0\gamma_{53}+0\gamma_{5out}, \tag{16}$$

$$\mu_4 = 0\gamma_{12}+0\gamma_{13}+0\gamma_{14}+0\gamma_{15}+0\gamma_{24}+0\gamma_{25}+0\gamma_{2out}+0\gamma_{34}+0\gamma_{3out}$$
$$+\mu_4\gamma_{42}+\mu_4\gamma_{43}+\mu_4\gamma_{45}+\mu_4\gamma_{4out}+0\gamma_{52}+0\gamma_{53}+0\gamma_{5out}, \tag{17}$$

$$\mu_5 = 0\gamma_{12}+0\gamma_{13}+0\gamma_{14}+0\gamma_{15}+0\gamma_{24}+0\gamma_{25}+0\gamma_{2out}+0\gamma_{34}+0\gamma_{3out}$$
$$+0\gamma_{42}+0\gamma_{43}+0\gamma_{45}+0\gamma_{4out}+\mu_5\gamma_{52}+\mu_5\gamma_{53}+\mu_5\gamma_{5out}. \tag{18}$$

From model equation (10 - 18) can be represented in the matrix form as:

$$\begin{bmatrix}
\mu_1 & 0 & 0 & 0 & 0 & 0 & 0 & 0 & 0 & \mu_4 & 0 & 0 & 0 & \mu_5 & 0 & 0 \\
0 & \mu_1 & 0 & 0 & 0 & 0 & 0 & 0 & 0 & 0 & \mu_4 & 0 & 0 & 0 & \mu_5 & 0 \\
0 & 0 & \mu_1 & 0 & \mu_2 & 0 & 0 & \mu_3 & 0 & 0 & 0 & 0 & 0 & 0 & 0 & 0 \\
0 & 0 & 0 & \mu_1 & 0 & \mu_2 & 0 & 0 & 0 & 0 & 0 & \mu_4 & 0 & 0 & 0 & 0 \\
\mu_1 & \mu_1 & \mu_1 & \mu_1 & 0 & 0 & 0 & 0 & 0 & 0 & 0 & 0 & 0 & 0 & 0 & 0 \\
0 & 0 & 0 & 0 & \mu_2 & \mu_2 & \mu_2 & 0 & 0 & 0 & 0 & 0 & 0 & 0 & 0 & 0 \\
0 & 0 & 0 & 0 & 0 & 0 & 0 & \mu_3 & \mu_3 & 0 & 0 & 0 & 0 & 0 & 0 & 0 \\
0 & 0 & 0 & 0 & 0 & 0 & 0 & 0 & 0 & \mu_4 & \mu_4 & \mu_4 & \mu_4 & 0 & 0 & 0 \\
0 & 0 & 0 & 0 & 0 & 0 & 0 & 0 & 0 & 0 & 0 & 0 & 0 & \mu_5 & \mu_5 & \mu_5
\end{bmatrix}
\begin{bmatrix}
\gamma_{12} \\ \gamma_{13} \\ \gamma_{14} \\ \gamma_{15} \\ \gamma_{24} \\ \gamma_{25} \\ \gamma_{2out} \\ \gamma_{34} \\ \gamma_{3out} \\ \gamma_{42} \\ \gamma_{43} \\ \gamma_{45} \\ \gamma_{4out} \\ \gamma_{52} \\ \gamma_{53} \\ \gamma_{5out}
\end{bmatrix}
=
\begin{bmatrix}
\lambda_2 \\ \lambda_3 \\ \lambda_4 \\ \lambda_5 \\ \mu_1 \\ \mu_2 \\ \mu_3 \\ \mu_4 \\ \mu_5
\end{bmatrix} \tag{19}$$

Equation (19) can be represented in the form

$$\begin{bmatrix} \gamma_{12} \\ \gamma_{13} \\ \gamma_{14} \\ \gamma_{15} \\ \gamma_{24} \\ \gamma_{25} \\ \gamma_{2out} \\ \gamma_{34} \\ \gamma_{3out} \\ \gamma_{42} \\ \gamma_{43} \\ \gamma_{45} \\ \gamma_{4out} \\ \gamma_{52} \\ \gamma_{53} \\ \gamma_{5out} \end{bmatrix} = \begin{bmatrix} \mu_1 & 0 & 0 & 0 & 0 & 0 & 0 & 0 & 0 & \mu_4 & 0 & 0 & 0 & \mu_5 & 0 & 0 \\ 0 & \mu_1 & 0 & 0 & 0 & 0 & 0 & 0 & 0 & 0 & \mu_4 & 0 & 0 & 0 & \mu_5 & 0 \\ 0 & 0 & \mu_1 & 0 & \mu_2 & 0 & 0 & \mu_3 & 0 & 0 & 0 & 0 & 0 & 0 & 0 & 0 \\ 0 & 0 & 0 & \mu_1 & 0 & \mu_2 & 0 & 0 & 0 & 0 & 0 & \mu_4 & 0 & 0 & 0 & 0 \\ \mu_1 & \mu_1 & \mu_1 & \mu_1 & 0 & 0 & 0 & 0 & 0 & 0 & 0 & 0 & 0 & 0 & 0 & 0 \\ 0 & 0 & 0 & 0 & \mu_2 & \mu_2 & \mu_2 & 0 & 0 & 0 & 0 & 0 & 0 & 0 & 0 & 0 \\ 0 & 0 & 0 & 0 & 0 & 0 & 0 & \mu_3 & \mu_3 & 0 & 0 & 0 & 0 & 0 & 0 & 0 \\ 0 & 0 & 0 & 0 & 0 & 0 & 0 & 0 & 0 & \mu_4 & \mu_4 & \mu_4 & \mu_4 & 0 & 0 & 0 \\ 0 & 0 & 0 & 0 & 0 & 0 & 0 & 0 & 0 & 0 & 0 & 0 & 0 & \mu_5 & \mu_5 & \mu_5 \end{bmatrix}^{+} \begin{bmatrix} \lambda_2 \\ \lambda_3 \\ \lambda_4 \\ \lambda_5 \\ \mu_1 \\ \mu_2 \\ \mu_3 \\ \mu_4 \\ \mu_5 \end{bmatrix} \tag{20}$$

(Note: the " + " sign above the coefficient matrix indicates that is a Pseoudo Inverse. This is because is a non square matrix)

## 2.3. Mathematical Formulation for new Departure Rate

Reducing waiting time of the customers in the banking hall and increasing the efficiency of the bank is thrust of this research, hence we formulate new departure rate of each of the nodes in our network system. This is done using equation (1 – 4), thus, we have the following equations.

$$\lambda_2 = \gamma_{12}\mu_1 + 0\mu_2 + 0\mu_3 + \gamma_{42}\mu_4 + \gamma_{52}\mu_5, \tag{21}$$

$$\lambda_3 = \gamma_{13}\mu_1 + 0\mu_2 + 0\mu_3 + \gamma_{43}\mu_4 + \gamma_{53}\mu_5, \tag{22}$$

$$\lambda_4 = \gamma_{14}\mu_1 + \gamma_{24}\mu_2 + \gamma_{34}\mu_3 + 0\mu_4 + 0\mu_5, \tag{23}$$

$$\lambda_5 = \gamma_{15}\mu_1 + \gamma_{25}\mu_2 + 0\mu_3 + \gamma_{45}\mu_4 + 0\mu_5. \tag{24}$$

Model equation (21-24) can be transform to matrix as in equation (25):

$$\begin{bmatrix} \gamma_{12} & 0 & 0 & \gamma_{42} & \gamma_{52} \\ \gamma_{13} & 0 & 0 & \gamma_{43} & \gamma_{53} \\ \gamma_{14} & \gamma_{24} & \gamma_{34} & 0 & 0 \\ \gamma_{15} & \gamma_{25} & 0 & \gamma_{45} & 0 \end{bmatrix} \begin{bmatrix} \mu_1 \\ \mu_2 \\ \mu_3 \\ \mu_4 \\ \mu_5 \end{bmatrix} = \begin{bmatrix} \lambda_2 \\ \lambda_3 \\ \lambda_4 \\ \lambda_5 \end{bmatrix}, \quad (25)$$

where,

the arrival rate $\lambda_i = \frac{1}{mean\ number\ of\ arrival}$, for i = 1,2,...5, (26)

the departure rate $\mu_i = \frac{1}{mean\ number\ of\ departure}$, for i= 1,2,…5, (27)

and

$$\rho = \frac{\lambda_i}{\mu_i}, \quad for\ i = 1, 2, \cdots 5. \quad (28)$$

The expected number in the queue is given as

$$l_q = \frac{\rho}{m-\rho}, \quad (29)$$

where m stands for the number of servers at the node.

The expected waiting time in the queue is given as:

$$w_{qi} = \frac{l_q}{\lambda_i}, \quad (30)$$

The expected number of customers in the system is given as

$$l_s = l_q + \rho. \quad (31)$$

Finally, the expected waiting time in the system for node 1-5 is given as

$w_i = \frac{l_s}{\lambda_i}$, For i = 1,2,…5.

## 3. Results and discussion

We begin this section with computation of mean arrival and departure time for all the nodes in the network system. The results of the computation obtained from the raw data collected for four weeks is presented in Table 1 below.

| | Node 1 | Node 2 | Node 3 | Node 4 | Node 5 |
|---|---|---|---|---|---|
| Mean arrival | 1.920 | 1.712 | 1.366 | 1.732 | 1.343 |
| Mean departure | 1.548 | 1.465 | 1.112 | 1.308 | 1.213 |

**Table 1:** Showing Data analysis for the Mean arrival as well as Mean departure

From Table 1 above, we obtained the Mean arrival and Mean departure for each node, the expected number of customers in the system, the expected number of customers in the queue and the expected waiting time in the system.

For node1, the arrival rate: $\lambda_1 = \frac{1}{mean\ number\ of\ arrival} = \frac{1}{1.920} = 0.52$ person per minute.

For node2, the arrival rate: $\lambda_2 = \frac{1}{mean\ number\ of\ arrival} = \frac{1}{1.712} = 0.58$ person per minute.

For node3, the arrival rate: $\lambda_3 = \frac{1}{mean\ number\ of\ arrival} = \frac{1}{1.366} = 0.73$ person per minute.

For node4, the arrival rate: $\lambda_4 = \frac{1}{mean\ number\ of\ arrival} = \frac{1}{1.732} = 0.58$ person per minute.

For node5, the arrival rate: $\lambda_2 = \frac{1}{mean\ number\ of\ arrival} = \frac{1}{1.343} = 0.74$ person per minute.

The departure rate for nodes is given as:

$$\mu_1 = \frac{1}{mean\ number\ of\ departure} = \frac{1}{1.548} = 0.646$$
$$\mu_2 = \frac{1}{mean\ number\ of\ departure} = \frac{1}{1.465} = 0.683$$
$$\mu_3 = \frac{1}{mean\ number\ of\ departure} = \frac{1}{1.112} = 0.899$$
$$\mu_4 = \frac{1}{mean\ number\ of\ departure} = \frac{1}{1.308} = 0.765$$
$$\mu_5 = \frac{1}{mean\ number\ of\ departure} = \frac{1}{1.213} = 0.824.$$

Node 1:

$\rho = \frac{\lambda_1}{\mu_1} = \frac{0.52}{0.646} = 0.8.$

The expected number of customer in the queue is given as

$l_q = \frac{\rho}{m-\rho} = \frac{0.8}{1-0.8} = 4.0,$

where m stands for the number of servers at the node1 (Meter Greeter Unit) .

The expected waiting time in the queue is given as

$w_{q1} = \frac{l_q}{\lambda_1} = \frac{4.0}{0.52} = 7.69$ minutes.

The expected number of customers in the system is given as

$l_s = l_q + \rho = 4.0 + 0.8 = 4.8.$

The expected waiting time in the system for node1 is given as
$w_1 = \frac{l_s}{\lambda_1} = \frac{4.8}{0.52} = 9.2$ minutes.

Node 2:
$\rho = \frac{\lambda_2}{\mu_2} = \frac{0.58}{0.683} = 0.8$.
The expected number of customers in the queue is given as
$l_q = \frac{\rho}{m-\rho} = \frac{0.8}{2-0.8} = 0.7$,
where m stands for the number of servers at the node2 (Customer Service Unit).

The expected waiting time in the queue is given as
$w_{q2} = \frac{l_q}{\lambda_2} = \frac{0.7}{0.58} = 1.2$ minutes.
The expected number of customers in the system is given as
$l_s = l_q + \rho = 0.7 + 0.8 = 1.5$.
The expected waiting time in the system for node 2 is given as
$w_2 = \frac{l_s}{\lambda_2} = \frac{1.5}{0.58} = 26$ minutes.

Node 3:
$\rho = \frac{\lambda_3}{\mu_3} = \frac{0.73}{0.899} = 0.8$.

The expected number of customers in the queue is given as
$l_q = \frac{\rho}{m-\rho} = \frac{0.8}{3-0.8} = 0.4$,
where m stands for the number of servers at the node3 (Marketing Unit).

The expected waiting time in the queue is given as
$w_{q3} = \frac{l_q}{\lambda_3} = \frac{0.4}{0.73} = 0.54$ Minute
The expected number of customers in the system is given as
$l_s = l_q + \rho = 0.4 + 0.8 = 1.2$
The expected waiting time in the system for node3 is given as
$w_3 = \frac{l_s}{\lambda_3} = \frac{1.2}{0.73} = 1.6 Minutes$.

Node 4:
.
$\rho = \frac{\lambda_4}{\mu_4} = \frac{0.58}{0.765} = 0.8$
The expected number of customers in the queue is given as
$l_q = \frac{\rho}{m-\rho} = \frac{0.8}{4-0.8} = 0.3$,
where m stands for the number of servers at the node4 (Tellers Unit).

The expected waiting time in the queue is given as

$$w_{q4} = \frac{l_q}{\lambda_4} = \frac{0.3}{0.58} = 0.52 \text{ minutes.}$$

The expected number of customers in the system is given as

$$l_s = l_q + \rho = 0.3 + 0.8 = 1.1.$$

The expected waiting time in the system for node 4 is given as

$$w_4 = \frac{l_s}{\lambda_4} = \frac{1.1}{0.58} = 1.9 \text{ minutes.}$$

Node 5:

$$\rho = \frac{\lambda_5}{\mu_5} = \frac{0.74}{0.824} = 0.9.$$

The expected number of customers in the queue is given as

$$l_q = \frac{\rho}{m-\rho} = \frac{0.9}{1-0.9} = 9.0,$$

where m stands for the number of servers at the node 5 (Customers Service Manager Unit).

The expected waiting time in the queue is given as

$$w_{q5} = \frac{l_q}{\lambda_5} = \frac{0.3}{0.74} = 0.41 \text{minutes.}$$

The expected number of customers in the system is given as

$$l_s = l_q + \rho = 9.0 + 0.9 = 9.9.$$

The expected waiting time in the system for node5 is given as

$$w_5 = \frac{l_s}{\lambda_5} = \frac{9.9}{0.74} = 13.4 Minutes.$$

However, the total expected waiting time in the system before modification is:

$$W_t = w_1 + w_2 + w_3 + w_4 + w_5 = 9.2 + 26 + 1.6 + 1.9 + 13.4 = 52.1 \cong 52 \min utes$$

Now substituting the departure rates and arrival rates calculated above into equation (20), we have:

$$\begin{bmatrix} \gamma_{12} \\ \gamma_{13} \\ \gamma_{14} \\ \gamma_{15} \\ \gamma_{24} \\ \gamma_{25} \\ \gamma_{2out} \\ \gamma_{34} \\ \gamma_{3out} \\ \gamma_{42} \\ \gamma_{43} \\ \gamma_{45} \\ \gamma_{4out} \\ \gamma_{52} \\ \gamma_{53} \\ \gamma_{5out} \end{bmatrix} = \begin{bmatrix} 0.65 & 0 & 0 & 0 & 0 & 0 & 0 & 0 & 0 & 0.77 & 0 & 0 & 0 & 0.82 & 0 & 0 \\ 0 & 0.65 & 0 & 0 & 0 & 0 & 0 & 0 & 0 & 0 & 0.77 & 0 & 0 & 0 & 0.82 & 0 \\ 0 & 0 & 0.65 & 0 & 0.68 & 0 & 0 & 0.89 & 0 & 0 & 0 & 0 & 0 & 0 & 0 & 0 \\ 0 & 0 & 0 & 0.65 & 0 & 0.68 & 0 & 0 & 0 & 0 & 0 & 0.77 & 0 & 0 & 0 & 0 \\ 0.65 & 0.65 & 0.65 & 0.65 & 0 & 0 & 0 & 0 & 0 & 0 & 0 & 0 & 0 & 0 & 0 & 0 \\ 0 & 0 & 0 & 0 & 0.68 & 0.68 & 0.68 & 0 & 0 & 0 & 0 & 0 & 0 & 0 & 0 & 0 \\ 0 & 0 & 0 & 0 & 0 & 0 & 0 & 0.89 & 0.89 & 0 & 0 & 0 & 0 & 0 & 0 & 0 \\ 0 & 0 & 0 & 0 & 0 & 0 & 0 & 0 & 0 & 0.77 & 0.77 & 0.77 & 0.77 & 0 & 0 & 0 \\ 0 & 0 & 0 & 0 & 0 & 0 & 0 & 0 & 0 & 0 & 0 & 0 & 0 & 0.82 & 0.82 & 0.82 \end{bmatrix} + \begin{bmatrix} 1.00 \\ 0.56 \\ 0.58 \\ 0.62 \\ 0.55 \\ 1.00 \\ 0.79 \\ 0.67 \\ 0.65 \end{bmatrix} \tag{32}$$

The coefficient of the unknown in equation (20) is a rectangular matrix, to find the inverse of this Matrix, we use Moore-Penrose Generalized Inverse. See the following ([4], [5], [6], [7], [8], [9], [10], [12], [18], [20]).

Hence, we obtain equation (22)

$$\begin{bmatrix} \gamma_{12} \\ \gamma_{13} \\ \gamma_{14} \\ \gamma_{15} \\ \gamma_{24} \\ \gamma_{25} \\ \gamma_{2out} \\ \gamma_{34} \\ \gamma_{3out} \\ \gamma_{42} \\ \gamma_{43} \\ \gamma_{45} \\ \gamma_{4out} \\ \gamma_{52} \\ \gamma_{53} \\ \gamma_{5out} \end{bmatrix} = \begin{bmatrix} 0.3529 & -0.0322 & -0.1548 & -0.1134 & 0.3715 & 0.0894 & -0.0774 & -0.0518 & -0.1069 \\ -0.0322 & 0.3529 & -0.1548 & -0.1134 & 0.3715 & 0.0894 & 0.0774 & -0.0518 & -0.1069 \\ -0.2222 & -0.2222 & 0.3901 & -0.1626 & 0.4388 & -0.0758 & -0.195 & 0.1517 & 0.1481 \\ -0.0986 & -0.0986 & -0.0805 & 0.3893 & 0.3567 & -0.103 & 0.0402 & -0.048 & 0.0657 \\ 0.0285 & 0.0285 & 0.4256 & -0.095 & -0.0969 & 0.38 & -0.2128 & 0.0095 & -0.019 \\ 0.1577 & 0.1577 & -0.0666 & 0.4824 & -0.1828 & 0.3516 & 0.0333 & -0.1995 & -0.1051 \\ -0.1862 & -0.1862 & -0.359 & -0.3874 & 0.2797 & 0.739 & 0.1795 & 0.19 & 0.1241 \\ 0.1405 & 0.1405 & 0.5135 & 0.1914 & -0.2465 & -0.235 & 0.305 & -0.1181 & -0.0937 \\ -0.1405 & -0.1405 & -0.5135 & -0.1914 & 0.2465 & 0.235 & 0.8185 & 0.1181 & 0.0937 \\ 0.4789 & 0.0227 & 0.0388 & -0.0515 & -0.1222 & 0.0043 & -0.0194 & 0.2122 & -0.1672 \\ 0.0227 & 0.4789 & 0.0388 & -0.0515 & -0.1222 & 0.0043 & -0.0194 & 0.2122 & -0.1672 \\ -0.056 & -0.056 & 0.1268 & 0.544 & -0.1397 & -0.2236 & -0.0634 & 0.2167 & 0.0374 \\ -0.4455 & -0.4455 & -0.2043 & -0.441 & 0.3841 & 0.2151 & 0.1022 & 0.6577 & 0.297 \\ 0.4901 & 0.0042 & 0.0863 & 0.1382 & -0.1797 & -0.0748 & -0.0431 & -0.1581 & 0.2417 \\ 0.0042 & 0.4901 & 0.0863 & 0.1382 & -0.1797 & -o.o748 & -0.0431 & -0.1581 & 0.2417 \\ -0.4943 & -0.4943 & -0.1726 & -0.2765 & 0.3594 & 0.1497 & 0.0863 & 0.3163 & 0.736 \end{bmatrix} \begin{bmatrix} 0.58 \\ 0.73 \\ 0.58 \\ 0.74 \\ 0.65 \\ 0.68 \\ 0.89 \\ 0.77 \\ 0.82 \end{bmatrix} \tag{33}$$

Solving equation (33) using maple 17 software, we obtain equation (34) below:

$$\begin{bmatrix} \gamma_{12} \\ \gamma_{13} \\ \gamma_{14} \\ \gamma_{15} \\ \gamma_{24} \\ \gamma_{25} \\ \gamma_{2out} \\ \gamma_{34} \\ \gamma_{3out} \\ \gamma_{42} \\ \gamma_{43} \\ \gamma_{45} \\ \gamma_{4out} \\ \gamma_{52} \\ \gamma_{53} \\ \gamma_{5out} \end{bmatrix} = \begin{bmatrix} 0.251085 \\ 0.308850 \\ 0.113229 \\ 0.326733 \\ -0.211641 \\ 0.435043 \\ 0.353324 \\ 0.407175 \\ 0.592740 \\ 0.211245 \\ 0.279675 \\ 0.300992 \\ 0.208421 \\ 0.310075 \\ 0.382960 \\ 0.307033 \end{bmatrix} \tag{34}$$

To normalize the values of the probabilities in equation (34), since we do not have negative probabilities, we take the absolute value of the estimates and rescaled them so that the sum of each node sums up to 1. Thus, we have

$$\begin{bmatrix} \gamma_{12} \\ \gamma_{13} \\ \gamma_{14} \\ \gamma_{15} \\ \gamma_{24} \\ \gamma_{25} \\ \gamma_{2out} \\ \gamma_{34} \\ \gamma_{3out} \\ \gamma_{42} \\ \gamma_{43} \\ \gamma_{45} \\ \gamma_{4out} \\ \gamma_{52} \\ \gamma_{53} \\ \gamma_{5out} \end{bmatrix} = \begin{bmatrix} 0.251111 \\ 0.308882 \\ 0.113241 \\ 0.326767 \\ 0.211639 \\ 0.435040 \\ 0.353321 \\ 0.407210 \\ 0.592790 \\ 0.211175 \\ 0.279582 \\ 0.300892 \\ 0.208352 \\ 0.310054 \\ 0.382934 \\ 0.307012 \end{bmatrix} \tag{35}$$

From equation (35), the following deductions are made:

At node 1 (Meter Greeter Unit), the weights are $\gamma_{12}, \gamma_{13}, \gamma_{14}$ and $\gamma_{15}$ with the values 0.251111, 0.308882, 0.113241 and 0.326767 respectively, shows that there is a high probability of a customer leaving node1 (Meter Greeter Unit) to join the queue for service at node5 (Customer Service Manager Unit) than any other node. The least probability is that a customer leaves node1 to node4 (Tellers Unit).

At node 2 (Customer Service Unit), the weights are $\gamma_{24}, \gamma_{25}$ and $\gamma_{2out}$ with values 0.211639, 0.435040 and 0.353321 respectively, shows that there is a high probability that a customer leaves node2 (Customer Service Unit) and goes directly to node5 (Customer Service Manager Unit).

At node 3 (Marketing Unit), the weights are $\gamma_{34}$ and $\gamma_{3out}$ with the values 0.407210 and 0.592790 respectively, which shows that there is a high probability that a customer leaves node3 (Marketing Unit) moves out of the system. The least probability is that a customer leaves node3 (Marketing Unit) to join the service at the node4 (Tellers Unit).

At node 4 (Tellers Unit), the weights are $\gamma_{42}, \gamma_{43}, \gamma_{45}$, and $\gamma_{4out}$ with the values 0.211175, 0.279582, 0.300892 and 0.208352 respectively, which shows that, there is a high probability that a customer leaves node4 (Tellers Unit) to join the service at the node5 (Customers Service Manager Unit).

At node 5 (Customers Service Manager Unit) the weights are $\gamma_{52}, \gamma_{53}$ and $\gamma_{5out}$ with the values 0.310054, 0.382934 and 0.307012 respectively, which shows that there is a high probability that a customer leaves node5 (Customer Service Manager Unit) to join the queue for service either at node3 (Marketing Unit). The least probability here is that a customer leaves node5 (Customer Service Manager Unit) and goes out of the system.

## 3.1. Solution For New Departure Rate

To obtain the new departure rate for the network system, we solve equation (25), this is done by substituting the values of $\gamma_{ij}$'s and arrival rates obtained in the previous section into equation (25) then we obtain equation (36):

$$\begin{bmatrix} \mu_1 \\ \mu_2 \\ \mu_3 \\ \mu_4 \\ \mu_5 \end{bmatrix} = \begin{bmatrix} 54.732 & 43.8693 & -0.1849 & 0.7306 \\ 6.2475 & -5.9549 & 0.2033 & 1.4693 \\ 17.8841 & 14.8199 & 2.3845 & -0.9486 \\ 69.3682 & 56.9901 & -0.0948 & 0.3747 \\ 6.0785 & -3.2277 & 0.2133 & -0.8430 \end{bmatrix} \begin{bmatrix} 0.58 \\ 0.73 \\ 0.58 \\ 0.74 \end{bmatrix} \tag{36}$$

Equation (36) becomes equation (37):

$$\begin{bmatrix}\mu_1\\ \mu_2\\ \mu_3\\ \mu_4\\ \mu_5\end{bmatrix}=\begin{bmatrix}16.023\\ 18.014\\ 18.022\\ 22.812\\ 7.4242\end{bmatrix} \tag{37}$$

Therefore, to serve Customer with the space interval of 5 minutes, we divide the values in equation (37) by 5. The recommended number of servers therefore for each node is given in equation (38):

$$\begin{bmatrix}\mu_1\\ \mu_2\\ \mu_3\\ \mu_4\\ \mu_5\end{bmatrix}=\begin{bmatrix}3.2046\\ 3.6028\\ 3.6044\\ 4.5624\\ 1.4848\end{bmatrix}\cong\begin{bmatrix}3\\ 4\\ 4\\ 5\\ 1\end{bmatrix} \tag{38}$$

The result in equation (38) shows that for the Bank to work optimally and to serve customers within the average time frame of 5 minutes, node1 will require a total of three servers, node2 will require a total of four servers, node3 will require a total of four servers, node4 will require a total of five servers, node five will require a total of one server. With the new estimated number of servers at each node given by equation (38). The arrival rates for each node are assumed to remain the same since we do not have control over it. A new departure rates and the expected waiting time for each node is estimated as follow.

The new departure rates for nodes are as follows:

$$\mu_1 = \textit{recommended departure rate per } 5\ \text{min.} = \tfrac{3}{5} = 0.6$$
$$\mu_2 = \textit{recommended departure rate per } 5\ \text{min.} = \tfrac{4}{5} = 0.8$$
$$\mu_3 = \textit{recommended departure rate per } 5\ \text{min.} = \tfrac{4}{5} = 0.8$$
$$\mu_4 = \textit{recommended departure rate per } 5\ \text{min.} = \tfrac{5}{5} = 1.0$$
$$\mu_5 = \textit{recommended departure rate per } 5\ \text{min.} = \tfrac{1}{5} = 0.2.$$

Finding the New Expected Waiting Time in the System.

Node 1:

$\rho = \frac{\lambda_1}{\mu_1} = \frac{0.52}{0.6} = 0.9$

The expected number of customers in the queue is given as

$, l_q = \frac{\rho}{m-\rho} = \frac{0.9}{3-0.9} = 0.4$

where m stands for the number of servers at the node1 (Meter Greeter Unit).

The expected waiting time in the queue is given as

$w_{q1} = \frac{l_q}{\lambda_1} = \frac{0.4}{0.52} = 0.8$ minutes

The expected number of customers in the system is given as
$l_s = l_q + \rho = 0.4 + 0.9 = 1.3$
The expected waiting time in the system for node1 is given as
$w_1 = \frac{l_s}{\lambda_1} = \frac{1.3}{0.52} = 2.5$ minutes.

Node 2:
$\rho = \frac{\lambda_2}{\mu_2} = \frac{0.58}{0.8} = 0.7$.
The expected number of customers in the queue is given as
$l_q = \frac{\rho}{m-\rho} = \frac{0.7}{4-0.7} = 0.2$,
where m stands for the number of servers at the node2 (Customer Service Unit).

The expected waiting time in the queue is given as
$w_{q2} = \frac{l_q}{\lambda_2} = \frac{0.2}{0.58} = 0.34$ minutes.

The expected waiting time in the system for node 2 is given as
$w_2 = \frac{l_s}{\lambda_2} = \frac{0.9}{0.58} = 1.6$ minutes.

Node 3:
$\rho = \frac{\lambda_3}{\mu_3} = \frac{0.73}{0.8} = 0.9$
The expected number of in the queue is given as
$l_q = \frac{\rho}{m-\rho} = \frac{0.9}{4-0.9} = 0.3$,
where m stands for the number of servers at the node3 (Marketing Unit).

The expected waiting time in the queue is given as
$w_{q3} = \frac{l_q}{\lambda_3} = \frac{0.3}{0.73} = 0.41$ minutes.
The expected number of customers in the system is given as
$l_s = l_q + \rho = 0.2 + 0.9 = 1.1$.

The expected waiting time in the system for node3 is given as
$w_3 = \frac{l_s}{\lambda_3} = \frac{1.1}{0.73} = 1.5$ minutes.

Node 4:
$\rho = \frac{\lambda_4}{\mu_4} = \frac{0.58}{1.0} = 0.6$
The expected number of customers in the queue is given as
$l_q = \frac{\rho}{m-\rho} = \frac{0.6}{5-0.6} = 0.1$,
where m stands for the number of servers at the node 4 (Tellers Unit).

The expected waiting time in the queue is given as
$w_{q4} = \frac{l_q}{\lambda_4} = \frac{0.1}{0.58} = 0.17$ minutes

The expected number of customers in the system is given as

$l_s = l_q + \rho = 0.1 + 0.6 = 0.7$

The expected waiting time in the system for node1 is given as

$w_4 = \frac{l_s}{\lambda_4} = \frac{0.7}{0.58} = 1.2$ minutes.

Node 5:

$\rho = \frac{\lambda_5}{\mu_5} = \frac{0.74}{1.0} = 0.7$.

The expected number of customers in the queue is given as

$l_q = \frac{\rho}{m-\rho} = \frac{0.7}{1-0.7} = 2.3$,

where m stands for the number of servers at the node5 (Customer Service Manager Unit).

The expected waiting time in the queue is given as

$w_{q5} = \frac{l_q}{\lambda_5} = \frac{2.3}{0.74} = 3.10$ minutes.

The expected number of customers in the system is given as

$l_s = l_q + \rho = 2.3 + 0.7 = 3.0$

The expected waiting time in the system for node1 is given as

$w_5 = \frac{l_s}{\lambda_5} = \frac{3.0}{0.74} = 4.1$minutes.

However, the total expected waiting time in the system after modification is

$W_t = w_1 + w_2 + w_3 + w_4 + w_5 = 2.5 + 1.6 + 1.5 + 1.2 + 4.1 = 10.9 \cong 11\, minutes$ .

The summary of the computed performance measure for determination of optimal number of servers at network queuing nodes to reduce waiting time at the First City Monument Bank, Minna branch, is given in Table 2.

| Nodes i | Number of Servers ($m_i$) | Probabilities ($\alpha_{ij}$) | $\varrho_i$ | Lq | Ls | $W_q$ | $W_S$ |
|---|---|---|---|---|---|---|---|
| 1 | 1 | 0.2511111.<br>0.308882<br>0.113241<br>0.326767 | 0.8 | 4.0 | 4.8 | 7.69 | 9.2 |
| 2 | 2 | 0.211639.<br>0.435040.<br>0.353321 | 0.8 | 0.7 | 1.5 | 1.20 | 26 |
| 3 | 3 | 0.407210.<br>0.592790. | 0.8 | 0.4 | 1.6 | 0.54 | 1.6 |
| 4 | 4 | 0.211175.<br>0.279582.<br>0.300892<br>0.208352 | 0.8 | 0.3 | 1.1 | 0.52 | 1.9 |
| 5 | 1 | 0.310054.<br>0.382934.<br>0.307012 | 0.9 | 9.0 | 9.9 | 0.41 | 13.4 |
| Total | 11 | | 4.1 | 14.4 | 18.9 | 10.36 | 52.1 |

**Table 2**: Showing all the results obtained before modification.

| Nodes i | Number of Servers ($m_i$) | $\varrho_i$ | Lq | Ls | $W_q$ | $W_S$ |
|---|---|---|---|---|---|---|
| 1 | 3 | 0.9 | 0.4 | 1.3 | 0.8 | 2.5 |
| 2 | 4 | 0.7 | 0.2 | 0.9 | 0.34 | 1.6 |
| 3 | 4 | 0.9 | 0.3 | 1.1 | 0.41 | 1.5 |
| 4 | 5 | 0.6 | 0.1 | 0.7 | 0.17 | 1.2 |
| 5 | 1 | 0.7 | 2.3 | 3.0 | 3.10 | 4.1 |
| Total | 17 | 3.8 | 3.3 | 7 | 4.8 | 10.9 |

**Table 3**: Showing all the results obtained after modification

| Nodes | Current number of servers | Optimal number of servers obtained |
|---|---|---|
| 1 | 1 | 3 |
| 2 | 2 | 4 |
| 3 | 3 | 4 |
| 4 | 4 | 5 |
| 5 | 1 | 1 |
| Total | 11 | 17 |

**Table 4**: Showing the comparison between current number of servers and optimal number of servers obtained

## 4. Conclusion

The network queuing system of First City Monument Bank, Minna branch has been effectively investigated and studied. The study has determined optimal number of banking personnel at different nodes of the bank network system to reduce waiting time of the customers. Results from

the study is a vital information to the management of the bank for proper planning and efficient service delivery. The network model could also be applied to other banks with little modifications.

## References

[1] Adaji I. (2018). A determination of optimal performance for the queuing system. Unpublished Thesis of Master Technology in Department of Mathematics, Federal University of Technology, Minna.

[2] Adaji I., Lawal A., Abdullahi A., and Abdulkadir A. (2021). Performance evaluation of outpatient department waiting line system in a city. J. Appl. Sci. Environ. Manage., 25(1): 65-70.

[3] Adamu L., Adaji I., and Abdulkadir A. (2019) A study of waiting and service cost of a mult-server queuing system at national health insurance scheme (NHIS) Unit of the General Hospital Minna. Transactions of the Nigerian Association of Mathematical Physics, 10: 177-184

[4] Asmaa M. K., Asma A. E., and Afaf A. (2019). Applications of the Moore-Penrose generalized inverse to linear systems of algebraic equations. American Journal of Applied Mathematics, 7(6): 152-156.

[5] Bahadur-Thapa G., Lam-Estrada P., and Lo`pez-Bonilla J. (2018). On the Moore-Penrose generalized inverse matrix. World Scientific News, 5(9): 100- 110.

[6] Ben-Israel A. (1980). Generalized Inverses of Matrices and Their Applications. Springer, 154-186.

[7] Campbell S. L. and Meyer C. D. (1979). Generalized Inverses of Linear Transformations. London: Pitman Publishers.

[8] Golub G. H. and Kahan W. (1965). Calculating the singular values and pseudo-inverse of a matrix. SIAM J. Numer. Anal., 2 (3): 421 – 433.

[9] Greville T. N. (1960). The Pseudoinverse of a rectangular singular matrix and its application to the solution of systems of linear equations. SIAM Rev., 3(1): 38-43.

[10] Hearon J. Z. (1968). Generalized inverses and solutions of linear systems. Journal of research of National Bureau of standards-B Mathematical Sciences, 72: 303-308.

[11] Ismaila A. and Lawal A. (2020). Determination of optimal number of servers at network queuing node to reduce waiting time. International Journal of Optimal Model, 3(1): 34 – 49.

[12] Kanan A. M. (2017). Solving the systems of linear equations using the Moore-Penrose generalized inverse. Journal Massarat Elmeya, 1(2): 3-8.

[13] Kandenmir C. and Cavas I. (2007). An application of queuing theory to the relationship between insulin level and number of insulin receptors. Turk. J Biochem., 32(27): 32-38.

[14] Kembe M. M, Onah E. S., and Lorkegh S. (2012). A study of waiting and service cost of a multi-server queuing model in a specialist hospital. International Journal of Scientific and Technology Research, 1(8): 19-23.

[15] Narayanamoorthy S. and Ramya L. (2017). Multi server fuzzy queuing model using dsw algorithm with hexagonal fuzzy number. International Journal of Pure and Applied Mathematics, 11: 117 - 212.

[16] Owoloko E., Ayoku A., Adeleke J., and Edeki S. (2015). On the application of the open Jackson queuing network. Global International Journal of Applied Mathematics, 11(4): 2299-2313.

[17] Penrose R. (1955). A generalized inverse for matrices. Proc. Camb. Phil. Soc., 4(51): 406-413.
[18] Rao C. R. and Mitra S. K (1971). Generalized inverse of a matrix and its applications. New York: Wiley, 601-620.
[19] Rotich T. (2016). Utility analysis of an emergency medical service model using queuing theory. British Journal of Mathematics and Computer Science, 19(1), 1-18.
[20] Zuhair N. M. (1976). Generalized inverses and applications. New York: Academic Press.

**International Journal of Mathematical Analysis and Modelling**
**Volume 5, Issue 1, May 2022, Pages 56 – 68**

# A Fermat polynomial method for solving optimal control problems

**M. U. Nduka*† and B. I. Oruh*‡**

**Abstract**

In this paper, we propose an efficient computational approach to solve optimal control problems subject to state constraints and boundary conditions. The idea is to obtain an approximate numerical value of the objective function. The method is based on state parameterization. The state variable is considered as a linear combination of Fermat polynomials with unknown coefficients such that the state differential equations are satisfied. The optimal control problem is converted to quadratic programming problem which we easily solved by Lagrange method. Some numerical examples are considered to illustrate the reliability of the method. The numerical results obtained are accurate when compared with the analytic solution and results obtained from literatures.

***Keywords:*** optimal control; parameterization; Fermat polynomials; optimization

## 1. Introduction

Control theory is a branch of optimization theory that deals with the minimization or maximization of an objective function subject to some state equations and constraints. It addresses the problem of how best to optimize or operate a dynamic system to optimize some given criteria or performance. From a general viewpoint, an optimal control problem is an optimization problem. Ever since its emergence, optimal control theories have been applied to a wide range of areas and disciplines such as finance, for biological models and computational biology, Economics for economic models and economics of recycling, Engineering for aerospace and robotics [14], [3], [9]. Optimal control problems consider the optimization of dynamic system characterized by state and control variables.

The goal of solving optimal control problems is to determine the control $U(t)$ and the state $X(t)$ of a dynamic system that either minimizes or maximizes a performance index or functional $J\big(u(t), x(t)\big)$ and at the same instant satisfying the dynamic constraints and boundary conditions [12]. The solutions to optimal control problems can be found using two major techniques, analytic and numerical techniques. Analytic techniques obtain the necessary optimality

* Department of Mathematics, Michael Okpara University of Agriculture, Umudike, Nigeria
† Corresponding Author; modesty1799@gmail.com
‡ ifeanyichi@mouau.edu.ng

conditions through the maximum principle which is a generalization of classical calculus of variation.

However, it is often difficult to obtain analytic solution of optimal control problems. Furthermore, as the complexity of optimal control problems increases it becomes almost impossible to solve optimal control problems analytically. As a result, numerical techniques for solving optimization problems are employed to solve optimal control problems. The availability of numerous nonlinear programming softwares has made numerical techniques a better alternative. Numerical techniques have presented an attractive field for researchers of mathematical sciences, which have produced different numerical computational techniques and efficient algorithms in solving optimal control problems. Numerical techniques are achieved by discretization or parameterization.

Parameterization methods give a robust technique for solving optimal control problems in finite dimensional spaces. The method expresses the state, and/or control of a system as a function of some independent quantities known as parameters. State parameterization converts an optimal control problem to a nonlinear optimization problem and finds $(n+1)$ unknown polynomial coefficients of degree, at most$n$, in the form $\sum_{i=0}^{n} a_i t^i$. Polynomials have been used by many authors [13], [2], [15], [11], [4], [8] as approximating functions to the state and/or control variables of an optimal control problem, which result to different approximate values of the performance index. In most cases, Chebyshev polynomials and Legendre polynomials are used. [6], [5] solved Duffing Oscillator problem. The solution is based on state parameterization using linear combination of Chebyshev polynomials with unknown coefficients. This approximation converts an $(n+1)$ dimensional optimization problem into one-dimensional optimization problem which can then be solved easily. [10] proposed the use of Chebyshev wavelets, the state variable is approximated by a new hybrid based on second kind Chebyshev wavelets. subsequent iterations result to better accuracy. [5] proposed a numerical approach for solving optimal control problems using the Boubaker polynomials expansion scheme. [1] presented a technique to solve nonlinear optimal control problems. The method is based on using Legendre scaling functions to parameterize the state variable. This approach replaces the nonlinear optimal control problem by a sequence of time-varying linear quadratic optimal control problems which gives a better result when compared with some other methods. In spite of the many advantages that the state parameterization offer, the method has not been used extensively as there are numerous functions that have not been used which can give a better approximation and result than the ones in the literature.

In this paper we present the Fermat polynomial as the approximating function. The state variable of an optimal control problem is considered as a linear combination of Fermat polynomials with unknown coefficients such that the state differential equations are satisfied. The optimal control problem is converted to a quadratic programming problem resulting from a linear quadratic optimal control problem which can easily be solved by existing optimization methods.

## 2. Problem statement

Find the optimal control $u^*$ and the optimal trajectory $x^*$ that optimizes the performance index;

$$J = \int_{t_0}^{t_1} L(x(\tau), u(\tau), \tau)dt, \tag{1}$$

subject to the state equations:

$$\dot{x}(\tau) = f(x(\tau), u(\tau), \tau), \tag{2}$$

and boundary conditions:

$$x(t_0) = x_0, x(t_1) = x_1 \tau \in [t_0, t_1], \tag{3}$$

where $f$ is a real-valued continuously differentiable function. $x(\tau): I \to \mathbb{R}^n$, $u(\tau): I \to \mathbb{R}^m$, $I = [t_0, t_1]$, $L$ is assumed to be continuously differentiable and equation (1.1) is known as *Lagrangian* problem. For easy reference we shall denote equations (1)-(3).

### 2.1. Material and methods

We state that the parameterization involves the approximation of the state variable(s) of an optimal control problem using a given trial function or polynomials.

#### 2.2.1. Fermat polynomials

Polynomial expansions are broadly used in many mathematical fields to obtain results for both numerical and analytical analysis. Many of these polynomials are obtained from difference equations. Fermat polynomials are among the polynomial sequences that are generated by difference equations.

Fermat polynomials can be generated by the difference equation:

$$f_{i+2}(t) = 3tf_{i+1}(t) - 2f_i(t), \qquad f_0(t) = 0, f_1(t) = 1, \qquad i \geq 0.$$

Fermat polynomials can also be obtained by setting $p(t) = 3t$, and $q(t) = -2$ in the Lucas polynomial sequence defined by:

$$F_n(t) = p(t)F_{n-1}(t) + q(t)F_{n-2}(t).$$

Fermat polynomials can be explicitly written as:

$$\mathcal{F}(t) = \begin{cases} \frac{\left(3t+\sqrt{9t^2-8}\right)^k - \left(3t-\sqrt{9t^2-8}\right)^k}{2^k\sqrt{9t^2-8}}, & t \neq \frac{2}{3} \qquad k = 1,2 \ldots \\ 2^{\frac{k}{2}} sin\left(\frac{\pi}{4}k\right), & t = \frac{2}{3} \end{cases}$$

The first few Fermat polynomials are:

$$\mathcal{F}_1(t) = 1,\ \mathcal{F}_2(t) = 3t, \mathcal{F}_3(t) = 9t^2 - 2,\ \mathcal{F}_4(t) = 27t^3 - 12t, \mathcal{F}_5(t) = 81t^4 - 54t^2 + 4.$$

It is necessary to note that $\mathcal{F}_k(t)$ is a polynomial of degree $(k-1)$ with integer coefficients.

### 2.2.2. State parameterization using Fermat polynomials

We approximate the system state variable by a sequence of Fermat polynomials with unknown coefficients. Let $Q \subset C^1([t_0, t_1])$ be set of all functions satisfying equation (3). The performance index in equation (1) can be expressed as a function of$x(t)$. Then optimal control problem (1)-(3) may be considered as a minimization of equation (1) on the set $Q$.

### 2.2.3. Approximation of state and control variables

Let $Q_n$ be a subset of $Q$ consisting of Fermat polynomials of degree up to $n$ as

$$x_n = \sum_{i=1}^{n} a_i \, \mathcal{F}_i(t) \; n = 1,2 \ldots \tag{4}$$

Now we consider the minimization of $J$ on $Q_n$ with $\{a_i\}_{i=0}^{n}$ as unknowns.

Equation (2) can be re-written as

$$u(t) = \phi(x(t), \dot{x}(t), t). \tag{5}$$

The control variable is then written as a function of the unknown parameters of the state variables by substituting equation (4) into equation (5)

$$u_n(t) = \phi\left(\sum_{i=0}^{n} a_i \mathcal{F}_i\,(t), \sum_{i=0}^{n} a_i \dot{\mathcal{F}}_i\,(t), t\right). \tag{6}$$

### 2.2.4 Approximation of the performance index

By substituting these approximations of state variables (4) and control variables (6) into the objective function (1) we get

$$\hat{J}(a_0, a_1, \ldots a_n) = \int_{t_0}^{t_1} L\left(\sum_{i=1}^{n} a_i \mathcal{F}_i(t)\,, \phi\left(\sum_{i=1}^{n} a_i \mathcal{F}_i\,(t), \sum_{i=1}^{n} a_i \dot{\mathcal{F}}_i(t), t\right)\right) dt. \tag{7}$$

The boundary conditions become

$$x_n(t_0) = \sum_{i=1}^{n} a_i \mathcal{F}_i(t_0) = x_0,$$

$$x_n(t_1) = \sum_{i=1}^{n} a_i \mathcal{F}_i(t_1) = x_1.$$

The integration of equation (7) yields an expression in terms of the unknown parameters we seek. The optimal control problem is converted into a mathematical programming problem of unknown parameters with equality constraints.

The resulting problem can be stated in the form

$$minimize \;\; \hat{J}(a_1, a_2, \dots a_n) = a'Ma, \tag{8}$$
$$subject\ to: \;\; g(a_1, a_2 \dots a_3) = b, \tag{9}$$

where $a \epsilon \mathbb{R}^n$, $\hat{J}$ is the approximate value of $J$, $M$ is an $n \times n$ matrix. We obtain the optimal control vector $a^*$ by using the Lagrangian multiplier method.

## 3. Algorithm

**Input**: Optimal Control Problem (1)-(3).
**Output**: The approximate optimal control, optimal trajectory and approximate performance index.
**Step 1**. Approximate the state variable by $nth$ Fermat series.
**Step 2**. Express the control variable as a function of the approximated state variable.
**Step 3**. Substitute the expressions in steps 1 and 2 into the performance index to obtain the approximate performance index $\hat{J}$.
**Step 4**. Find the set of equality constraints from the initial and final conditions and calculate the matrix $M$.
**Step 5**. Find the optimal parameters $a^*$ by solving the optimization problem (8)-(9).
**Step 6**. Substitute $a^*$ into equations (4), (6), and (7) to find the approximate optimal trajectory, approximate optimal control and the performance index respectively.

## 4. Numerical results

### 4.1. Example 1

We consider the minimization problem:

$$minimize\ J = \frac{1}{2}\int_0^1 (3x(t)^2 + u(t)^2)\, dt, \tag{10}$$
$$Subject\ to \quad u = \dot{x} + x \tag{11}$$
$$with\ conditions\ x(0) = 0, x(1) = 2. \tag{12}$$

#### 4.1.1. Analytic Approach

First, we attempt the problem analytically using Pontryagin-Minimum-Principle. We construct the Hamiltonian of the problem:

$$H(x,u,\lambda) = 3x^2 + u^2 + \lambda(u - x), \tag{13}$$

$$\frac{\partial H}{\partial u} = 0 \Longrightarrow 2u + \lambda = 0,$$

$$u = -\frac{\lambda}{2}. \tag{14}$$

Substitute equation (13) into equation (14) and simplify

$$H = 3x^2 - \frac{\lambda^2}{2} - \lambda x. \tag{15}$$

Differentiate equation (15) with respect to $x$ and $\lambda$

$$\frac{\partial H}{\partial x} = -\dot{\lambda} \Longrightarrow 6x - \lambda = -\dot{\lambda}, \qquad \frac{\partial H}{\partial \lambda} = \dot{x} \Longrightarrow -\frac{2\lambda}{4} - x = \dot{x}.$$

Simplifying we have

$$\ddot{x} - 4x = 0. \tag{16}$$

Hence, the solution to equation (16) is

$$x(t) = Acosh(2t) + Bsinh(2t).$$

Apply the boundary conditions to obtain the optimal state function

$$x^*(t) = \frac{2\sinh(2t)}{\sinh(2)}. \tag{17}$$

And the optimal control function

$$u^*(t) = \frac{4\cosh(2t) + 2\sinh(2t)}{\sinh(2)}. \tag{18}$$

Substitute (17) and (18) into equation (10)

$$J = \frac{1}{2}\int_0^1 \left(3\left(\frac{4sinh^2(2t)}{sinh^2(2)}\right) + \left(\frac{16cosh^2(2t) + 16\cosh(2t)\sinh(2t) + 4sinh^2(2t)}{sinh^2(2)}\right)\right)dt$$

$$J = \frac{8}{sinh^2(2)}\int_0^1 (sinh^2(2t) + cosh^2(2t) + \cosh(2t)\sinh(2t))dt$$

$$J = 6.14925721.$$

Hence $J = 6.14925721$ is the exact numerical solution of the optimal control problem (10)-(12).

### 4.1.2. The Proposed Approach

We approximate the state variable with 5th order Fermat polynomial

$$x \approx \sum_{i=1}^{5} a_i \mathcal{F}_i = a_1\mathcal{F}_1 + a_2\mathcal{F}_2 + a_3\mathcal{F}_3 + a_4\mathcal{F}_4 + a_5\mathcal{F}_5,$$

$$\hat{x}(t) = 81a_5t^4 + 27a_4t^3 + (9a_3 - 54a_5)t^2 + (3a_2 - 12a_4)t + a_1 - 2a_3 + 4a_5 \quad (19)$$

and the approximate control function

$$\hat{u}(t) = 81a_5t^4 + (27a_4 + 324a_5)t^3 + (9a_3 + 81a_4 - 54a_5)t^2 + (3a_2 + 18a_3 - 12a_4 - 108a_5)t + a_1 + 3a_2 - 2a_3 - 12a_4 + 4a_5 \quad (20)$$

The squares of equations (19) and (20) are substituted into equation (10) to obtain the approximate objective function in terms of the unknown parameters
Integrating and simplifying we have

$$\hat{J} = 2{a_1}^2 + 9a_1a_2 + 13a_1a_3 + 18a_1a_4 + \frac{179a_1a_5}{5} + 15{a_2}^2 + 63a_2a_3 + \frac{534a_2a_4}{5} + 198a_2a_5 + \frac{929{a_3}^2}{10} + \frac{819a_3a_4}{2} + \frac{5611a_3a_5}{7} + \frac{19659{a_4}^2}{35} + \frac{4923a_4a_5}{2} + \frac{213119{a_5}^2}{70} \quad (21)$$

The boundary conditions are substituted into equation (19) to obtain algebraic equations

$$a_1 - 2a_3 + 4a_5 = 0,$$

$$a_1 + 3a_2 + 7a_3 + 15a_4 + 31a_5 - 2 = 0. \quad (22)$$

The optimal control problem is finally reduced to an optimization problem. Our task is to minimize equation (21) subject to equation (22).

The solution of the system of equations yields $a^* = \left(\frac{307}{3913}, \frac{2939}{7206}, \frac{751}{1488}, \frac{137}{12060}, \frac{67}{11917}\right)$, and $\lambda^* = \left(\frac{1190}{1079}, -\frac{5067}{824}\right)$ which is the value that minimizes $J$.

Hence, $J(a^*) = 6.14927031$ is the approximate numerical solution of the optimal control problem, which is an acceptable approximation for the exact numerical solution $J^* = 6.14925721$.

The approximate optimal state and control functions are obtained by substituting the value of $a^*$ into equations (19) and (20) as

$$x(t) = \frac{5427}{11917}t^4 + \frac{411}{1340}t^3 + \frac{27136}{18014}t^2 + \frac{12241}{11259}t + \frac{15433}{34694}$$
$$u(t) = \frac{5427}{11917}t^4 + \frac{47925}{22518}t^3 + \frac{48224}{45036}t^2 + \frac{31267}{22518}t + \frac{10118}{93056}$$

The graph of the state and control function are plotted below.

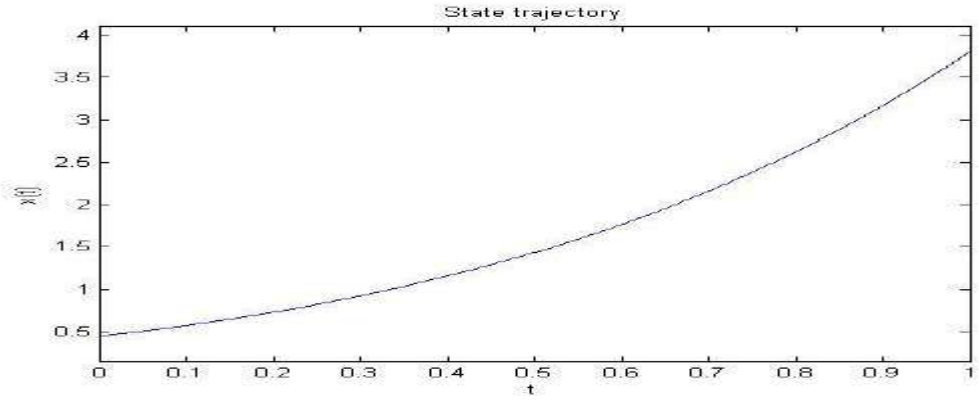


**Figure 1a.**

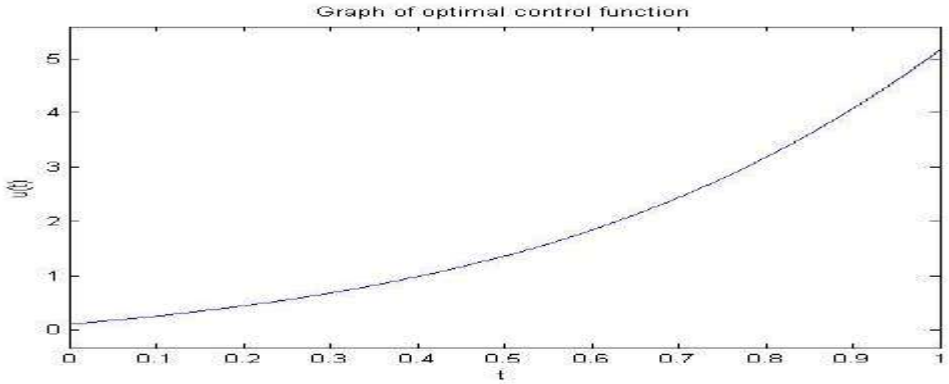


**Figure 1b.**

## 4.2. Example 2

$$Minimize \quad J = \int_0^1 \left(x^2(t) + \frac{1}{2}u^2(t)\right) dt, \tag{23}$$

$$Subject\ to\colon\ \dot{x}(t) = \frac{1}{2}x(t) + u(t),\ \ x(0) = 1. \tag{24}$$

The optimal solution is:

$$x^*(t) = \frac{2e^{3t} + e^3}{2e^{3t/2}(2 + e^3)}, \qquad u^*(t) = \frac{2e^{3t} - e^3}{2e^{3t/2}(2 + e^3)}.$$

And the exact solution for the performance index is:

$$J = \frac{e^6 + e^3 - 2}{e^6 + 4e^3 + 4} = 0.8641644978.$$

Using our approach, we approximate $x(t)$ by Fermat polynomial of order 7

$$x \approx \sum_{i=1}^{5} a_i \mathcal{F}_i,$$

$$\begin{aligned} x = {} & 729a_7t^6 + 243a_6t^5 + (81a_5 + 810a_7)t^4 + (27a_4 - 216a_6)t^3 \\ & + (9a_3 - 54a_5 + 216a_7)t^2 + (3a_2 - 12a_4 + 36a_6)t + a_1 - 2a \\ & + 4a_5 - 8a_7. \end{aligned} \tag{25}$$

From equation (24) we have:

$$\begin{aligned} u = {} & -\frac{729a_7}{2}t^6 + \left(4374a_7 - \frac{243a_6}{2}\right)t^5 + \left(1215a_6 - \frac{81a_5}{2} - 405a_7\right)t^4 \\ & + \left(324a_5 - \frac{27a_4}{2} + 108a_6 + 3240a_7\right)t^3 \\ & + \left(81a_4 - \frac{9a_3}{2} + 27a_5 - 648a_6 - 108a_7\right)t^2 \\ & + \left(18a_3 - \frac{3a_2}{2} + 6a_4 - 108a_5 - 18a_6 + 432a_7\right)t - \frac{a_1}{2} + 3a_2 \\ & + a_3 - 12a_4 - 2a_5 + 36a_6 + 4a_7 \end{aligned} \tag{26}$$

Then substituting equations (25) and (26) into equation (23) gives:

$$J(a_1, a_2, \dots a_7) = \frac{9}{8}{a_1}^2 + \frac{15}{8}a_1a_2 - \frac{9}{4}a_1a_3 - \frac{93}{16}a_1a_4 - \frac{171}{20}a_1a_5 - \frac{171}{8}a_1a_6 - \frac{3771}{28}a_1a_7 + \frac{45}{8}{a_2}^2 + \frac{399}{16}a_2a_3 + \frac{639}{20}a_2a_4 + 48a_2a_5 + \frac{16551}{140}a_2a_6 + \frac{144267}{32}a_2a_7 + \frac{2079}{40}{a_3}^2 + 231a_3a_4 + \frac{61407}{140}a_3a_5 + \frac{28179}{32}a_3a_6 + \frac{454311}{20}a_3a_7 + \frac{104499}{280}{a_4}^2 + \frac{54579}{32}a_4a_5 + \frac{477873}{140}a_4a_6 + \frac{5424159}{80}a_4a_7 + \frac{127665}{56}{a_5}^2 + \frac{805509}{80}a_5a_6 + \frac{251430813}{1540}a_5a_7 + \frac{38100861}{3080}{a_6}^2 + \frac{28615023}{80}a_6a_7 + \frac{134572923999}{40040}{a_7}^2.$$

Minimize $J(a_1, a_2, \dots a_7)$ subject to $x(t_0, a_1, a_2, \dots a_7) = x_0$. The solution is

$a^* = \left(\frac{5509605}{43424277}, -\frac{62695946}{13027283}, \frac{20145943}{14474759}, -\frac{24125360}{13027283}, \frac{35048278}{14474759}, -\frac{24431921}{13027283}, \frac{59827196}{43424277}\right)$ and $\lambda^* = -\frac{70048008}{40529325}$.

The approximate solution is $J(a^*) = 0.864164498$ which agrees with the exact solution.

| | Method | J | Error |
|---|---|---|---|
| Exact Value | | 0.8641644978 | 0 |
| Kafash, B. and Delavarkhalafi, A. | Restarted State Parameterization | 0.8643546452 | $1.9e^{-04}$ |
| Eisa, B.M. and Awadalla, T.A. | Legendre | 0.8641645132 | $1.5e^{-09}$ |
| This Research | Fermat | 0.8641644978 | 0 |

**Table 1.** Comparison of the optimal value with other methods

We calculate the state and control variables as:

$$x(t) = \frac{2895}{2882}t^6 - \frac{1642}{3603}t^5 + \frac{7468}{3603}t^4 - \frac{5174}{1126}t^3 + \frac{5066}{4504}t^2 - \frac{1729}{1407}t + 1$$

$$u(t) = -\frac{2895}{5765}t^6 + \frac{1169}{1407}t^5 - \frac{3732}{1126}t^4 + \frac{4769}{4504}t^3 - \frac{8741}{4504}t^2 + \frac{6449}{2252}t - \frac{2551}{1476}.$$

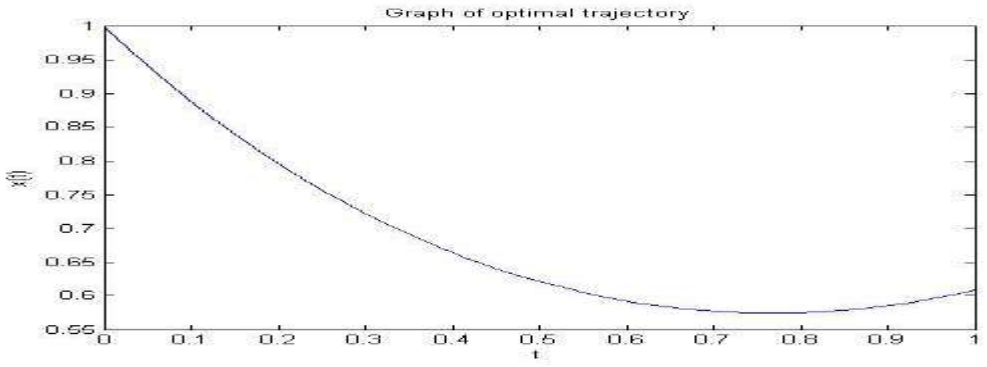


**Figure 2a.**

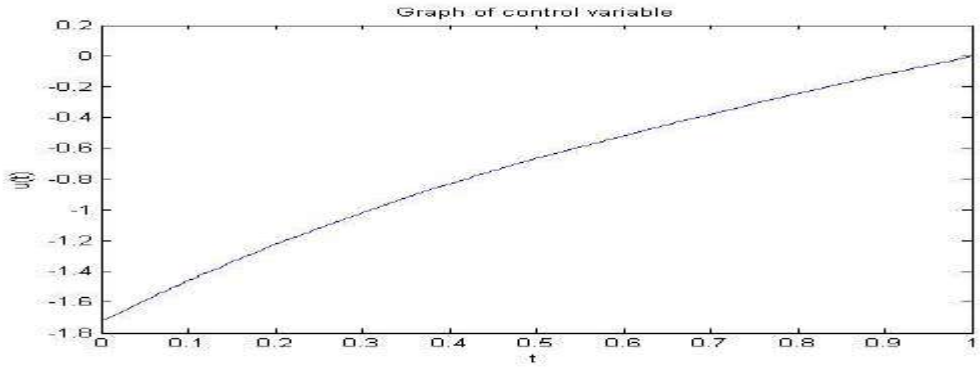


**Figure 2b.**

## 5. Convergence analysis

The convergence of parameterization method is generally based on Weierstrass Approximation Theorem, which have been rigorously proved by many researchers.

**Theorem 1.** (Weierstrass Approximation Theorem). Let $f \epsilon C([a,b],\mathbb{R})$. Then, there is a sequence of polynomials, $P_n(x)$, that converges uniformly to $f(x)$ on $[a,b]$.

**Proof**: See [6], [15].

**Theorem 2.** (Kafash and Delavarkhalafi, 2014). If, $\alpha_n = inf_{Q_n} J$, for $n = 1,2, \ldots$, then $lim_{n\to\infty}\alpha_n$, where $\alpha = inf_Q J$.

**Proof**. Let $\hat{\alpha} > J(X(.))$ be the limit of non-increasing sequence $\{\alpha_n\}$. If $\hat{\alpha} > \alpha$, then $\varepsilon = \frac{\hat{\alpha}-\alpha}{2} > 0$, so; there exist $X(.)\epsilon Q,\ J\big(X(.)\big) < \varepsilon + \alpha = \frac{\hat{\alpha}-\alpha}{2} + \alpha = \frac{\hat{\alpha}+\alpha}{2} < \hat{\alpha}$ such that $\hat{\alpha} > J(X(.))$, which contradicts the continuity of $J$ and Theorem 1.

## 6. Conclusion

This paper proposed numerical approach to solve optimal control problems based on state parameterization. We showed that Fermat polynomials can be used to approximate the state variables of optimal control problems which convert optimal control problems into quadratic programming problem. From the numerical results obtained, we can conclude that our proposed approach gives better and reliable result when compared with other methods.

## References


[1] Eisa B.M. and Awadalla T.A. (2017). Optimal state and control variables parameterization. International Journal of Trend in Research and Development, 4(2): 2394-2433.

[2] El-Kady M. and Elbarbary E.M.E. (2002). A Chebyshev expansion method for solving nonlinear optimal control problems. Journal of Computational and Applied Mathematics, 129: 171-182.

[3] Highfill J. and McAsey M. (2001). An application of optimal control to the economics of recycling. Society for Industrial and Applied Mathematics, 43(4): 679-693.

[4] Jaddu H.M. (2002). Direct solution of nonlinear optimal control problems using quasilinearization and Chebyshev polynomials. Journal of Franklin Institute, 339: 479-498.

[5] Kafash B. and Delavarkhalafi A. (2014). Restarted state parameterization method for optimal control problems. Journal of Mathematics and Computer Science, 14: 151-161.

[6] Kafash B., Delavarkhalafi A. and Karbassi S.M. (2012a). Application of Chebyshev polynomials to derive efficient algorithms for the solution of optimal control problems. Journal of Scientifica Iranica, 19(3): 795-805.

[7] Kafash B., Delavarkhalafi A. and Karbassi S.M. (2012b). Numerical solution of nonlinear optimal control problems based on state parameterization. Iranian Journal of Science and Technology, 36(3): 331-340.

[8] Kafash B., Delavarkhalafi A., Karbassi S.M. and Boubaker K. (2014). A numerical approach for solving optimal control problems using the Boubaker polynomials expansion scheme. Journal of Interpolation and Approximation in Scientific Computing, 2014: 1-18.

[9] Lenhart S. and John T.W. (2007). Optimal control applied to biological models. Mathematical and Computational Biology. Chapman and Hall, CRC press, London.

[10] Mehdi R. (2016). Numerical solution of optimal control problems using a new second kind Chebyshev wavelet. Journal of Computational Methods for Differential Equations, 4(2), 162-169.

[11] Mehne H.H. and Borzabadi A.H. (2006). A numerical method for solving optimal control problems using state parameterization. Journal of Numerical Algorithm, 42: 165-169.

[12] Patterson M. (2013). Efficient solutions to nonlinear optimal control problems using adaptive mesh orthogonal collocation methods. Ph.d. Dissertation. University of Florida.

[13] Phelps C. and Kaminer I. (2014). Consistent approximation of a nonlinear optimal control problem with uncertain parameters. Automatic, 50(12): 2987-2997.

[14] Ping C and Sardar M.N.I. (2005). Optimal control models in finance: a new computational approach. Springer.

[15] Tohidi E., Samadi O.R.N., and Farah M.H. (2011). Legendre approximation for solving class of nonlinear optimal control problems. Journal of Mathematical Finance, 1: 8-13.

**International Journal of Mathematical Analysis and Modelling**
**Volume 5, Issue 1, May 2022, Pages 69 – 76**

# CATANOVA analysis of academic performance of pupils in primary schools and districts - a tool for conflict resolution

**D. M. O. Omebo[*], A. Y. Emmanuel[†], and G. Aimufua[‡]**

**Abstract**

This paper is an extract of the research findings that was carried out in Ofu local government area of Kogi state in 2021 which was used to resolve the conflict that broke out as a result of the establishment of Government Special Science College by the Kogi state Government. The bone of contention then was which of the three districts of the local government should have the new special science college. This necessitated the research to find out if performance depends on the district or not. An analysis of variance for categorical data (CATANOVA) was used in carrying out the test. It was discovered that performance depends on the district, and that pupils from Igalaogba district performed better than the other two districts. Hence the new Government Special Science College, should be sited in this particular district. All the findings were based on the performance of pupils in primary six using common entrance examination results for 2019 since there was no common entrance examination for 2020 due to covid-19 pandemic.

***Keywords***: districts; Chi- square; catanova; performance

## 1. Introduction

The growth of statistics has made itself felt in almost every phase of human endeavor. Statistics provides models that are needed to study situations involving uncertainties. One of such is that which confronted Ofu Local government area of Kogi state in 2021.

[*] Corresponding Author: Department of Statistics, Federal University of Lafia, PMB 146, Lafia, Nigeria; damebo2002@yahoo.co.uk

[†] Department of Mathematics, Federal University of Lafia, PMB 146, Lafia, Nigeria; atanyiemmanuel@gmail.com

[‡] Department of Computer Science, Nasarawa State University, Keffi, Nasarawa, Nigeria; aimufuagio@yahoo.com

The Kogi state government of Nigeria established a new special science college to be located in Ofu local government Area of the state. As usual every district began to give reasons why it should be located in their district. All efforts to result this problem to no avail. This necessitated a research to find out if performance is dependent on the district or not. This is because the district that performed better will be able to feed the college with the desired quality and quantity of students needed by the new school. There are three districts in Ofu Local Government. These include Ugwolawo, Igalaogba and Itobe districts.

This study is therefore aimed at finding out if performance across the districts is the same or not. Hence, this study investigates the comparative academic performances of primary six pupils across the districts of Ofu local government area of Kogi state.

## 1.1. Aim and objectives of the study

i. To ascertain if performance is dependent on districts.
ii. To determine which of the districts should have the school.
iii. To resolve the conflict already created by this agitation.

## 1.2. Nature and scope of study

There are 53 primary schools in Ofu Local Government Area of Kogi State out of which samples of 20 primary schools were taken. The primary schools in kogi state like their counterparts in other states are controlled by the state primary Education Board which is now called state universal basic Education Board (SUBEB) which in turn is controlled by the state ministry of education. It is this state ministry of education that provides an approved syllabus to be followed by the primary schools and at the end of the six-year programme, the pupils sit for common entrance examination which qualify them to go to secondary schools. The examination is made up of three papers. These are: Paper 1(English language), paper 2 (Mathematics) and Paper 3 (General paper). At the end of the examination, successful candidates are classified into five groups – Distinction(A), Good (B), Credit (C), Fair (D) and Pass (E). Similarly, unsuccessful candidates are awarded (F). All findings are based on the analysis of this examination results from the sampled schools from the various districts.

## 1.3. Sampling techniques

Out of the 53 primary schools in Ofu Local government Area, I sampled 20 primary schools according to the classification below.

Sampling distribution of the primary schools in Ofu local government area

| Districts | Number of schools |
|---|---|
| Ugwolawo | 9 |
| Igalaogba | 6 |
| Itobe | 5 |

The researcher used stratified random sampling techniques to represent the entire Ofu Local Government Area. The local Government has three districts so that communities were used as the

stratifying factor. Ofu Local Government Area comprises of eighteen communities, which is grouped into three districts forming the strata, from which simple random sampling was used. Ugwolawo district consists of Ugwolawo, Ogegume, Ojofa, Obagwu, Umomi, Akpagidigbo, Alome, Ikagbo, and Ugbogbo, while Igalaogba district is made up of Aloma, Igah, Ejule, Ogbonicha, Ogbulu and Ikeje. Finally, Itobe district comprises of Ojodu, Adumu, Aloji, Itobe and Ochadamu. Also, I used proportional allocation of sample size according to the weight (number of the communities that each group consists in terms of number of primary schools in each group).

## 2. Literature review

Even though many studies have been carried out to ascertain the dependence of performance on one factor or the other, majority of them if not all were carried out using the results from examinations such as first school leaving certificate (FSLCE), Senior school certificate examination (SSCE), University matriculation Examinations (UME) among others as their only source of data for the analysis which this study frown at due to gross examination malpractice usually associated with the conduct and marking of the scripts by the authorities concern.

In order to ascertain if boys are more brilliant than girls, [5] investigated into the performance of boys and girls in a sample of 32 primary schools Nsukka Educational Zone. From the report of his findings, he asserted that boys are more brilliant than girls all within primary school age.

Another research carried out by [1] on how the shift system affects the academic performance of primary school pupils in Enugu using qualitative data based on 1978 only, he came up with the following results: first, that the morning session pupils performed better than the afternoons. Secondly, that this disparity in performance was as a result of the fact that shift one had relatively more qualified and trained teachers than shift two. [12] carried out research on school location and academic performance of pupils in English language in primary schools. He reported that there is a significant difference in the academic performance of pupils in urban and rural primary schools in English language.

## 3. Methodological framework

The methodological framework for this study is a two-way analysis of variance for categorical data (CATANOVA).

### 3.1. A two-way catanova with chi-square tests for interaction

Consider a two-way experimental situation with a k-dimensional vector of responses
$\{(n_{ijk})\ K, i=1,2,\ldots I, j=1,2,\ldots,J\}$ recorded in frequencies in the $(ij)^{th}$ plot. We assume a multinomial probability model, namely,

$\Pr(\{n_{ijk}\}k/\{\pi_{ijk}\}\ k,n_{ij}) = nij\ !/\ \prod_k\{nijk!\}$ $(\pi ijk)\prod_k(n^{ijk}$
$nijk = 0,1,\ldots,n_{ij}$
$0 \leq \pi_{ijk} \leq 1$
$Nij = \sum_k nijk$ is held fixed

Nijk, ni/ j/ k are independent ∀ i≠ i/

The hypothesis to be tested are:
HR: $\prod ijk == \prod jk$ , there is no row effect.
HC: : $\prod ijk == \prod ik$ , there is no column effect.
HRC: : $\prod ijk == \prod k$ , there is no row x column interaction.

The expectation of the sample estimate of : $\prod ijk$ is given by the linear model
E ($\prod^{\wedge} ijk$) $\boldsymbol{\mu}$k + Tik + Bjk + $\boldsymbol{\lambda}$ijk,
where $\boldsymbol{\mu}$k, Bjk and $\boldsymbol{\lambda}$ijk assume their usual meaning of constant, row effect, column effect and interaction respectively. The hypothesis, HR, HC, and HRC will be seen to be respectively equivalent to
Hi: Tik = 0 ∀i, HB: Bjk = 0 ∀j and $\boldsymbol{\lambda}$ijk = 0 ∀i,j.

The parameters: $\prod ijk$ may be considered fixed or random with probability density h( $\prod ijk$), over {0,1} depending on whether I and J are random or not [13,14]. Specially,

g( $\prod ijk$) if I and J are random, o≤ $\prod ijk$≤ 1,
h( $\prod ijk$) = g ($\prod jk$) if I is fixed and J random 0≤ $\prod jk$≤ 1,
g($\prod ik$) if I is random and J fixed, 0≤ : $\prod ik$ ≤ 1.

We shall now consider the sum of squares (SS) for {nijk }k. This may be obtained, [6,7,8,9,10,11] also [2,3], as the trace of the sample variance- covariance matrix. That is

$$SS(nijk) = \Sigma_k \text{ var } (nijk).$$

Upon further simplification, we have that
TSS = n - $\sum_k$ n2..k/n , as the total sum of squares
BRSS = n - $\sum_{ik}$ n2i.k/ni , as the between row sum of squares
BCSS = n - $\sum_{jk}$ n2.jk/nj , as the between column sum of squares
WUSS = n - $\sum_{ijk}$ n2ijk/nij, as the within unit sum of squares,
where

N = $\sum_i$ ni = $\sum_j$ nj $\sum_{ij}$ ni j
RSS = TSS – BRSS = $\sum_k$ n2i.k/ni - $\sum_k$ n2..k/n
CSS = TSS – BCSS = = n - $\sum_{jk}$ n2.jk/nj - $\sum_k$ n2..k/n
NSS = BRSS + BCSS – TSS – WUSS
= n - $\sum_{ijk}$ n2ijk/nij - $\sum_{ik}$ n2i.k/ni - $\sum_{jk}$ n2.jk/nj + $\sum_k$ n2..k/n.

We may reject HR, HC and HRC respectively at specified ά-level of error if
$\chi^2_R \geq \chi^2(\acute{\alpha})_{(I-1)(J-1)(K-1)}$,
where
$\chi^2_R$ = (K-1)(n-1)RSS/ TSS
$\chi^2_C$ = (K-1)(n-1)css/TSS

$\chi^2_{NT}$ = (K-1)(n-1)NSS/TSS

## 3.2. Materials and methods

Below is the data layout for a two – way analysis of variance for categorical data (CATANOVA). This was given by [4]

| | Districts | Ugwolawo | | | | | | | Igalaogba | | | | | | | Itobe | | | | | | |
|---|---|---|---|---|---|---|---|---|---|---|---|---|---|---|---|---|---|---|---|---|---|---|
| i | Responses | A | B | C | D | E | F | T | A | B | C | D | E | F | T | A | B | C | D | E | F | T |
| | Males | $n_{111}$ | $n_{112}$ | $n_{113}$ | $n_{114}$ | $n_{115}$ | $n_{116}$ | $n_{11.}$ | $n_{121}$ | $n_{122}$ | $n_{123}$ | $n_{124}$ | $n_{125}$ | $n_{126}$ | $n_{12.}$ | $n_{131}$ | $n_{132}$ | $n_{133}$ | $n_{134}$ | $n_{135}$ | $n_{136}$ | $n_{13.}$ |
| | Females | n211 | n212 | n213 | n214 | n215 | n216 | n21. | n221 | n222 | n223 | n224 | n225 | n226 | n22. | n231 | n232 | n233 | n234 | n235 | n236 | n23. |
| | n.jk | n.11 | n.12 | n.13 | n.14 | n.15 | n.16 | n.1. | n.21 | n.22 | n.23 | n.24 | n.25 | n.26 | n.2. | n.31 | n.32 | n.33 | n.34 | n.35 | n.36 | n.3. |

**Table 1**: Data layout for two way catanavo

| | Ugwolawo | | | | | | | Igalaogba | | | | | | | Itobe | | | | | | T | | | | | | | |
|---|---|---|---|---|---|---|---|---|---|---|---|---|---|---|---|---|---|---|---|---|---|---|---|---|---|---|---|---|
| sex | A | B | C | D | E | F | ni1. | A | B | C | D | E | F | ni2. | A | B | C | D | E | F | ni3. | ni.k | | | | | | ni.. |
| male | 139 | 62 | 58 | 10 | 55 | 83 | 407 | 71 | 75 | 45 | 24 | 36 | 52 | 303 | 107 | 52 | 53 | 5 | 45 | 75 | 337 | 317 | 189 | 156 | 39 | 136 | 210 | 1047 |
| fem-ale | 80 | 51 | 48 | 11 | 50 | 85 | 325 | 39 | 48 | 29 | 37 | 39 | 51 | 243 | 43 | 20 | 26 | 6 | 30 | 64 | 189 | 162 | 119 | 103 | 54 | 119 | 200 | 757 |
| Total | 219 | 113 | 106 | 21 | 105 | 168 | 732 | 110 | 123 | 74 | 61 | 75 | 103 | 546 | 150 | 72 | 79 | 11 | 75 | 139 | 526 | 479 | 308 | 259 | 93 | 255 | 410 | 1804 |

**Table 2**: Two – way catanova test on performance of male and female pupils of primary in Ofu local Government Area of Kogi State in common entrance examination for the year 2021 DISTRICTS

Total sum of squares (TSS) = n - $\sum_k n2..k/n$

= 1804 - $(479^2 + 308^2 + 259^2 + 93^2 + 255^2 + 410^2)/ 1804$

= 1804 – 633160/1804

= 1804 – 350.9756

TSS = 1453.0244.

Between sex sum of squares (BSSS) = n - $\sum_{ik} n2i.k/n\,i$

= 1804 – $(317^2 + 189^2 + 156^2 + 39^2 + 136^2 + 210^2)/1047 + (162^2 + 119^2 + 103^2 + 54^2 + 119^2 + 200^2) / 757$

= 1804 - (214.5778 + 142.7886)

= 1804 - 357.3664

BRSS = 1446.6336.

Between districts sum of squares (BDSS) = n - $\sum_{jk} n2.jk/nj$

= 1804 - $(219^2 + 113^2 + 106^2 + 21^2 + 105^2 + 168^2)/ 732 + (110^2 + 123^2 + 74^2 + 11^2 + 75^2 + 139^2)/526$

= 1804 - (152.5355 + 96.4469 + 112.1521)

= 1804 - 361.1345

BDSS = 1442.8655.

Row sum of squares (RSS) = TSS – BDSS

= 1453.0244 – 1446.6336

= 6.3908

RSS = 6.3908.

Column sum of squares (CSS) = TSS – BDSS

= 1453.0244 - 1442.8655

= 10.1588

| Source of variance | Degree of freedom | Sum of squares |
|---|---|---|
| Row or factor levels or sexes | 1 | 6.3908 |
| Districts | 2 | 10.1588 |
| Sex x districts | 10 | 1.3334 |
| Residual | 1790 | 1435.1414 |
| Total | 1803 | 1453.0244 |

**Table 3**: Catanova table

Ho: Performance is independent of the districts.
H1: Performance is dependent on the districts.

The test statistic = $\chi^2_{cal}$ = k – 1(n-1)CSS/ TSS

= (6-1)1804 – 1) 10.1588/ 1453.0244

= 63.0282.

$\chi^2_{tab} = \chi^{2\,(0.05)}_{(J-1)(K-1)} = \chi^{2\,(0.05)}_{(3-1)(6-1)} = 18.307.$

Decision Rule: Reject Ho if $\chi^2_{cal}$ is greater than $\chi^2_{tab}$

Conclusion:
Since $\chi^2_{cal} = 63.0283 > \chi^2_{tab} = 18.307$, we reject Ho and conclude that performance depends on the districts.

To determine which of the districts perform best, we compute the proportions of students that passed and failed in each districts as follows:
Proportion of pupils in Ugwolawo district that passed is
$P_{ug\ passed}$ = nug pass/ Nug 0.77.
Proportion of pupils in Ugwolawo district that failed is
$P_{ug\ failed}$ = nug failed/Nug = 168/732 = 0.23.
Proportion of pupils in Igalaogba district that passed is
$P_{ig\ passed}$ = nIg passed/NIg= 443/546 = 0.81.
Proportion of pupils that failed in Igalaogba is
$P_{ig\ failed}$ = nig failed/Nig = 103/546 = 0.19.
Proportion of pupils in Itobe that passed is
$P_{It\ passed}$ = nIt passed/NIt = 387/526 = 0.74.
Proportion of pupils in Itobe that failed is
$P_{it\ failed}$ = nIt failed/NIt = 139/526 = 0.26.

The proportions of pupils that passed in each district in the decreasing order is as follows:
Igalaogba = 0.81
Ugwolawo = 0.77
Itobe = 0.74.

Similarly, the proportion of pupils that failed in each district in the increasing order is as follows:
Igalaogba = 0.19
Ugwolawo = 0.23
Itobe = 0.26.

## 4. Conclusion

From the foregoing, it shows that performance depends on the district. This means that performance of any chosen pupil depends on which district the pupil comes from. From the result obtained, pupils from Igalaogba district performed better than the other two districts with the Itobe district having the poorest. The researcher therefore recommended that the government special science college should be located at Igalaogba district.

## References


[1] Ajuwe (1990). Shift system and academic performance on primary schools in Enugu state (unpublished research), 11-14.

[2] Anderson T. W. (1958). Catanova for multidimensional contingency tables: Nominal-scale response, 56.

[3] Anderson T. W. (1958). An introduction to multivariate analysis. John Wiley, New York.

[4] Fisher R. A. (1970). Statistical methods for research workers 14th Edition, 4-6.

[5] Oladele F. (1972). Performance of boys and girls' primary schools Nsukka Educational Zone (Unpublished research), 7-9.

[6] Onukogu I.B. (2014). Analysis of variance of categorical data-nested designs. Journal of Statistics: Advances in Theory and Applications, 12:109-116.

[7] Onukogu I.B. (1985) Reasoning by analogy from ANOVA to CATANOVA, Biom J., 27:839-849.

[8] Onukogu I.B. (2014). Analysis of variance of categorical data-nested designs. Journal of Statistics: Advances in Theory and Applications, 12:109-116.

[9] Onukogu I.B. (1982). One degree of freedom for non-additivity in a contingency table and its multivariate extension, Biometrical Journal, 115-125.

[10] Onukogu I.B. (1981). One degree of freedom for interaction in a two-way classification without replication. Biometrical journal, Vol. 24 (8): 1-7.

[11] Onukogu I.B. (1982). An analysis of variance of nominal data. Biometrical journal., 7-8.

[12] Peter H.L. (2021). School location and academic performance of pupils in English language in primary schools. Onlineproject.com.ng, 4-5.

[13] Scheffe H. (1959). The analysis of variance. Wiley, New York, p8-10.

[14] Scheffé H. (1959). The analysis of variance. Wiley: New York, p477.

**International Journal of Mathematical Analysis and Modelling**
**Volume 5, Issue 1, May 2022, Pages 77 – 89**

# Numerical solutions of higher-order second kind Fredholm integro-differential equations with modified homotopy analysis method

**M. D. Aloko[*], J. A. Osilagun[†], and Johnson D. Audu[‡]**

**Abstract**

We present a modified Homotopy Analysis Method (MHAM) for solving higher-order nonlinear Fredholm integro-differential equations. This approach utilizes the homotopy principles but introduces two auxiliary parameters to construct a modified homotopy. The Parameters make it easier to analyze linear and strongly nonlinear problems without linearizing the problems directly. The series solution including the recurrence relations are carefully developed and presented explicitly without the need of applying any discretization. The error estimates are tabulated while the solution plots are graphically displayed. When compared with exact solutions and other traditional methods, our scheme proved reliable, efficient, and cost-effective.

***Keywords***: homotopy; higher order; Fredholm- integro-differential equations; decomposition.

## 1. Introduction

Nonlinear Fredholm equations naturally serve as model equations for many memory-dependent dynamical systems. These include population dynamics, epidemiology, and diffusion [20]. As a result, a lot of research has been directed towards approximating different kinds of Nonlinear Fredholm equations. Cubic spline collocation methods have recently been used for Integro-Differential equation systems [18], convolution integral approach [12], application of Legendre polynomials [18], Taylor collocation [18,6], and method of Chebyshev's polynomials [14]. Maleknejadel et al applied Berstein Operation Matrix to solve higher order-Volterra-Fredholm Integral-Differential equations [17]. More recent, high-order approximations techniques are employed in [4, 5]. Parameter variation approach for different problems related to Integro-differential equation systems is presented in [16]. In [18], a

[*] National Agency for Science and Engineering Infrastructure, FMST, Abuja, Nigeria
[†] Department of Mathematics, University of Lagos, Lagos, Nigeria
[‡] Corresponding Author: King Fahd University of Petroleum and Minerals, Dhahran, Saudi Arabia; Johnsonaudu@gmail.com

new modified Adomian method is presented while a numerical solution for the Taylor expansion method for Fredholm integral equations is contained in [19].

In this paper, we propose and implement an iterative scheme modified Homotropy Analysis Method (MHAM) to approximate the following integro-differential equation.

$$\mathrm{u}^{(\mathrm{m})}(x) = \beta(x) + \mu \int_{\mathrm{a}}^{\mathrm{g(x)}} \mathrm{G}(x, \mathrm{s})\mathrm{u}^{(n)}(\mathrm{s})\,\mathrm{ds}, \quad (1)$$

subject to the initial conditions

$$\mathrm{u}^{(k)}(0) = c_k,$$

where $c_k, k = 0, 1, \ldots (m-1)\,,\ k, n\,,\ and\ \ m$ are integers with $n < m$.

It is worthy to note that some complicated problems that cannot be handled with our classical method are covered in [13, 3, 9].

In the remainder of this section, we present a general framework of the problem. In Section 2, the main ideas of homotopy including the series solutions and recurrence equations are presented while our modified homotopy scheme is provided in Section 3. In Section 4, we numerically implemented our scheme on some higher-order integro-differential equations and compared our approximate solution with the exact solution and conventional HAM.

## 2. Homotopy analysis method (HAM)

The Homotopy analysis method employs the concepts of homotopy from topology to generate a convergent series solution from nonlinear systems, however, instead of using the traditional homotopy, a nonzero auxiliary parameter $h$, referred to as the convergence –control parameter was introduced and nonzero auxiliary function $H(x)$ is used to construct the homotopy Analysis Method. We consider the following differential equation

$$\aleph u(x) = 0, \quad (2)$$

where, $\aleph$ is non-linear operator, $u(x)$ is an unknown function of independent variable $x$. Let $u_0(x)$ denotes an initial approximation of $u(x)$ and $\mathcal{L}$ denotes an auxiliary linear operator with the property:

$$\mathcal{L}[\beta(x)] = 0 \text{ when } \beta(x) = 0. \quad (3)$$

Using equation (1), we define the non-linear operator as

$$\aleph[u(x)] = u^{(m)}(x) - \beta(x) - \mu \int_{\mathrm{a}}^{\mathrm{g(x)}} \mathrm{G}(x, \mathrm{s})\mathrm{u}^{(n)}(\mathrm{s})\,\mathrm{ds}\,. \quad (4)$$

Let $\mathcal{L} = I\ and\ H(x) = 1$, then to construct the so- called homotopy method, the following family of equation is used

$$(1-r)\mathcal{L}[\varphi(x; r, h) - u_0(x)] = rhH(x)\aleph[\varphi(x; r, h)], \quad (5)$$

where, $r \in [0,1]$ is an embedding parameter, $\varphi(x,r)$ is a function of $x$ $and$ $r$, $h$ is a non-zeros auxiliary parameter and $H(x)$ is a non-zero auxiliary function. When $r = 0$, from equation (5), we have

$$\mathcal{L}[\varphi(x;0,h) - u_0(x)] = 0. \tag{6}$$

It follows that

$$\left.\begin{array}{l} \phi(x;0,h) = u_0(x), \\ r = 1, \\ \aleph[(\phi(x;1,h)] = 0; x \geq 0, \\ subject \\ \phi(x;1,h) = 0. \end{array}\right\} \tag{7}$$

Since $h \neq 0, H(x) \neq 0$ and from the definition in equation (4), equations (7) are equivalent provided $\varphi(x;1,h) = u(x)$.

As the embedding parameter $r$ increases from 0 to 1, the solution $\varphi(x;r)$ of equation (2) depends upon the embedding parameter $r$ and varies from the initial approximation $u_0(x)$ to the solution $u(x)$ of equation (2), see [3]. In topology, such a kind of continuous variation is called deformation. The zeroth-order deformation for equation (1) is constructed as

$$\aleph[u(x)] = u^{(n)}(x) - \beta(x) - \mu \int_a^{h(x)} k(x,s)u^{(m)}(s)\,ds\,. \tag{8}$$

$$\left.\begin{array}{c} (1-r)[\varphi(x;r,h) - u(x;0,h)] = rh(x)\left[\frac{\partial^n \varphi(x;r,h)}{\partial x^n} - \beta(x) - \mu \int_a^{h(x)} k(x,s)u^{(n)}(s)\,ds\right], \\ or \\ (1-r)[\varphi(x;r,h) - u_0(x)] = rh(x)\aleph[\varphi(x;r,h)]. \end{array}\right\} \tag{9}$$

Expand $\varphi(x;r,h)$ in Taylor series with respect to $r$ , we get

$$\varphi(x;r,h) = \varphi(x;0,h) + \sum_{m=1}^{\infty} \frac{r^m}{m!} \frac{\partial^m}{\partial r^m} \varphi(x;r,h)\Big|_{r=0}. \tag{10}$$

Let $u_m(x,h) = \frac{1}{m!}\frac{\partial^m \varphi(x;r,h)}{\partial r^m}|_{r=0}$ . Using equations (5) and (6), if the auxiliary linear operator, the initial approximation, the auxiliary parameter $h$ and the auxiliary function are properly chosen, the series equation (9) converges at r=1, then we have

$$\phi(x;r,h) = u_0(x) + \sum_{m=1}^{\infty} u_m(x,h)r^m\,. \tag{11}$$

Equation (11) provide a relationship between the initial approximation $u_0(x)$) and the exact solution $u(x)$ by means of the terms $u_m(x)$ $(m = 1, 2, \dots)$ which are unknown and defining the vector $\vec{u}_n = \{u_0(x), u_1(x), \dots u_n(x)\}$.

Differentiating equation (9) with respect to $r$ yields

$$(1-r)\frac{\partial\varphi(x;r,h)}{\partial \mathrm{r}} - \varphi(x;r,h) - u_0(x) = h\aleph[\varphi(x;r,h)] + rh\frac{\partial\aleph(\varphi(x;r,h))}{\partial \mathrm{r}}. \tag{12}$$

Setting $r = 0$, equation (12) yields

$$\frac{\partial\varphi(x;r)}{\partial \mathrm{r}}|_{r=0} = h\aleph[\varphi(x;r)]|_{r=0}. \tag{13}$$

Differentiating equation (11) with respect to $r$, gives

$$\frac{\partial\varphi(x;r,h)}{\partial r} = \sum_{m=1}^{\infty} mu_m(x,h)r^{m-1},$$
$$= u_1(x,h) + \sum_{m=2}^{\infty} mu_m(x,h)r^{m-1}. \tag{14}$$

Using equation (14) and equation (13), the deformation equation of first-order is obtained as:

$$\left.\begin{array}{c} u_1(x,h) = h\aleph(u_0(x,h)), \\ u_1(x,h) = h\left(u_0(x) - \beta(x) - \mu\int_{\mathrm{a}}^{\mathrm{h(x)}}(\mathrm{k}(x,\mathrm{s})u_0{}^{(n)}(\mathrm{s})\,ds\right). \end{array}\right\} \tag{15}$$

Differentiating equation (12) with respect to $r$ and setting $r = 0$,

$$-2\frac{\partial\varphi(x;r,h)}{\partial \mathrm{r}} + (1-r)\frac{\partial\varphi(x;r,h)}{\partial \mathrm{r}} = 2h\frac{\partial\aleph(\varphi(x;r,h))}{\partial \mathrm{r}} + rh\frac{\partial^2\aleph(\varphi(x;r,h))}{\partial \mathrm{r}^2}.$$

Using equation (14) and equation (15), to obtain

$$-2u_1(x,h) + \sum_{m=2}^{\infty} mu_m(x,h)r^{m-1} + (1-r)[2u_2(x,h) + \sum_{m=2}^{\infty} m(m-1)u_m(x,h)r^{m-2}$$
$$= -2h[u_1(x,h) + \sum_{m=2}^{\infty} mu_m(x,h)r^{m-1}] - 2h\aleph(u_0(x,h) + qh\frac{\partial^2\aleph(\varphi(x,r)}{\partial r^2}.$$

Setting $r = 0$, the second-order deformation equation is also obtained as

$$u_2(x,h) = (1+h)u_1(x,h) - \mathrm{h}\mu(\int_{\mathrm{a}}^{\mathrm{h(x)}}(\mathrm{k}(x,\mathrm{s})u_0{}^{(n)}(\mathrm{s}))ds).$$

To determine the $m^{th}$ -order deformation, differentiating equation (11) $m$ –times with respect to $r$ and then setting $r = 0$, using equations (13)-(15), we have

$$\frac{\partial^m}{\partial r^m}(1-r)[\varphi(x;r,h)-u_0(x)]$$
$$=\frac{\partial^m}{\partial r^m}\left(rh\aleph[\varphi(x;r,h)]-\beta(x)-\mu\int_{\mathrm{a}}^{\mathrm{h(x)}}\mathrm{k}(x,\mathrm{s})\mathrm{u}^{(n)}(x;r,h)\right)ds.$$

Substituting the homotopy series and dividing by $m!$, then $m-order$ deformation equation is obtained as

$$u_m(x,h)=(1+h)u_{m-1}(x)-\frac{\mathrm{h}}{(m-1)!}\int_{\mathrm{a}}^{\mathrm{h(x)}}\frac{\partial^{m-1}\varphi(x;r)}{\partial r^{m-1}}\mathrm{k}(x,\mathrm{s},)\mathrm{u}^{(n)}(x;r)|_{r=0}ds. \quad (16)$$

A partition of $[\mathrm{a},h(x)]$, can be chosen as follows:

$a=x_1<x_2<\cdots<x_n=h(x)=b$ and $u_m(x_i)$ is computed as
$$u_m(x_i,h)=(1+h)u_{m-1}(x_i,h)$$
$$-\frac{1}{(m-1)!}\int_{\mathrm{a}}^{\mathrm{h}(x_i)}\frac{\partial^{m-1}\varphi(x;r,h)}{\partial r^{m-1}}\mathrm{k}(x,\mathrm{s})\mathrm{u}^{(n)}(x;r,h)|_{r=0,\ x=x_i}ds.$$

Using equations (6) and (7), taking inverse $\mathcal{L}^{-1}$, (9) yields

$$\left.\begin{array}{c}u_0=u(x;0,h)=\mathcal{L}^{-1}(\beta(x))=b_i\\ and\\ u(x;1,h)=u(x)\end{array}\right\}. \quad (17)$$

Also equation (16) can be expressed as

$$\mathcal{L}[u_m(x)-x_m u_{m-1}(x)]=hR_m\vec{u}_{m-1}(x). \quad (18)$$

where $R_m\vec{u}_{m-1}=\frac{1}{(m-)!}\frac{\partial^{m-1}\aleph[\varphi(x;r,h)]}{\partial r^{m-1}}|_{r=0}$ and $x_m=\begin{cases}0, & m\le 1\\ 1, & m>1\end{cases}$. (19)

Using equation (18)

$$u_m(x)=(1-x_m)u_{m-1}(x)+h\mathcal{L}^{-1}H(x)R_m\vec{u}_{m-1}(x). \quad (20)$$

## 3. Derivation of modified homotopy analysis method (MHAM)

A new recursion algorithm is obtained for $u_m(x)$ such that the initial approximant $u_0(x)=b_i$ obtained is decomposed into two parts $b_i(x)=b_{0i}(x)+b_{1i}(x)$ and replacing the two components by a series say $b_l$ of infinite component expressed as: $b_l(x)=\sum_{n=0}^{\infty}b_{in}(x)$.

Taking $\mathcal{L}^{-1}$ of equation (18) and using equation (17).

The scheme for the Modified Homotopy Analysis Method (MHAM) is constructed as

$$\left.\begin{aligned} u_0 &= b_{10}(x), \\ u_1 &= b_{11}(x) + h\mathcal{L}^{-1}R_m\vec{u}_0(x), \\ u_2 &= b_{12}(x) + h\mathcal{L}^{-1}R_m\vec{u}_1(x), \\ u_3 &= b_{13}(x) + h\mathcal{L}^{-1}R_m\vec{u}_2(x), \\ &\vdots \\ u_m &= b_{i,m}(x) - h\mathcal{L}^{-1}R_m\vec{u}_{m-1}(x), m = 2,3, \dots \end{aligned}\right\} \quad (21)$$

It easy to obtain where the $m-th$ approximation of $u(x)$ for $m \geq 1$, that is given by

$$u(x) \approx u_0 + \sum_{m=1}^{k} u_m(x). \quad (22)$$

Equation (21) reduces the number of terms involved in each component, and hence the size of calculations is minimized compared to the conventional Homotopy Analysis method only. When $k \to \infty$, an accurate approximate of equation (21) can be obtained with the series solution of equation (2) by using the initial conditions [7, 8, 1, 6]. Thus, the Modified Homotopy Analysis Method (MHAM) provides a numerical method for solving integro-differential classes of problems and overcome the difficulty of decomposing $u(x)$ with an efficient improvement over the traditional Homotopy Analysis Method.

## 4. Numerical experiment

In order to analyze the results, three numerical examples are given to illustrate the accuracy and effective properties of the method and MAPLE- 17 package on Window 2010 is used to carry-out the calculation. Results are displayed in tables and graphical plots.

**Example 1 [21].**

Consider the third order Non-linear Fredholm integro differential equation of the second kind.

$$u'''(x) = xe^x + \frac{1079}{360}e^x + \frac{1}{120}\int_0^1 e^{(x-2s)}\mathrm{u}^2(\mathrm{s})\mathrm{ds}, \quad (23)$$

for $\mathrm{x} \in [0,1]$ with the initial condition $u(0) = 2, u'(0) = 1, u''(0) = 2$ , and the exact solution $u(x) = xe^x$.

Using the MHAM algorithm (21), the zero deformation equation, and the Taylor series expansion:

$$b_l(x) = x + x^2 + \frac{1}{360} - \frac{359}{360}x - \frac{719}{720}x^2 + (x - \frac{1}{360})e^x \equiv x + x^2 + \frac{1}{360} - \frac{359}{360}x - \frac{719}{720}x^2 + \left(x - \frac{1}{360}\right)\left(1 + x + \frac{1}{2}x^2 + \frac{1}{6}x^3 + \frac{1}{24}x^2 + 0(x^5\right) \equiv x + x^2 + \frac{1079}{2160}x^3 + \frac{1439}{8640}x^4 + \frac{1}{24}x^5$$

Let $b_{10}(x) = x + x^2 = u_0(x),\ b_{11}(x) = +\frac{1079}{2160}x^3 + \frac{1439}{8640}x^4,\ b_{12}(x) = \frac{1}{24}x^5$

Setting $\mathrm{h} = -1$ for each approximation,

$$u_1(x) = b_{11}(x) - h\frac{1}{120}\int_0^{\mathrm{x}}\int_0^{\mathrm{x}}\int_0^{\mathrm{x}}(\int_0^1 exp(\xi - 2r)\,\mathrm{u}^2{}_0(\mathrm{r})dr)d\xi d\xi d\xi,$$

$$u_1(x) = \frac{7}{480}x^2 - \frac{3}{32}\mathrm{e}^{-2}x^2 - \frac{7}{480}\mathrm{e}^x x^2 + \frac{3}{32}\mathrm{e}^x\mathrm{e}^{-2}x^2 + x^3$$

$$\begin{aligned} u_2(x) = & -\frac{922699}{36864000}\mathrm{e}^x\mathrm{e}^{-2}x^2 - \frac{6130109}{552960000}x^2 + \frac{922699}{36864000}\mathrm{e}^{-2}x^2 \\ & + \frac{2943}{163840}\mathrm{e}^{-4}x^2 - \frac{15739}{30720}\mathrm{e}^{-3}x^2 - \frac{63}{163840}\mathrm{e}^{-6}x^2 \\ & + \frac{219709}{2764800}\mathrm{e}^{-1}x^2 + \frac{39}{4096}\mathrm{e}^{-5}x^2 + \frac{15739}{30720}\mathrm{e}^{-3}\mathrm{e}^x x^2 \\ & + \frac{63}{163840}\mathrm{e}^x\mathrm{e}^{-6}x^2 + \frac{6130109}{552960000}\mathrm{e}^x x^2 - \frac{2943}{163840}\mathrm{e}^x\mathrm{e}^{-4}x^2 \\ & - \frac{219709}{2764800}\mathrm{e}^{-1}\mathrm{e}^x x^2 - \frac{39}{4096}\mathrm{e}^{-5}\mathrm{e}^x x^2 - \frac{3}{8}\mathrm{e}^x\mathrm{e}^{-2}x^3 \\ & + \frac{7}{120}\mathrm{e}^x x^3 - 6x^3 + \frac{7}{480}\mathrm{e}^x x^4 - \frac{3}{32}\mathrm{e}^x\mathrm{e}^{-2}x^4 + \frac{1}{24}x^5 \end{aligned}$$

:::

$$u_n(x) = b_{i,n}(x) - h\int_0^{\mathrm{x}}\int_0^x\int_0^1(\xi\mathrm{r})\mathrm{u}_{n-1}^2(\mathrm{r})\mathrm{drd}\xi\mathrm{d}\xi$$

The approximation solution by MHAM for the same Example 1 is written in the form:

$$\begin{aligned} u(x) = u_0(x) + u_1(x) + u_2(x) + \cdots + u_n(x) = \\ x - 5x^3 + \frac{1}{24}x^5 + \frac{7}{120}\mathrm{e}^x x^3 + \frac{2943}{163840}\mathrm{e}^{-4}x^2 - \frac{15739}{30720}\mathrm{e}^{-3}x^2 \\ + \frac{219709}{2764800}\mathrm{e}^{-1}x^2 - \frac{63}{163840}\mathrm{e}^{-6}x^2 + \frac{39}{4096}\mathrm{e}^{-5}x^2 \\ + \frac{7}{480}\mathrm{e}^x x^4 - \frac{3}{8}\mathrm{e}^x\mathrm{e}^{-2}x^3 + \frac{15739}{30720}\mathrm{e}^{-3}\mathrm{e}^x x^2 - \frac{39}{4096}\mathrm{e}^{-5}\mathrm{e}^x x^2 \\ + \frac{2533301}{36864000}\mathrm{e}^x\mathrm{e}^{-2}x^2 + \frac{63}{163840}\mathrm{e}^x\mathrm{e}^{-6}x^2 + \frac{554893891}{552960000}x^2 \\ - \frac{2533301}{36864000}\mathrm{e}^{-2}x^2 - \frac{1933891}{552960000}\mathrm{e}^x x^2 - \frac{219709}{2764800}\mathrm{e}^{-1}\mathrm{e}^x x^2 \\ - \frac{3}{32}\mathrm{e}^x\mathrm{e}^{-2}x^4 - \frac{2943}{163840}\mathrm{e}^x\mathrm{e}^{-4}x^2 \end{aligned}$$

| $x_i$ | Exact Sol | HAM | | MHAM | |
|---|---|---|---|---|---|
| | | $u^5{}_{MHAM}$- APR Sol | ABS-E | $u^5{}_{MHAM}$- APR Sol | ABS-E |
| 0.1 | 0.110517 | 0.110517 | 1.51E-07 | 0.110517 | 5.12E-11 |
| 0.2 | 0.244281 | 0.244279 | 1.24E-06 | 0.244281 | 3.82E-10 |
| 0.3 | 0.404958 | 0.404953 | 4.29E-06 | 0.404958 | 1.31E-09 |
| 0.4 | 0.596730 | 0.596719 | 1.04E-05 | 0.596730 | 3.17E-09 |
| 0.5 | 0.824361 | 0.824340 | 2.09E-05 | 0.824361 | 6.36E-09 |
| 0.6 | 1.093271 | 1.093234 | 3.72E-05 | 1.093271 | 1.13E-08 |
| 0.7 | 1.409627 | 1.409566 | 6.06E-05 | 1.409627 | 1.84E-08 |
| 0.8 | 1.780433 | 1.780340 | 9.31E-05 | 1.780433 | 2.83E-08 |
| 0.9 | 2.213643 | 2.213506 | 1.36E-04 | 2.213643 | 4.14E-08 |
| 1.0 | 2.718282 | 2.718089 | 1.93E-04 | 2.718282 | 5.85E-08 |

**Table 1**: Comparison of Absolute Error Table for Example **1**

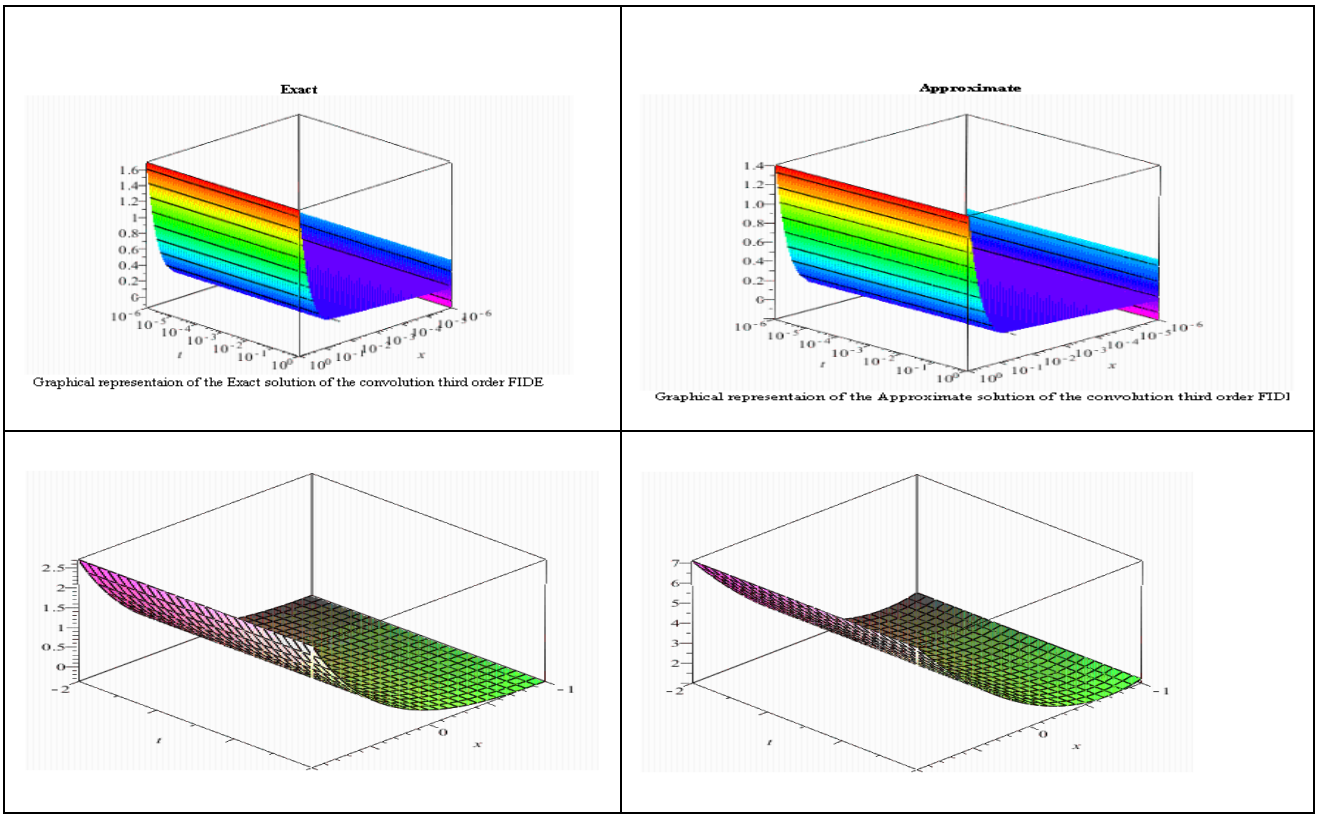


**Figure 1:** Graphical representation using 3-iterate of FIDE Example 1

**Example 2**: Consider the initial value problem [10]

$$u'''(x) = e^{x} - \frac{1}{4}(e^{x} + 1) + \int_0^1 xs(u'')^2(s)ds, \qquad (24)$$

$$u(0) = u'(0) = u''(0) = 1.$$

Using the MHAM algorithm (21), the zero deformation using equation, and Taylor series expansion for

$$b_l(x) = \frac{1}{4} + \frac{x}{4} + \frac{x^2}{8} + \frac{3}{4}e^x - \frac{x^3}{24}$$
$$\equiv 1 + x + \frac{x^2}{2} + \frac{x^3}{12} + \frac{x^4}{32} + \frac{x^5}{160} + \frac{x^6}{960} + \frac{x^7}{6720} + \frac{x^8}{53760} + \frac{x^9}{483840} + \frac{x^{10}}{4838400}$$
$$+ \frac{x^{11}}{53222400} + \frac{x^{12}}{6386688000} + \frac{x^{13}}{8302694400} + \frac{x^{14}}{116237721600} + O(x^{15})$$
$$\equiv 1 + x + \frac{x^2}{2} + \frac{x^3}{12} + \frac{x^4}{32} + \frac{x^5}{160} + \frac{x^6}{960} + \frac{x^7}{6720} + \frac{x^8}{53760} + \frac{x^9}{483840} + \frac{x^{10}}{4838400}$$
$$+ \frac{x^{11}}{53222400} + \frac{x^{12}}{6386688000} + \frac{x^{13}}{8302694400} + \frac{x^{14}}{116237721600}$$

Let $b_{10}(x) = 1 + x = u_0(x)$, $b_{11}(x) = \frac{x^2}{2} + \frac{x^3}{12}$, $b_{12}(x) = \frac{x^5}{160} + \frac{x^6}{960}$, $b_{13}(x) = \frac{x^7}{6720} + \frac{x^8}{53760}$, $b_{14}(x) = \frac{x^9}{483840} + \frac{x^{10}}{4838400}$, ...,

Setting $\mathrm{h} = -1$ for each approximation,

$$u_1(x) = b_{11}(x) - h\int_0^x \int_0^x \int_0^x \left(\int_0^1 (\xi r)(u''_0)^2(\mathrm{r})dr\right) d\xi d\xi d\xi = \frac{1}{2}x^2 + \frac{1}{12}x^3$$
$$u_2(x) = b_{12}(x) - h\int_0^x \int_0^x \int_0^x (\int_0^1 (\xi r)(u''_1)^2(\mathrm{r})dr) d\xi d\xi d\xi = \frac{1}{32}x^4 + \frac{1}{160}x^5 - \frac{43}{1152}hx^4$$
$$u_3(x) = b_{13}(x) - h\int_0^x \int_0^x \int_0^x (\int_0^1 (\xi r)(u''_2)^2(\mathrm{r})dr) d\xi d\xi d\xi =$$
$$\frac{1}{960}x^6 + \frac{1}{6720}x^7 - \frac{139}{86016}hx^4 + \frac{43}{14336}h^2x^4 - \frac{1849}{1327104}h^3x^4$$
$$u_4(x) = b_{14}(x) - h\int_0^x \int_0^x \int_0^x (\int_0^1 (\xi r)(u''_3)^2(\mathrm{r})dr) d\xi d\xi d\xi =$$
$$\frac{1}{53760}x^8 + \frac{1}{483840}x^9 - \frac{461}{81100800}hx^4 + \frac{3015977}{187280916480}h^4x^4$$
$$+ \frac{7367}{990904320}h^2x^4 - \frac{202367}{12331253760}h^3x^4$$
$$- \frac{3418801}{1761205026816}h^7x^4 - \frac{5393533}{399532621824}h^5x^4$$
$$+ \frac{79507}{9512681472}h^6x^4$$

$$u_5(x) = b_{15}(x) - h\int_0^x \int_0^x \int_0^x (\int_0^1 (\xi r)\,(u''_4)^2(\mathrm{r})dr)d\xi d\xi d\xi =$$
$$\frac{1}{4838400}x^{10} + \frac{1}{53222400}x^{11} - \frac{461}{81100800}hx^4 + \frac{3015977}{187280916480}h^4x^4 + \frac{7367}{990904320}h^2x^4 - \frac{202367}{12331253760}h^3x^4 - \frac{3418801}{1761205026816}h^7x^4 - \frac{5393533}{399532621824}h^5x^4 + \frac{79507}{9512681472}h^6x^4$$

::

$$u_m(x) = b_{im}(x) - h\int_0^x \int_0^x \int_0^x (\int_0^1 (\xi r)\,(u''_{m-1})^2(\mathrm{r})dr)d\xi d\xi d\xi =$$

The approximation solution by MHAM for the same Example **2** is written in the form:

$$u(x) = u_0(x) + u_1(x) + u_2(x) + \cdots + u_n(x)$$

| | | **MHAM** | | **[10]** | |
|---|---|---|---|---|---|
| $x_i$ | **Exact Sol** | **APR Sol n=7** | **ABS-E** | $u^7{}_{MHAM}$**- APR Sol** | **ABS-E** |
| **0.0** | **1.00000** | **1.00000** | **0.00E+00** | **1.00000** | **0.00E+00** |
| **0.1** | **1.10517** | **1.10517** | **2.51E-13** | **1.10517** | **2.22E-08** |
| **0.2** | **1.22140** | **1.22140** | **6.49E-11** | **1.22140** | **7.58E-07** |
| **0.3** | **1.34986** | **1.34986** | **1.68E-09** | **1.34985** | **6.12E-06** |
| **0.4** | **1.49182** | **1.49182** | **1.70E-08** | **1.49180** | **2.74E-05** |
| **0.5** | **1.64872** | **1.64872** | **1.03E-07** | **1.64863** | **8.85E-05** |
| **0.6** | **1.82212** | **1.82212** | **4.46E-07** | **1.82189** | **2.33E-04** |
| **0.7** | **2.01375** | **2.01375** | **1.55E-06** | **2.01322** | **5.31E-04** |
| **0.8** | **2.22554** | **2.22554** | **4.56E-06** | **2.22445** | **1.09E-03** |
| **0.9** | **2.45960** | **2.45959** | **1.18E-05** | **2.45753** | **2.08E-03** |
| **1.0** | **2.71828** | **2.71825** | **2.79E-05** | **2.71458** | **3.70E-03** |

**Table 2:** Results and Comparison of Absolute Error Table for FIDE Example **2**

## 5. Conclusion

In this paper, we provided a modified Homotopy Analysis (MHAM) approach for approximating strongly nonlinear physical models in engineering and applied sciences that are governed by higher-order Fredholm integro -differential equation of the second kind.
The implementation and the numerical examples both show that our technique is efficient. The scheme is simple to implement, it reduces the computational difficulty associated with other traditional methods.

**Acknowledgement:** The authors would like to thank National Agency for Science and Engineering Infrastructure (NASENI), University of Lagos (UNILAG), and King Fahd University of Petroleum and Minerals (KFUPM) for their support**.**

## References

[1] Al-Hayani W. (2013). Solving nth-order integro-differential equations using the combined Laplace transform- Adomian decomposition method. Applied Mathematics, 4: 882-886.

[2] Chandru M., Das P., and Ramos H. (2018). Numerical treatment of two-parameter singularly perturbed parabolic convection diffusion problems with non-smooth data. Mathematical Methods in the Applied Sciences, 41(14): 5359-5387.

[3] Das P. (2018). A higher order difference method for singularly perturbed parabolic partial differential equations. Journal of Difference Equations and Applications, 24(3): 452-477.

[4] Das P. (2019). An a posteriori based convergence analysis for a nonlinear singularly perturbed system of delay differential equations on an adaptive mesh. Numerical Algorithms, 81(2): 465-487.

[5] Das P. and Natesan S. (2014). Optimal error estimate using mesh equidistribution technique for singularly perturbed system of reaction–diffusion boundary-value problems. Applied mathematics and computation, 249: 265-277.

[6] Das P. and Vigo-Aguiar J. (2019). Parameter uniform optimal order numerical approximation of a class of singularly perturbed system of reaction diffusion problems involving a small perturbation parameter. Journal of Computational and Applied Mathematics, 354: 533-544.

[7] Das P., Rana S., and Ramos H. (2020). A perturbation-based approach for solving fractional-order Volterra–Fredholm integro differential equations and its convergence analysis. International Journal of Computer Mathematics, 97(10): 1994-2014.

[8] Das P., Rana S., and Ramos H. (2020). On the approximate solutions of a class of fractional order nonlinear Volterra integro-differential initial value problems and boundary value problems of first kind and their convergence analysis. Journal of Computational and Applied Mathematics, 113116.

[9] Das P., Rana S., and Vigo-Aguiar J. (2020). Higher order accurate approximations on equidistributed meshes for boundary layer originated mixed type reaction diffusion systems with multiple scale nature. Applied numerical mathematics, 148: 79-97.

[10] Hemeda A. A. (2012). New iterative method: application to nth-order integro-differential equations. International Mathematical Forum, 47(7): 2317 – 2332.

[11] Jafarzadeh Y. and Keramti B. (2018). numerical method for a system of integro-differentials equations and convergence analysis by Taylor collocation, Ain Shams Engineering Journal,

9(4): 1433-1438.

[12] Katsidelis J. T. (2019). numerical solution of integro-differentials equations with convolution integrals. Archive of Applied Mechanics, 89(10): 2019–2032.

[13] Keshvaraz E. and Ordokhani Y. (2019). A fast numerical algorithm based on the Taylor wavelets for solving the fractional integro-differential equations with weakly singular kernels. Maths Meth Appl. Sci., 42: 4427-4443.

[14] Kurt N. and Sezer M. (2008). Polynomial solution of high-order linear Fredholm integro-differential equations with constant coefficients. Journal of the Franklin Institute, 345(8): 839-850.

[15] Liao S. (2005). Comparison between the homotopy analysis method and homotopy perturbation method. Applied Mathematics and Computation, 169(2): 1186-1194.

[16] Noor M.A., Waheed K.I., and Al-Said E.A. (2016). Variation of parameters method for solving system of nonlinear system of Volterra integro-differential equations. Computer Mathematics Application, 62: 2126-2131.

[17] Maleknejad K., Basirat B., and Hashemizadeh E. (2011). Hybrid Legendre polynomials and Block-Pulse functions approach for nonlinear Volterra- Fredholm integro-differential equations. Computer and Mathematics with Applications, 61: 2821-2828.

[18] Memudu W.W. and Taiwo O.A. (2016). Exponentially fitted collocation approximation method for the numerical solutions of Higher Order Linear Fredholm Integro-differential-Difference Equations. Theoretical Mathematics and Applications, 6(1): 131-150.

[19] Sezer M. (1994). Taylor polynomial solutions of Volterra integral equations. International Journal of Mathematical Education in Science and Technology, 25(5): 625-633.

[20] Vahdati S., Abbas Z., and Ghasemi M. (2010). Math. Application of homotopy analysis method to Fredholm and Volterra integral equations. Mathematical Sciences Quarterly Journal.

[21] Wazwaz A. M. (2011). Linear and nonlinear integral equations: methods and applications, Springer.

**International Journal of Mathematical Analysis and Modelling**
**Volume 5, Issue 1, May 2022, Pages 90 – 99**

# On the performance of Nigerian security agencies: a learning rate and learning curve perspective

**A. O. Abam[*] and E. F. Nsien[†]**

**Abstract**

Effective management of workforce is one of the most critical functions affecting the performance of security agencies. The development of an agency is dependent on the degree of performance of the workforce. The performance of workforce is the resultant effect of the learning curves, learning rates and level of teamwork of the personnel. Considering that security is key in the wellbeing of any economy and bearing in mind that learning curves and rates of Corps affects the performances of the agency, this work seeks to assess the Performance of security agencies considering their learning differences. A conceptual framework model for security agencies' workforce was proposed and formulated for assessing the learning differences of personnel. The findings reveal that the higher the rank of Personnel, the lesser the amount of time required to recover as a result of experience compared to the low rank Corps. That, Corps have a chance to observe breaks which is always stated in the Corps condition of service like off duty, annual leave, tea breaks. Performance depends on Corps' traits and skills acquired, on-the-job trainings, different learning rates, learning curves and the operational strategies employed for recruitments, trainings, identification of Corps' experiences and productivity.

***Keywords*:** learning curve; process; rate; performance.

## 1. Introduction

The growth and development of any organization or industry is dependent on the degree of performance or productivity of the workforce. Meanwhile, the performance of a workforce or productivity of any industry is measured based on the learning curves, learning rates and level of teamwork of the personnel. Considering the different operations regarding airlines, Wright in 1936 brought to limelight the development of learning curves by assembling the costs of airlines' decrement through repeated operations ([32], [4]). The work of [11] cited in [4] defined a learning curve as a mathematical description of workers' performances in repetitive tasks while [1] revealed that learning curves, rates and skills of personnel contributes to the efficient operations and performance of security agencies. Research conducted by [29], [16], [10] defined learning curve as an efficient weapon that assesses workers' performance in repetitive tasks, leading to reduced process loss due to workers' inability in the first production cycle [4]. That

[*] Corresponding Author: Department of Statistics, Federal University of Lafia, Nasarawa State, Nigeria; abamayeni@gmail.com; +2347035489880
[†] Department of Statistics, University of Uyo, Uyo, Nigeria; nsiened@gmail.com; +2348037927439

learning curves depend on some variables like the time of the first operations, unit numbers produced at each time interval, production costs and the percent of non-conforming units [12]. In another development, [10] revealed that repetition leads to less time demand because of due familiarity with working tools, strategies and operational procedures or processes. The work carried out by [17] as cited in [28] opined that there exist a binding force and relationship between workers' personality characteristics/traits and their academic motivation with different effective teaching strategies. The workers' experiences, forgetting processes, workers' assignment strategy and trainings contribute to the wellbeing and productivity of any industry or security agency. In the light of the above, this paper seeks to assess the performance of Corps of the Nigerian Security Agencies using their learning rates and learning curves.

Effective management of labor resources and workforce is one of the most critical functions affecting performance of manufacturing systems. An agency or industries' growth and development is hinged on the performance and productivity of her workers. Inefficient skills regarding learning rates, learning curves and teamwork had contributed to the poor performances of security agencies. This further reveal that the security agencies are either not been equipped or prepared to cope with the demanding technological changes, trends and developments of the present economy and security challenges. Different security agencies have failed in performing or exercising their duties to the citizens and the nation generally. This is owing to the fact that Corps' individual differences in terms learning curves, rates and lack of teamwork is not adequate to bring desired performance. In the light of the above, the aim of the study is to formulate and propose a conceptual framework model for security agencies' learning differences, learning curves and learning rates.

Objectively, this will be achieved by:

i. Assessing the factors that contribute to the differences in learning curves of the personnel.
ii. Identifying the determinants of learning rates of Corps that motivate their agility and top performances.
iii. Formulate a Conceptual framework model for learning curves and learning rates of the Nigerian Security Agencies' workforce using the determinant factors of learning curves and rates.

Different scholars have studied Learning processes which generally, are used in choice menu configuration, job scheduling, job rotation, production development, estimation of lot conclusion time, evaluation of production cost reduction, optimization of tasks allocation to workers based on learning profiles, mitigating or checking of production losses after interruptions, breaks and fatigues. [8], [30] states that learning processes are affected by some factors like structure of the training programs. Workers' motivations in performing their duties or tasks given to them were assessed by [21], [3] as another teething problem of learning processes. [23], [24] [22] revealed that prior or previous experiences gained in the duty or assignment given to a worker affects his/her learning process. However, [22] added that the respective task or assignment complexities affect the workers' learning processes. The research of [5] states that mass customization popularity, a production strategy in manufacturing, service industry is an advantage of workers' learning curves. [9], [15], [7] believes that learning curves are used in analyzing and controlling the companies productivity and operations. Learning curves are

also seen as a way to allocate responsibilities or tasks to workers according to their experiences or histories of learning profiles ([23], [6]). Research conducted by [20] sees learning curves as a means of measuring production costs as workers gain experiences while [26], [27] believes that learning curves estimates cost consulting and technology implementation.

## 2. Brief history of learning curves

The Wright (1936) log-linear model was the first organizational learning curve given as

$$y = C_1 x^b \qquad (1)$$

where, y is the average time or cost needed per unit production; C is the time (cost) for the first unit production; x is the number of units and b is the slope of the learning curve that describes the learning rates of workers ([10], [31]). [14] modified Wrights model by monitoring the process with high percentage of non-conforming and reworked units as:

$$y = C_1 (x + B)^b \qquad (2)$$

where B is the number of units of prior experiences. [23] developed the exponential learning curve as

$$y = C_1 x^b e^{dx} \qquad (3)$$

where d is a second constant; e is the exponential value and other parameters are as defined above. In another development, [4] modified equation (3) above resulting to a multivariate learning curve analyzed using surface graphs stated as:

$$y = k \prod_{i=1}^{n} C_i x_i^{b_i} \qquad (4)$$

where $C_i$ is the coefficient for the independent variable $x_i$; k is the performance cost to producing the first unit.

Recall that:

$$\text{Total Factor Productivity} = \frac{Price \times Output}{Wage \times Input} \qquad (5)$$

The power form or traditional model for experience and performance by [18] is given as

$$Cp = C_1 q^{-b} \qquad (6)$$

where Cp is the cost of performance or production; $C_1$ is the unit cost to produce first units; b represents the learning rates and q is the number of units.

# 3. Proposed models

## 3.1. Proposed model for learning curves of Nigerian security agencies workforce

According to [23], the support for counter terrorism operations is sustained and effectively maintained with the help of understanding the learning abilities and capabilities of the workforce. From (4) above, modifying [4] model by introducing other parameters of Nigerian Security Agencies we have the following proposed model.

$$\min y = \sum_{i=1}^{n} k[\prod_{i=1}^{n} U_i x_i^{b_i}]; U = \{a, c, d, f, h\} \qquad (7)$$

$$y = ka_i x_i^{b_i} + kc_i x_i^{b_i} + kd_i x_i^{b_i} + kf_i x_i^{b_i} + k\, h_i x_i^{b_i} (8)$$

$$y = k[a_i x_i^{b_i} + c_i x_i^{b_i} + d_i x_i^{b_i} + f_i x_i^{b_i} + h_i x_i^{b_i}] (9)$$

From equations (9) and (10), "y" is the average time or cost needed per unit performance or production. "k" is the performance cost of producing the first unit; "U" is a multi-objective function comprising of the learning curve, learning rate, fatigue, interruptions and breaks. "U" is the coefficient for the independent variable $x_i$; "a" is the learning rate deviation; "c" is the learning curve deviation; "d" is the breaks deviation; "f" is the fatigue deviation; "h" is the interruptions deviation; "x" is the independent variable representing the number of units in the production process; "b" is the slope of the learning curve that describes the learning rates of workers.

## 3.2. Proposed conceptual model for learning curves and learning rates of Nigerian security agencies workforce

In order to develop the conceptual model for the learning curves and rates of Nigerian Security Agencies' Workforce, the [19] organizational learning curve was modified. [2] defined the learning curve of a workforce as the constituent of the performance, capabilities, learning abilities and responses of a security agency's workforce. Meanwhile, learning curve consists of the movement from an individual action (personal experiences got) to organizational action (actions taken by Corps dependent on the agencies' vision and mission statements) to environmental responses and finally individual beliefs. This is represented in a circular form below.

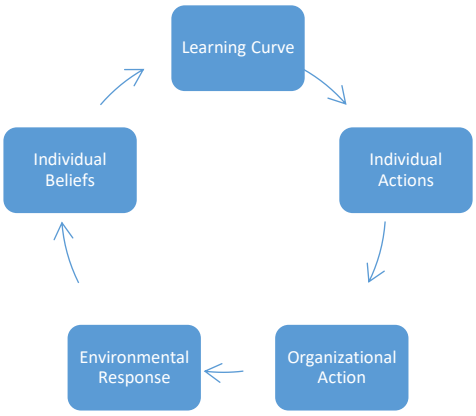


**Figure 1**: Organizational Learning cycle (Adopted from [19]).

Recall that, "Organizations can differ in terms of the amount of experience, the nature of experience, the ability to learn from experience, the amount of deliberate learning activities, the nature of deliberate learning activities, the ability to learn from deliberate activities, the ability to translate learning into better organizational knowledge, the ability to change behavior in response to better organizational knowledge, and the ability to obtain better organizational performance as a result of changed behavior" [18]. [13] revealed that, resources allocation is a proponent of the learning process since the personnel awareness contributes to the learning curves, rates and learning processes of an organization. Meanwhile, the elements of organizational learning processes include: the vision and mission of the organization, better knowledge acquired (on-the-job training or refresher courses), improving actions resulting from the experiences got from the in-house training or refresher courses and on-going efforts (the continuous objective processes, activities of achievements obtained from the agencies' set goals and objectives).

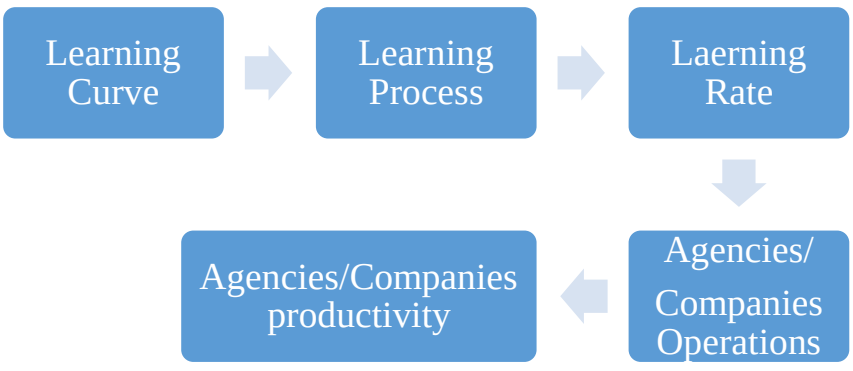


**Figure 2**: Proposed Conceptual framework model for the Learning Process of Security Agencies Workforce

From Figure 2, above each of the stages is represented in a conceptual model framework as shown below.

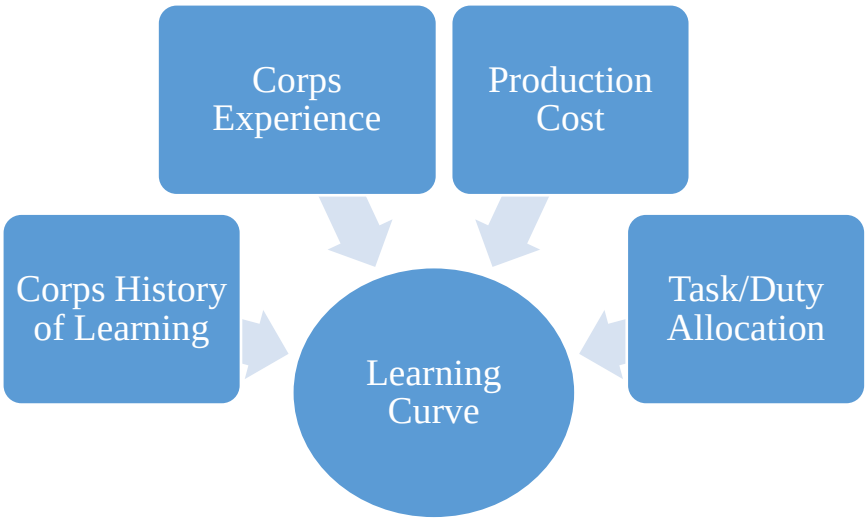


**Figure 3**: Proposed determinants of the Learning Curve of the Security Agencies' workforce.

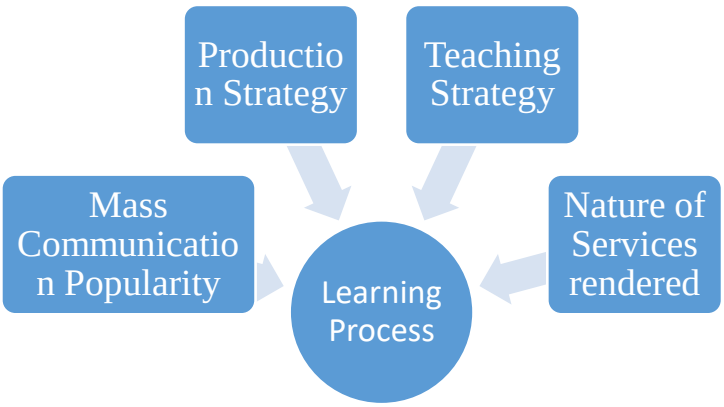


**Figure 4**: Proposed determinants of the Learning Process of the Security Agencies' workforce.

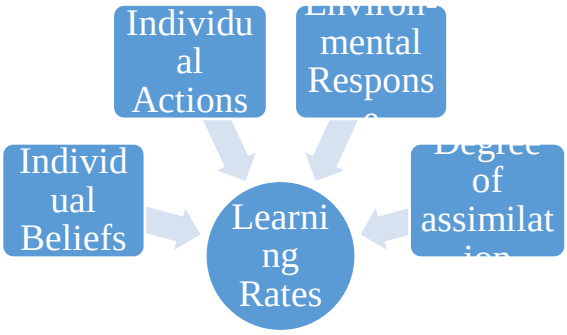


**Figure 5**: Proposed determinants of the Learning Rate of the Security Agencies' workforce.

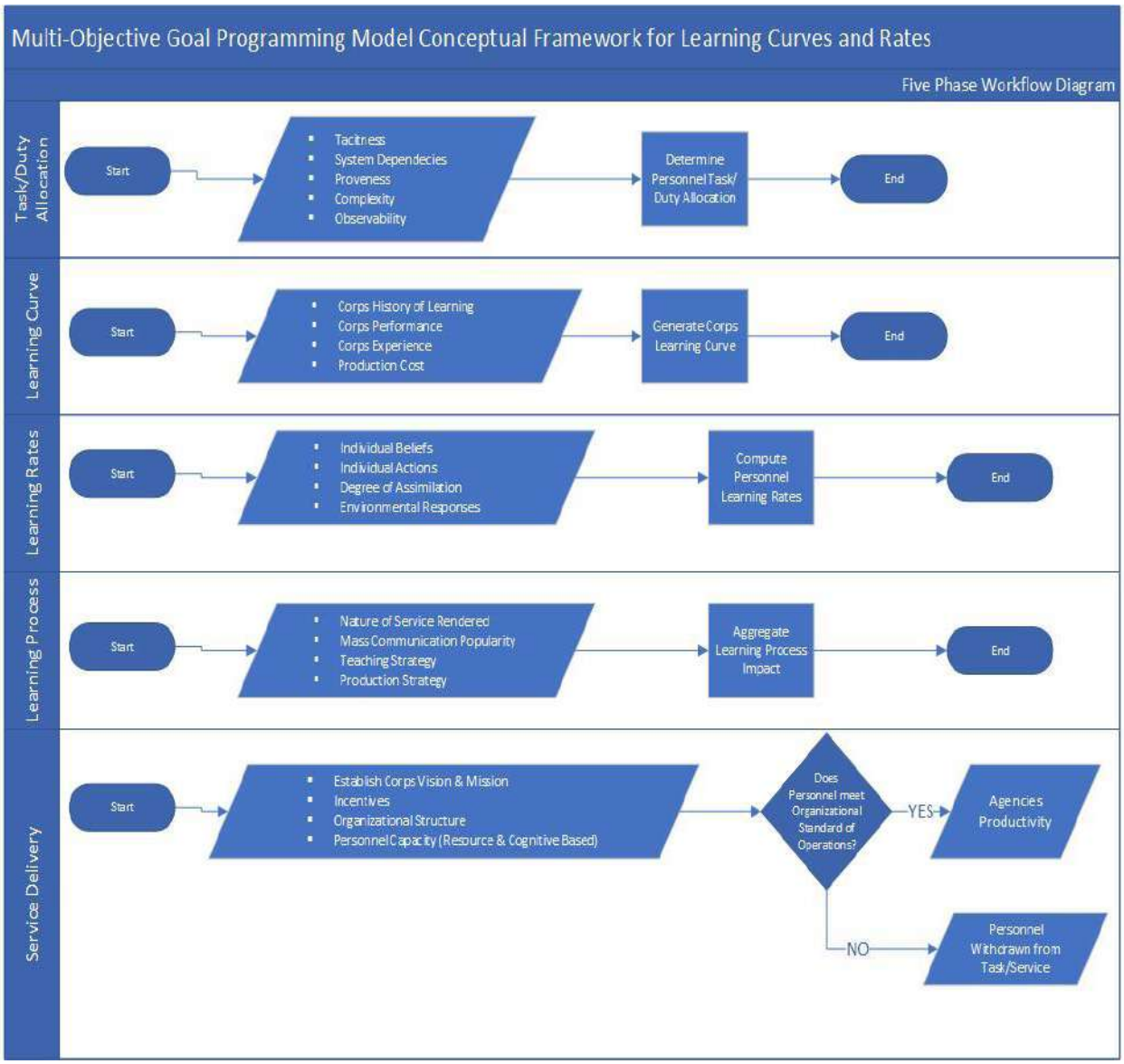


**Figure 6**: Conceptual Framework/Model of the Learning Curves of Personnel

## 4. Discussion

Task or schedules allotted to personnel on the first phase of the conceptual framework depends on their provenness, tacitness and personal observable traits. The second phase (the learning curves) handles the corps history of learning, performances, experience and demands in the course of carrying out their duties. Meanwhile, the third phase (learning rates) has proponent factors of the corps' beliefs, actions, level/degree of assimilations and environmental responses while the fourth phase called the learning process involves the nature of services rendered, teaching and production strategies with impacts of communication skills. However, the service delivery (final phase) uses the corps' vision and mission statements with operational structures to achieve the agencies' set objectives. At this stage, each personnel thrive to meet the standards of the operations of the corps, thereby evaluating the agency as either being productive (personnel is awarded) or unproductive (personnel is withdrawn from the task or service).

Generally, at every planning stage, Corps on-the-job training, skills acquired, overtime task carried out, availability to a task or scheduled duty, tea breaks or off-duties given, different interruptions, personality traits/ranks and fatigue are considered so as to inform decision makers on what, how, when to employ (hire), dismiss, sack or retrench (fire) and train personnel (induction/refresher courses and on-the-job trainings). This research work reveals that corps differences in terms of ranks, skills and handling of machines (arms) aid predictions in recruitment/employment, retrenchment (retirement /dismissal), training as well as the nature of breaks given. However, Corps on off duty (not working at regular times) do not have breaks. The findings posit that the higher the rank of Personnel (Corps) the lower or the lesser the amount of time required to recover as a result of experience gathered compared to the low ranking Corps. More Corps employed/recruited and trained at the entry point seems to have very low skills and personality level regarding the job.

## 5. Conclusion

From the findings, every Corp has a chance to observe break time as stated in the Corps condition of service regarding off duty, annual leave, tea breaks etc. That, Corps performance depends on the traits or skills acquired, on-the-job trainings, different learning rates and learning curves and the operational strategies employed by agencies in recruitments, trainings, identification of different Corps' experiences and productivity. The research work proposed conceptual model of learning curves, and rates of personnel of the Nigerian Security Agencies.

## References

[1] Abam A.O. and Oladejo M.O. (2021). A goal programming model for the efficient operations of security agencies in Nigeria. International Conference on Contemporary Developments in Mathematical Sciences ICCDMS 2021, Book of Proceedings: 857-875.

[2] Abam A. O., Oladejo M. O., and Emmanuel A. Y. (2020). Modelling fatigue and performance capabilities in Nigerian security agencies workforce. Journal of Physical Mathematics, 11(3): 319. doi:10.37421/jpm.2020.11.319.

[3] Agrell P.J., Bogetoft P., and Tind J. (2002). Incentive plans for productive efficiency, innovation and learning. International Journal of Production Economics 78(1): 1-11.

[4] Anzanello M.J. and Fogliatto F.S. (2011a). Learning curves models and applications: Literature review and research directions. International Journal of Industrial Ergonomics, 41: 573-583.

[5] Anzanello M.J. and Fogliatto F.S. (2011b). Selecting the best clustering variables for grouping mass-customized products involving workers learning. International Journal of Production Economics 130 (2): 268-276.

[6] Anzanello M.J. and Fogliatto F.S. (2007). Learning curve modelling of work assignment in mass customized assembly lines. International Journal of Production Research 45(13): 2919-2938.

[7] Anzanello M.J. and Fogliatto F.S. (2010). Scheduling learning dependent jobs in customized assembly lines. International Journal of Production Research. 48 (13): 6683-6699.

[8] Azizi N., Zolfaghari S., and Liang M. (2010). Modeling job rotation in manufacturing systems: the study of employee's boredom and skill variations. International Journal of Production Economics 123 (1): 69-85.

[9] Chen C., Lo C., and Liao Y. (2008). Optimal lot size with learning consideration on an imperfect production system with allowable shortages. International Journal of Production Economics, 113 (1): 459- 469.

[10] Dar-El E. M. (2000). Human learning: from learning curves to learning organizations. Kluver Academic Publishers, Massachusetts.

[11] Fioretti G. (2007). The organizational learning curve. European Journal of Operational Research, 177 (3): 1375-1384.

[12 Franceschini F. and Galetto M. (2002). Asymptotic defectiveness of manufacturing plants: an estimate based on process learning. International Journal of Production Research, 40 (3): 537-545.

[13] Udoh I. J., Alabi O. I., and Abam A. O. (2021). Resources allocation queue-fairness model of multi-server petroleum products distribution system. International Journal of Trend in Scientific Research and Development (IJTSRD), 5(2): 770-788. www.ijtsrd.com e-ISSN: 2456 –6470

[14] Jaber M. and Guiffrida A. (2004). Learning curves for process generating defects requiring reworks. European Journal of Production Research 159 (3): 663-672.

[15] Jaber M. and Saadany A. (2011). An economic production and manufacturing Model with learning effects. International Journal of Production Economics, 131 (1): 115-127.

[16] Jaber M., Goyal S., and Imran M. (2008). Economic production quantity model for items with imperfect quality subject to learning effects. International Journal of Production Economics, 115 (1): 143-150.

[17] Komarraju M. and Karau S. J. (2005). The relationship between the big five personality traits and academic motivation. Personal. Indiv. Diff., 39: 557-567.

[18] Lapre M. A. and Nembhard I. M. (2010). Inside the organizational learning curve: understanding the organizational learning process. Foundations and Trends in Technology, Information and Operations Management. 4(1): 1-103.

[19] March J. G. and Olsen J. P. (1975). The uncertainty of the past: organizational learning under ambiguity. In: J. G. March (1988), Decisions and Organizations. Oxford:Blackwell: 335-58.

[20] Nadeau M., Kar A., Roth R., and Kirchain R. (2010). A dynamic process-based Cost modeling approach to understand learning effects in manufacturing. International Journal of Production Economics, 128 (1): 223-234.

[21] Natter M., Mild A., Feurstein M., Dorffner G., and Taudes A. (2001). The Effect of incentive schemes and organizational arrangements on the new product development process. Management Science, 47 (8): 1029-1045.

[22] Nembhard D.A. and Osothsilp N. (2002). Task complexity effects on between -individual learning/forgetting variability. International Journal of Industrial Ergonomics 29 (5): 297-306.

[23] Nembhard D.A. and Uzumeri M.V. (2000a). An individual-based description of learning within an organization. IEEE Transactions on Engineering Management 47 (3): 370-378.

[24] Nembhard D.A. and Uzumeri M.V. (2000b). Experimental learning and forgetting for manual and cognitive tasks. International Journal of Industrial Ergonomics, 25(3): 315-326.

[25] Oladejo M.O., Udoh I. J., and Abam A. O. (2021). Optimizing the community's supports in counter- terrorism operations: a stick – carrot game theoretic model. Current Journal of Applied Science and Technology, 39(47): 45-67. ISSN: 2457-1024 (Past name: British Journal of Applied Science & Technology, ISSN: 2231-0843, NLM ID: 101664541).

[26] Plaza M. and Rohlf K. (2008). Learning and performance in ERP implementation projects: a learning-curve model for analyzing and managing consulting costs. International Journal of Production Economics, 115 (1): 72-85.

[27] Plaza M., Ngwenyama O., and Rohlf K. (2010). A comparative analysis of Learning curves: implications for new technology implementation management. European Journal of Operational Research, 200 (2): 518-528.

[28] Rafiei H., Rabbani M., and Koushan N. (2012). Effect of Motivation & Learning Curve in Dynamic Cell Formation and the Worker Assignment Problem. International Journal of Engineering Sciences & Research Technology 1(9): 481-497.

[29] Salameh M. and Jaber M. (2000). Economic production quantity model for items with imperfect quality. International Journal of Production Economics, 4 (1): 59-64.

[30] Serel D.A., Dada M., Moskowitz H., and Plante R.D. (2003). Investing in quality under autonomous and induced learning. IIE Transactions, 35(6): 545-555.

[31] Teplitz C.J. (1991). The learning curve desk book: a reference guide to theory, calculations and applications. Quorum Books, New York.

[32] Wright T. P. (1936). Factors affecting the costs of airplanes. Journal of Aeronautical Science, 3: 122–128.

**International Journal of Mathematical Analysis and Modelling**
**Volume 5, Issue 1, May 2022, Pages 100 – 120**

# Sensitivity analysis of Nipah virus Malaysian variant ($NiV_m$) with transmission dynamics

**S. I. S. Abang[*†], A. L. Ozioko[‡†], O. N. Nze[*§], G. C. E. Mbah[†**] , and C. T. Onyia[††]**

**Abstract**

In this paper, we established the basic reproductive number of the Nipah virus disease, the DFE and endemic equilibrium of the SIR disease model. We deploy the next generation matrix approach to obtain sufficient conditions under which the basic reproductive number was obtained. We then perform a sensitivity analysis of the model, which helped us come up with some proposed policies to assist stake holders on the right policies to apply. The study aimed at analyzing the sensitivity of the parameters in relations to the basic reproductive number of the proposed disease model; to achieve this we use the following objectives: (1) obtain the basic reproductive number of the model (2) perform sensitivity analysis of the model. From our analysis, some of the followings were drawn as conclusions. It was discovered that some parameters were found to be positively contributing to the spread of the disease, parameters like $\Lambda_H$, which is the recruitment parameter for the model, $\beta_1$, this parameter is the effective contact rate, while some other parameters reduce the spread of the disease, parameters like $\tau_1$, which is the proportion of infected that goes for treatment, while $\mu_H$, natural death.

[*] Corresponding Author: National Centre for Technology Management, an Agency of the Federal Ministry of Science & Technology, PRODA Training Institute, Independence Layout, Enugu, Nigeria; sunnyscott2010@gmail.com; 07033911987
[†] Department of Mathematics, University of Nigeria Nsukka, Nigeria
[‡] Department of Mathematics, Federal University, Lokoja, Nigeria; arinze.luke@fulokoja.edu.ng; 08034198454
[§] obynnekanze@gmail.com; 08062627262
[**] godwin.mbah@unn.edu.ng; 08032198708
[††] Department of Statistics, Institute of Management Technology (IMT), Enugu, Nigeria; chukwuemekaonyia@gmail.com; 07035410292

# 1. Introduction

Nipah virus (NiV) infection is an emerging pathogen endemic to Southeast Asia that can be transmitted from its reservoir (wild animals, fruit bats, pigs etc) to human. NiV is a zoonotic virus (that is, it is transmitted from animals to humans) and can also be transmitted through contaminated food or directly between people [13]. It was first detected in the 1998–1999 outbreaks in Kampung Sungai Nipah, Malaysia and then Singapore, with seasonal outbreaks in Bangladesh and India since 2001, and a suspected 2014 outbreak in the Philippines. It derived its name from Sungai Nipah, a village in Malaysia where the virus was first detected in 1998 [1]. In Africa there has been an outbreak in Madagascar, which shows that Africa is not spear of this new deadly zoonotic virus [5].

In the 1998-99 Malaysia outbreak, NiV spillover occurred from bats to pigs, which led to pig-to-pig, pig-to-human, and suspected, although limited, human-to-human NiV transmission [11]. After the first noticeable outbreak in Malaysia, NiV infection has subsequently been recognized in Bangladesh in 2001 and nearly annual outbreaks have occurred in this country ever since, with disease also identified periodically in eastern India; case fatality rates during outbreaks in these countries have ranged from 75% to 100%. Other regions may be at risk for NiV infection, as serologic evidence for NiV has been found in the known natural reservoir (Pteropus bat species) and several other bat species in a number of other countries, including Cambodia, Thailand, Indonesia, Madagascar, Ghana, and the Philippines [12]; [8].

# 2. Model formulation

## 2.1. Model assumption

The development of the model is based on the following assumptions:

i. Those recruited into the system are not infected or contacted the disease.
ii. We focus on the Malaysia ($NiV_M$) strain.
iii. There is an Intensive supportive care for those infected with the virus that goes for treatment.
iv. The treatment given to those infected is the combinational therapy method, because as the time of this study there is no single specific approach or method for treating Nipah virus disease.
v. Nipah virus is seen to be a highly emerging disease and no single drug is available yet for its treatment.
vi. Humans can contact the disease by contact with infected bats, infected pigs or infected humans.
vii. The infected individual can recover either by care giving/combinational therapy or naturally.
viii. One can recover from the infection without treatment.
ix. Once recovered a person or animal cannot get the virus again.
x. We assume the latent class is merge with the infectious class.
xi. Pigs get infected by contact with infectious pigs or infectious bats.

xii. People or pigs can die naturally or as a result of the disease.
xiii. Bats are natural carrier of Nipah virus disease.
xiv. The pigs are caged so that they do not roam to eat defecations from humans that are infected.

Now, putting these assumptions together we have a model flow diagram and thus the model equations for the transmission dynamics of the Nipah virus and its control.

**Model variables for the Nipah virus model**

$S_H$ - susceptible humans
$I_H$ - infectious humans
$I_{HT}$- infectious humans receiving treatment
$R_H$ - recovered humans
$S_P$ - susceptible pigs
$I_P$ - infectious pigs
$I_{PT}$- infectious pigs receiving treatment
$R_P$ - recovered pigs
$S_B$ - Susceptible bats, with strong immune response capable of controlling the infection.
$I_B$ - infectious bats

**Parameters and their interpretations for the Nipah virus model**

$\Lambda_H$ - Constant recruitment of human through birth and migration
$\Lambda_P$ - Constant recruitment of pig through birth and purchase of new pigs into the animal society
$\Lambda_B$ - Constant recruitment of bats by births and migration of bats into the bat population.
$N_H$ – Total human population
$N_P$ – Total pig population
$N_B$ – Total bat population
$\mu_H$ - Natural death rate for humans
$\mu_P$ - Natural death rate for pigs
$\mu_B$ – Natural death rate for bats.
$\beta_1$ - Effective contact rate for humans
$\beta_2$- Effective contact rate of pigs
$\beta_3$ - Effective contact rate of bats
$\tau_1$ – Proportion of infected human that goes for treatment
$\tau_2$- Proportion of infected pigs taken for treatment
$\delta_1$ -rate at which humans die as a result of the disease in the infectious human class

$\delta_2$- rate at which humans die as a result of the disease in the infectious treated human class undergoing treatment.
$\delta_3$ -rate at which pigs die as a result of the disease in the infectious pig class not undergoing treatment.
$\delta_4$- rate at which pig dies as a result of the disease in the infectious pig class undergoing treatment.

$\delta_5$ -rate at which bats die as a result of human activities.
$\gamma_1$ - rate at which infectious human recovers
$\gamma_2$- rate at which infectious human undergoing treatment recovers
$\gamma_3$ - rate at which infectious pigs recovers
$\gamma_4$- rate at which infectious treated pigs recovers
$n_0$ - modification parameter associated with reduced infectiousness of infected humans, $0 \leq n_0 \leq 1$
$n_1$ - modification parameter associated with reduced infectiousness of infected pigs as compared to infected humans, $0 \leq n_1 \leq 1$
$n_2$ - - modification parameter associated with reduced infectiousness of infected pigs as compared to infected humans, $0 \leq n_2 \leq 1$.
$\lambda$ – this is the force of infection

## 2.2. Model equations on NiV infection without inhibiting parameters

$$\frac{dS_H}{dt} = \Lambda_H - \frac{\beta_1[\, n_0 I_H + n_1 I_P + n_2 I_B] S_H}{N_H} - \mu_H S_H \,, \quad (1)$$

$$\frac{dI_H}{dt} = \frac{\beta_1[\, n_0 I_H + n_1 I_P + n_2 I_B] S_H}{N_H} - [\gamma_1 + \tau_1 + \mu_H + \delta_1] I_H, \quad (2)$$

$$\frac{dI_{HT}}{dt} = \tau_1 I_H - [\gamma_2 + \mu_H + \delta_2] I_{HT}, \quad (3)$$

$$\frac{dR_H}{dt} = \gamma_1 I_H + \gamma_2 I_{HT} - \mu_H R_H, \quad (4)$$

$$\frac{dS_P}{dt} = \Lambda_P - \frac{\beta_2[I_P + n_2 I_B] S_P}{N_P} - \mu_P S_P, \quad (5)$$

$$\frac{dI_P}{dt} = \frac{\beta_2[I_P + n_2 I_B] S_P}{N_P} - [\gamma_3 + \tau_2 + \mu_P + \delta_3] I_P, \quad (6)$$

$$\frac{dI_{PT}}{dt} = \tau_2 I_P - [\gamma_4 + \mu_P + \delta_4] I_{PT}, \quad (7)$$

$$\frac{dR_P}{dt} = \gamma_3 I_P + \gamma_4 I_{PT} - \mu_P R_P, \quad (8)$$

$$\frac{dS_B}{dt} = \Lambda_B - \frac{\beta_3 I_B S_B}{N_B} - \mu_B S_B \,, \quad (9)$$

$$\frac{dI_B}{dt} = \frac{\beta_3 I_B S_B}{N_B} - [\mu_B + \delta_5] I_B. \quad (10)$$

## 3. Positivity of solutions

Since there is a portion of the system of equations in (4.1) to (4.10) represents the non-inhibitor populations, it is necessary to reflect on the fact that the associated population sizes can never be negative. Thus, we establish the positive invariance of $\Omega_1$ to be given as:

$\Omega_1 = \{ (S_H(t), I_H(t), I_{HT}(t), R_H(t), S_P(t), I_P(t), I_{PT}(t), R_P(t), S_B(t), I_B(t)) \in \Re_+^{10} \}$ then
$\{S_H(t), I_H(t), I_{HT}(t), R_H(t), S_P(t), I_P(t), I_{PT}(t), R_P(t), S_B(t), I_B(t) \text{ and } N_1(t)\} \geq 0, \forall\, t \geq 0$

There is need for all the variables to be non-negative for all time. This analysis ensures that the model is well posed and that it is realistic in representing the populations with non-negative values. A Mathematical equation is said to be well posed, if it has a solution and that solution should be unique and the solution must depend continuously on the data and parameters [9]; [2].

**Theorem 1**: The solutions set for the non-inhibitor sub-model $(S_H(t), I_H(t), I_{HT}(t), R_H(t), S_P(t), I_P(t), I_{PT}(t), R_P(t), S_B(t), I_B(t)) \in \Re_+^{10}$, are contained in the feasible solution $\Omega_1$. We describe the feasible solution to be such a state, where at the origin of the disease, the $(S_H(t), I_H(t), I_{HT}(t), R_H(t), S_P(t), I_P(t), I_{PT}(t), R_P(t), S_B(t), I_B(t))$ are non-zero;

**Proof**: Let $\{S_H(t), I_H(t), I_{HT}(t), R_H(t), S_P(t), I_P(t), I_{PT}(t), R_P(t), S_B(t), I_B(t) \ and \ N_1(t)\} \geq 0, \forall\, t \geq 0$.

We show that $\Omega_1$ is positively invariant so that it is sufficient to consider the dynamics of the model system

From (1):

$$\frac{dS_H}{dt} = \Lambda_H - \frac{\beta_1[\,\eta_0 I_H + \eta_1 I_P + \eta_2 I_B]S_H}{N_H} - \mu_H S_H$$
$$\Rightarrow \frac{dS_H}{dt} \geq -\left[\frac{\beta_1[\,\eta_0 I_H + \eta_1 I_P + \eta_2 I_B]}{N_H} + \mu_H\right] S_H \ .$$

Next, we integrate both sides

$$\int \frac{dS_H}{S_H} \geq -\int \left[\frac{\beta_1[\,\eta_0 I_H + \eta_1 I_P + \eta_2 I_B]}{N_H} + \mu_H\right] dt$$
$$\ln S_H \geq -\left[\frac{\beta_1[\,\eta_0 I_H + \eta_1 I_P + \eta_2 I_B]}{N_H} + \mu_H\right] t + S(t)$$

Take exponential of both sides

$$S_H \geq S_{H1}(t) e^{-\left[\frac{\beta_1[\,\eta_0 I_H + \eta_1 I_P + \eta_2 I_B]}{N_H} + \mu_H\right] t} \ .$$

At t=0,

$$S_H \geq S(0) \ .$$

This implies that

$$S_H \geq 0.$$

Similarly, we do this approach for the other variables, by this we have shown that all the solutions of (1 to 10) are in $\Re_+^{10}$, provided that the initial conditions are positive. Thus, our feasible region, $\Omega_1$ is positively invariant. Therefore, the model is mathematically well posed and epidemiologically reasonable. Hence, it is sufficient to consider the dynamic of the model (1 to 10 ) in $\Omega_1$ [7].

## 4. Disease free equilibrium (DFE)

Using the sub-model for the human without inhibitor as control, the force of infection for the non-inhibitor sub-model is given to be $\lambda_H = \frac{\beta_1[n_0 I_H + n_1 I_P + n_2 I_B]S_H}{N_H}$

Before we go further into the analysis, we must first determine the equilibrium points of the modelled system of equations.

To find the equilibrium point(s) for the non-inhibitor human compartment, we need to set the above equations (1), (2), (3), and (4) to zero, that is:

$$\frac{dS_H}{dt} = 0, \frac{dI_H}{dt} = 0, \frac{dI_{HT}}{dt} = 0, \frac{dR_H}{dt} = 0,$$

we have the following:

$$0 = \Lambda_H - \frac{\beta_1[n_0 I_H + n_1 I_P + n_2 I_B]S_H}{N_H} - \mu_H S_H, \quad (11)$$

$$0 = \frac{\beta_1[n_0 I_H + n_1 I_P + n_2 I_B]S_H}{N_H} - [\gamma_1 + \tau_1 + \mu_H + \delta_1]I_H, \quad (12)$$

$$0 = \tau_1 I_H - [\gamma_2 + \mu_H + \delta_2]I_{HT}, \quad (13)$$

$$0 = \gamma_1 I_H + \gamma_2 I_{HT} - \mu_H R_H \quad (14)$$

From (11), we replace $\beta_1$ with $q_1 I_H$, then solve for $S_H$

$$S_H = \frac{\Lambda_H N_H}{N_H \mu_H + q_1 I_H[n_0 I_H + n_1 I_P + n_2 I_B]} \quad (15)$$

From (12), we let $\beta_1 = q_1 I_H$ , then solve for $I_H$

$$0 = \left(\frac{q_1[n_0 I_H + n_1 I_P + n_2 I_B]S_H}{N_H} - [\gamma_1 + \tau_1 + \mu_H + \delta_1]\right) I_H \quad (16)$$

From (16), we found $I_H = 0$ or $\left(\frac{q_1[n_0 I_H + n_1 I_P + n_2 I_B]S_H}{N_H} - [\gamma_1 + \tau_1 + \mu_H + \delta_1]\right) = 0$ , considering this result from (16), it shows us that we would have two equilibrium points.

$$\Rightarrow \left(\frac{q_1 n_0 I_H S_H}{N_H} + \frac{q_1 n_1 I_P S_H}{N_H} + \frac{q_1 n_2 I_B S_H}{N_H} - [\gamma_1 + \tau_1 + \mu_H + \delta_1]\right) = 0$$

$$I_H = \left(\frac{N_H[\gamma_1 + \tau_1 + \mu_H + \delta_1] - [n_1 I_P + n_2 I_B]q_1 S_H}{q_1 n_0 S_H}\right).$$

Now, substitute the new value of $S_H$ in (15) into (12).

$$\Rightarrow I_H = 0 \; or \; I_H = \left(\frac{N_H[\gamma_1+\tau_1+\mu_H+\delta_1]-[n_1 I_P+n_2 I_B]q_1\Lambda_H}{q_1 n_0 \Lambda_H}\right).$$

Now we input $I_H = 0$ into (13), (14) and (15) to get the values for $I_{HT}$, $R_H$ and $S_H$ respectively.

For (13),

$$0 = \tau_1 I_H - [\gamma_2 + \mu_H + \delta_2] I_{HT}$$
$$I_{HT} = \frac{\tau_1 I_H}{[\gamma_2+\mu_H+\delta_2]},$$
$$I_{HT} = \frac{\tau_1 (0)}{[\gamma_2+\mu_H+\delta_2]} = 0$$
$$\therefore I_{HT} = 0.$$

For (14), we solve for $R_H$ and then substitute $I_H = 0$ and $I_{HT} = 0$ into the result

$$0 = \gamma_1 I_H + \gamma_2 I_{HT} - \mu_H R_H$$
$$R_H = \frac{\gamma_1 I_H + \gamma_2 I_{HT}}{\mu_H}$$
$$\Rightarrow R_H = \frac{\gamma_1(0)+\gamma_2(0)}{\mu_H} = 0$$

Then $R_H = 0$.

Next, we substitute $I_H = 0$ into (15)

$$S_H = \frac{\Lambda_H N_H}{N_H \mu_H + q I_H[n_0 I_H + n_1 I_P + n_2 I_B]}$$
$$S_H = \frac{\Lambda_H N_H}{N_H \mu_H + q(0)[n_0(0) + n_1 I_P + n_2 I_B]}$$
$$\Rightarrow S_H = \frac{\Lambda_H}{\mu_H}$$

Thus, we have the values for $S_H$, $I_H$, $I_{HT}$, and $R_H$.

Hence the first equilibrium point (which is popularly referred to as the DFE), to be given as:
$(S_H, I_H, I_{HT}, R_H) = \left(\frac{\Lambda_H}{\mu_H}, 0, 0, 0\right)$.

For the second equilibrium point, we substitute the value $I_H^* = \left(\frac{N_H[\gamma_1+\tau_1+\mu_H+\delta_1]-[n_1 I_P+n_2 I_B]q_1 n_0 \Lambda_H}{q_1 n_0 \Lambda_H}\right)$ into the following (13), (14), and (15) to get new values for $I_{HT}$, $R_H$, and $S_H$.

$$I_H^* = \left(\frac{N_H[\gamma_1+\tau_1+\mu_H+\delta_1]-[n_1 I_P+n_2 I_B]q_1 n_0 \Lambda_H}{q_1 n_0 \Lambda_H}\right) = W_2.$$

For (13),

$$0 = \tau_1 I_H^* - [\gamma_2 + \mu_H + \delta_2] I_{HT}^*$$

$$I_{HT}^* = \frac{\tau_1 I_H^*}{[\gamma_2+\mu_H+\delta_2]},$$

$$I_{HT}^* = \frac{\tau_1(N_H[\gamma_1+\tau_1+\mu_H+\delta_1]-[n_1 I_P+n_2 I_B]q_1 n_0 \Lambda_H)}{q_1 n_0 \Lambda_H\ [\gamma_2+\mu_H+\delta_2]} = W_3.$$

For (14), we solve for $R_H$ and then substitute $I_H^* = \left(\frac{N_H[\gamma_1+\tau_1+\mu_H+\delta_1]-[n_1 I_P+n_2 I_B]q_1 n_0 \Lambda_H}{q_1 n_0 \Lambda_H}\right)$ and $I_{HT}^* = \frac{\tau_1(N_H[\gamma_1+\tau_1+\mu_H+\delta_1]-[n_1 I_P+n_2 I_B]q_1 n_0 \Lambda_H)}{q_1 n_0 \Lambda_H\ [\gamma_2+\mu_H+\delta_2]}$ into (14).

$$0 = \gamma_1 I_H^* + \gamma_2 I_{HT}^* - \mu_H R_H^*$$

$$R_H^* = \frac{\gamma_1 I_H^* + \gamma_2 I_{HT}^*}{\mu_H}$$

$$R_H^* = \frac{\gamma_1(N_H[\gamma_1+\tau_1+\mu_H+\delta_1]-[n_1 I_P+n_2 I_B]q_1 n_0 \Lambda_H)\,[\gamma_2+\mu_H+\delta_2] + \gamma_2(\,\tau_1(N_H[\gamma_1+\tau_1+\mu_H+\delta_1]-[n_1 I_P+n_2 I_B]q_1 n_0 \Lambda_H))}{\mu_H(q_1 n_0 \Lambda_H)\ [\gamma_2+\mu_H+\delta_2]}$$

$$R_H^* = W_4.$$

For (15), we substitute $I_H^* = \left(\frac{N_H[\gamma_1+\tau_1+\mu_H+\delta_1]-[n_1 I_P+n_2 I_B]q_1 n_0 \Lambda_H}{q_1 n_0 \Lambda_H}\right)$ into (15):

$$S_H^* = \frac{\Lambda_H\ N_H}{N_H\,\mu_H + q_1\left(\frac{N_H[\gamma_1+\tau_1+\mu_H+\delta_1]-[n_1 I_P+n_2 I_B]q_1 n_0 \Lambda_H}{q_1 n_0 \Lambda_H}\right)\left[\, n_0\left(\frac{N_H[\gamma_1+\tau_1+\mu_H+\delta_1]-[n_1 I_P+n_2 I_B]q_1 n_0 \Lambda_H}{q_1 n_0 \Lambda_H}\right)+n_1 I_P+ n_2 I_B\right]}$$

$$S_H^* = \frac{\Lambda_H\ N_H\ q_1 n_0 \Lambda_H}{(N_H\,\mu_H)q_1 n_0 \Lambda_H + q_1(N_H[\gamma_1+\tau_1+\mu_H+\delta_1]-[n_1 I_P+n_2 I_B]q_1 n_0 \Lambda_H)[\, n_0(\,N_H[\gamma_1+\tau_1+\mu_H+\delta_1]-[n_1 I_P+n_2 I_B]q_1 n_0 \Lambda_H)+(n_1 I_P+ n_2 I_B)\, q_1 n_0 \Lambda_H]}$$

We then let $S_H^* = W_1$ . Now, we have the values for $S_H^*$, $I_H^*$, $I_{HT}^*$, and $R_H^*$ .

Hence the second equilibrium point (that is the EE), which is given as:
$S_H^*, I_H^*, I_{HT}^*, R_H^*) = (W_1, W_2, W_3, W_4)$.

We call the first equilibrium point the disease free equilibrium (DFE), while the second equilibrium point is called the endemic equilibrium (EE).

Since we have gotten the equilibrium points for our non-linear system of equation for the uncontrolled disease sub-model for human, we will then analyze these equilibrium points, as they are necessary for our study, because it is at these points, that we will discuss the stability of the modelled system.

Next, we find the equilibrium for the pig compartment of the non-inhibitor compartment:

$$\frac{dS_P}{dt} = \Lambda_P - \frac{\beta_2[I_P + n_2 I_B]S_P}{N_P} - \mu_P S_P, \quad (5)$$
$$\frac{dI_P}{dt} = \frac{\beta_2[I_P + n_2 I_B]S_P}{N_P} - [\gamma_3 + \tau_2 + \mu_P + \delta_3]I_P, \quad (6)$$
$$\frac{dI_{PT}}{dt} = \tau_2 I_P - [\gamma_4 + \mu_P + \delta_4]I_{PT}, \quad (7)$$
$$\frac{dR_P}{dt} = \gamma_3 I_P + \gamma_4 I_{PT} - \mu_P R_P . \quad (8)$$

At this point of our discussion, we replace $\beta_2$ with $gI_P$, which is the rate at which susceptible pigs become exposed to the disease.

To find the equilibrium point, we need to set the above equations (5), (6), (7), (8) to zero, that is:

$$\frac{dS_P}{dt} = 0, \frac{dI_P}{dt} = 0, \frac{dR_P}{dt} = 0,$$
$$0 = \Lambda_P - \frac{\beta_2[n_1 I_P + n_2 I_B]S_P}{N_P} - \mu_P S_P, \quad (17)$$
$$0 = \frac{\beta_2[n_1 I_P + \eta_2 I_B]S_P}{N_P} - [\gamma_3 + \tau_2 + \mu_P + \delta_3]I_P, \quad (18)$$
$$0 = \tau_2 I_P - [\gamma_4 + \mu_P + \delta_4]I_{PT}, \quad (19)$$

$$0 = \gamma_3 I_P + \gamma_4 I_{PT} - \mu_P R_P. \quad (20)$$

From (17) we solve for $S_P$:

$$S_P = \frac{\Lambda_P N_P}{N_P \mu_P + \beta_2[n_1 I_P + n_2 I_B]} \quad (21)$$

We let $\beta_2 = q_2 I_P$ , then we solve for $I_P$

$$0 = \left(\frac{q_2[n_1 I_P + \eta_2 I_B]S_P}{N_P} - [\gamma_3 + \tau_2 + \mu_P + \delta_3]\right) I_P. \quad (22)$$

For $\left(\frac{q_2[n_1 I_P + \eta_2 I_B]S_P}{N_P} - [\gamma_3 + \tau_2 + \mu_P + \delta_3]\right) = 0$ ,

$$\Rightarrow \left(\frac{q_2 n_1 I_P S_H}{N_P} + \frac{q_2 n_2 I_B S_H}{N_P} - [\gamma_1 + \tau_1 + \mu_H + \delta_1]\right) = 0$$

$$I_P = \left(\frac{N_P[\gamma_3 + \tau_2 + \mu_P + \delta_3] - [n_1 I_P + n_2 I_B]q_2 n_1 S_P}{q_2 n_1 S_P}\right).$$

From (38), we found $I_P = 0$ or $0 = \left(\frac{q_2[n_1 I_P + \eta_2 I_B]S_P}{N_P} - [\gamma_3 + \tau_2 + \mu_P + \delta_3]\right)$ considering this result from (38), it shows us that we would have two equilibrium points, one for $I_P = 0$ and the other when $I_P = \left(\frac{N_P[\gamma_3+\tau_2+\mu_P+\delta_3]-[n_1 I_P+n_2 I_B]q_2 n_1 S_P}{q_2 n_1 S_P}\right)$.

Now, substitute the new value of $S_P$ in (21) into the other value for $I_P$:

$$I_P^* = \frac{q_2\,[\,n_1 I_P + n_2 I_B]\Lambda_P \;\; -[\gamma_3+\tau_2+\mu_P+\delta_3]\,N_P\,\mu_P}{q_2\,[\,n_1 I_P + n_2 I_B]} = \; W_6 \; . \qquad (23)$$

Now we input $I_P = 0$ into (19), (20) and (21) to get the values for $I_{HT}$, $R_H$ and $S_H$ respectively.

For (19),

$$0 = \;\; \tau_2 I_P - [\gamma_4 + \mu_P + \delta_4] I_{PT},$$
$$I_{PT} = \frac{\tau_2 I_P}{[\gamma_4+\mu_P+\delta_4]} \;\; ,$$
$$I_{PT} = \frac{\tau_2\,(0)}{[\gamma_4+\mu_P+\delta_4]} = 0,$$
$$\therefore \; I_{PT} = \; 0\,.$$

For (20), we solve for $R_P$ and then substitute $I_P = 0$ and $I_{PT} = 0$ into the result

$$0 = \; \gamma_3 I_P + \; \gamma_4 I_{PT} \; - \; \mu_P R_P,$$
$$R_P = \frac{\gamma_3 I_P + \gamma_4 I_{PT}}{\mu_P}$$
$$\Rightarrow \;\; R_P = \frac{\gamma_3(0) + \gamma_4(0)}{\mu_P} = 0$$

Then $R_P = 0$.

Next, we substitute $I_P = \; 0$ into (15):

$$S_P = \frac{\Lambda_P \;\; N_P}{N_P \;\mu_P + \; q_2 I_P[\,n_1 I_P + n_2 I_B]}$$
$$S_P = \frac{\Lambda_P \;\; N_P}{N_P \;\mu_P + \; q_2(0)[n_1(0) + n_2 I_B]}$$
$$\Rightarrow \; S_P = \frac{\Lambda_P}{\mu_P}.$$

Thus, we have the values for $S_P$, $I_P$, $I_{PT}$, and $R_P$ . Hence the first equilibrium point (that is the DFE), which is given as:

$$(S_P\,, I_P, I_{PT}, R_P) = \left(\frac{\Lambda_P}{\mu_P}\,, 0, 0, 0\right).$$

For the second equilibrium point, we substitute (23) into the following (19), (20), and (21) to get new values for $I_{PT}$, $R_P$, and $S_P$

For (19),

$$0 = \tau_2 I_P^* - [\gamma_4 + \mu_P + \delta_4] I_{PT}^*$$
$$I_{PT}^* = \frac{\tau_2 I_P^*}{[\gamma_4+\mu_P+\delta_4]} ,$$
$$I_{PT}^* = \frac{\tau_2(q_2 [n_1 I_P + n_2 I_B]\Lambda_H - [\gamma_3+\tau_2+\mu_P+\delta_4] N_P \mu_P)}{q_2 [n_1 I_P + n_2 I_B] [\gamma_4+\mu_P+\delta_4]} = W_7.$$

For (20), we solve for $R_H$ and then substitute $I_P^* = \frac{q_2 [n_1 I_P + n_2 I_B]\Lambda_P - [\gamma_1+\tau_1+\mu_H+\delta_1] N_H \mu_H}{q_2 [n_0 I_H + n_1 I_P + n_2 I_B]}$ and $I_{HT}^* = \frac{\tau_2(q_2 [n_1 I_P + n_2 I_B]\Lambda_P - [\gamma_3+\tau_2+\mu_P+\delta_3] N_P \mu_P)}{q_2 [n_1 I_P + n_2 I_B] [\gamma_4+\mu_P+\delta_4]}$ into the result

$$0 = \gamma_3 I_P^* + \gamma_4 I_{PT}^* - \mu_P R_P^*$$
$$R_P^* = \frac{\gamma_3 I_P^* + \gamma_4 I_{PT}^*}{\mu_P}$$
$$R_P^* = \frac{\gamma_2(q_2 [n_1 I_P + n_2 I_B]\Lambda_P - [\gamma_3+\tau_2+\mu_P+\delta_3] N_H \mu_H) [\gamma_2+\mu_H+\delta_2] + \gamma_2(\tau_1(q_2 [n_1 I_P + n_2 I_B]\Lambda_P - [\gamma_3+\tau_2+\mu_P+\delta_3] N_P \mu_P))}{\mu_P(q_2 [n_1 I_P + n_2 I_B] [\gamma_4+\mu_P+\delta_4])}$$
$$R_H^* = W_8 .$$

For (21), we substitute $I_P^* = \frac{q_2 [n_1 I_P + n_2 I_B]\Lambda_P - [\gamma_3+\tau_2+\mu_P+\delta_3] N_P \mu_P}{q_2 [n_1 I_P + n_2 I_B]}$ into (21):

$$S_P^* = \frac{\Lambda_P N_P}{N_P \mu_P + q_2 I_P [n_1 I_P + n_2 I_B]}$$
$$S_P^* = \frac{\Lambda_P N_P ([n_1 I_P + n_2 I_B])}{N_P \mu_P ([n_1 I_P + n_2 I_B]) + (q_2 [n_1 I_P + n_2 I_B]\Lambda_P - [\gamma_3+\tau_2+\mu_P+\delta_3] N_P \mu_P)[n_1 I_P + n_2 I_B]}$$
$$\Rightarrow S_P^* = \frac{\Lambda_P N_P}{N_P \mu_P + (q_2 [n_1 I_P + n_2 I_B]\Lambda_P - [\gamma_3+\tau_2+\mu_P+\delta_3] N_P \mu_P)} = W_5 .$$

Now, we have the values for $S_P^*$, $I_P^*$, $I_{PT}^*$, and $R_P^*$ . Hence the second equilibrium point (that is the EE), which is given as:
$(S_P^* , I_P^*, I_{PT}^*, R_P^*) = (W_5, W_6, W_7, W_8)$.

Similarly, we find the equilibrium point for the bat compartment. Recall

$\lambda_B = \frac{\beta_3 I_B S_P}{N_P}$ = FOI for bats

$$\frac{dS_B}{dt} = \Lambda_P - \frac{\beta_3 I_B S_B}{N_B} - \mu_B S_B \qquad (9)$$

$$\frac{dI_B}{dt} = \frac{\beta_3 n_2 I_B S_B}{N_B} - [\mu_B + \delta_5]I_B \ . \qquad (10)$$

At this point of our discussion, we replace $\beta_3$ with $q_3 I_B$, which is the rate at which susceptible bats become exposed to the disease.

To find the equilibrium point or fixed point, we need to set the above equations (9), (10) to zero, that is:

$$\frac{dS_B}{dt} = 0, \frac{dI_B}{dt} = 0, \frac{dB}{dt} = 0$$

$$0 = \Lambda_B - \frac{\beta_3 n_2 I_B S_B}{N_B} - \mu_B S_B \qquad (24)$$

$$0 = \frac{\beta_3 n_2 I_B S_B}{N_B} - [\mu_B + \delta_5]I_B \ . \qquad (25)$$

From (24) we have the following:

$$0 = \Lambda_B - \frac{\beta_3 n_2 I_B S_B}{N_B} - \mu_B S_B$$

$$S_B = \frac{\Lambda_B N_B}{N_B \mu_B + \beta_3 n_2 I_B} \ . \qquad (26)$$

Now, we let $\beta_3 = q_3 I_B$ , then we solve for $I_B$ in (25)

$$0 = \frac{q_3 I_B n_2 I_B S_B}{N_B} - [\mu_B + \delta_5]I_B$$

$$0 = \left(\frac{q_3 I_B n_2 S_P}{N_B} - [\mu_B + \delta_5]\right) I_B$$

$$\Rightarrow I_B = 0 \ and \ 0 = \left(\frac{q_3 I_B n_2 S_P}{N_P} - [\mu_B + \delta_5]\right).$$

For $\left(\frac{q_3 I_B n_2 S_P}{N_B} - [\mu_B + \delta_5]\right) = 0$

$$\Rightarrow \left(\frac{q_3 I_B n_1 S_P}{N_B} - [\mu_B + \delta_5]\right) = 0$$

$$I_B = \left(\frac{N_B[\mu_B + \delta_5]}{q_3 n_2 S_B}\right).$$

From (25), we found $I_B = 0$ or $0 = \left(\frac{q_3[n_2 I_B] S_B}{N_B} - [\mu_B + \delta_5]\right)$ considering this result from (25), it shows us that we would have two equilibrium points, one for $I_B = 0$ and when $I_B = \left(\frac{N_B[\mu_B + \delta_5]}{q_3 n_2 S_B}\right)$

Now, substitute (26) into the other value for $I_B$:

$$I_B^* = \left(\frac{N_B([\mu_B+\delta_5]N_B\,\mu_B+[\mu_B+\delta_5]\,q_3n_2I_B)}{q_3n_2\Lambda_B\;N_B}\right) = \; W_{10}\,. \qquad (27)$$

Now we input $I_P = 0$ into (26) to get the value for $S_H$. For (26),

$$S_B = \frac{\Lambda_B\;N_B}{N_B\,\mu_B+\,q_3\,I_Bn_2I_B}$$
$$S_B = \frac{\Lambda_B\;N_B}{N_B\,\mu_B+\,q_3\,(0)n_2(0)}$$
$$\Rightarrow S_B = \frac{\Lambda_B}{\mu_B}\;.$$

Hence the first equilibrium point is given as $(S_B\,, I_B) = \left(\frac{\Lambda_B}{\mu_B}\,, 0\right)$. Next, we compute the second equilibrium point

Put $I_B^* = \left(\frac{N_B([\mu_B+\delta_5]N_B\,\mu_B+[\mu_B+\delta_5]\,q_3n_2I_B)}{q_3n_2\Lambda_B\;N_B}\right)$ into (26) to find the endemic value for $S_B$

$$S_B^* = \frac{\Lambda_B\;N_B\,(q_3n_2\Lambda_B\;N_B)^2}{N_B\,\mu_B(q_3n_2\Lambda_B\;N_B)^2+\,q_3\,n_2(N_B([\mu_B+\delta_5]N_B\,\mu_B+[\mu_B+\delta_5]\,q_3n_2I_B))^2}.$$

Therefore, the second equilibrium point the bat compartment is:

$$(\,S_B^*\,, I_B^*) = \left(\frac{\Lambda_B\;N_B\,(q_3n_2\Lambda_B\;N_B)^2}{N_B\,\mu_B(q_3n_2\Lambda_B\;N_B)^2+\,q_3\,n_2(N_B([\mu_B+\delta_5]N_B\,\mu_B+[\mu_B+\delta_5]\,q_3n_2I_B))^2}\,, \left(\frac{N_B([\mu_B+\delta_5]N_B\,\mu_B+[\mu_B+\delta_5]\,q_3n_2I_B)}{q_3n_2\Lambda_B\;N_B}\right)\right).$$

Hence, the disease free equilibrium, $E^0$, (DFE) for the non-inhibitor Niv model are:

$$(S_H(0)^0, I_H(0)^0, I_{HT}(0)^0, R_H(0)^0, S_P(0)^0, I_P(0)^0, I_{PT}(0)^0, R_P(0)^0, S_B(0)^0, I_B(0)^0\,) =$$
$$\left(\frac{\Lambda_H}{\mu_H}\,, 0, 0, 0, \frac{\Lambda_P}{\mu_P}\,, 0, 0, 0, \frac{\Lambda_B}{\mu_B}\,, 0\;\right)$$

where, the endemic equilibrium, $E^*$, (EE) for the non-inhibitor Niv model are:

$$(S_H(0)^*, I_H(0)^*, I_{HT}(0)^*, R_H(0)^*, S_P(0)^*, I_P(0)^*, I_{PT}(0)^*, R_P(0)^*, S_B(0)^*, I_B(0)^*) =$$
$$\left( \frac{[\gamma_1+\tau_1+\mu_H+\delta_1]N_H}{q[n_0I_H+n_1I_P+n_2I_B]}, \frac{\Lambda_H q[n_0I_H+n_1I_P+n_2I_B]-[\gamma_1+\tau_1+\mu_H+\delta_1]N_H}{q[n_0I_H+n_1I_P+n_2I_B]}, \frac{\tau_1(\Lambda_H q[n_0I_H+n_1I_P+n_2I_B]-[\gamma_1+\tau_1+\mu_H+\delta_1]N_H)}{q[n_0I_H+n_1I_P+n_2I_B][\gamma_2+\mu_H+\delta_2]}, \right.$$
$$\gamma_1 \frac{\Lambda_H q[n_0I_H+n_1I_P+n_2I_B]-[\gamma_1+\tau_1+\mu_H+\delta_1]N_H}{q[n_0I_H+n_1I_P+n_2I_B]\mu_H}, \frac{[\gamma_3+\tau_2+\mu_P+\delta_3]N_P}{g[n_1I_P+n_2I_B]}, \frac{\Lambda_P g[I_P+n_2I_B]-[\gamma_3+\tau_2+\mu_P+\delta_3]T_P}{g[n_1I_P+n_2I_B]}, \tau_2 \frac{\Lambda_P g[n_1I_P+n_2I_B]-[\gamma_3+\tau_2+\mu_P+\delta_3]N_P}{g[n_1I_P+n_2I_B][\gamma_4+\mu_P+\delta_4]},$$
$$\left. \gamma_3 \frac{\Lambda_P g[n_1I_P+n_2I_B]-[\gamma_3+\tau_2+\mu_P+\delta_3]T_P}{g[n_1I_P+n_2I_B]\mu_P}, \frac{[\mu_B+\delta_5]N_B}{\beta_3}, \left[ \frac{\Lambda_B-S_B\mu_B}{S_B} \right] \frac{N_B}{\beta_3} \right)$$

## 5. The basic reproductive number ($R_0$) for the study

Epidemiologists calculate $R_0$ using various approaches, like individual-level contact tracing data obtained at the beginning of the pandemic. Once a person is diagnosed, his/her contacts are traced and tested. $R_0$ is then figured out by averaging over the number of secondary cases of all diagnosed individuals. If one or more infected person(s), is introduced into the community, the disease could either spread or die out [10]. This approach is based upon the definition of $R_0$, but it does not ensure that the calculated $R_0$ is also an epidemic doorstep parameter.

Now, rewriting the inhibitor free model, starting with the disease compartment, we have:

$$\frac{dI_H}{dt} = \frac{\beta_1[n_0I_H+n_1I_P+n_2I_B]S_H}{N_H} - [\gamma_1+\tau_1+\mu_H+\delta_1]I_H,$$
$$\frac{dI_{HT}}{dt} = \tau_1 I_H - [\gamma_2+\mu_H+\delta_2]I_{HT},$$
$$\frac{dI_P}{dt} = \frac{\beta_2[I_P+n_2I_B]S_P}{N_P} - [\gamma_3+\tau_2+\mu_P+\delta_3]I_P,$$
$$\frac{dI_{PT}}{dt} = \tau_2 I_P - [\gamma_4+\mu_P+\delta_4]I_{PT},$$
$$\frac{dI_B}{dt} = \frac{\beta_3 n_2 I_B S_B}{N_B} - [\mu_B+\delta_5]I_B$$
$$\frac{dS_H}{dt} = \Lambda_H - \frac{\beta_1[n_0I_H+n_1I_P+n_2I_B]S_H}{N_H} - \mu_H S_H,$$
$$\frac{dS_P}{dt} = \Lambda_P - \frac{\beta_2[I_P+n_2I_B]S_P}{N_P} - \mu_P S_P$$
$$\frac{dS_B}{dt} = \Lambda_B - \frac{\beta_3 n_2 I_B S_B}{N_B} - \mu_B S_B$$
$$\frac{dR_H}{dt} = \gamma_1 I_H + \gamma_2 I_{HT} - \mu_H R_H$$
$$\frac{dR_P}{dt} = \gamma_3 I_P + \gamma_4 I_{PT} - \mu_P R_P.$$

From the above model of our study, we have:

$X$ = vector of the infected classes, such as exposed, carrier, infectious etc.
$Y$ = vector of uninfected classes, such as susceptible, recovered etc.

Therefore,
$$X = \begin{pmatrix} I_H \\ I_{HT} \\ I_P \\ I_{PT} \\ I_B \end{pmatrix},\ Y = \begin{pmatrix} S_H \\ S_P \\ S_B \\ R_H \\ R_P \end{pmatrix}$$

$$f = \begin{bmatrix} f_1 \\ f_2 \\ f_3 \\ f_4 \\ f_5 \end{bmatrix},\ v = \begin{bmatrix} v_1 \\ v_2 \\ v_3 \\ v_4 \\ v_5 \end{bmatrix}$$

$$f = \begin{bmatrix} \frac{\beta_1[\,n_0 I_H + n_1 I_P + n_2 I_B]S_H}{N_H} \\ 0 \\ \frac{\beta_2[n_1 I_P + n_2 I_B]S_P}{N_P} \\ 0 \\ \frac{\beta_3 n_2 I_B\, S_B}{N_B} \end{bmatrix},\quad v = \begin{bmatrix} [\gamma_1+\tau_1+\mu_H+\delta_1]I_H \\ -\tau_1 I_H + [\gamma_2+\mu_H+\delta_2]I_{HT} \\ [\gamma_3+\tau_2+\mu_P+\delta_3]I_P \\ -\tau_2 I_P + [\gamma_4+\mu_P+\delta_4]I_{PT} \\ [\mu_B+\delta_5]I_B \end{bmatrix},$$

$$F = \begin{bmatrix} \frac{\partial f_1}{\partial I_H} & \frac{\partial f_1}{\partial I_{HT}} & \frac{\partial f_1}{\partial I_P} & \frac{\partial f_1}{\partial I_{PT}} & \frac{\partial f_1}{\partial I_B} \\ \frac{\partial f_2}{\partial I_H} & \frac{\partial f_2}{\partial I_{HT}} & \frac{\partial f_2}{\partial I_P} & \frac{\partial f_2}{\partial I_{PT}} & \frac{\partial f_2}{\partial I_B} \\ \frac{\partial f_3}{\partial I_H} & \frac{\partial f_3}{\partial I_{HT}} & \frac{\partial f_3}{\partial I_P} & \frac{\partial f_3}{\partial I_{PT}} & \frac{\partial f_3}{\partial I_B} \\ \frac{\partial f_4}{\partial I_H} & \frac{\partial f_4}{\partial I_{HT}} & \frac{\partial f_4}{\partial I_P} & \frac{\partial f_4}{\partial I_{PT}} & \frac{\partial f_4}{\partial I_B} \\ \frac{\partial f_5}{\partial I_H} & \frac{\partial f_5}{\partial I_{HT}} & \frac{\partial f_5}{\partial I_P} & \frac{\partial f_5}{\partial I_{PT}} & \frac{\partial f_5}{\partial I_B} \end{bmatrix},\ V = \begin{bmatrix} \frac{\partial V_1}{\partial I_H} & \frac{\partial V_1}{\partial I_{HT}} & \frac{\partial V_1}{\partial I_P} & \frac{\partial V_1}{\partial I_{PT}} & \frac{\partial V_1}{\partial I_B} \\ \frac{\partial V_2}{\partial I_H} & \frac{\partial V_2}{\partial I_{HT}} & \frac{\partial V_2}{\partial I_P} & \frac{\partial V_2}{\partial I_{PT}} & \frac{\partial V_2}{\partial I_B} \\ \frac{\partial V_3}{\partial I_H} & \frac{\partial V_3}{\partial I_{HT}} & \frac{\partial V_3}{\partial I_P} & \frac{\partial V_3}{\partial I_{PT}} & \frac{\partial V_3}{\partial I_B} \\ \frac{\partial V_4}{\partial I_H} & \frac{\partial V_4}{\partial I_{HT}} & \frac{\partial V_4}{\partial I_P} & \frac{\partial V_4}{\partial I_{PT}} & \frac{\partial V_4}{\partial I_B} \\ \frac{\partial V_5}{\partial I_H} & \frac{\partial V_5}{\partial I_{HT}} & \frac{\partial V_5}{\partial I_P} & \frac{\partial V_5}{\partial I_{PT}} & \frac{\partial V_5}{\partial I_B} \end{bmatrix}.$$

Therefore, we have

$$F = \begin{bmatrix} \frac{\beta_1 n_0\, S_H}{N_H} & 0 & \frac{\beta_1 n_1\, S_H}{N_H} & 0 & \frac{\beta_1 n_2\, S_H}{N_H} \\ 0 & 0 & 0 & 0 & 0 \\ 0 & 0 & \frac{\beta_2 n_1 S_P}{N_P} & 0 & \frac{\beta_2 n_2 S_P}{N_P} \\ 0 & 0 & 0 & 0 & 0 \\ 0 & 0 & 0 & 0 & \frac{\beta_3 n_2 S_B}{N_B} \end{bmatrix},$$

$$V = \begin{bmatrix} [\gamma_1+\tau_1+\mu_H+\delta_1] & 0 & 0 & 0 & 0 \\ 0 & -\tau_1 I_H + [\gamma_2+\mu_H+\delta_2] & 0 & 0 & 0 \\ 0 & 0 & [\gamma_3+\tau_2+\mu_P+\delta_3] & 0 & 0 \\ 0 & 0 & -\tau_2 & [\gamma_4+\mu_P+\delta_4] & 0 \\ 0 & 0 & 0 & 0 & [\mu_B+\delta_5] \end{bmatrix}.$$

Next, we evaluate $F$ at DFE. Therefore, we have

$$F = \begin{bmatrix} \frac{\beta_1 n_0 \Lambda_H}{N_H \mu_H} & 0 & \frac{\beta_1 n_1 \Lambda_H}{N_H \mu_H} & 0 & \frac{\beta_1 n_2 \Lambda_H}{N_H \mu_H} \\ 0 & 0 & 0 & 0 & 0 \\ 0 & 0 & \frac{\beta_2 n_1 \Lambda_P}{N_P \mu_P} & 0 & \frac{\beta_2 n_2 \Lambda_P}{N_P \mu_P} \\ 0 & 0 & 0 & 0 & 0 \\ 0 & 0 & 0 & 0 & \frac{\beta_3 n_2 \Lambda_B}{N_B \mu_B} \end{bmatrix},$$

$$V = \begin{bmatrix} [\gamma_1+\tau_1+\mu_H+\delta_1] & 0 & 0 & 0 & 0 \\ 0 & [\gamma_2+\mu_H+\delta_2] & 0 & 0 & 0 \\ 0 & 0 & [\gamma_3+\tau_2+\mu_P+\delta_3] & 0 & 0 \\ 0 & 0 & -\tau_2 & [\gamma_4+\mu_P+\delta_4] & 0 \\ 0 & 0 & 0 & 0 & [\mu_B+\delta_5] \end{bmatrix}.$$

We then compute $V^{-1}$, using Maple 2019:

$$\begin{bmatrix} \left[\frac{1}{\gamma 1 + \tau 1 + \mu H + \delta 1}, 0, 0, 0, 0\right], \\ \left[0, \frac{1}{\gamma 2 + \mu H + \delta 2}, 0, 0, 0\right], \\ \left[0, 0, \frac{1}{\gamma 3 + \tau 2 + \mu P + \delta 3}, 0, 0\right], \\ \left[0, 0, \frac{\tau 2}{(\gamma 3 + \tau 2 + \mu P + \delta 3)(\gamma 4 + \mu P + \delta 4)}, \frac{1}{\gamma 4 + \mu P + \delta 4}, 0\right], \\ \left[0, 0, 0, 0, \frac{1}{\mu B + \delta 5}\right] \end{bmatrix}$$

Since we have gotten $V^{-1}$ and we also have F, then, we can then compute the Next Generation Matrix (NGM) for the uncontrolled disease model.

$$\left[\left[\frac{\beta 1(n0)\,\Lambda H}{(\gamma 1+\tau 1+\mu H+\delta 1)\,NH(\mu H)},\ 0,\ \frac{\beta 1(n1)\,\Lambda H}{(\gamma 1+\tau 1+\mu H+\delta 1)\,NH(\mu H)},\ 0,\ \frac{\beta 1(n2)\,\Lambda H}{(\gamma 1+\tau 1+\mu H+\delta 1)\,NH(\mu H)}\right],\ \left[0,0,0,0,0\right],\ \left[0,0,\frac{\beta 2(n1)\,\Lambda P}{(\gamma 3+\tau 2+\mu P+\delta 3)\,NP(\mu P)},0,\frac{\beta 1(n2)\,\Lambda P}{(\gamma 3+\tau 2+\mu P+\delta 3)\,NP(\mu P)}\right],\ \left[0,0,\frac{\tau 2\,\beta 2(n1)\,\Lambda P}{(\gamma 3+\tau 2+\mu P+\delta 3)\,(\gamma 4+\mu P+\delta 4)\,NP(\mu P)},0,\frac{\tau 2\,\beta 1(n2)\,\Lambda P}{(\gamma 3+\tau 2+\mu P+\delta 3)\,(\gamma 4+\mu P+\delta 4)\,NP(\mu P)}\right],\ \left[0,0,0,0,\frac{\beta 1(n2)\,\Lambda B}{(\mu B+\delta 5)\,NB(\mu B)}\right]\right]$$

Next, we determine the eigenvalues of our non-inhibitor model. Now we compute $|FV^{-1}-A_iI|=0$, where $A_i$ is given as the Eigen values.

The eigenvalues for the non-inhibitor model is given as:

$$\begin{bmatrix} 0 \\ 0 \\ \dfrac{\beta 2(n1)\,\Lambda P}{(\gamma 3+\tau 2+\mu P+\delta 3)\,NP(\mu P)} \\ \dfrac{\beta 1(n0)\,\Lambda H}{(\gamma 1+\tau 1+\mu H+\delta 1)\,NH(\mu H)} \\ \dfrac{\beta 1(n2)\,\Lambda B}{(\mu B+\delta 5)\,NB(\mu B)} \end{bmatrix}$$

Therefore, $R_0 = \frac{\beta_1 n_0\,\Lambda_H}{[\gamma_1+\tau_1+\mu_H+\delta_1]\,N_H\mu_H}$. This is the basic Reproductive number for our non-inhibitor model. Result for $R_0$, was first recognized by [10], many other works have been done on $R_0$, such as [6].

In practice, $R_0$ does not depend on the assumptions about immunity subsequent to the infectious period. The $R_0$ concept is based on an assumed situation where one infective is introduced into a large susceptible population [4] In reality, such situations hardly ever occur, such that one has to base estimates of Ro on data available in endemic situations where the infection is present for a long time. However, this requires detailed knowledge about the density-dependent regulation of the

transmission process which determines the equilibrium endemic level. It also assumes knowledge about the heterogeneities in transmission patterns, as it is obvious that estimates of Ro based on equilibrium data are highly dependent on the availability of this required information or on the degree to which the assumed mechanisms reflect reality.

## 6. Sensitivity indices of NiV infection model parameters

In this section, we try to determine how changes in each of the parameters affect the transmission and spread of the disease. In order to achieve this, a sensitivity analysis of the non-inhibitor model is carried out. This is also done in order for us to see the response of the model output (in this case $R_0$) to parameter(s) variation.

In 2017, [3], gave us a clear succinct definition of sensitivity analysis where he stated that the normalized forward- sensitivity index of a variable, $v$, depends on a parameter of interest, p, which is defined as:

$$\mathrm{r}_p^v = \frac{\partial v}{\partial p} \times \frac{p}{v}.$$

In particular, the sensitivity indices, of the basic reproduction number, $R_0$, with respect to the model parameters are examined.

The positive sign of sensitivity indices of $R_0$ to the model parameters illustrates that an increase (or decrease) in the value of each of the parameter in the model, may lead to an increase (or decrease) in $R_0$ of the model (1-10) and asymptotically result into persistency (or elimination) of the disease in the community. On the contrary, the negative sign of S.I of $R_0$ to the model parameter indicates that an increase (or decrease) in the value of each of the parameter in each case leads to a corresponding decrease (or increase) in $R_0$ of the model (1-10). Hence, with sensitivity analysis, one can get insight on the appropriate intervention strategies to prevent and control the spread of the disease described in model (1-10).

Recall that

$$R_0 = \frac{\beta_1 n_0 \Lambda_H}{[\gamma_1+\tau_1+\mu_H+\delta_1] N_H \mu_H},$$

and that $n_0 > 0$.

Hence:

$$\boldsymbol{r}_{\mu_H}^{R_0} = \frac{\partial R_0}{\partial \mu_H} \times \frac{\mu_H}{R_0}$$
$$= -\left(\frac{\beta_1 n_0 \Lambda_H}{[\gamma_1+\tau_1+\mu_H+\delta_1] N_H \mu_H^2} + \frac{\beta_1 n_0 \Lambda_H}{[\gamma_1+\tau_1+\mu_H+\delta_1]^2 N_H \mu_H}\right) \times \frac{[\gamma_1+\tau_1+\mu_H+\delta_1] N_H \mu_H^2}{\beta_1 n_0 \Lambda_H}$$

$$= -\left(\frac{\beta_1 n_0 \Lambda_H[\gamma_1+\tau_1+\mu_H+\delta_1] + \beta_1 n_0 \Lambda_H \mu_H}{[\gamma_1+\tau_1+\mu_H+\delta_1]^2 N_H \mu_H{}^2}\right) \times \left(\frac{[\gamma_1+\tau_1+\mu_H+\delta_1]\, N_H \mu_H{}^2}{\beta_1 n_0 \Lambda_H}\right)$$

$$= -\left(\frac{[\gamma_1+\tau_1+\mu_H+\delta_1] + \mu_H}{[\gamma_1+\tau_1+\mu_H+\delta_1]^2 N_H \mu_H{}^2}\right) \times ([\gamma_1 + \tau_1 + \mu_H + \delta_1]\, N_H \mu_H{}^2)$$

$$= -\left(\frac{[\gamma_1+\tau_1+\mu_H+\delta_1] + \mu_H}{[\gamma_1+\tau_1+\mu_H+\delta_1]\mu_H}\right) \quad (negative)$$

Summarily, the table below shows the signs of S.I. of $R_0$:

$\beta_1 - positive$
$\Lambda_H - positive$
$n_0 - positive$
$\delta_1 - negaive$
$N_H - negative$
$\tau_1 - negative$
$\gamma_1 - negative$
$\mu_H - negative$

Thus, if we increase (decrease) any of the parameters $\beta_1, \Lambda_H, n_0$, then $R_0$ will increase (decrease). Also, if we increase (decrease) any of $N_H$, $\mu_H$, $\gamma_1$,$\tau_1$, $\delta_1$, then $R_0$ will decrease (increase). Sensitive index of other parameters that did not appear in $R_0$ are zero, that is, the increase or decrease of such parameter has no influence on the reproductive number.

## 6. Conclusion

The periodic outbreaks of deadly Nipah virus infections in Malaysia have become the most public health concerns because of the highly mortality rates. Once an outbreak occurs in any region of the country, the virus can be transmitted to the whole family and/or even in the community. The study derives an estimate of $R_0$ based on Nipah virus epidemic and endemic situations to interpret $R_0$, from our assumptions and theories of existing researches. During the last twenty years $R_0$ has emerged as a basic concept in infectious disease epidemiology, but it has also become apparent how difficult it is to apply in actual field situations [4]. It was discovered that some parameters were found to be positively contributing to the spread of the disease, parameters like $\Lambda_H$, which is the recruitment parameter for the model, $\beta_1$, this parameter is the effective contact rate, while some other parameters reduce the spread of the disease, parameters like $\tau_1$, which is the proportion of infected that goes for treatment, while $\mu_H$, natural death. It is our hope that this survey will motivate further research in this direction.

## References


[1] Ang B. S. P., Lim T. C. C., and Wang L. (2018). Nipah virus infection. Accessed on 22nd June 2019 from https://www.ncbi.nlm.nih.gov/pmc/articles/PMC5971524/.

[2] Bartuccelli M. V, Gourley S. A., and Woolcock C. J. (1997). Conditions for positivity of solutions of a class of dissipative partial differential equations. Accessed on 19th January, 2022 from https://www.researchgate.net/publication/242802652_Conditions_for_positivity_of_solutions_of_a_class_of_dissipative_partial_differential_equations.

[3] Bertrand L. and Andrea S. (2017). Introduction to sensitivity analysis. Accessed on 22nd of December, 2021 from https://link.springer.com/referenceworkentry/10.1007/978-3-319-12385-1_31?noAccess=true

[4] Dietz K. (1993). The estimation of the basic reproduction number for infectious diseases. Accessed on 11th July, 2021 from https://journals.sagepub.com/doi/10.1177/096228029300200103 or https://www.researchgate.net/publication/14938541_The_Estimation_of_the_Basic_Reproduction_Number_for_Infectious_Diseases/link/55b6868708ae092e9656ecd6/download.

[5] Giangasper M. (2013). Tropical medicine and surgery. Accessed on 14th March, 2022 from https://www.researchgate.net/publication/269552982_Nipah_Virus/link/552f52ce0cf2acd38cbbf3ee/download.

[6] Heffernan J. M, Smith R. J., and Wahl L. M. (2005). Perspectives on the basic reproductive ratio. Accessed on 22nd January, 2022 from https://www.ncbi.nlm.nih.gov/pmc/articles/PMC1578275/#bib42.

[7] Hethcote H. W. (2000). The mathematics of infectious disease. Accessed on 23rd April, 2021 from https://epubs.siam.org/doi/epdf/10.1137/S0036144500371907.

[8] Hosono H., Kono H., Ito S., and Shirai J. (2006). Economic impact of the Nipah Virus infection outbreak in Malaysia. Accessed on 14th June, 2019 from http://www.sciquest.org.nz/elibrary/download/63964/T6-1.3.1+-+Economic+impact+of+nipah+virus+infection+outbreak+in+Malaysia.

[9] Kirwa P.I., Rotich T., Obogi R., and Tanui P.K. (2017). Boundedness and positivity of a mathematical model of the immune response to HIV infection. Accessed on 12th March, 2022 from https://www.researchgate.net/publication/321796765_Boundedness_and_Positivity_of_a_Mathematical_Model_of_the_Immune_Response_to_HIV_Infection

[10] Kermack W.O. and McKendrick A.G. (1927). A contribution to the mathematical theory of epidemics. Proc. R. Soc. 1927;115:700–721, Accessed on 7th March, 2022 from https://royalsocietypublishing.org/doi/pdf/10.1098/rspa.1927.0118

[11] Reddy K. R. (2018). Nipah Virus (NiV) Infection: An Emerging Zoonosis of Public Health Concern. Accessed on 11th January, 2022 from https://www.researchgate.net/publication/331574912_Nipah_Virus_NiV_Infection_An_Emerging_Zoonosis_of_Public_Health_Concern/link/5c8155f392851c6950608118/download.

[12] World Health Organization (WHO). 2018 Nipah research and development (R&D) roadmap. Accessed on 10th July, 2020 from https://www.who.int/teams/blueprint/nipah

[13] World Health Organization (WHO). 2018. Nipah virus. Accessed on 22nd June 2019 from https://www.who.int/news-room/fact-sheets/detail/nipah-virus.

**International Journal of Mathematical Analysis and Modelling**
**Volume 5, Issue 1, May 2022, Pages 121 – 127**

# Analysis of drought and flood occurrence using markov chain

**O. K. Musa[*], L. Adamu[*†], E. N. Didigwu[‡], A. Abdullahi[§], and S. D. Yakubu[**]**

**Abstract**

Flood and drought are among the most common natural disasters affecting the world. In this paper, Markov model has been used to analyse and predict flood and drought occurrences in Birnin Kebbi, Nigeria. The Standardized Precipitation index(SPI) was used to classify the annual rainfall of Birnin Kebbi into three states (flood, normal and drought). After some successful iterations of the model, the model stabilized to equilibrium probabilities, revealing that in the long-run 20% of the years in Birnin Kebbi will experience flood, 60% will experience normal rainfall and 20% will experience drought. It was also observed that, a drought year cannot be followed by a flood year and the probability of a drought year to be followed by a normal year is high while the probability of a normal year to be followed by a drought year and a drought year to be followed by another drought year is extremely small. Results from this research is an important information to the government and people of Kebbi state for better understanding of rainfall dynamics in their locality.

***Keywords***: markov model; annual rainfall, standardized precipitation index, transition probability, equilibrium probabilities.

## 1. Introduction

Floods and droughts are among the most disastrous natural hazards in the world ([1] and [4]). Drought occurs when there is significant rainfall deficit that causes hydrological imbalances and affects the land productive systems. Drought practically occurs in all climatic regions with both high and low mean rainfalls [11]. It can result in damaging agricultural production and the natural environment [2].

[*] Department of Mathematics, Federal University of Technology, Minna, Nigeria
[†] Corresponding Author
[‡] Department of Mathematics, Enugu State University of Science and Technology, Enugu, Nigeria
[§] Department of Mathematics, Faculty of Science, Air Force Institute of Technology, Kaduna, Nigeria
[**] Department of Mathematical Science, Ibrahim Badamasi Babagida University, Lapai, Nigeria

Drought is often seen as a "creeping" phenomenon with slow onset and cessation. As a result, an effective drought monitoring system is the most important tool for developing and implementing efficient mitigation strategies. However, not only can the onset of drought conditions be rapid, an indication of how long drought conditions may continue will enable improved planning and resource allocation. For this reason, a capability to accurately forecast the onset, persistence and cessation of drought conditions will enable more effective drought mitigation strategies to be developed [10]. [12] defines flood as significant rise of water level in a stream, lake, reservoir or coastal region. Also, [8] defined flood as excessive water run-off or the rise in water level in a particular area which is more than what the particular environment can absorb. Flood and drought are one of the most devastating natural disasters in the world. In Nigeria, the story is not different as these has caused serious havoc to our environment and the economy. However, little or nothing can be done to avoid its occurrence but prior information such as prediction of flood and drought can assist the farmers, stakeholders and the general public to take adequate proactive measure in order to mitigate their effects. Hence, the result from this model will provide adequate information about flood and drought in some upcoming years for the studied areas. According to NEMA, in 2012 alone, floods caused more than N2.6 trillion in economic damage, much of which could be attributed to large-scale transboundary floods (from rivers Niger and Benue). In 2019, about 126 deaths were recorded, over 48,000 people were displaced and property worth millions of Naira destroyed across the country (Nigeria Hydrological Services Agency, 2020).The Standard Precipitation Index (SPI) was introduced by [7] as measure of the precipitation deficit that is uniquely related to probability. It can be calculated for any accumulation timescale, usually from monthly precipitation observations, and is typically expressed as SPI-n, where n is the number of months of accumulation. The time series is analogous to a moving average in the sense that a new value is calculated each month and is auto-correlated to previous months depending on the accumulation timescale [10].

## 2. Materials and method

Birnin Kebbi is the capital city of Kebbi state, is located in north-western Nigeria on (12° 27′ N and 4° 11′ E).The data used for this research work were obtained from the National Oceanic and Atmospheric Administration (NOAA) for the period of thirty years (1991 to 2020). After which the SPI was used to classify the rainfall into states

### 2.1. Model formulation

Suppose that the SPI rainfall classification for a year is considered as a random variable $x$, the collection of these random variables over the years constitute a stochastic process $\chi_n$, n=0,1,2,3,…, We assume that this stochastic process satisfies Markov property. Let the annual rainfall be modelled by a three-state Markov model based on the SPI classification

State 1: Flood (SPI Value ≥1)
State 2: Normal (-0.99≤SPI Value ≤0.99)

State 3: Drought (SPI Value ≤ -1)
The transition probability matrix is represented by

$$P=\begin{bmatrix} P_{11} & P_{12} & P_{13} \\ P_{21} & P_{22} & P_{23} \\ p_{31} & P_{32} & P_{33} \end{bmatrix}. \quad (1)$$

Following [5], let $P^{(n)}$ be the probability state vectors of the Markov chain, where n=0,1,2,3,… and let $P_i^{(n)}$ be the probability that the annual rainfall is in the i$^{th}$state at the n$^{th}$ year. $P^{(0)}$ is the initial state vector of the Markov chain and p$^{(n)}$ is the state vector at the n$^{th}$ year. Then, by induction we have that

$$P^{(n)} = P^{(n-1+1)} = P^{(n-1)}.P = P^n \quad (2)$$

On iteration we have,

$$P^{(n)} = P^{(0)}P^n. \quad (3)$$

That is, the initial state vector $P^{(0)}$ and the transition matrix $P$ determine the state vector $P^{(n)}$ at the n$^{th}$ year. If we now let

$$P^{(n)} = \begin{bmatrix} P_1^n & P_2^n & P_3^n \end{bmatrix}. \quad (4)$$

Denote the probabilities of finding the annual rainfall in any of the three states at the n$^{th}$ year and also let

$$P^{(0)} = \begin{bmatrix} P_1^0 & P_2^0 & P_3^0 \end{bmatrix}. \quad (5)$$

Denote the initial state vector and its elements, the Markov chain model for annual rainfall based on SPI classification in the study area can be represented by

$$\begin{bmatrix} P_1^n & P_2^n & P_3^n \end{bmatrix} = \begin{bmatrix} P_1^0 & P_2^0 & P_3^0 \end{bmatrix} \begin{bmatrix} P_{11} & P_{12} & P_{13} \\ P_{21} & P_{22} & P_{23} \\ P_{31} & P_{32} & P_{33} \end{bmatrix}^n \quad (6)$$

**Limiting State Probability**

The limiting state probability is represented by equation (7) below and is obtained when n → ∞ in equation (3).

$$\pi = \pi P, \tag{7}$$

where $\pi = \begin{bmatrix} \pi_1 & \pi_2 & \pi_3 \end{bmatrix}$

$$\pi = \sum_{i=1}^{3} \pi_i = 1. \tag{8}$$

These equations will be use to find the limiting state probabilities for our model.

## 3. Results and discussion

| SPI classification | frequency | State |
|---|---|---|
| SPI value ≥ 1 | 6 | Flood |
| -0.99≤ SPI value≤ 0.99 | 18 | Near normal |
| SPI value ≤ -1 | 6 | Drought |

**Table 1**: A summary of SPI annual rainfall classification of BerninKebbi.

From Table 1, we obtained the transition count presented in equation (9)

$$C = \begin{bmatrix} 2 & 2 & 2 \\ 4 & 10 & 3 \\ 0 & 5 & 1 \end{bmatrix}. \tag{9}$$

The probability transition matrix obtained from equation (9) is presented below

$$P = \begin{bmatrix} 0.333 & 0.333 & 0.333 \\ 0.235 & 0.588 & 0.176 \\ 0 & 0.833 & 0.167 \end{bmatrix}. \tag{10}$$

Calculating $P^n$ , on iteration we have

$$P^2 = \begin{bmatrix} 0.189 & 0.584 & 0.225 \\ 0.216 & 0.571 & 0.211 \\ 0.196 & 0.629 & 0.174 \end{bmatrix} \quad (11)$$

$$P^4 = \begin{bmatrix} 0.206 & 0.585 & 0.205 \\ 0.205 & 0.584 & 0.206 \\ 0.207 & 0.582 & 0.207 \end{bmatrix} \quad (12)$$

$$P^8 = \begin{bmatrix} 0.206 & 0.583 & 0.205 \\ 0.205 & 0.583 & 0.205 \\ 0.206 & 0.583 & 0.206 \end{bmatrix} \quad (13)$$

$$P^{20} = \begin{bmatrix} 0.204 & 0.577 & 0.204 \\ 0.204 & 0.577 & 0.203 \\ 0.203 & 0.578 & 0.203 \end{bmatrix} \quad (14)$$

$$P^{30} = \begin{bmatrix} 0.202 & 0.573 & 0.202 \\ 0.202 & 0.572 & 0.202 \\ 0.202 & 0.573 & 0.202 \end{bmatrix} \quad (15)$$

$$P^{50} = \begin{bmatrix} 0.199 & 0.563 & 0.199 \\ 0.199 & 0.563 & 0.199 \\ 0.199 & 0.563 & 0.199 \end{bmatrix} \quad (16)$$

**Limiting State Probabilities**

As n increases, $p^n$ gets closer to equation (16) that is, n≥50 the transition probabilities stabilise to equation (16), and from equation (3) with the initial state probability vector

$$P^0 = \begin{bmatrix} 1 & 0 & 0 \end{bmatrix}$$

$$P^{(n)} = P^0 P^n = \begin{bmatrix} 1 & 0 & 0 \end{bmatrix} \begin{bmatrix} 0.199 & 0.563 & 0.199 \\ 0.199 & 0.563 & 0.199 \\ 0.199 & 0.563 & 0.199 \end{bmatrix}$$

$$P^{(n)} = [0.199 \quad 0.563 \quad 0.199]. \quad (16)$$

Correcting to one decimal place, we have:

$$P^{(n)} = [0.2 \quad 0.6 \quad 0.2].$$

This is the probability of finding the annual rainfall based on SPI classification fall in any of three states for large n (1.e n ≥ 50).

From equation (3), we obtained the limiting state probability vector that is equation (7).
Thus: $\pi = \pi P\ (0.2\ \ 0.6\ \ 0.2)$.

The interpretation of this result is that, in the long-run 20% of the years during rainy season in BirninKebbi will experience flood, 60% will experience normal rainfall while 20% will experience drought.As it can be seen from equation (10) (transition probability matrix) a drought year cannot be followed by a flood yearand the probability of a drought to be followed by a normal year is high while the probability of a normal year to be followed by a drought and a drought year to be followed by another drought year is extremely small.

## 4. Conclusion

The rainfall pattern of Birnin Kebbi, Kebbi state has been analysed using Markov Chain with the help of Standardized Precipitation Index (SPI). Results from the research is an important information to the government and people of Kebbi state for better understanding of rainfall dynamics and viable agricultural production.

## References

[1] Bates D., Maechler M., Bolker B., and Walker S. (2014). Linear mixed-effects models using Eigen and S4. R Package Version 1:1–23.

[2] Gidey E., Dikinya O., Sebego R., Segosebe E., and Zenebe A. (2018). Analysis of the long-term agricultural drought onset, cessation, duration, frequency, severity and spatial extent using vegetation health index (VHI) in Raya and its environs, northern Ethiopia. Environmental Research System 7 (13). https://doi.org/10.1186/s40068-018-0115-z.

[3] Guha-Sapir D., Vos F., Below R., and Ponserre S. (2012). Annual disaster statistical review 2011: The numbers and trends. Brussels: Centre for Research on the Epidemiology of Disasters, Institute of Health and Society (IRSS), and Universitécatholique de Louvain.

[4] IPCC. (2007). Summary for Policymakers. In: Climate Change 2007: Impacts, Adaptation and Vulnerability. Contribution of Working Group II to the Fourth Assessment Report of the Inter-governmental Panel on Climate Change, M.L. Parry, O.F. Canziani, J.P. Palutikof, P.J. van der Linden and C.E. Hanson, Eds., Cambridge University Press, Cambridge, UK, 7-22.

[5] Lawal A. (2017). Stochastic model of rainfall precipitations for crop production in some selected states of north central Nigeria. Unpublised Phd thesis, Department of Mathematics, Federal University Technology, Minna, Nigeria.

[6] Lawal A., Abubakar U.Y., Danladi H., and Andrew S. G. (2016). Markovian approach for the analysis and prediction of weekly rainfall pattern in Makurdi, Benue State, Nigeria. J. Appl. Sci. Environ. Manage Vol. 20 (4) 965-971.

[7] McKee T. B., Doesken N. J., and Kliest J. (1993). The relationship of drought frequency and duration to time scales. In: Proceedings of the 8th Conference on Applied Climatology, Anaheim, CA, America. Meteorol. Soc. Boston, pp. 179–184.

[8] Nelson D. R., Adger W. N., and Brown K. (2007). Adaptation to environmental change: contributions of a resilience framework. Annual Review of Environment and Resources, 32(1): 395-419.

[9] Nigeria Hydrological Services Agency, (2020). Annual Flood Outlook. https://www.google.com/url?sa=t&source=web&rct=j&url=https://nihsa.gov.ng/wp-content/uploads/2020/06/2020-NIHSA-Annual-Flood-Outlook-AFO-5-2.pdf&ved=2ahUKEwiS7rSEx6LzAhWsDmMBHV82DVQQFnoECBUQAQ&usg=AOvVaw1JaPlygzezDG70hkgW0tXJ.

[10] Singleton A. (2012). Forecasting drought in europe with the standardized precipitation index: an assessment of the performance of the european centre for medium range weather forecasts variable resolution ensemble prediction system. Journal of the International Society for the Prevention and Mitigation of Natural Hazards, DOI 10.1007/s11069-019-03665-6.

[11] Um M., Kim Y., Park D., and Kim J. (2017). Effects of different reference periods on drought index estimations from 1901 to 2014. Hydrology and Earth System Sciences, 21: 4989–5007.

**International Journal of Mathematical Analysis and Modelling**
**Volume 5, Issue 1, May 2022, Pages 128 – 161**

# Simulation of the optimal control strategies to mitigate smartphone virus infection transmission dynamics

**T. I. Chinebu[*†], G. C. E. Mbah[‡], E. A. Jooda[*], E. O. Ezennorom[§], and I. V. Udegbe[‡]**

**Abstract**

In this study, a mathematical model of the optimal control strategies of Smartphone virus infection transmission dynamics incorporating vaccination, quarantine and treatment as the control parameters is presented. Pontryagin's maximum principle is used to characterize the optimal controls and the optimality system is solved by an iteration method. We performed some numerical simulations to verify the theoretical analysis with Runge-Kutta method of order four in MATLAB. The numerical simulation of the model shows that effective vaccination, quarantine and treatment as control strategies can eradicate Smartphone virus infection form the population. Finally, our findings strongly suggest that high coverage of vaccination, quarantine and treatment are critical to the success of Smartphone virus infection control.

***Keywords***: smartphone virus; optimal control; vaccination; quarantine; treatment; pontryagin's maximum principle

## 1. Introduction

The Smartphone enable users to have a device with a good processing power, internet access and functions of traditional mobile phones in one device, small enough to fit in a pocket. However, the wealth of private information which is stored on those devices made them an interesting target for malicious users and cyber criminals [18], who then invade these Smartphone with virus. Smartphone virus is a mischief program written to proliferate from one phone to another and it takes control of Smartphone devices by exploiting its vulnerability. Continuous improvement in Smartphone device hardware and Smartphone communication technologies has led to a highly interconnected world,

[*]Department of Applied Sciences, Federal College of Dental Technology and Therapy, P.M.B. 01473, Trans Ekulu Enugu, Nigeria
[†] Corresponding Author
[‡] Department of Mathematics, University of Nigeria, Nsukka, Nigeria
[§] Department of Computer Science, Madonna University Nigeria, Elele, Nigeria

but also a world grown highly vulnerable. Cyber criminals have proven significantly efficient in uncovering new vulnerabilities in popular applications (apps)[14]. As a result, more and more

Smartphone malware families are introduced every year [19]. Just in 2017, more than 20 million malware samples have been detected [17], while other studies show that the chances for monetization is a key factor responsible for the rise of Smartphone malware [12][23].

The cyber attacker who was able to install malware on some system can install or delete programs, modify files, download sensitive information and use them to impersonate the user's action and keystrokes, capture users screen, use camera and retrieve photos or videos, use the infected system as a source of DDoS attack [18][22]. Smartphone can become infected either through downloading infected files using the phone internet browser, transferring files between phones using Bluetootth interface, synchronizing with an infected computer, assessing an infected physical memory card, opening infected files attached to multimedia message service (MMS) or email [4][5]. Zhang [28] discovered that Smartphone virus can also propagate through multi-layered network. He concluded that Smartphone viruses can use any network (3G, 4G, Wi-Fi or Bluetooth). When an unsuspected user accepts the infected attachment file, using a phone susceptible to the virus, then the virus is installed and infects the target phone which then begins to perform as an attacked phone [6][25]. Smartphone virus can seize the victim's mobile device by running malicious exploit and this infected device will in turn, scan and infect other Smartphones in the mobile network [25].

Some response mechanisms completely stop further virus propagation, but others simply slow the propagation rate of the virus. Both types of response can be used. Ideally, the response mechanism would always quickly and completely stop Smartphone virus propagation. However, some viruses spread so quickly that a first response mechanism that slows the spread could buy time to enable activation of a second response mechanism that completely halts the propagation process. Actually, in phone user education response, the consent of the phone user to accept the message and infect the phone is required, therefore, a user not accepting an infected message has a direct effect on virus propagation. Also, other response mechanism such as immunization can prevent infection even if the user accepts the MMS message attachment [9]. A virus scans of all MMS attachments as they pass through an MMS gateway is completely effective against viruses with known virus signature. For that reason, after the new virus signature is added to the list of known viruses, the gateway virus scan is able to completely halt virus propagation [24].

The immunization response mechanism operates using software placed directly on each Smartphone [21]. After a Smartphone service provider detects virus that exploits a vulnerable Smartphone, the service provider begins developing a patch to fix that vulnerability [26]. Once the patch is developed, the immunization software resident in each Smartphone automatically installs any immunization patch available [28]. Bandwidth constraint prevents most Smartphones from receiving the patch simultaneously, so the patch is rolled out to the entire Smartphone population uniformly over a period of time [16]. The more servers that are dedicated to distributing these patches, the faster the deployment to susceptible Smartphones in the network [2]. When the patch

arrives at a particular Smartphone, it becomes immunized from virus if not infected, or the patch stops further propagation attempts from Smartphone if it is already infected [24].

Because Smartphone viruses have potential to attack in many different ways, an optimal response strategy must incorporate mechanisms to counteract a wide variety of virus behaviors. The hope of stopping Smartphone virus before it degrades the utility and value of Smartphones is quick and concerted action on the part of all universal mobile telecommunications service (UMTS) data networksthat their mobile devices use; Wi-Fi networks have no such protection. And while some carriers already filter their MMS streams to remove messages bearing malicious attachments, all should do so [12].

Some of the manufacturers have joined the trusted computing group, which has been hammering on industry standards micro circuiting inside phones that will make it harder for malware to get a sensitive data in the devices memory or to hijack its payment mechanism. Symbian released a version of its operating system that does an improved job of protecting key files which requires software to obtain digital certificate from the company. This Symbian system refuses to install programs not accompanied by a certificate. Unless disabled by a user the system effectively excludes all mobile malware discovered [12].

## 2. Related literature

Virus attack is a serious threat in Smartphone network environment and is still multiplying as time continues to pass. Controlling these virus attacks in Smartphone is very necessary. Several mathematical models have been developed to simulate, analyze and understand Smartphone virus propagation and its control strategies, in related works, Guillen et al [11] used the theory of optimal control that is associated to systems of ordinary differential equations to find a new function to control malware epidemic through time, while Liu and Zhong [15] employed the optimal control theory to study malware immunization strategies, aiming to keep the total economic loss of security investment and infection loss as low as possible.

Van Ruitenbeek and Stevens [24] proposed response mechanisms for mobile phone viruses and used their model to obtain insight on the effectiveness of the virus mitigation technique. To study the fundamental spreading patterns that characterize a mobile virus outbreak, Wang et al [25] modeled the mobile benign worm based on two stages of repairing mechanisms. Chinebu et al [6] proposed an SVEIQRS model that control virus attack through vaccination and quarantine. Their model has a globally asymptotically stable virus free equilibrium when $R_0 < 1$ and a unique endemic equilibrium when $R_0 > 1$ . Yang et al [27] proposed two different propagation models of mobile phone viruses under the complex network.

Our aim in this paper is to highlight the seriousness of Smartphone virus propagation, particularly exposed $(E(t))$ Smartphone that is infected without symptom which can transmit the infection to susceptible$(S(t))$ Smartphone. Likewise, there can be transmission from infected Smartphone $(I(t))$ to susceptible. In addition, we included complication with virus infected Smartphone $(C(t))$. Furthermore, we have the quarantined Smartphone $(Q(t))$ and finally the recovered Smartphone $(R(t))$.

A continuous mathematical model was proposed in this paper and it describes the dynamics of a population infected by Smartphone virus. Moreover, we gave the optimal control model in

section 3. We presented the optimal control problem for the model where various results regarding the existence and characterization of the optimal control using Potryagin's Maximum Principle was given in section 4. Matlab was used for the Numerical Simulation and is presented in section 5. Lastly, the conclusion was presented in section 6.

## 3. Mathematical model formulation

We consider a mathematical model that describes the Sensitivity analysis of Smartphone virus infection transmission dynamics as proposed in Chinebu et al [8]. The entire Smartphone population denoted by $\mathrm{N(t)}$ was divided into six compartments.

### 3.1. Description of the smartphone model compartments

The schematic diagram of the proposed Smartphone virus transmission dynamics is shown in Figure 1

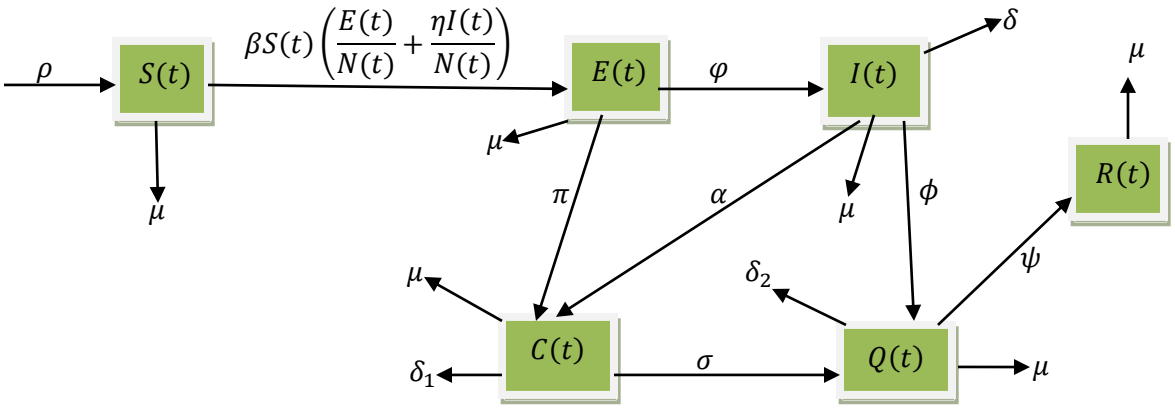


Figure 1: Schematic diagram of the model.

Let us denote the force of infection by

$$\lambda = \beta\left(\frac{\eta E(t) + I(t)}{N}\right), \qquad (1)$$

where $\beta$ is the Smartphone virus infection transmission rate and $\eta$ is the modification factor for the exposed Smartphones.

The susceptible compartment is increased by $\rho$, which denotes the incidence of susceptible Smartphone. All the compartments is decreased by the amount $\mu$ (natural Death), $\frac{\beta\eta S(t)E(t)}{N}$ (the number of Smartphone that are infected with the virus by contact with the exposed Smartphone) and $\frac{\beta S(t)I(t)}{N}$ (the number of Smartphone that were infected with the virus by communication with infected Smartphone). $\varphi$, is the number of Smartphones that become infectious, and$\pi$ is the number of Smartphones that have upgraded to the development of rapid and dangerous virus, thereby, having complications due to antivirus deficiency. Smartphones that have severe complications such as Apps crashing over and over again is denoted by $\alpha$. $\delta$ is death rate due to virus infection and $\phi$, progression rate from infected to quarantine. Death rate due to virus infection is denoted by $\delta_1$ and progression rate from infected with complications to quarantine by $\sigma$. $\psi$ represent the movement from quarantined to recovered Smartphones and quarantined Smartphones that cannot be repaired again is represented by $\delta_2$. The natural death rate is denoted by $\mu$.

Based on the above assumptions and the schematic diagram, we thus present the Smartphone virus infection transmission dynamics model by the following systems of differential equation as proposed in Chinebu et al [8]:

$$\left.\begin{aligned}
\frac{dS(t)}{dt} &= \rho - \mu S(t) - \lambda S(t),\\
\frac{dE(t)}{dt} &= \lambda S(t) - (\mu + \varphi + \pi)E(t),\\
\frac{dI(t)}{dt} &= \varphi E(t) - (\mu + \alpha + \phi + \delta)I(t),\\
\frac{dC(t)}{dt} &= \pi E(t) + \alpha I(t) - (\mu + \delta_1 + \sigma)C(t),\\
\frac{dQ(t)}{dt} &= \phi I(t) + \sigma C(t) - (\mu + \delta_2 + \psi)Q(t),\\
\frac{dR(t)}{dt} &= \psi Q(t) - \mu R(t),
\end{aligned}\right\} \qquad (2)$$

where the initial states are $S(0) \geq 0, E(0) \geq 0, I(0) \geq 0, C(0) \geq 0, Q(0) \geq 0, R(0) \geq 0$.

## 4. Formulation as an optimal control problem

The goal of this study is to use three control strategies $\tau_1(t), \tau_2(t)$ and $\tau_3(t)$ in terms of combined effort of vaccination, quarantine and treatment (repair) for $t \in [0, t_f]$ that would minimize the number infected Smartphones which will subsequently be destroyed (When there is less/no possibility of the Smartphone being repaired) due to virus infection and its complications. And at the same time, also minimize the cost of vaccination, quarantine and treatment of the population. First control is the proportion of Smartphones that are subjected to vaccination. Therefore, $\tau_1$ denotes vaccination strategy to susceptible Smartphones at time $t$. Second control is the proportion of Smartphones that were quarantined and is denoted by $\tau_2\big(I(t) + C(t)\big)$ which are infected and complicated Smartphones that are quarantined at time $t$. The third control is denoted by $\tau_3 Q(t)$ which represents quarantined Smartphones that underwent treatment (repair) at time $t$. Thus, we obtain

$$\left.\begin{aligned}
\frac{dS(t)}{dt} &= \rho - \mu S(t) - \beta\left[\big(1-\tau_1(t)\big)\left(\frac{\eta E(t) + I(t)}{N}\right)\right] S(t),\\
\frac{dE(t)}{dt} &= \beta\left[\big(1-\tau_1(t)\big)\left(\frac{\eta E(t) + I(t)}{N}\right)\right] S(t) - (\mu + \varphi + \pi)E(t),\\
\frac{dI(t)}{dt} &= \varphi E(t) - (\mu + \alpha + \phi + \delta)I(t) - \tau_2(t)I(t),\\
\frac{dC(t)}{dt} &= \pi E(t) + \alpha I(t) - (\mu + \delta_1 + \sigma)C(t) - \tau_2(t)C(t),\\
\frac{dQ(t)}{dt} &= \phi I(t) + \sigma C(t) - (\mu + \delta_2 + \psi)Q(t) + \tau_2(t)I(t) + \tau_2(t)C(t) - \tau_3(t)Q(t),\\
\frac{dR(t)}{dt} &= \psi Q(t) - \mu R(t) + \tau_3(t)Q(t).
\end{aligned}\right\} \quad (3)$$

The problem is to minimize the objective functional

$$J(\tau_1, \tau_2, \tau_3) = E(t_f) + I(t_f) + C(t_f) + Q(t_f) + \int_0^{t_f} \left( E(t_f) + I(t_f) + C(t_f) + Q(t_f) + \frac{B_1}{2}\tau_1^2(t) + \frac{B_2}{2}\tau_2^2(t) + \frac{B_3}{2}\tau_3^2(t) \right) dt, \quad (4)$$

where $B_1 \geq 0, B_2 \geq 0$ and $B_3 \geq 0$ are the cost coefficients of $\tau_1(t), \tau_2(t)$ and $\tau_3(t)$ at time $t, t_f$ being the final time. Hence, we seek the optimal controls $\tau_1^*, \tau_2^*$ and $\tau_3^*$ such that

$$J(\tau_1^*, \tau_2^*, \tau_3^*) = \min_{\tau_1, \tau_2, \tau_3 \in W} J(\tau_1, \tau_2, \tau_3), \tag{5}$$

where $W$ is the set of admissible control defined by

$$\begin{aligned} W = \{\tau_1, \tau_2, \tau_3 : & 0 \leq \tau_{1min} \leq \tau_1(t) \leq \tau_{1max} \leq 1, \\ & 0 \leq \tau_{2min} \leq \tau_2(t) \leq \tau_{2max} \leq 1, \\ & 0 \leq \tau_{3min} \leq \tau_3(t) \leq \tau_{3max} \leq 1, \\ & t \in [0, t_f]\} \end{aligned} \tag{6}$$

## 4.1. The optimal control: existence and characterization

We shall first show the existence of solutions of system (3), after which we shall prove the existence of optimal control [10].

## 4.2. Existence of an optimal control

**Theorem 4**: Consider the control problem with system (3). There exists an optimal control $(\tau_1^*, \tau_2^*, \tau_3^*) \in W$ such that

$$J(\tau_1^*, \tau_2^*, \tau_3^*) = \min_{\tau_1, \tau_2, \tau_3 \in W} J(\tau_1, \tau_2, \tau_3).$$

**Proof**: We can prove the existence of the optimal control through the following four conditions as was discussed in [7]:

Proof of Condition 1.
The theorems 3 and 4 indicate that the set of controls and corresponding state variables is not empty. We shall use Boyce and DiPrima [3] simplified version of an existence result to prove that the set of controls and the corresponding state variables are non empty. Let $y_i' = Fy_i(t, y_1, y_2, \dots, y_6)$ with $i = 1, 2, \dots, 6$ where $(y_1, y_2, y_3, y_4, y_5, y_6) = (S(t), E(t), I(t), C(t), Q(t), R(t))$ where $y_1, y_2, y_3, y_4, y_5, y_6$ form the right hand side of the system of equation (3). Let $\tau_1, \tau_2$ and $\tau_3$ for some constants and since all parameters are constant with $y_1, y_2, y_3, y_4, y_5$ and $y_6$ being continuous, then, it implies that $F_S$, $F_E, F_I, F_C, F_Q$ and $F_R$ are also continuous. More so, the partial derivatives $\frac{\partial F y_i}{\partial y_i}$ with $i = 1, 2, \dots, 6$ are all continuous. Therefore, there exists a unique solution $(S(t), E(t), I(t), C(t), Q(t), R(t))$ that satisfies the initial conditions. Consequently, the set of control and the control variables is non-empty, hence, condition 1 is satisfied.

Proof of Condition 2.
The control space of equation (4)

$$J(\tau_1,\tau_2,\tau_3) = E(t_f) + I(t_f) + C(t_f) + Q(t_f) + \int_0^{t_f} \left( E(t_f) + I(t_f) + C(t_f) + Q(t_f) + \frac{B_1}{2}\tau_1^2(t) + \frac{B_2}{2}\tau_2^2(t) + \frac{B_3}{2}\tau_3^2(t) \right) dt$$

is convex in $W$ and closed by definition. Take any controls $\tau_1, \tau_2 \in W \; and \; \Omega \in [0,1]$. Then, $0 \leq \Omega\tau_1 + (1-\Omega)\tau_2$. Furthermore, we observe that $\Omega\tau_1 \leq \Omega \; and (1-\Omega)\tau_2 \leq (1-\Omega)$, then, $\Omega\tau_1 + (1-\Omega)\tau_2 \leq \Omega + (1-\Omega) = 1$. Therefore, $0 \leq \Omega\tau_1 + (1-\Omega)\tau_2 \leq 1$, for all $\tau_1, \tau_2 \in W$ and $\Omega \in [0,1]$. So, $W$ is convex and therefore, condition 2 is satisfied.

Proof of Condition 3.
All the right hand sides of the equations in system (4) are continuous, bounded above by a sum of bounded control and state, and can be written as a linear function of $\tau_1, \tau_2, \tau_3$ with coefficients depending on time and state. The control space $W = \{\tau_1, \tau_2, \tau_3 : 0 \leq \tau_{1min} \leq \tau_1(t) \leq \tau_{1max} \leq 1, 0 \leq \tau_{2min} \leq \tau_2(t) \leq \tau_{2max} \leq 1, 0 \leq \tau_{3min} \leq \tau_3(t) \leq \tau_{3max} \leq 1, t \in [0, t_f]\}$ is convex and closed by definition.

From system (3), we have

$$\frac{dN(t)}{dt} = \rho - \mu N,$$
$$\lim_{t\to\infty} Sup\, N(t) \leq \frac{\rho}{\mu}.$$

Therefore, all solutions of system (3) are bounded. So, there exists $y_1, y_2, y_3, y_4, y_5 \; and \; y_6$ such that$\forall\, t \in [0, t_f]: S(t) \leq y_1, E(t) \leq y_2, I(t) \leq y_3, C(t) \leq y_4, Q(t) \leq y_5 \; and \; R(t) \leq y_6$. If we consider

$$\begin{cases} F_S = S(t) \leq \rho \\ F_E = E(t) \leq D_1 E \\ F_I = I(t) \leq \varphi E - D_2 I \\ F_C = C(t) \leq \pi E(t) + \alpha I(t) - \tau_2(t) y_4 \\ F_Q = Q(t) \leq \phi I(t) + \sigma C(t) + \tau_2(t)(y_3 + y_4) - \tau_3(t) y_5 \\ F_R = R(t) \leq \psi Q(t) + \tau_3(t) y_5 \end{cases}$$

So, we can rewrite system (3) in matrix form as

$$F(t, S(t), E(t), I(t), C(t), Q(t), R(t)) \leq \rho + VY(t) - FW(t)$$

where $F\big(t, S(t), E(t), I(t), C(t), Q(t), R(t)\big) = \big[F_S, F_E, F_I, F_C, F_Q, F_R\big]^T$

$$Y(t) = [S(t), E(t), I(t), C(t), Q(t), R(t)]^T$$

$$W(t) = [\tau_1, \tau_2, \tau_3]^T$$

and

$$V := \begin{pmatrix} 0 & 0 & 0 & 0 & 0 & 0 \\ 0 & 0 & 0 & 0 & 0 & 0 \\ 0 & 0 & 0 & 0 & 0 & 0 \\ 0 & \pi & \alpha & 0 & 0 & 0 \\ 0 & 0 & \phi & \sigma & 0 & 0 \\ 0 & 0 & 0 & 0 & \psi & 0 \end{pmatrix}$$

$$F := \begin{pmatrix} -\beta\left(\frac{\eta ES + IS}{N}\right) & 0 & 0 \\ \beta\left(\frac{\eta ES + IS}{N}\right) & 0 & 0 \\ 0 & -I & 0 \\ 0 & -C & 0 \\ 0 & I + C & -Q \\ 0 & 0 & Q \end{pmatrix}$$

which gives the linear function of the control vector defined by time and state variables. Then we find out the bound of the right hand side. It is noted that all parameters are constant and greater than or equal to zero. Therefore, we can write

$$F\big(t, S(t), E(t), I(t), C(t), Q(t), R(t)\big) \leq \|\rho\| + \|V\|\|Y(t)\| + \|F\|\|W(t)\|$$
$$\leq \mathfrak{O} + \gamma(\|Y(t)\| + \|W(t)\|)$$
$$where\ \ \mathfrak{O} \leq \rho\ and\ \gamma = max(\|V\|, \|F\|)\,.$$

.

Hence, we say that the right hand side is bounded by a sum of the state and control. Therefore, condition 3 is satisfied.

Proof of Condition 4.

The integrand in the objective functional $E\big(t_f\big) + I\big(t_f\big) + C\big(t_f\big) + Q\big(t_f\big) + \frac{B_1}{2}\tau_1^2(t) + \frac{B_2}{2}\tau_2^2(t) + \frac{B_3}{2}\tau_3^2(t)$ is clearly convex in $W$.

We then show that there exists constants $\xi_1, \xi_2, \xi_3, \xi_4 > 0$, and $\xi$ such that $E(t_f) + I(t_f) + C(t_f) + Q(t_f) + \frac{B_1}{2}\tau_1^2(t) + \frac{B_2}{2}\tau_2^2(t) + \frac{B_3}{2}\tau_3^2(t)$ satisfies $E(t_f) + I(t_f) + C(t_f) + Q(t_f) + \frac{B_1}{2}\tau_1^2(t) + \frac{B_2}{2}\tau_2^2(t) + \frac{B_3}{2}\tau_3^2(t) \geq \xi_1 + \xi_2|\tau_1|^{\xi} + \xi_3|\tau_2|^{\xi} + \xi_4|\tau_3|^{\xi}$.

The state variable being bounded, let $\xi_1 = \inf_{t\in[0,t_f]} E(t_f) + I(t_f) + C(t_f) + Q(t_f), \xi_2 = \frac{B_1}{2}, \xi_3 = \frac{B_2}{2}, \xi_4 = \frac{B_3}{2}$ $and$ $\xi = 2$, then it follows that: $E(t_f) + I(t_f) + C(t_f) + Q(t_f) + \frac{B_1}{2}\tau_1^2(t) + \frac{B_2}{2}\tau_2^2(t) + \frac{B_3}{2}\tau_3^2(t) \geq \xi_1 + \xi_2|\tau_1|^{\xi} + \xi_3|\tau_2|^{\xi} + \xi_4|\tau_3|^{\xi}$.

Therefore, condition 4 is also satisfied. From the above discussion the existence of the objective functional has been established. Then from Fleming and Rishel [10], we conclude that there exists an optimal control.

## 4.3. Characterization of the optimal control

In order to derive the necessary conditions for the optimal control, we apply Pontryagin's Maximum Principle $(PMP)$[26] to the Hamiltonian $H$.

**Theorem 5**: Given optimal controls $(\tau_1^*, \tau_2^*, \tau_3^*)$ and solutions$S^*, E^*, I^*, C^*, Q^*$ $and$ $R^*$ of the corresponding system (3), there exist adjoint variables$\lambda_1, \lambda_2, \lambda_3, \lambda_4, \lambda_5$ $and$ $\lambda_6$ satisfying

$$\left.\begin{aligned}
\dot{\lambda}_1 &= \lambda_1\left(\mu + \beta(1-\tau_1(t))\left(\frac{\eta E(t) + I(t)}{N}\right)\right) - \lambda_2\left(\beta(1-\tau_1(t))\left(\frac{\eta E(t) + I(t)}{N}\right)\right)\\
\dot{\lambda}_2 &= -1 + \lambda_1\left(\beta(1-\tau_1(t))\left(\frac{\eta S(t)}{N}\right)\right) - \lambda_2\left(\beta(1-\tau_1(t))\frac{\eta S(t)}{N} - A\right) - \lambda_3\varphi - \lambda_4\pi\\
\dot{\lambda}_3 &= -1 + \lambda_1\left(\beta(1-\tau_1(t))\left(\frac{S(t)}{N}\right)\right) - \lambda_2\left(\beta(1-\tau_1(t))\frac{S(t)}{N}\right) + \lambda_3(B + \tau_2(t)) - \lambda_4\alpha - \lambda_5(\phi + \tau_2(t))\\
\dot{\lambda}_4 &= -1 - \lambda_4(G + \tau_2(t)) - \lambda_5(\sigma + \tau_2(t))\\
\dot{\lambda}_5 &= -1 + \lambda_5(K + \tau_3(t)) - \lambda_6(\psi + \tau_3(t))\\
\dot{\lambda}_6 &= \lambda_6\mu
\end{aligned}\right\} (7$$

With transversality conditions at time $t_f$: $\lambda_1(t_f) = 0, \lambda_2(t_f) = -1, \lambda_3(t_f) = -1, \lambda_4(t_f) = -1, \lambda_5(t_f) = -1, \lambda_6(t_f) = 0$. Moreover, the optimal controls $\tau_1^*, \tau_2^*$ $and$ $\tau_3^*$ are given by

$$\left.\begin{aligned}\tau_1^* &= min\left(1, max\left(0, \frac{\lambda_2-\lambda_1}{B_1}\left(\beta\left(\frac{\eta E(t)+I(t)}{N}\right)S(t)\right)\right)\right)\\ \tau_2^* &= min\left(1, max\left(0, \frac{\lambda_3 I(t)+\lambda_4 C(t)-\lambda_5(I(t)+C(t))}{B_2}\right)\right)\\ \tau_3^* &= min\left(1, max\left(0, \frac{(\lambda_5-\lambda_6)Q(t)}{B_3}\right)\right)\end{aligned}\right\} (8)$$

Proof: The Hamiltonian $H$ is defined as follows:

$H(t) = E(t_f) + I(t_f) + C(t_f) + Q(t_f) + \frac{B_1}{2}\tau_1^2(t) + \frac{B_2}{2}\tau_2^2(t) + \frac{B_3}{2}\tau_3^2(t) + \dot{\lambda}_1 S(t) + \dot{\lambda}_2 E(t) + \dot{\lambda}_3 I(t) + \dot{\lambda}_4 C(t) + \dot{\lambda}_5 Q(t) + \dot{\lambda}_6 R(t)$.

The adjoint variables $\dot{\lambda}_1, \dot{\lambda}_2, \dot{\lambda}_3, \dot{\lambda}_4, \dot{\lambda}_5, \dot{\lambda}_6$ are obtained by the following system:

$$\dot{\lambda}_1 = -\frac{\partial H}{\partial S}, \dot{\lambda}_2 = -\frac{\partial H}{\partial E}, \dot{\lambda}_3 = -\frac{\partial H}{\partial I}, \dot{\lambda}_4 = -\frac{\partial H}{\partial C}, \dot{\lambda}_5 = -\frac{\partial H}{\partial Q}, \dot{\lambda}_6 = -\frac{\partial H}{\partial R} (9)$$

For $t \in [0, t_f]$, the adjoint equations and transversality conditions can be obtained by using Pontryagin's Maximum Principle [20][13][1], such that

$$\left.\begin{aligned}
\dot{\lambda}_1 &= -\frac{\partial H}{\partial S} = \lambda_1\left(\mu + \beta\big(1-\tau_1(t)\big)\left(\frac{\eta E(t)+I(t)}{N}\right)\right) - \lambda_2\left(\beta\big(1-\tau_1(t)\big)\left(\frac{\eta E(t)+I(t)}{N}\right)\right)\\
\dot{\lambda}_2 &= -\frac{\partial H}{\partial E} = -1 + \lambda_1\left(\beta\big(1-\tau_1(t)\big)\left(\frac{\eta S(t)}{N}\right)\right) - \lambda_2\left(\beta\big(1-\tau_1(t)\big)\frac{\eta S(t)}{N} - A\right) - \lambda_3\varphi - \lambda_4\pi\\
\dot{\lambda}_3 &= -\frac{\partial H}{\partial I} = -1 + \lambda_1\left(\beta\big(1-\tau_1(t)\big)\left(\frac{S(t)}{N}\right)\right) - \lambda_2\left(\beta\big(1-\tau_1(t)\big)\frac{S(t)}{N}\right) + \lambda_3\big(B+\tau_2(t)\big)\\
&\qquad -\lambda_4\alpha - \lambda_5\big(\phi+\tau_2(t)\big)\\
\dot{\lambda}_4 &= -\frac{\partial H}{\partial C} = -1 - \lambda_4\big(G+\tau_2(t)\big) - \lambda_5\big(\sigma+\tau_2(t)\big)\\
\dot{\lambda}_5 &= -\frac{\partial H}{\partial Q} = -1 + \lambda_5\big(K+\tau_3(t)\big) - \lambda_6\big(\psi+\tau_3(t)\big)\\
\dot{\lambda}_6 &= -\frac{\partial H}{\partial R} = \lambda_6\mu
\end{aligned}\right\} \quad (10)$$

The optimal control $\tau_1^*, \tau_2^*\ and\ \tau_3^*$ derived from the optimality condition

$$\frac{\partial H}{\partial \tau_1} = 0, \frac{\partial H}{\partial \tau_2} = 0, \frac{\partial H}{\partial \tau_3} = 0$$

$$\left.\begin{aligned}
-\frac{\partial H}{\partial \tau_1} &= -B_1\tau_1(t) + (\lambda_2-\lambda_1)\left(\beta\left(\frac{\eta E(t)+I(t)}{N}\right)S(t)\right) = 0\\
-\frac{\partial H}{\partial \tau_2} &= -B_2\tau_2(t) + \lambda_3 I(t) + \lambda_4 C(t) - \lambda_5(I(t)+C(t)) = 0\\
-\frac{\partial H}{\partial \tau_3} &= -B_3\tau_3(t) + (\lambda_5-\lambda_6)Q(t) = 0
\end{aligned}\right\}$$

Then, we have

$$\left.\begin{aligned}\tau_1(t) &= \frac{\lambda_2-\lambda_1}{B_1}\left(\beta\left(\frac{\eta E(t)+I(t)}{N}\right)S(t)\right)\\ \tau_2(t) &= \frac{\lambda_3 I(t)+\lambda_4 C(t)-\lambda_5(I(t)+C(t))}{B_2}\\ \tau_3(t) &= \frac{(\lambda_5-\lambda_6)Q(t)}{B_3}\end{aligned}\right\}$$

By substituting the optimal control $\tau_1^*, \tau_2^* \; and \; \tau_3^*$ ino the state system (3) and the adjoint system (9), we obtain the corresponding $S^*, E^*, I^*, C^*, Q^*, R^*$and $\lambda_i^*, i = 1, 2, \dots, 6$, with the help of the transversality condition $\lambda_i^*(t_f), i = 1, 2, \dots, 6$

## 5. Numerical simulations

In this section, we present the result obtained by solving the optimal control system numerically having the initial conditions for the state variables. Thus, the optimal control system is a two-point boundary value problem with separate boundary conditions at time steps $i = 0 \; and \; i = t_f$. We solve the optimality system by using Runge Kutta method of order four (RK4). The numerical simulations were carried out with the parameters in Table 1.

| *Paramete* | *Description* | *Value* |
|---|---|---|
| $\rho$ | Incidence of Smartphone | 100 |
| $\mu$ | Natural death rate | 0.057 |
| $\beta$ | Contact rate of infected Smartphones with susceptible | 0.85 |
| $\eta$ | Modification factor for the exposed Smartphones | 0.0002 |
| $\varphi$ | The rate at which exposed Smartphones become infectious | 0.045 |
| $\pi$ | The rate at which exposed Smartphones develop complication due to virus infection | 0.04 |
| $\alpha$ | The rate at which infected Smartphones develop complication due to virus infection | 0.21 |
| $\phi$ | Quarantine rate of infected Smartphones before treatment | 0.083 |
| $\delta$ | Disease induced death rate of infected Smartphones | 0.01 |
| $\delta_1$ | Disease induced death rate of infected with complication Smartphones | 0.01 |
| $\delta_2$ | Disease induced death rate of quarantined Smartphones | 0.01 |
| $\sigma$ | Quarantine rate of infected with complication Smartphones before treatment | 0.02 |
| $\psi$ | The rate at which quarantined Smartphones recover from virus infection after treatment. | 0.017 |

**Table 1**: Parameter value for the simulation

For the optimality of the model, we have the initial value for the susceptible, exposed, infected, infected with complication, quarantined and recovered as $S(0) = 100, E(0) = 10, I(0) = 4, C(0) = 2, Q(0) = 3\ and\ R(0) = 5$.

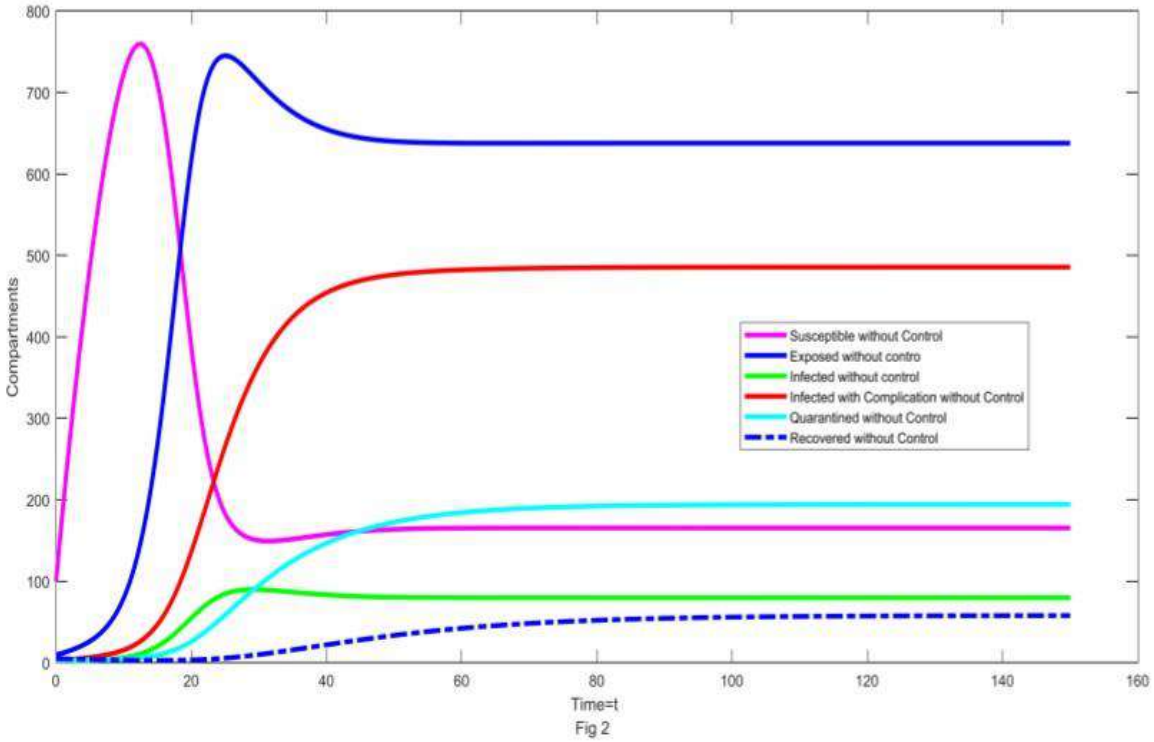


**Figure 2**: The Dynamics of Susceptible, Exposed, Infected, Infected with Complication, Quarantined and Recovered Smartphones without Vaccination, quarantine and treatment Control strategies $(\tau_1(t), = \tau_2(t) = \tau_3(t) = 0)$.

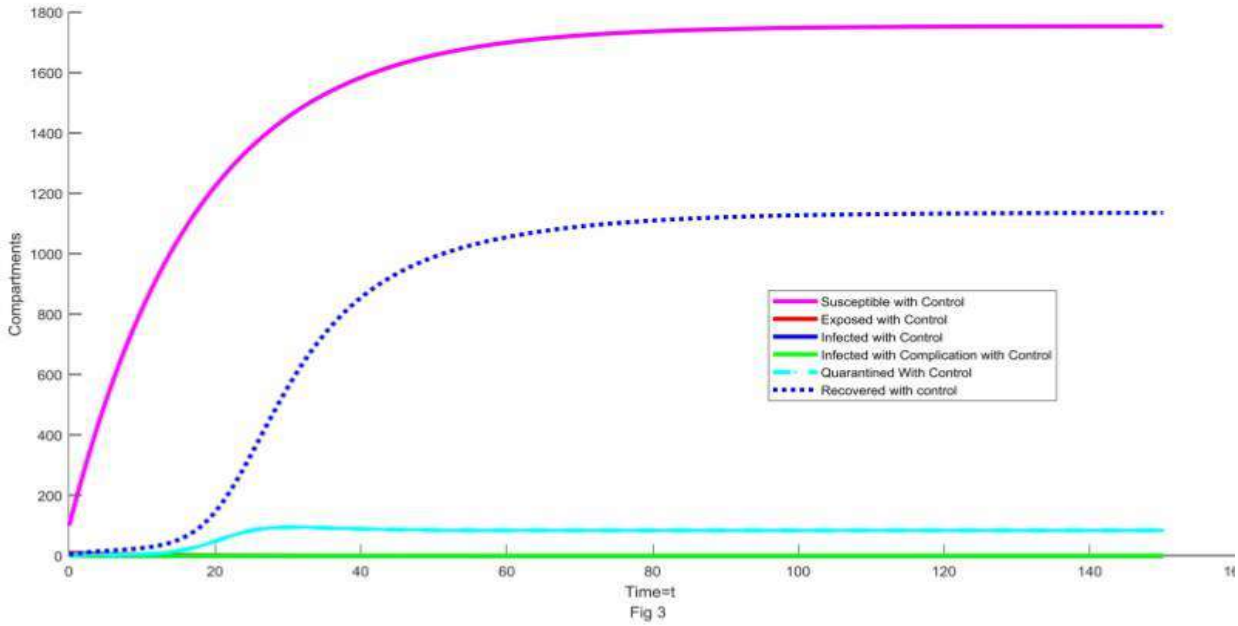


**Figure 3**: The Dynamics of Susceptible, Exposed, Infected, Infected with Complication, Quarantined and Recovered Smartphones with Vaccination, quarantine and treatment Control strategies $(0 < \tau_3(t), \tau_3(t), \tau_3(t) < 1)$.

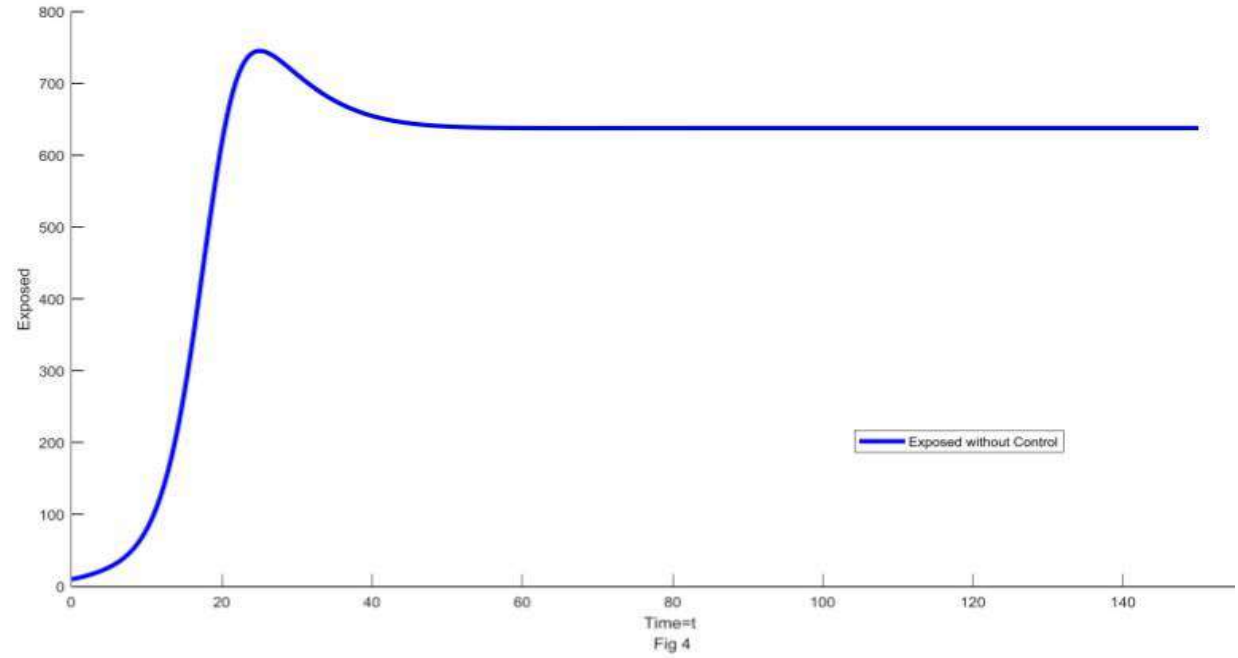


**Figure 4**: The Dynamics of Exposed Smartphones without Vaccination, quarantine and treatment Control strategies $(\tau_1(t), = \tau_2(t) = \tau_3(t) = 0)$.

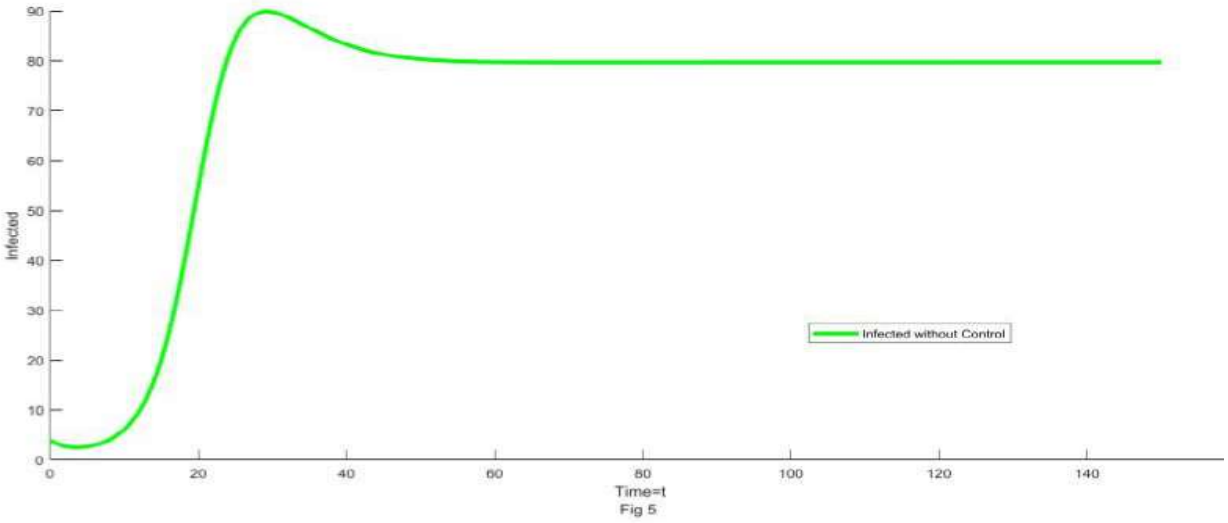


**Figure 5**: The Dynamics of Infected Smartphones without Vaccination, quarantine and treatment Control strategies $(\tau_1(t), = \tau_2(t) = \tau_3(t) = 0)$.

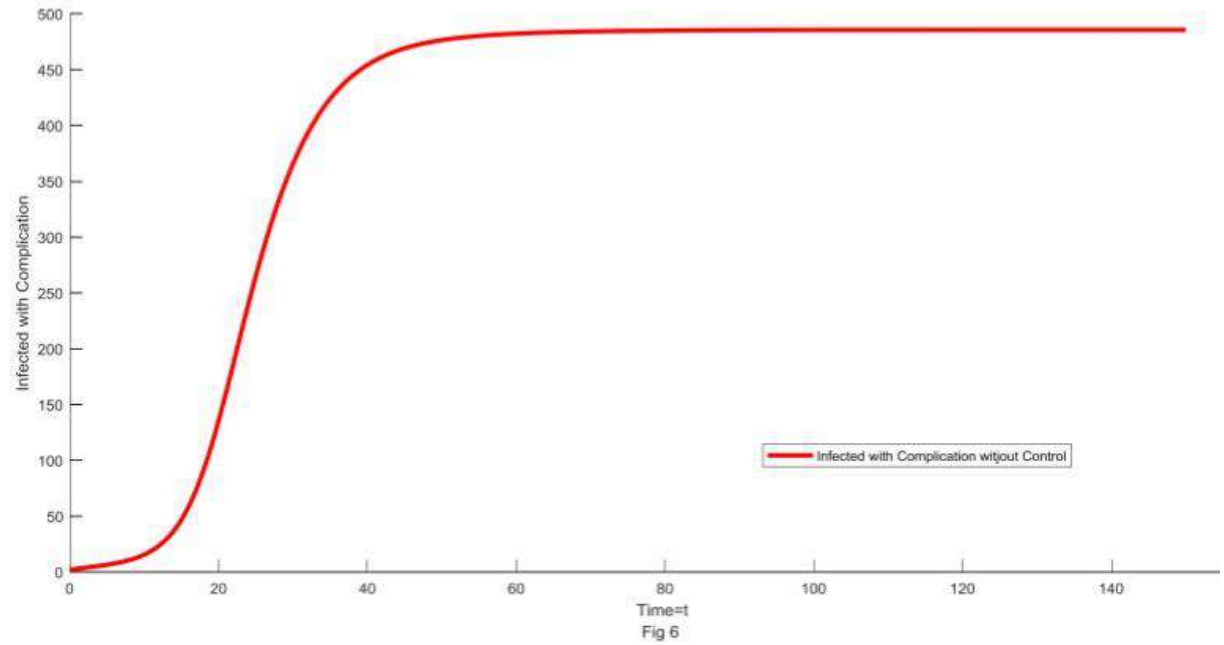


**Figure 6**: The Dynamics Infected with Complication Smartphones without Vaccination, quarantine and treatment Control strategies $(\tau_1(t), = \tau_2(t) = \tau_3(t) = 0)$.

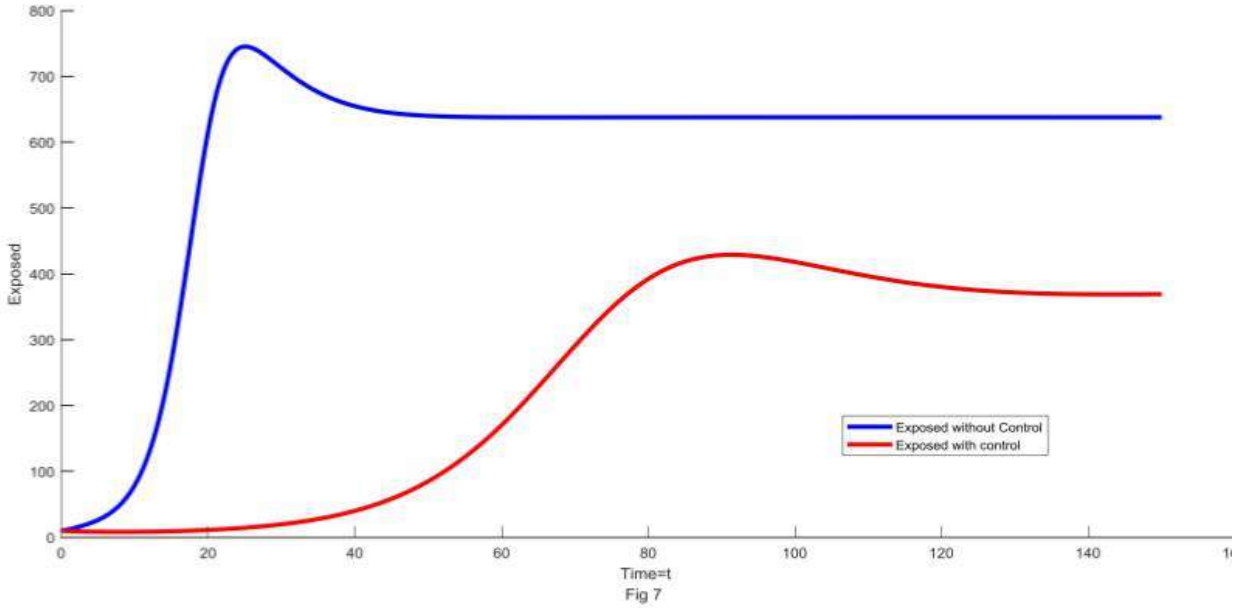


**Figure 7**: The Dynamics of Exposed Smartphones with vaccination Control strategy only $(0 < \tau_1(t) < 1, and\ \tau_2(t) = \tau_3(t) = 0)$.

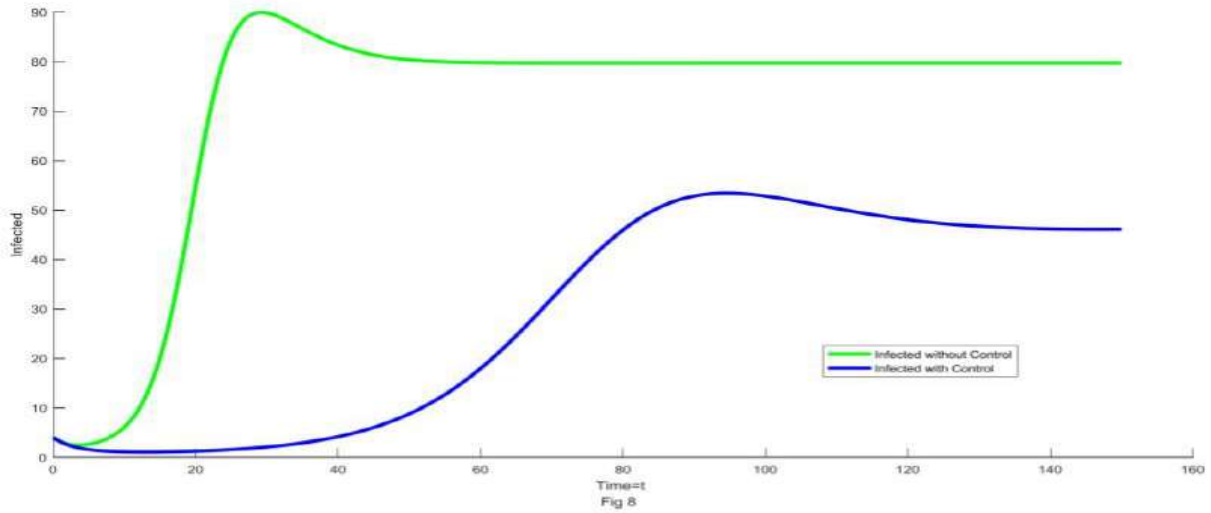


**Figure 8**: The Dynamics of Infected Smartphones with vaccination Control strategy only $(0 < \tau_1(t) < 1, and\ \tau_2(t) = \tau_3(t) = 0)$.

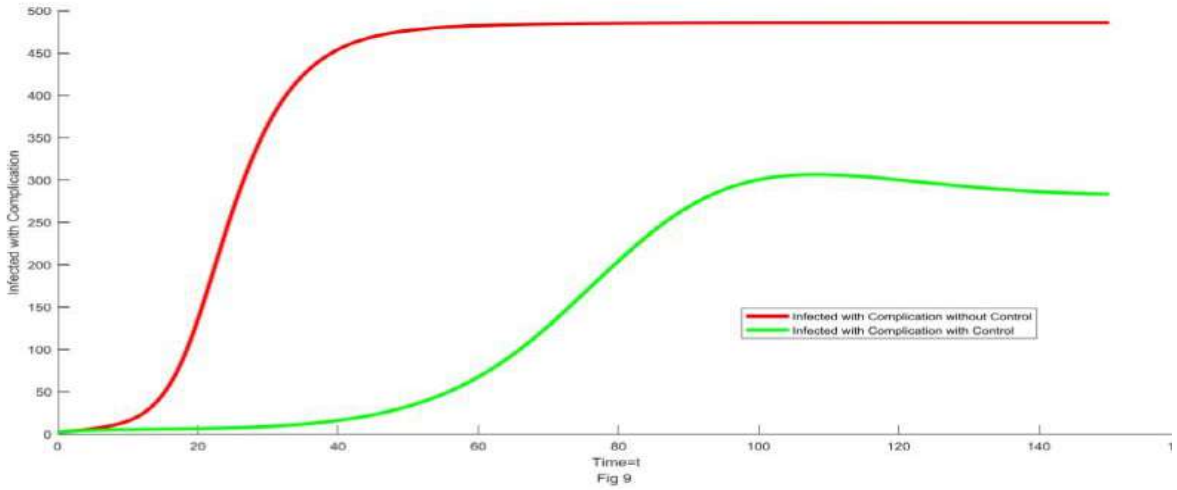


**Figure 9**: The Dynamics of Infected with Complication Smartphones with vaccination Control strategy only $(0 < \tau_1(t) < 1, and\ \tau_2(t) = \tau_3(t) = 0)$.

| Without and with control $\tau_1(t)$ after $t = 150$ | Without control | With control | Percentage of decreasing |
|---|---|---|---|
| Exposed | 637.8093 | 369.1904 | 42.12 |
| Infected | 79.7262 | 46.1296 | 42.14 |
| Infected with Complication | 637.8093 | 369.1904 | 41.70 |

**Table 2**: Percentage of the decreasing number of Exposed, Infected and Infected with Complication without and with control $\tau_1(t)$

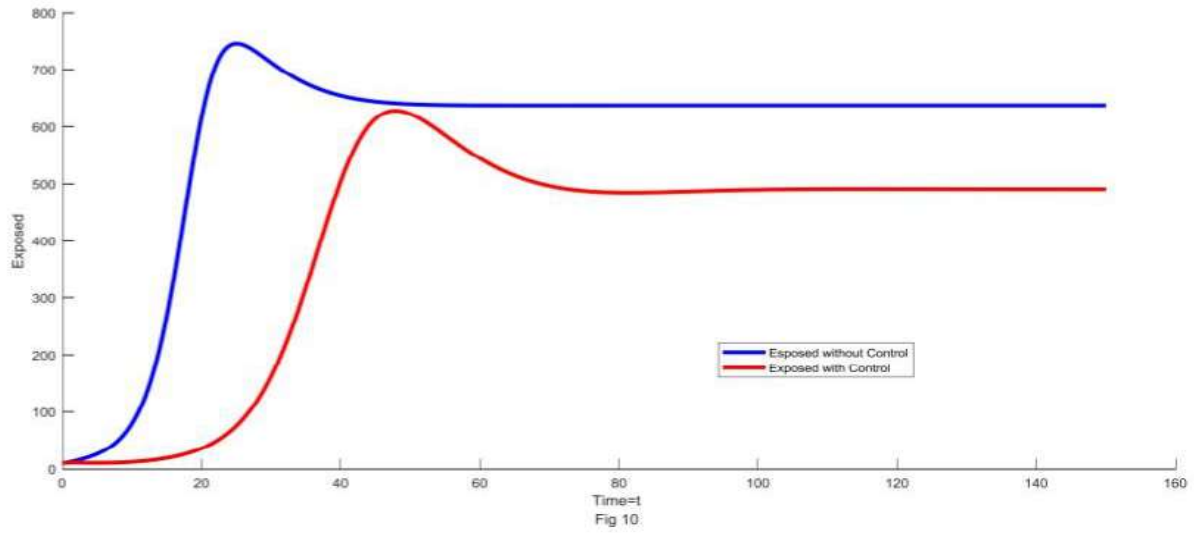


**Figure 10**: The Dynamics of Exposed Smartphones with quarantine control strategy only $(0 < \tau_2(t) < 1, and\ \tau_1(t) = \tau_3(t) = 0)$.

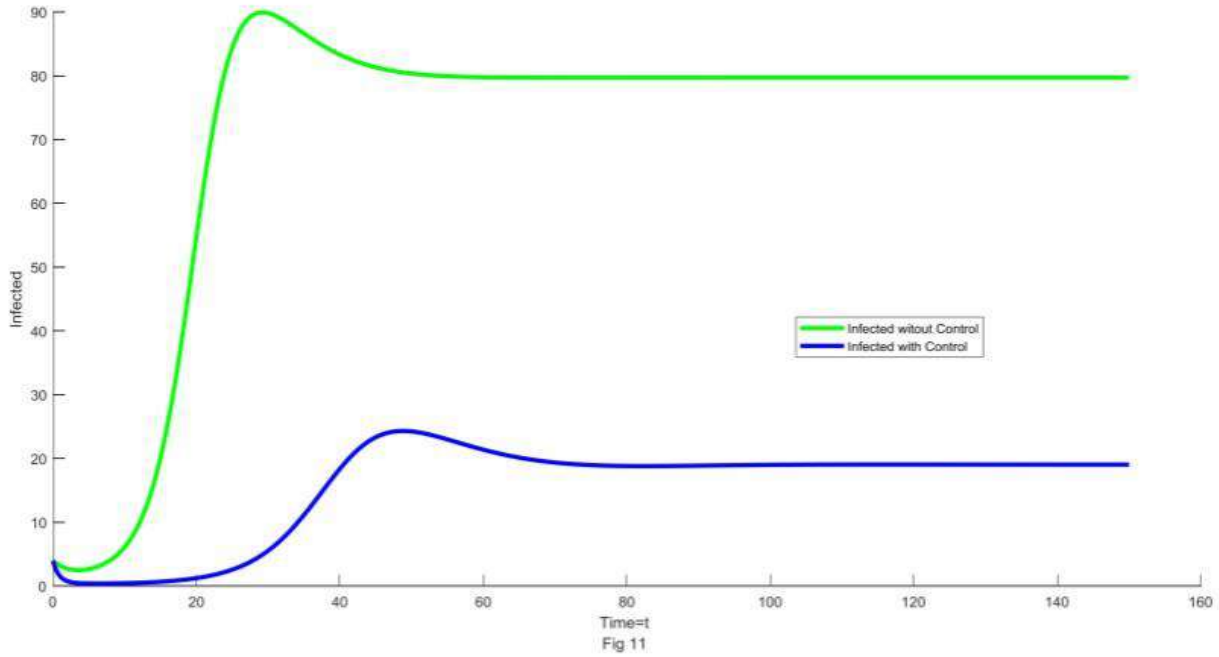


**Figure 11**: The Dynamics of Infected Smartphones with quarantine control strategy only $(0 < \tau_2(t) < 1, and\ \tau_1(t) = \tau_3(t) = 0)$.

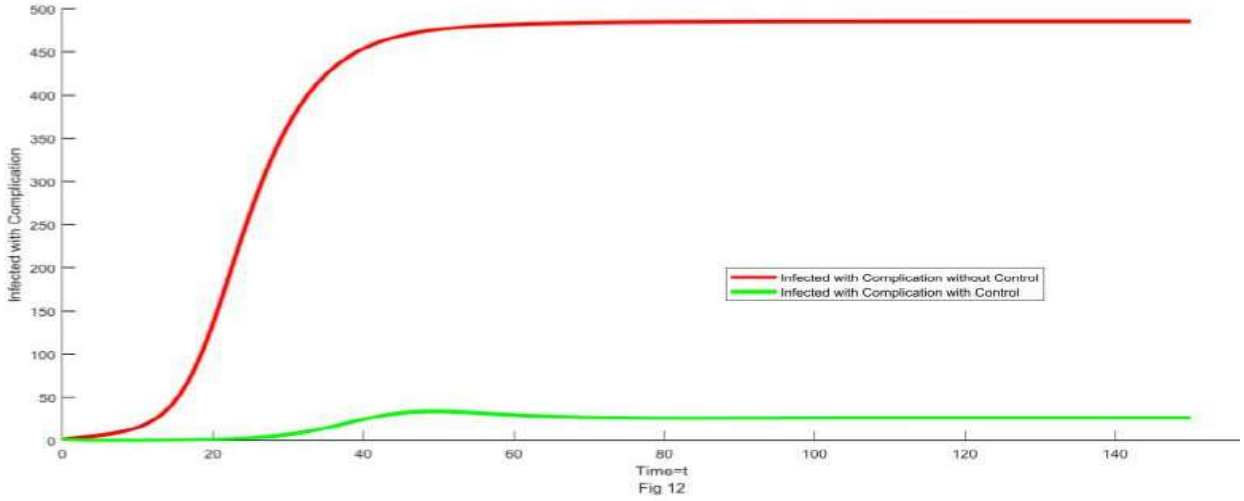


**Figure 12**: The Dynamics of Infected with Complication Smartphones with quarantine control strategy only $(0 < \tau_2(t) < 1, and\ \tau_1(t) = \tau_3(t) = 0)$.

| Without and with control $\tau_2(t)$ after $t = 150$ | Without control | With control | Percentage of decreasing |
|---|---|---|---|
| Exposed | 637.8093 | 490.9569 | 23.04 |
| Infected | 79.7262 | 19.0457 | 76.11 |
| Infected with Complication | 637.8093 | 26.6492 | 94.51 |

**Table 3**: Percentage of the decreasing number of Exposed, Infected and Infected with Complication without and with control $\tau_2(t)$

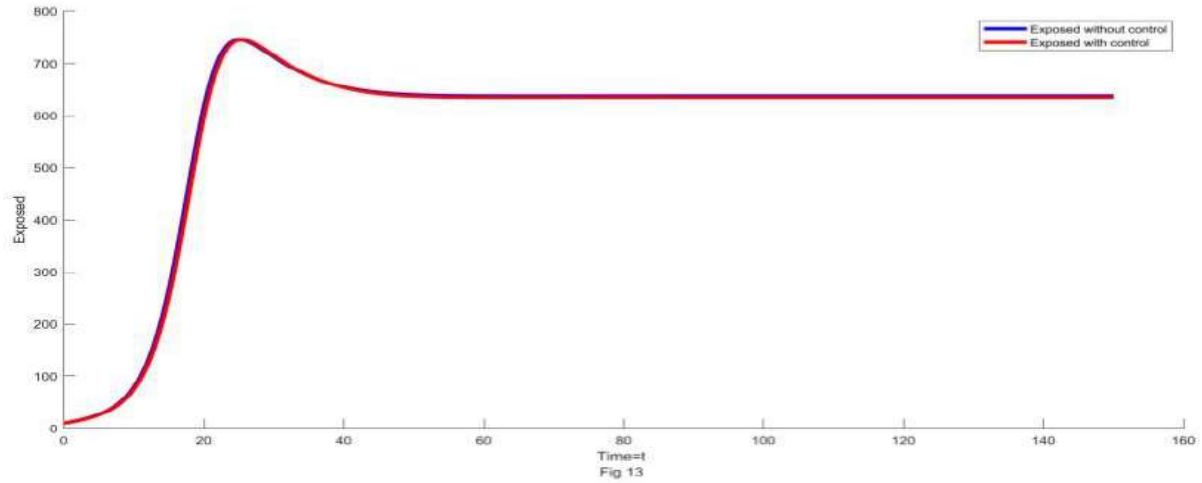


**Figure 13**: The Dynamics of Exposed Smartphones with treatment control strategy only $(0 < \tau_3(t) < 1, and\ \tau_1(t) = \tau_2(t) = 0)$.

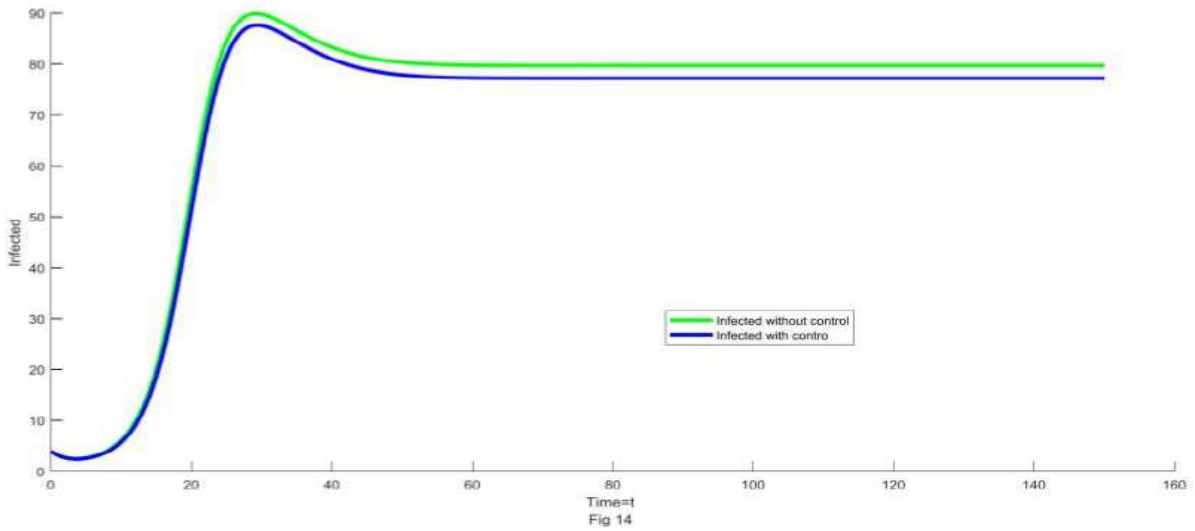


**Figure 14**: The Dynamics of Infected Smartphones with treatment control strategy only $(0 < \tau_3(t) < 1, and\ \tau_1(t) = \tau_2(t) = 0)$.

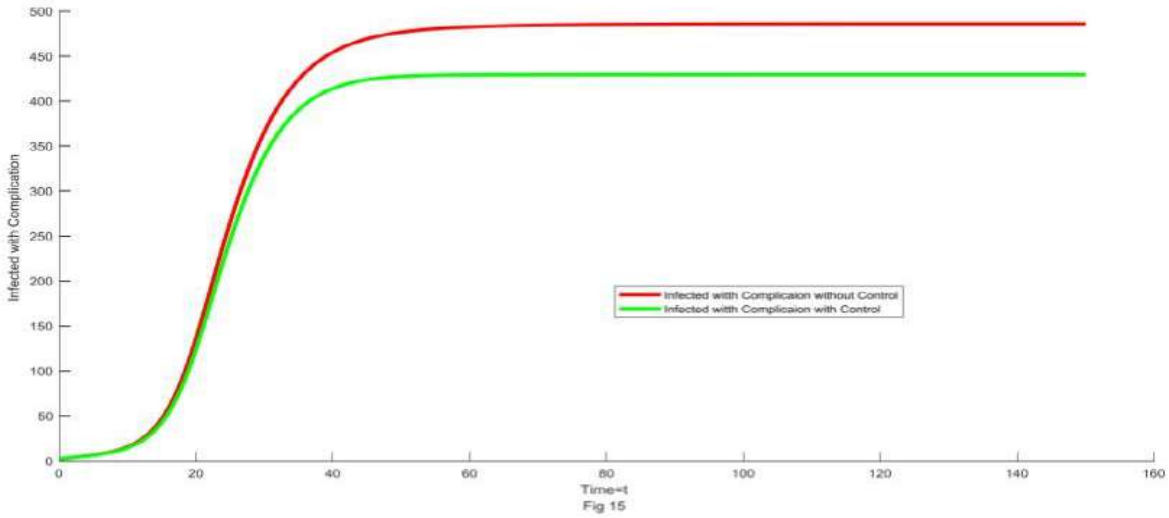


**Figure 15**: The Dynamics of Infected with Complication Smartphones with treatment control strategy only $(0 < \tau_3(t) < 1, and\ \tau_1(t) = \tau_2(t) = 0)$.

| Without and with control $\tau_3(t)$ after $t = 150$ | Without control | With control | Percentage of decreasing |
|---|---|---|---|
| Exposed | 637.8093 | 635.2779 | 0.87 |
| Infected | 79.7262 | 77.2635 | 3.09 |
| Infected with Complication | 637.8093 | 429.2418 | 1.16 |

**Table 4**: Percentage of the decreasing number of Exposed, Infected and Infected with Complication without and with control $\tau_3(t)$

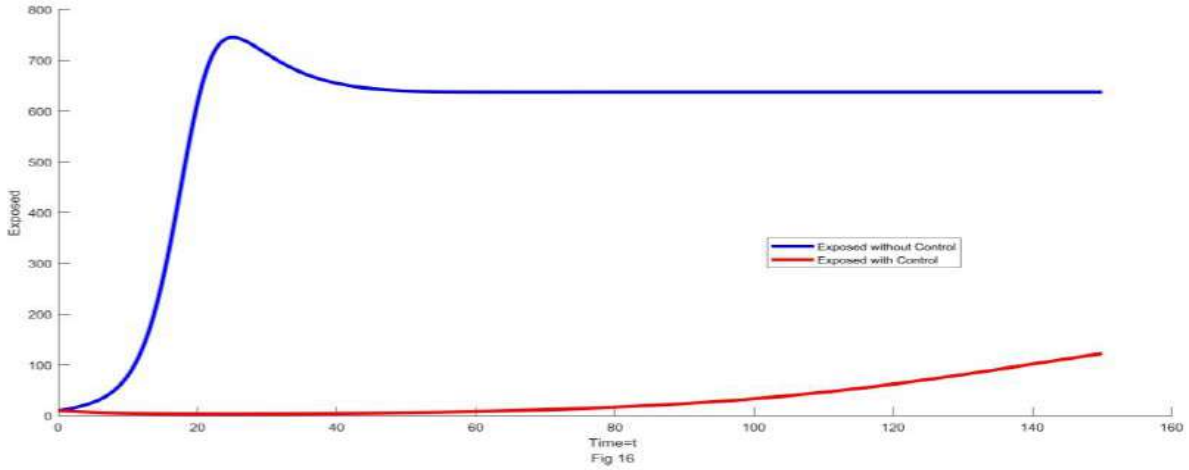


**Figure 16**: The Dynamics of Exposed Smartphones with vaccination and quarantine Control strategies only $(0 < \tau_1(t), \tau_2(t) < 1 \; and \; \tau_3(t) = 0)$ .

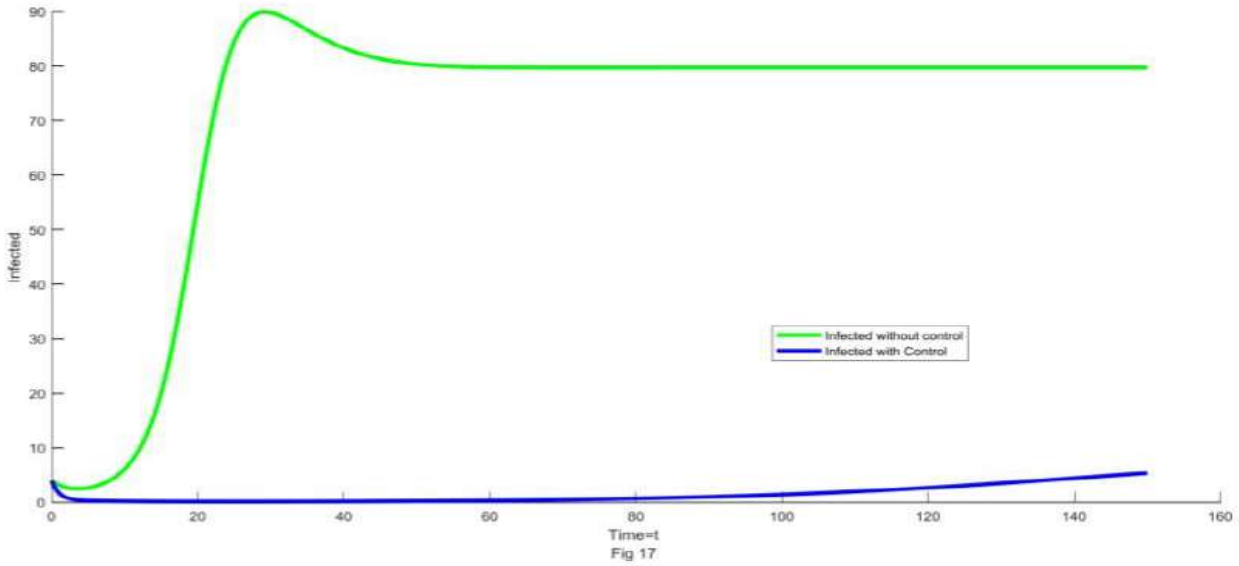


**Figure 17**: The Dynamics of Infected Smartphones with vaccination and quarantine Control strategies only $(0 < \tau_1(t), \tau_2(t) < 1 \; and \; \tau_3(t) = 0)$ .

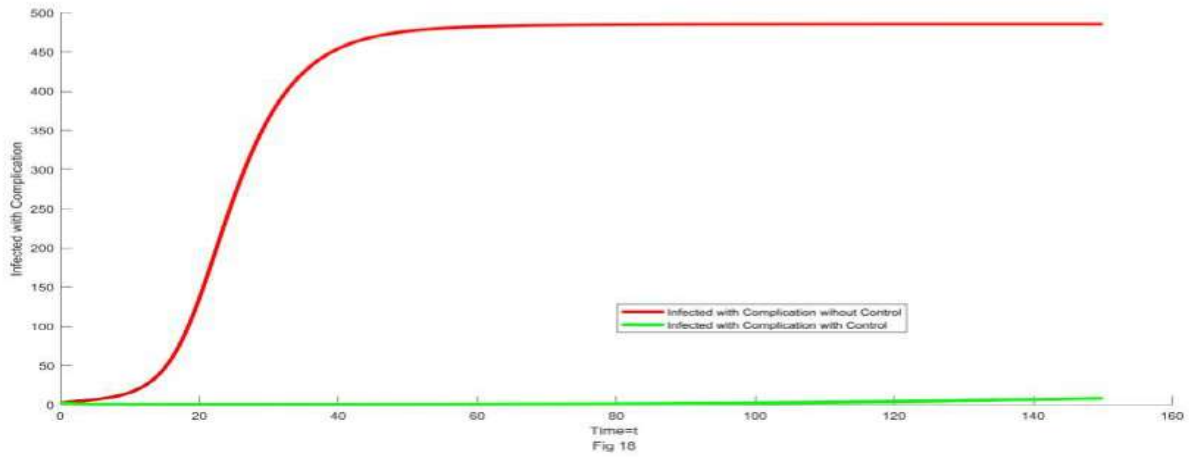


**Figure 18**: The Dynamics of Infected with Complication Smartphones with vaccination and quarantine Control strategies only $(0 < \tau_1(t), \tau_2(t) < 1 \; and \; \tau_3(t) = 0)$ .

| Without and with control $\tau_1(t) and \; \tau_2(t)$ after $t = 150$ | Without control | With control | Percentage of decreasing |
|---|---|---|---|
| Exposed | 637.8093 | 122.5242 | 80.79 |
| Infected | 79.7262 | 5.3701 | 93.26 |
| Infected with Complication | 637.8093 | 7.9962 | 98.35 |

**Table 5**: Percentage of the decreasing number of Exposed, Infected and Infected with Complication without and with control $\tau_1(t) and \; \tau_2(t)$.

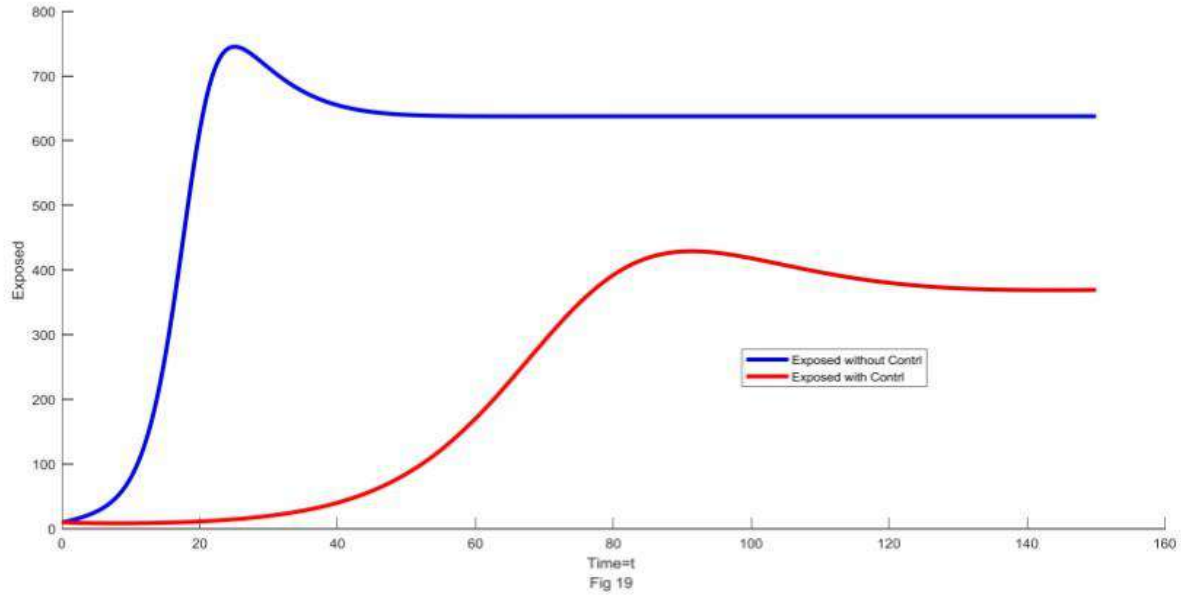


**Figure 19**: The Dynamics of Exposed Smartphones with vaccination and treatment Control strategies only $(0 < \tau_1(t), \tau_3(t) < 1 \; and \; \tau_2(t) = 0)$.

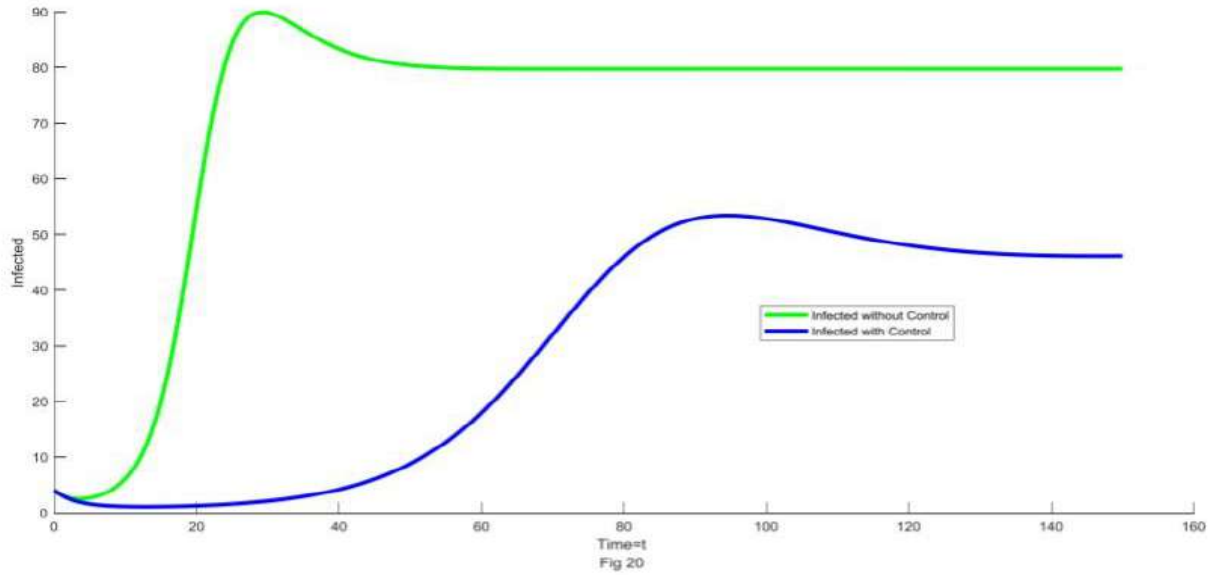


**Figure 20**: The Dynamics of Infected Smartphones with vaccination and treatment Control strategies only $(0 < \tau_1(t), \tau_3(t) < 1 \; and \; \tau_2(t) = 0)$ .

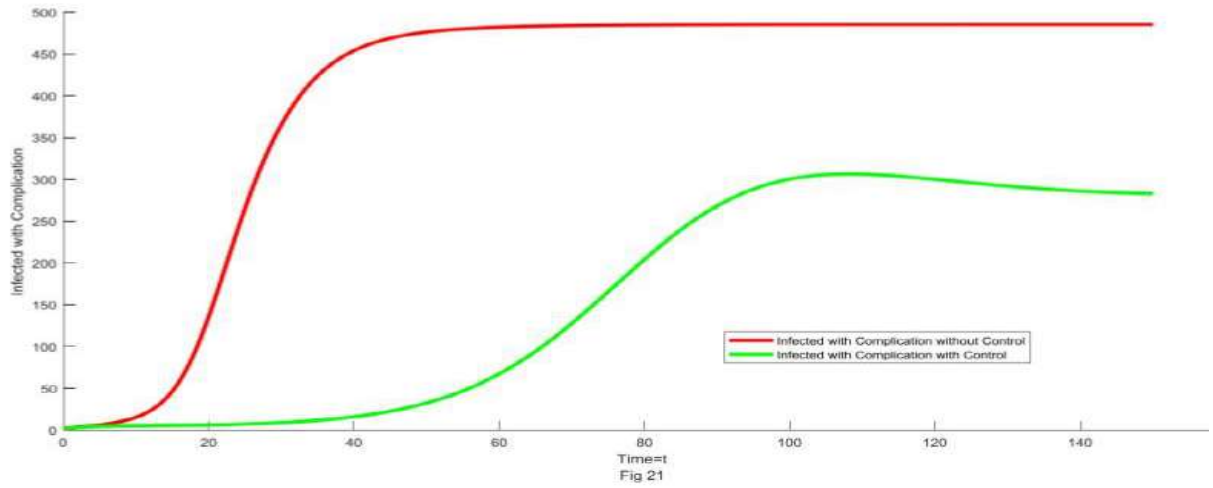


**Figure 21**: The Dynamics of Infected with Complication Smartphones with vaccination and treatment Control strategies only $(0 < \tau_1(t), \tau_3(t) < 1 \; and \; \tau_2(t) = 0)$ .

| Without and with control $\tau_1(t) and \; \tau_3(t)$ after $t = 150$ | Without control | With control | Percentage of decreasing |
|---|---|---|---|
| Exposed | 637.8093 | 369.1904 | 42.12 |
| Infected | 79.7262 | 46.0457 | 42.14 |
| Infected with Complication | 637.8093 | 283.1645 | 41.70 |

**Table 6**: Percentage of the decreasing number of Exposed, Infected and Infected with Complication Without and with control $\tau_1(t) and \; \tau_3(t)$.

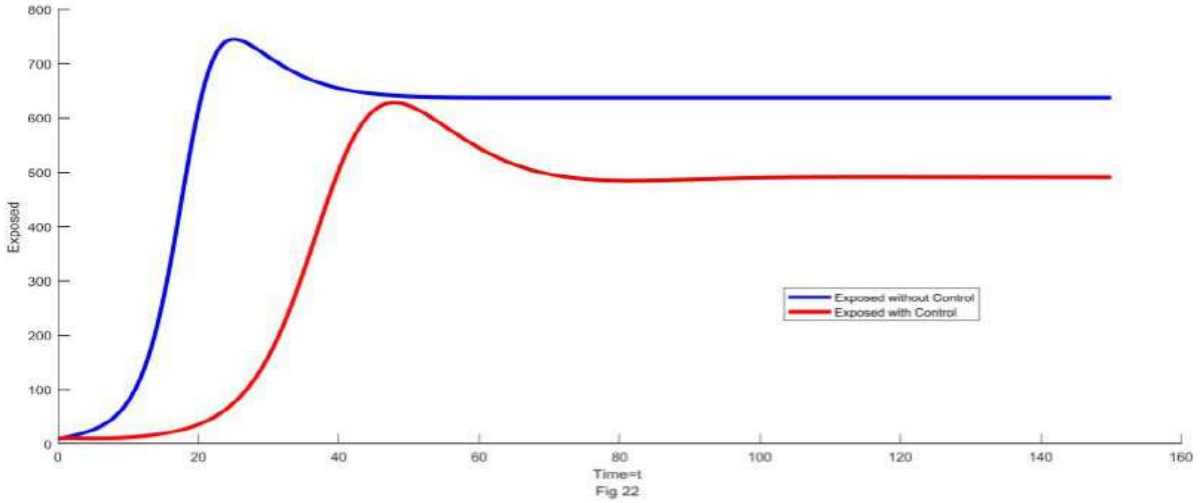


**Figure 22**: The Dynamics of Exposed Smartphones with quarantine and treatment Control strategies only $(0 < \tau_2(t), \tau_3(t) < 1 \; and \; \tau_1(t) = 0)$ .

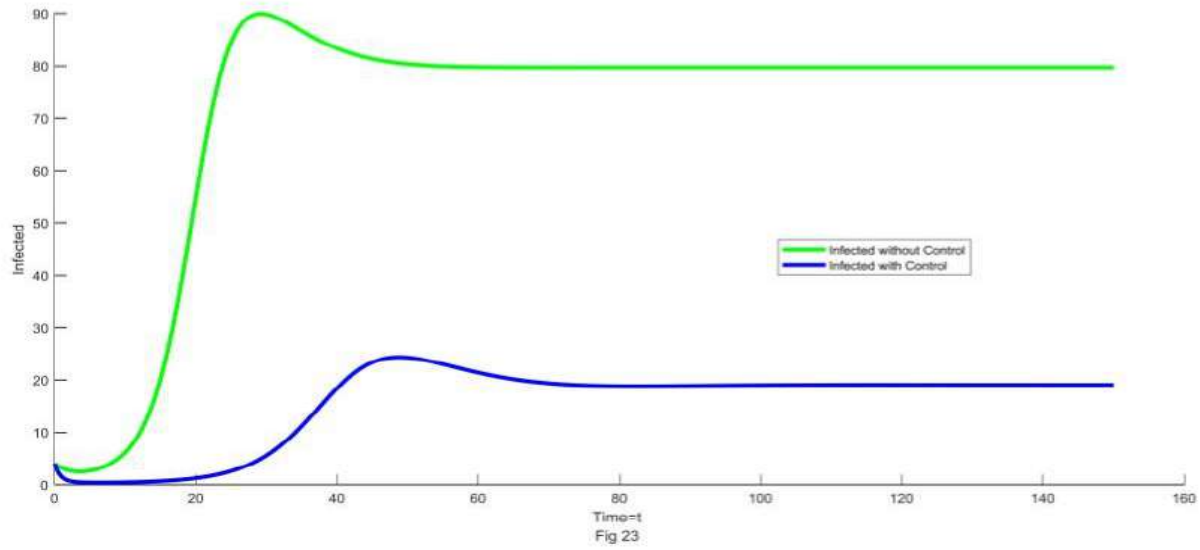


**Figure 23**: The Dynamics of Infected Smartphones with quarantine and treatment Control strategies only $(0 < \tau_2(t), \tau_3(t) < 1 \; and \; \tau_1(t) = 0)$ .

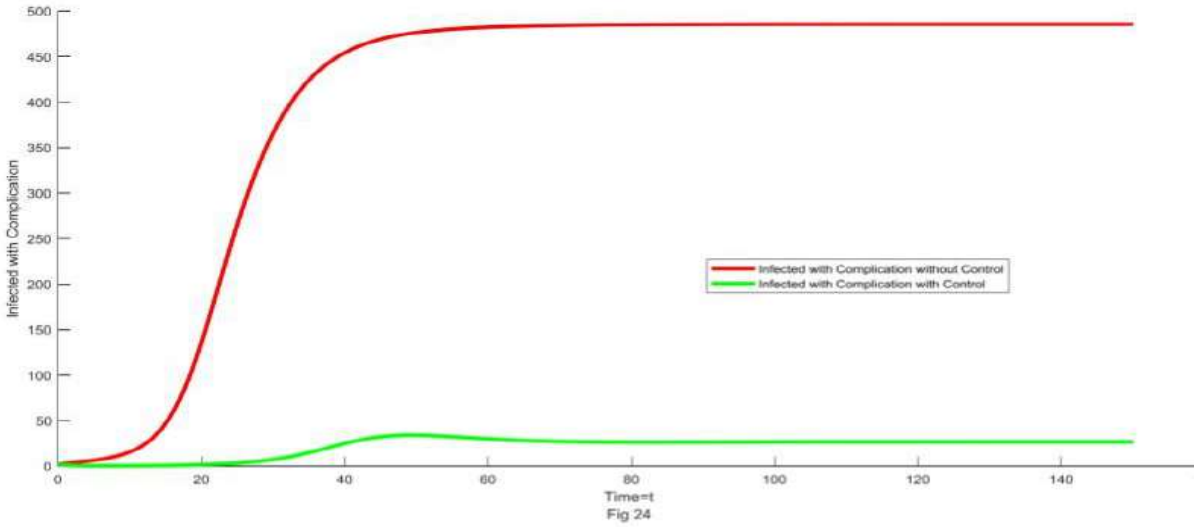


**Figure 24**: The Dynamics of Infected with Complication Smartphones with quarantine and treatment Control strategies only $(0 < \tau_2(t), \tau_3(t) < 1 \; and \; \tau_1(t) = 0)$.

| Without and with control $\tau_2(t) and \; \tau_3(t)$ after $t = 150$ | Without control | With control | Percentage of decreasing |
|---|---|---|---|
| Exposed | 637.8093 | 490.9569 | 23.02 |
| Infected | 79.7262 | 19.0457 | 76.11 |
| Infected with Complication | 637.8093 | 26.6492 | 94.51 |

**Table 7**: Percentage of the decreasing number of Exposed, Infected and Infected with Complication without and with control $\tau_2(t) and \; \tau_2(t)$.

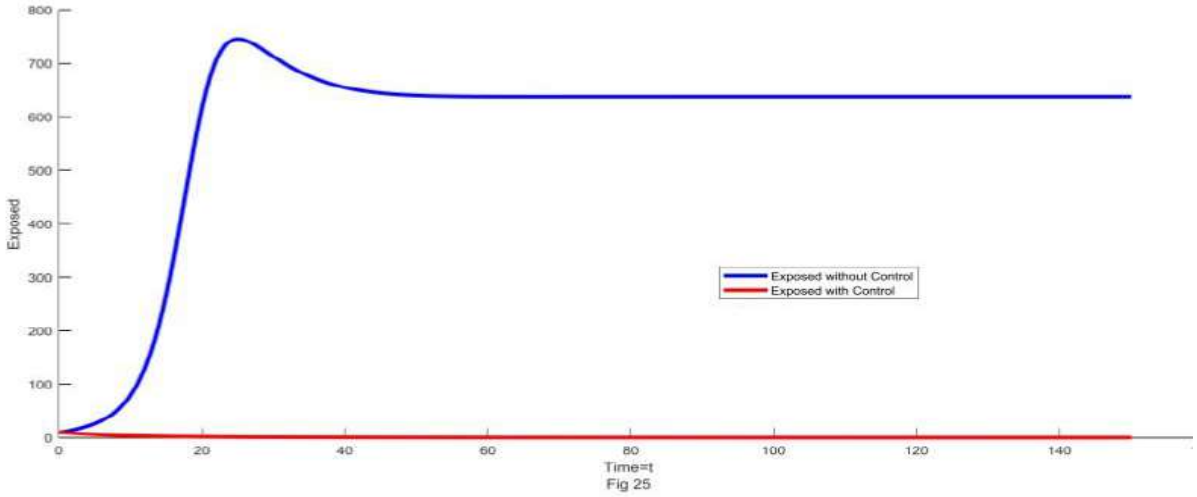


**Figure 25**: The Dynamics of Exposed Smartphones with vaccination, quarantine and treatment Control strategies $(0 < \tau_1(t), \tau_2(t), \tau_3(t) < 1)$.

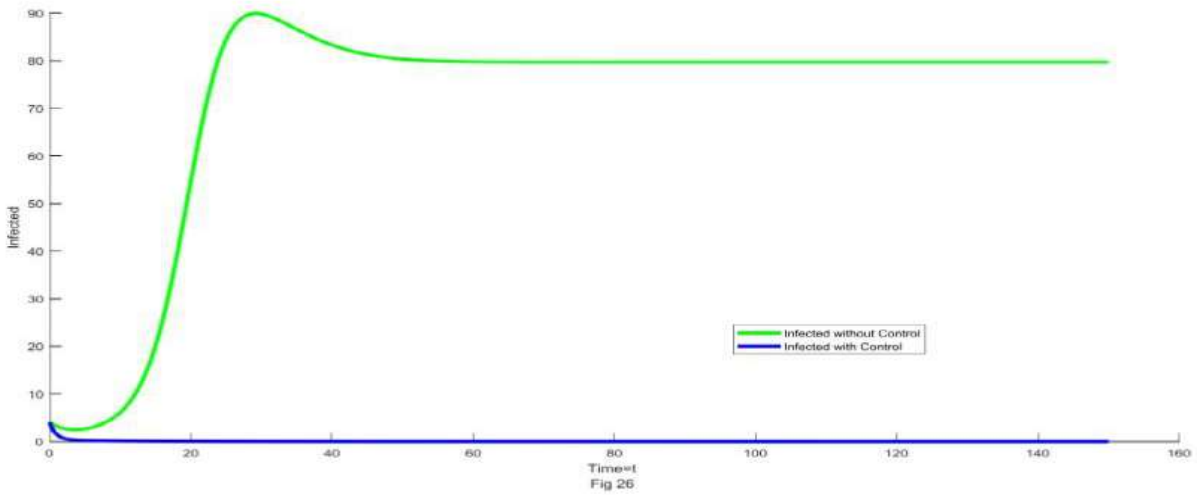


**Figure 26**: The Dynamics of Infected Smartphones with vaccination, quarantine and treatment Control strategies $(0 < \tau_1(t), \tau_2(t), \tau_3(t) < 1)$.

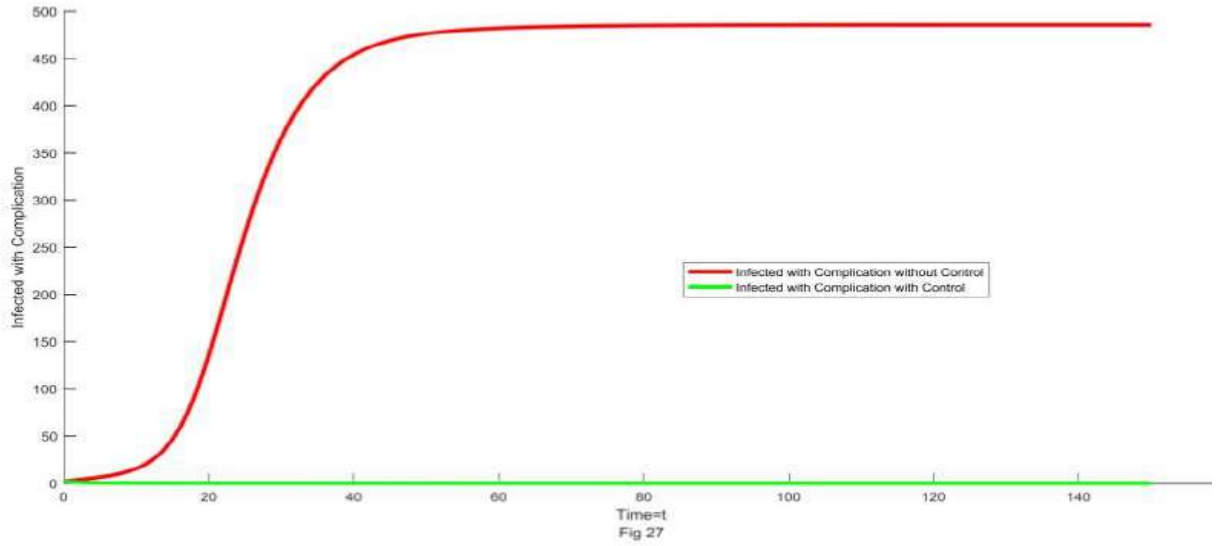


**Figure 27**: The dynamics of Infected with Complication Smartphones with vaccination, quarantine and treatment Control strategies $(0 < \tau_1(t), \tau_2(t), \tau_3(t) < 1)$ .

| Without and with control $\tau_1(t), \tau_2(t) and\ \tau_3(t)$ after $t = 150$ | Without control | With control | Percentage of decreasing |
|---|---|---|---|
| Exposed | 637.8093 | 0.0029371 | 99.9995 |
| Infected | 79.7262 | 0.00011848 | 99.9995 |
| Infected with Complication | 637.8093 | 0.00016898 | 99.9999 |

**Table 8**: Percentage of the decreasing number of Exposed, Infected and Infected with Complication without and with control $\tau_1(t), \tau_2(t) and\ \tau_2(t)$.

Figures 2 and 3 reveal the dynamics of the six compartments without and with optimal control respectively. From Figure 2, the population of exposed, infected and infected with complication were seen to be increasing because of lack of optimal control strategies. Also, we shall observe from figure 3 that the population of exposed, infected and infected with complication were drastically reduced whereas susceptible and recovered population increases due to the effectiveness of the optimal control strategies. The result of the individual compartments of exposed, infected and

infected with complications were respectively displayed in Figures 4, 5 and 6 and it shows that without optimal control strategies, the Smartphone virus infection will continuously be transmitted from one Smartphone to another.

When we used only the optimal control $\tau_1(t)$, (Vaccination), there is an increase in the population of Smartphones protected from virus and the result were shown in Figures 7 (Exposed Smartphones), figure 8 (Infected Smartphones) and figure 9 (Infected with Complication Smartphones). This simply means that if Smartphones are adequately and effectively installed with antivirus, there will be a decrease in the exposed, infected and infected with complication Smartphones in the population. The percentage decrease is represented in table 2. In Figures 10, 11 and 12, we use only the optimal control $\tau_2(t)$. Here, the quarantine strategy was adopted for all Smartphones in the compartments of infected and infected with complication. The result of this optimal control strategy, indicates a slight decrease in the population of the exposed as in Figure 10, and a greater percentage decrease in the population of the infected and infected with complication Smartphones as shown in Figure 11 and Figure 12 respectively, which implies that the strategy is effective. Also, the percentage decreases in the required compartments were given in Table 3. Table 4 displayed the result of only the optimal control $\tau_3(t)$, which is treatment (repair). We observe that treatment only as an optimal control strategy for Smartphone virus is not strong enough to reduce the population of exposed, infected and infected with complication Smartphones. From Figure 13, we observe that treatment (repair) does not have effect on exposed Smartphones, and similar results were displayed in Figure 14 and Figure 15.

In Table 5, we show the result of combined optimal control strategies for $\tau_1(t)\ and\ \tau_2(t)$, (vaccination and quarantined). Figure 16 displayed the effect of vaccination and quarantine on the exposed Smartphone population, Figure 17 shows the effect of vaccination and quarantine on the infected Smartphone population whereas Figure 18 displayed the effect of vaccination and quarantine on the infected with complication. From these figures, we observe that vaccination and quarantine have a great effect by decreasing the population of the exposed, infected and infected with complication Smartphones. Also, table 6 presents the effect of combined optimal control strategies for $\tau_1(t)\ and\ \tau_3(t)$ (Vaccination and treatment). The outcome of vaccination and treatment on the exposed Smartphones is demonstrated in Figure 19. More so, the outcome of vaccination and treatment on the infected Smarphone population is presented in Figure 20 while the outcome of the same vaccination and treatment on infected with complication is shown in Figure 21. Examining these figures, we notice that the combined optimal control strategies of vaccination and treatment does not have much effect on the exposed, infected and infected with complication Smartphones. In the same way, we displayed the result of the combined optimal control strategies for $\tau_2(t)\ and\ \tau_3(t)$ (quarantine and treatment) on the exposed, infected and infected with complication Smartphones in table 7. In Figure 22, we demonstrated that quarantine and treatment does not have much effect on the exposed Smartphone population. it was presented in Figure 23, that quarantine and treatment have much effect on infected Smartphone population and also Figure 24 showed that it has great effect on infected with complication. From the results of these combinations, we observed that $\tau_1(t)\ and\ \tau_2(t)$, (vaccination and quarantined) optimal control strategy is more effective than the other two combinations. Since the main objective of this model is to minimize Smartphone virus infection in the population, we merged the three optimal control

strategies $\tau_1(t), \tau_2(t), and\ \tau_3(t)$, that is, vaccination, quarantine and treatment. Based on Table 8 which shows the percentage of the decreasing number of exposed, infected and infected with complication Smartphones, we observe that the combination of the three optimal control strategies (vaccination, quarantine and treatment) has the greatest decreasing effect on the exposed Smartphones as in Figure 25, infected Smartphones as in Figure 26 and infected with complication Smartphones as in Figure 27. From these outcomes, we noticed that combined intervention of $\tau_1(t), \tau_2(t), and\ \tau_3(t)$ is a better control strategy for Smartphone virus infection and need to be deployed early in order to reduce Smartphone virus infection to the barest minimum.

## 6. Conclusion

In this study, we proposed the optimal control strategies to mitigate Smartphone virus infection transmission dynamics. In order to minimize the number of infected and infected with complication, we introduced three control strategies $\tau_1(t), \tau_2(t), and\ \tau_3(t)$, which respectively represents Vaccination, quarantined and treatment (repair). We also obtained the characterization of the optimal controls by applying the results of the control theory. The model was solved numerically by Runge – Kutta method of order four in MATLAB. Numerical simulation of the model shows the effectiveness of vaccination, quarantine and treatment, combination of any of the two control strategies and even the three control strategies. However, the results revealed that a combination of vaccination, quarantine and treatment is a better control strategy for Smartphone virus infection.

## Reference

[1] Balatif O., Khajji B., and Rachik M. (2020). Mathematical modeling, analysis and optimal control of abstinence behavior of registration on electoral list, Discrete Dyn. Nat. Soc., 9738934.

[2] Batista F.K., del Rey Á. M., Quintero-Bonilla S., and Queiruga-Dios A. (2017). A SEIR model for computer virus spreading based on cellular automata. In International Joint Conference SOCO'17-CISIS'17-ICEUTE'17 León, Spain, September 6–8, 2017, Proceeding (pp. 641-650).

[3] Boyce W. E. and DiPrima R.C. (2000). Elementary differential equations and boundary value problems, John Wiley and Sons, New York, 2000.

[4] Chandrasekar S. and Jayaprakasan V. (2014). Automatic detection and restraining mobile virus propagation using android. International Journal of Computer Science and Mobile Computing, 3(1): 526-532.

[5] Chinebu T.I., Udegbe I.V., and Eberendu A.C. (2021). Epidemic model and mathematical study of impact of vaccination for the control of malware in computer network. Journal of Advances in Mathematics and Computer Science. 36(3): 72-96.

[6] Chinebu T.I., Eberendu A.C., and Udegbe I.V. (2021) Analysis of a mathematical model for the dynamics of smartphone virus propagation: a guide from epidemiological model. Global Scientific Journals, 9(6).

[7] Chinebu T.I., Udegbe I.V., and Ezennorom E.O. (2021). Analysis of optimal control strategies for preventing computer virus infection and reducing program files damage with other symptoms. Journal of Scientific Research and Reports, 27(1): 8-29.

[8] Chinebu T.I., Mbah G.C.E., Jooda E.A., Ezennorom E.O., and Udegbe I.V. (2021). Sensitivity analysis of smartphone virus infection transmission dynamics. Journal of the Nigerian Society for Mathematical Biology, 4: 76 – 95.

[9] Fan Y., Zheng K., and Yang Y. (2010). Epidemic model of mobile phone virus for hybrid spread mode with preventive immunity and mutation, In Proc. 6th International Conference on wireless communications networking and mobile computing (WiCOM 2010), Chengdu, China.

[10] Fleming W.H. and Rishel R.W. (1975). Deterministic and stochastic optimal control. Springer, New York.

[11] Guillen J.D.H., del Rey A.M., and Vara R.C. (2020). On the optimal control of a malware propagation model. Mathematics, doi: 10.3390/math8091518.

[12] Hypponen M. (2006). Malware goes mobile. Scientific American, Inc. www.Sciam.com.

[13] Kouidere A., Balatif O., Ferjouchia H., Boutayeb A., and Rachik M. (2019). Optimal control strategy for a discrete time to the dynamics of a population of diabetic with highlighting the impact of living environment. Discreet Dyn. Nat. Soc., 6342169.

[14] Kouliaridis V., Barmpatsalou K., Kambourakis G., and Chen S. (2020). A survey on mobile malware detection techniques, IEICE Transacions on Information and Systems vol. E103 No. 2.

[15] Liu W. and Zhong S. (2017). Web malware spread modelling and optimal control strategies. Scientific Reports, doi:10.1038/srep42308.

[16] MadhuSudanan V. and Geetha R. (2020). Dynamics of epidemic computer virus spreading model with delays. Wireless Personal Communications, 115(3): 2047-2061.

[17] McAfee. Mobile Threat Report, hppts://www.mcafee.com/enterprise/en-us/assets/reports/rp-mobile-threat-report-2018.pdf, accessed May 10, 2018.

[18] Milosevic N., Dehghantanha A., and Choo K.K.R. (2017). Machine learning aided malware classification of android. Computers and Electrical Engineering, 61: 266 – 274.

[19 Peng S., Min W., Wang G., and Yu S. (2014). Propagation of smartphone worm based on semi-markov process and social relationship graph. Comput. Secr., 44: 92-103.

[20] Pontryagin L.S., Boltyanskii V.G., Gamkrelidze R.V., and Mischenko E.F. (1962). The mathematical theory of optimal processes. Willy, New York.

[21] Racic R., Ma D., and Chen H. (2006). Exploiting MMS vulnerabilities to stealthily exhaust mobile phone's battery. In 2006 Secure Comm and Workshops (pp. 1-10). IEEE.

[22] Skoudis E. and Zeltser L. (2004). Malware: fighting malicious code. Prentice Hall Professional, New Jersey, USA.

[23] Symantec, Motivations of Recent Android Malware, hppt://www.symantec,com/content/en/us/enterprise/media/security_response/whitepapers/motivations_of_recent_android_malware.pdf, accessed Dec 10, 2018.

[24] van Ruitenbeek E., Courtney T., Sander W. H., and Stevens F. (2007). Quantifying the effectiveness of mobile phone viruse response mechanism. In Proceeding of the 37th

Annual IEEE/IFTP International Conference on Dependable System and Networks (DNS 07), 790-799.

[25] Wang M., Chen Z., Xu L., and Zhan H. (2014). Spread and control of mobile benign worm based on two-stage repairing mechanism. Journal of Applied Mathematics.

[26] Yang L.X., Li P., Yang X., and Tang Y.Y. (2017). Distributed interaction between computer virus and patch: A modeling study. arXiv preprint arXiv:1705.04818.

[27] Yang W., Wei X., Guo H., An G., Guo L., and Yao Y. (2014). Modeling the propagation of mobile phone virus under complex network. The Scientific World Journal, hppt://dx.doi.org/10.1155/2014/207457.

[28] Zhang C. (2021). Global behavior of a computer virus propagation model on multilayer networks. Security and Communication Networks, 9 (6).

# International Journal of Mathematical Analysis and Modelling

**Scope:** The International Journal of Mathematical Analysis and Modelling (IJMAM), formerly known as the Journal of the Nigerian Society for Mathematical Biology, is the official journal of the Nigerian Society for Mathematical Biology, designed to disseminates original research findings in all areas of pure and applied mathematics. The aim of the journal is to cause to be published, original research, that shows the connection between pure and applied mathematicians, statisticians, operations researchers, physicists, engineers, computer scientists and specialists in any field of human endeavour such as in agriculture, medicine, pharmacy, life sciences, physical sciences, engineering, social sciences, humanities, arts, etc., at the crossroad of theoretical, experimental and field studies with the mathematical sciences, in order to provide solutions to problems that cut across these fields through exchange of ideas and collaborations.

Submitted papers should provide rigorous mathematical analysis of any real-world problem being discussed; at the same time, the results obtained should be useful and easily understandable by non-mathematicians. The journal will accept different kinds of articles, ranging from review articles to special invitations. All submitted manuscript will be assessed by the Editor-in-Chief before being sent out for peer-review.

Areas covered in the IJMAM include, mathematical modelling, numerical analysis, fluid mechanics, real and complex analysis, functional analysis, operator theory, statistics, algebra, computational mathematics and differential equations. Articles that show the connections between different areas of mathematics when solving real-world problems are especially welcome in the IJMAM.

**Manuscript Information and guidelines for Authors**

This is to invite you to submit high-quality research articles to the International Journal of Mathematical Analysis and Modelling (IJMAM), formerly known as the Journal of the Nigerian Society for Mathematical Biology.

Manuscripts should be written either using MS Word (most preferred) or in LaTeX. Initial submissions for review can be in MS Word or PDF. There will be a page restriction of a maximum of 26 pages per accepted article. The article should be concise and details of well-established mathematical methods should be omitted. Articles that do not contain significant mathematical content and results will not be accepted for publication.

Citations within the manuscript should be done using the number system i.e., “Following the idea in [7], we have that …”. Theorems, Lemmas, Propositions,

Remarks, e.t.c., should be numbered using the Section number where they appear e.g., Theorem 2.1 will appear in Section 2.

References should follow the format shown below:

[1] Anderson R. M. and May M. (1991). Infectious Diseases of Humans: dynamics and Control. Oxford University Press, UK.

[2] Castillo-Chavez C. and Song B. (2004). Dynamical models of tuberculosis and their applications, Math. Biosci. Eng., 1: 361-404.

References should be in alphabetical order in the list of references, which should be the last section in the manuscript.

Manuscripts should be submitted to the Editor-in-Chief, via the following email address: mcsb@uniben.edu. Please note that this is the **only** acceptable channel for manuscript submission at this time.

There is a publication charge for each accepted article. Payment details will be corresponded to the author(s) at the time of manuscript acceptance for publication in the IJMAM.

**Subscription rates:** This is subject to change from time to time. Please, contact the Editor-in-Chief for the current rates, for local and foreign subscriptions.

**International Journal of Mathematical Analysis and Modelling**
**(Formerly Journal of the Nigerian Society for Mathematical Biology)**
**Volume 5, Issue 1 (May), 2022**

## Contents